Investigation of T cell signalling events regulating immunity and tolerance *in vivo*

Angela Mary Young Morton

A thesis submitted to the Faculty of Medicine, University of Glasgow for the degree of Doctor of Philosophy

Division of Immunology, Infection and Inflammation
Glasgow Biomedical Research Centre
120 University Place
University of Glasgow
Glasgow
G12 8TA

November 2007

Declaration

The work presented in this thesis represents original work carried out by the author. This thesis has not been submitted in any form to any other University.

Angela Mary Young Morton
University of Glasgow
November 2007

Dedicated to my brother, Alastair Young Morton

Acknowledgements

Firstly, I would like to thank my supervisors Professor Maggie Harnett, Professor Paul Garside and Professor Allan Mowat for all of their support, advice and encouragement over the years. It has been a pleasure to work for all three of you. In particular, I would like to give special thanks to Maggie for her guidance in the writing of this thesis.

All members, past and present, of Lab 207, Team Mowat, the Michie lab and the Harnett lab have also given me help and support (and cups of tea) during the course of my PhD, so thank you all. Those who deserve a particular mention are listed below.

Special thanks to Karen Smith and Kim Kennedy for introducing me to the joys of immunohistochemistry and for their great friendship during my time in Lab 207. Thank you to Dr Claire Adams for her help during our collaborative development of the *in vitro* and *in vivo* priming and tolerance models. Thanks also to Dr Jim Brewer for his expertise in fluorescence technology and Paul Mitchell for his help in developing some of the immunofluorescence techniques. Andy, Elinor and Yvonne, thank you for your good chat. Thank you to all of the current members of the Harnett lab, who had to put up with me during my write-up. Very special thanks are due to Mairi McGrath and Theresa Thalhamer for keeping me sane and very kindly reading my thesis.

Thanks also to Laura Denby and Andy Baker for their kind help and technical expertise with the adenoviral work.

I would also like to thank the Medical Research Council, UK for their funding, without which this research would not have been possible.

Thank you to all of my friends for putting up with me during the writing of this thesis. Sara, Jill, Becky and Kirsty Rice deserve a special mention.

I would also like to thank my mum and brother who have always supported me, and my late father, who always encouraged me to do my best.

Finally, a very special mention to two amazing people who are also great friends, Anne Donachie and Barbara McManus. Thank you both for everything (including the adoptive transfers!).

Table of contents

List of figures and tables

Chapter 1 – General Introduction

Chapter 2 – Materials and Methods

Chapter 3 - Development of technologies for examining T cell signalling *in situ*

Chapter 4 - Analysing the role of ERK MAPK signalling and potential cell cycle modulators in priming and tolerance of antigen-specific T cells *in vitro*

Chapter 5 – Analysing the role of Rap1 signalling in tolerance and priming

Chapter 6 – General Discussion

List of Abbreviations

The following abbreviations are used in this thesis:

3'-phosphoinositide-dependent protein kinase	PDK
3, 3', 5, 5'-tetramethylbenzidine peroxidase	TMB
4',6-diamido-2-phenylindole hydrochloride	DAPI
Activating transcription factor	ATF
Activator protein 1	AP-1
Adenosine tri-phosphate	ATP
Adenovirus	Ad
Antibody	Ab
Antigen	Ag
Antigen Presenting Cell(s)	APC
Apoptosis inducing factor	AIF
Autoimmune polyendocrinopathy-candidiasis-ectodermal dystrophy	APECED
Autoimmune regulator protein	AIRE
B7-related protein-1	B7RP-1
B cell antigen receptor	BcR
B cell lymphoma-2	Bcl-2
Bcl-2 homology	BH
Bone Marrow derived Dendritic Cell(s)	BMDC
B regulatory cell	B_{reg}
c-Jun N-terminal kinase	JNK
Calcium	Ca^{2+}
Central-supramolecular activation cluster	c-SMAC
Cholera toxin	CT
Clusters of differentiation	CD
Complete Freunds' adjuvant	CFA
Constitutively active	CA
Counts per minute	cpm
Cyclin-dependent kinase	CDK
Cytotoxic T lymphocyte(s)	CTL
Cytotoxic T lymphocyte-associated antigen	CTLA
Delayed-type hypersensitivity	DTH

Dendritic Cell(s)	DC
Deoxyribonucleic acid	DNA
Detergent-insoluble glycolipid-rich domains	DIG
Diacylglycerol	DAG
Diacylglycerol kinase	DGK
Dominant negative	DN
Double negative	DN
Double positive	DP
E twenty-six	ETS
Early growth response	EGR
Enzyme Linked Immuno Sorbent Assay	ELISA
Experimental autoimmune encephalomyelitis	EAE
Fluorescein Isothiocyanate	FITC
fms-like tyrosine kinase ligand	flt3L
Fas associated protein with a death domain	FADD
Flow cytometry	FC
Fluorescence resonance energy transfer	FRET
Forkhead box P3	FoxP3
Forward Scatter	FSC
Foetal Calf Serum	FCS
Glycolipid-enriched microdomains	GEM
Glyosylphosphatidylinositol-anchored protein	GPI-AP
Granulocyte-macrophage colony-stimulating factor	GM-CSF
Green Fluorescent Protein	GFP
Growth factor receptor-bound protein 2	Grb2
GTPase-activating protein	GAP
Guanosine 5'-(trihydrogen diphosphate)	GDP
Guanosine 5’-tri-phosphate	GTP
Guanine nucleotide exchange factor	GEF
Gut-associated lymphoid tissue	GALT
High endothelial venule	HEV
Human Coxsackie/Adenovirus Receptor	hCAR
IL-2 tyrosine kinase	Itk
Inducible T cell co-stimulator	ICOS
Immunoglobulin	Ig

Immuno-Histo-Chemistry	IHC
Immunoreceptor tyrosine-based activation motif	ITAM
Inflammatory bowel disease	IBD
Inositol 1, 4, 5-triphosphate	IP_3
Intercellular adhesion molecule	ICAM
Interferon	IFN
Interfollicular regions	IFR
Interleukin	IL
Intra-epithelial cells	IEC
Intra-peritoneal	i.p.
Intravenous	i.v.
kilo Daltons	kD
Lamina propria	LP
Laser Scanning Cytometry	LSC
Linker of Activated T cells	LAT
Lipopolysaccharide	LPS
Lymphocyte function-associated antigen	LFA
Major Histocompatibility Complex	MHC
Mammalian target of rapamycin complex 2	mTORC2
Mean Fluorescence Intensity	MFI
Medullary epithelial cells	mTECs
Mesenteric lymph node(S)	MLN
Messenger ribonucleic acid	mRNA
Mitochondrial membrane potential	MMP
Mitogen-activated protein kinase	MAPK
Mitogen-activated protein kinase kinase	MEK
Mitogen-activated protein kinase kinase kinase	MEKK
Mitosis	M
Monoclonal Ab	mAb
Mothers against decapentaplegic homology	mad
Multiplicity of Infection	MOI
Natural killer T cell	NK
Nuclear Factor-kappa B	NF-κB
Nuclear factor of activated T cells	NF-AT
Optical density	OD

Ovalbumin	OVA
Ovalbumin in Complete Freunds Adjuvant	OVA/CFA
p44/42 MAPKinase	ERK
$p56^{lck}$	Lck
$p59^{fyn}$	Fyn
Phosphorylated	p
Peripheral lymph node(s)	PLN
Peripheral-supramolecular activation cluster	p-SMAC
Peyer's Patch(es)	PP
Phosphatase and Tensin homolog deleted on chromosome 10	PTEN
Phosphate Buffered Saline	PBS
Phosphatidylinositol (3,4,5)-triphosphate	$PI(3,4,5)P_3$
Phospho-p44/42 MAP Kinase	pERK
Phosphoinositide 3 kinase	PI3K
Phospholipase C-γ1	PLC-γ1
Phycoerythrin	PE
Pleckstrin Homology	PH
Programmed death-1	PD-1
Propidium Iodide	PI
Protein kinase C	PKC
Protein tyrosine kinases	PTK
Reactive oxygen species	ROS
Receptor(s)	R
Recombinase activator gene	Rag
Red Fluorescent Protein	RFP
Regulator for cell adhesion and polarisation type 1	Rap1
Retinoblastoma protein	Rb
Ribonucleic acid	RNA
Severe combined immunodeficiency	Scid
SH2-domain-containing leukocyte-specific phosphoprotein of 76 kDa	SLP-76
Side scatter	SSC
Son of Sevenless	SOS
Stress activated protein kinases	SAPK
Subcutaneous	s.c.
Superantigen	SAg

Supramolecular activation cluster	SMAC
T cell Receptor	TcR
T helper cell type 1	T_H1
T helper cell type 2	T_H2
T helper cell type 3	T_H3
T helper cell type 17	T_H17
Ternary Complex Factor	TCF
Tissue-specific antigen(s)	TSA
T regulatory cell	T_{reg}
T regulatory 1 cell	Tr1
Toll-like receptor	TLR
Transforming growth factor	TGF
Transgenic	Tg
Transitional 2-marginal zone precursor	T2-MZP
Tumour necrosis factor	TNF
Zeta-chain-associated protein kinase 70 kDa	ZAP-70

gram	g
milligram	mg
microgram	µg
nanogram	ng
molar	M
millimolar	mM
micromolar	µM
millilitres	ml
revolutions per minute	rpm
times gravity	*g*

Summary

The ability of the immune system to discriminate between pathogenic and self or food antigens is essential not only for the generation of a productive immune response against invasive pathogens, but also for a state of antigen-specific tolerance to be elicited against harmless antigens. A breakdown in such tolerance can result in the development of a variety of autoimmune diseases including rheumatoid arthritis, Type 1 diabetes, inflammatory bowel disease and coeliac disease. Despite a wealth of studies in this field, however, the mechanisms by which the immune system can distinguish harmless and pathogenic antigens remain to be fully elucidated. If these mechanisms were better understood, such information could be exploited to help develop better therapies for autoimmune diseases, improve the rate of successful transplantations and increase the efficacy of vaccines.

The primary means of maintaining tolerance to self antigens is to prevent self-reactive T cells from exiting the thymus following their development therein (central tolerance). However, some self-reactive T cells escape thymic deletion and as such, central tolerance is incomplete. Indeed, peripheral tolerance is required for an individual to elicit tolerance to all self-antigens, developmental antigens and some food and environmental antigens which are not present in early life. Peripheral tolerance is defined as a state of antigen-specific hyporesponsiveness, which is induced by exposure of T cells to antigen under sub-optimal activating conditions. For a T cell to become fully activated, and therefore productively primed, it must recognise its cognate antigen in the context of MHC and receive co-stimulation via the interaction of its CD28 receptor with CD80/86 on an antigen-presenting cell (APC). Clonal anergy, one of the proposed mechanisms of peripheral tolerance, describes a state of long lasting unresponsiveness to antigen in the T cell. Such anergy is induced when the TcR is ligated in the absence of co-stimulation and can be evidenced, upon re-stimulation with antigen, by reduced IL-2 production, cell cycle progression and proliferation, relative to that observed in primed cells.

It has been widely proposed that both qualitative and quantitative differences in T cell signalling may underlie the differential functional outcomes of priming and tolerance. However, the majority of these studies have relied upon biochemical assessment of signalling in T cell lines or clones, at the population level following polyclonal stimulation *in vitro*, and thus has led to the generation of conflicting data. Moreover, and most importantly, these data do not necessarily reflect the responses of individual antigen-specific T cells within their environmental niche within primary or

secondary lymphoid tissue. In addition, as such data represents the responses of all cell types in the sample population at any one time, they do not provide any information pertaining to the differential kinetics, amplitude or subcellular localisation of signals generated by functionally distinct subgroups within the population.

A relatively new technology, laser scanning cytometry (LSC), offers an attractive means of investigating such responses, as it essentially marries the quantitative capabilities of flow cytometric analysis of cells in suspension with the ability to analyse spatially the fluorescence of large numbers of individual cells, either in suspension or in tissue in a slide-based format. Moreover, the adoptive transfer system, in which limited numbers of TcR transgenic (Tg) T cells are distributed evenly throughout the thymus-dependent area of the lymph node, provides an attractive means of studying antigen-specific responses occurring at near physiological frequencies *in situ*. Such antigen-specific T cells can be readily distinguished from endogenous T cells by LSC, following fluorescent staining of their TcR, as they are sparsely situated amongst the endogenous T cell population within the lymph node. Use of the adoptive transfer system, in combination with LSC analysis, has therefore enabled the development, in this thesis, of a quantitative imaging technology with which to study T cell signalling in individual antigen-specific T cells *in vitro* and *in situ*.

In T cells, the maintenance phase of anergy has been reported to reflect defective activation of transcription factors, such as c-Jun/c-Fos, that are involved in formation of the AP-1 complex, which is required for inducing transcription of the IL-2 gene and optimal activation and effector function of T cells. In turn, this appears to be determined by the lack of recruitment of the ERK, JNK and p38 MAPK signalling cascades. The small GTPase, Rap1, has long been implicated in such desensitisation of ERK, and the consequent reduced IL-2 production, observed in tolerised T cells. However, as noted above, the majority of these findings were obtained from *in vitro* studies of T cell lines or clones and as such are not necessarily representative of physiological responses of primary antigen-specific T cells *in situ*.

This study therefore describes, for the first time, an inverse relationship between ERK activation (pERK) and Rap1 expression in individual primary antigen-specific T cells during the maintenance phases of tolerance and priming, both *in vitro* and *in vivo.* Analysis at the single cell level further revealed that the proportion of antigen-stimulated cells expressing pERK was lower in the anergic relative to primed groups *in vitro* and *in vivo,* and the few anergised T cells expressing pERK did so at a lower level than the primed cells *in vitro*. By contrast, Rap1 was found to be expressed in a greater

proportion of anergic antigen-specific T cells, and at considerably higher levels, compared with primed T cells following re-stimulation with antigen both *in vitro* and *in vivo*. An additional inverse relationship was observed between pERK and Rap1, concerning their subcellular localisation, with pERK appearing to co-localise with lipid raft structures in primed but not anergic cells and Rap1 appearing to be targeted to lipid rafts in anergic but not primed cells. These data suggests that Rap1 may be up-regulated and recruited to the immunological synapse upon re-stimulation with Ag in anergic T cells and that such Rap1 localisation and expression may contribute to the downregulation of ERK recruitment and activation in these cells. It is important to note that this inverse relationship between the accumulation of Rap1 and antagonism of ERK activation was only observed during the maintenance, and not induction, phases of both systemic and oral tolerance *in vivo*.

Furthermore, assessment of the activation status of downstream cell cycle modulators in priming and tolerance, revealed that downregulation of ERK activation and upregulation of $p27^{kip1}$ might not be sufficient for maintenance of the anergic state, as indicated by G_1 arrest, and hence, one or more additional negative signals may be required. Indeed, this study suggests that perhaps such a negative signal could be provided by the downregulation of p-Rb and/or increased expression of inactive cyclin dependent kinases (CDKs).

In summary, defective ERK signalling correlates with the up-regulation of Rap1 expression in tolerised relative to primed antigen-specific $CD4^+$ T cells during the maintenance phases of tolerance *in vitro* and *in vivo*. As this association occurs after the induction of both systemic and oral routes of tolerance, these data suggest that Rap1 antagonism of pERK signalling may play an important and general role in the maintenance of antigen-specific $CD4^+$ T cell tolerance. Moreover, as oral tolerance induction has been proposed as a potential therapy for autoimmune disorders and, oral administration of compounds offers a more attractive route for drug delivery in humans, these findings may have potential clinical applications. By advancing our knowledge of these key signals in regulating tolerance and priming at the single cell level *in vitro* and *in vivo*, we will therefore increase our understanding of an important physiological process at the molecular level, ultimately leading to identification of potential targets for enhancing or inhibiting immunity and tolerance.

Chapter 1

General Introduction

1. Introduction

1.1 Overview of the immune system

The immune system is a complex defence system in vertebrates which offers protection to the host from a variety of pathogenic microorganisms, including bacteria and viruses. The immune system comprises a multi-faceted array of cells and molecules capable of recognising (specifically and non-specifically), and eliminating an immense range of pathogens. There are two distinct, but intertwined, arms of the immune response, namely the innate and adaptive immune responses. Innate immunity is non-specific and represents the first line of defence against any invading pathogen. By contrast, adaptive immunity is specific and develops as the innate response occurs. Moreover, whilst the innate immune response does not differ upon repeated exposure to the same pathogen, adaptive immunity allows a memory response to develop so that subsequent encounters with the same antigen are treated with increased alacrity and efficacy by the host.

1.1.1 Innate immunity

Innate immunity comprises four types of defensive barriers: anatomical, physiological, endocytic/phagocytic and inflammatory. Anatomical defences include the skin, which acts as a physical barrier to pathogen entry and has an acidic pH (3-5), which diminishes growth of microorganisms on the body's surface. Similar functions are fulfilled by the mucous membranes which line the conjunctivae and alimentary, respiratory and urogenital tracts. The majority of pathogens invade the body by penetrating the mucous membranes but there are a number of further obstacles to this incursion. For example, mucus, secreted by the epithelial cells which line the mucous membranes, ensnares foreign microorganisms and epithelial cells in the lower respiratory and gastrointestinal tracts possess hair-like projections, called cilia, which beat synchronously to propel the entrapped microorganisms out of these tracts. Also, non-pathogenic bacteria preferentially colonise the epithelial cells on mucosal surfaces and out-compete pathogenic microorganisms for nutrients and space.

Physiological barriers include temperature, pH and chemical mediators. Thus, even normal body temperature or that associated with a fever is often sufficient to inhibit growth of some pathogens. Similarly, the stomach has an acidic pH that kills the majority of ingested microorganisms. Chemical mediators comprise a wide range of soluble proteins

including: (i) lysozyme, which can disrupt the integrity of the bacterial cell wall by cleaving the peptidoglycan layer; (ii) interferons, which are secreted by virally infected cells and are capable of protecting neighbouring cells from viral infection and (iii) complement, which contributes to clearance of pathogens by lysing their membranes or facilitating their phagocytosis.

A variety of cell types can internalise and degrade extracellular macromolecules and whole organisms, by endocytosis and/or phagocytosis. Macromolecules can be endocytosed in one of two ways, namely pinocytosis whereby material is non-specifically internalised in relation to its extracellular concentration or receptor-mediated endocytosis, in which specific molecules are internalised after they have bound to their specific receptor on the cell surface. Both types of endocytosis result in the formation of endosomes which then fuse with lysosomes to form secondary lysosomes wherein the biological material is degraded by a variety of digestive enzymes and the products are secreted from the cell. Phagocytosis can be only carried out by specialised innate cell types, including neutrophils, monocytes and macrophages, collectively termed phagocytes. Phagocytosis enables the internalisation and degradation of much larger material e.g. microorganisms, in much the same way as endocytosis occurs.

Inflammatory barriers arise when tissue damage and infection result in phagocytes and serum proteins, including acute phase proteins, leaking from the vasculature into the affected area. An increase in the concentration of acute phase proteins facilitates lysis or phagocytosis of the pathogen, both of which are mediated by complement. However, the innate immune response is dependent upon pathogens expressing common surface molecules that can be recognised by phagocytes and as such, many pathogens have evolved to avoid detection by the innate immune system. Adaptive immunity evolved in turn to equip the body with an enhanced detection system and a more comprehensive and specific range of defences.

1.1.2 Adaptive Immunity

In addition to its specificity and ability to elicit a memory response, the normal, functional adaptive immune response can also be hugely diverse. It can recognise a vast range of different antigens (Ag), as well as being able to distinguish self from non-self antigens thus, preventing autoimmune disorders from developing. There are two major cell types involved in the generation of adaptive immunity, namely lymphocytes and antigen-

presenting cells (APC). Lymphocytes constitute 20-40 % of the white blood cell population and they continually circulate around the body via the vasculature and lymphoid system, and have the ability to migrate into lymphoid organs and tissues. B and T cells are the two major subtypes of lymphocytes.

Upon ligation of the B cell antigen receptor (BcR) by its specific antigen, mature B cells proliferate and differentiate into populations of antibody-secreting plasma cells or memory B cells. Affinity maturation and isotype class switching occur in the germinal centres during this process. Antibodies (Abs) are immunoglobulin proteins which consist of re-arranged heavy (H) and light (L) chains which contain variable (V) regions that bind to specific antigens and facilitate their clearance by neutralisation, opsonisation or complement activation. As B cells constitutively express major histocompatibility complex (MHC) class II molecules and are efficient at acquiring cognate Ag, they can also act as APC for T cells. However, they are not the most efficient APC as they must be activated to induce expression of additional molecules such as the B7 molecules CD80, CD86 and CD40 that, via bidirectional signalling, promote T cell activation.

Evidence for B cells having a regulatory function (B_{regs}) also exists. Such B_{regs} can hamper the development of and/or promote recovery from inflammation via the production of IL-10 and TGFβ-1, and contact-dependent or -independent (through secreted Abs) interactions with other immune cells (Figure 1.1). The phenotype of such IL-10-secreting B cells has been proposed as $CD11b^{-}$ $CD5^{-}$ IgD^{+} (1, 2) and moreover, the suppressive function of these cells has been attributed to a $CD21^{hi}$ $CD23^{hi}$ IgM^{hi} B cell subtype (3), previously known as transitional 2-marginal zone precursor (T2-MZP) B cells. B cells have been shown to produce the regulatory cytokine IL-10 under a variety of inflammatory conditions *in vitro* and *in vivo*. Such IL-10 can act to dampen the inflammatory response by regulating the T_H1/T_H2 balance and downregulating innate cell-mediated inflammatory responses (4-7). IL-10 producing B cells were first described as being capable of modulating acute experimental autoimmune encephalomyelitis (EAE; (8)) and more recently, another subset of B_{regs} has been identified which can produce TGF-β1 (9-11) and may play a role in the induction of low dose oral tolerance (9, 10).

1.1.2.1 T cells

T cells are involved in a plethora of immunological activities and are essential to combat pathogens that evade detection by antibodies, and supply B cell help which subsequently leads to cognate Ab production.

1.1.2.2 T cell activation

A T cell requires two signals to become fully activated, with signal 1 being the recognition of peptide in the context of MHC and signal 2 being co-stimulation provided via the interaction of CD28 on the T cell with CD80/86 on the APC (Figure 1.2a). When a T cell receives both signal 1 and 2 it proliferates, differentiates and has effector function. In contrast, when a T cell receives only signal 1 i.e. lacks co-stimulation, it can undergo apoptosis or become anergic (Figure 1.2b). The induction of anergy is an active process and ligation of the TcR (signal 1) does result in activation (up-regulation of CD69 (12)) and proliferation of the T cell (13). The recent identification of novel co-stimulatory molecules has indicated that multiple signals may be required to elicit optimal co-stimulation of T cells (14). One such molecule is the inducible T cell co-stimulator (ICOS; also known as CD278 (15)). ICOS is another member of the CD28 family of co-stimulatory molecules which is not expressed on resting cells, but is induced on all activated T cells within 24-48 h of T cell activation (16). When expressed, it can bind to its ligand, B7-related protein-1 (B7RP-1), which is found on a number of cells including DC and B cells (15). ICOS is believed to be important in the co-stimulation of effector T_H2 cell responses, as it induces expression of IL-4 and IL-10, but not IL-2 (17). However, ICOS:B7RP-1 interactions have also been shown to be important for the clonal expansion, and capacity to provide B cell help, of naive, T_H1 and T_H2 cells (18).

1.1.2.3 T cell subtypes

T cells can be split into two main types: $CD8^+$ and $CD4^+$ T cells. $CD8^+$ T cells, known as cytotoxic T cells (T_C), exhibit MHC class I restriction and upon recognising their specific antigen in association with MHC class I in the presence of appropriate cytokines (e.g. IL-2 secreted by $CD4^+$ T cells), such T_C proliferate and differentiate into effector cells known as cytotoxic T lymphocytes (CTL). CTL are responsible for eliminating tumour cells, grafted cells or virally infected cells from the body. $CD4^+$ T cells are MHC class II

restricted and are known as T helper (T_H) cells as they act to stimulate other cells of the immune system to participate in the immune response.

1.1.2.4 $CD4^+$ T cell differentiation

$CD4^+$ T_H cells are activated upon recognition of their specific antigen complexed with MHC class II on an APC, in the presence of co-stimulation, and this activation causes the T_H cell to proliferate, thus generating a clone of effector T_H cells. Depending on the cytokine milieu in which an antigenic stimulus is received, either T_H1 or T_H2 effector cells are generated, each with different capabilities (Figure 1.3). T_H1 cells are known to express the transcription factor T-bet (19) and can produce IL-2, IFNγ and TNF-α. IFNγ upregulates IL-12 production by DC and macrophages and this IL-12, in turn, causes an increase in IFNγ production in T_H cells and so promotes T_H1 cell differentiation in a positive feedback loop. Moreover, IFNγ downregulates IL-4 production thus, further promoting a T_H1 phenotype. For example, IFNγ can post-transcriptionally downregulate IL-4-induced IL-4 receptor (IL-4R) gene expression (20). T_H1 cells contribute to the cellular (T_H1) immune response by improving the killing efficacy of macrophages and also stimulating proliferation of CTL. For example, IFNγ, produced by T_H1 cells, rapidly primes macrophages via the JAK1/2-STAT1 pathway (21). This pathway promotes intracellular killing of phagocytosed bacteria, rather than inducing the macrophage to process and present the antigen on its surface. T_H1 cells do, however, promote the production of IgG2a antibodies (in the mouse).

T_H2 cells express the transcription factor GATA-3 (22) and can produce IL-4, IL-5, IL-6, IL-10 and IL-13 and skew adaptive immunity towards a humoral (T_H2) immune response, by stimulating B cells to proliferate, isotype switch and secrete IgG1 antibodies (in the mouse). IL-4 stimulates T_H cells to differentiate into T_H2 cells and IL-10 inhibits IL-2 and IFNγ production, as well as IL-12 production by DC and macrophages, thus directing a T_H2 profile.

Another lineage of effector $CD4^+$ T cells, namely T_H17 cells, has recently been described which is characterised by its expression of the orphan nuclear receptor RORγT (23), as well as its cytokine production profile IL-17 (also known as IL-17A), IL-17F and IL-6. Moreover, the pathways which lead to the differentiation of T_H17 cells are distinct from those which promote development of T_H1 or T_H2 lineages (reviewed in (24, 25)).

However, T cell-produced TGF-β is required for the generation of both T_H1 and T_H17 lineages (26).

The existence of another subset of $CD4^+$ T cells, $CD4^+$ $CD25^+$ $Foxp3^+$ regulatory T cells (T_{reg}) has been validated in recent years. T_{reg} (previously known as suppressor T cells) have been shown to suppress pathological immune responses to self antigens in autoimmune disorders or foreign antigens in transplantation and graft versus host disease (27). A fuller description of the different T_{reg} classes including details of their specificity, phenotype and mechanism of suppression, is provided in Section 1.2.2.3 and Table 1.1. Briefly, T_{reg} exert their effects by downregulating the proliferation of other T cell populations both *in vitro* and *in vivo*. It is believed that, in addition to these naturally occurring T_{reg} generated in the thymus, so called adaptive or induced T_{reg} (T_{reg}, also known as T_H3 or Tr1 cells) exist in the periphery. These are T_{reg} which develop during an immune response *in vivo* (28) where $CD4^+$ $CD25^-$ T_H cells have been shown to upregulate expression of Foxp3 and differentiate into T_{reg} upon ligation of the T cell receptor (TcR) with low levels of antigen or antigen presented in an inappropriate cytokine environment (29).

1.2 The need for tolerance

The immune system in a normal healthy individual is capable of distinguishing self from non-self antigens. When a new antigen is encountered, it is this discriminatory capacity which allows the generation of a productive immune response against invasive pathogens or for a state of antigen-specific tolerance to be elicited. Such antigen-specific tolerance prevents harmful immune responses against self components (30) or non-dangerous food or environmental antigens. A breakdown in tolerance within an individual can result in the development of a variety of autoimmune disorders.

1.2.1 Central Tolerance

The primary means of maintaining tolerance to self antigens is to prevent self-reactive T cells from exiting the thymus following their development therein. Lymphoid progenitor cells are produced in the bone marrow or fetal liver before migrating to the thymus whereupon they start out as double negative (DN) thymocytes (31, 32), as they lack expression of CD4 and CD8. Subsequently, DN thymocytes which possess a functional TcR-β chain are selected to differentiate into double positive (DP) $CD4^+$ $CD8^+$ cells (33,

34). This process is termed β-selection. Such DP thymocytes then undergo positive and negative selection, processes which promote the differentiation of single positive (SP) $CD4^+$ or $CD8^+$ αβ-T cells, that are MHC-restricted and self-tolerant (35).

When the TcR of a developing thymocyte is strongly ligated by peptide:MHC, expressed on an APC (stromal or bone marrow-derived cells) in the thymus, it is programmed to die by apoptosis. Such a response constitutes the foundation of negative selection (also termed clonal deletion) in which encounter of thymocytes with self Ag:self MHC complexes, at affinities or avidities that are high, in the thymus results in deletion of self-reactive, and therefore potentially harmful, immature T cells from the T cell repertoire. Although it is easy to envision T cells encountering ubiquitous antigens in the thymus it has, until recently, been difficult to reconcile how thymic T cells 'see' tissue-specific antigens (TSA) (36) such as pancreatic insulin, which would be unlikely to be expressed in the thymus. It is proposed that aberrant (also known as "promiscuous") expression of peripheral Ag in the thymus enables thymic T cells to experience TSA (37, 38). Such thymic TSA expression is predominantly limited to medullary epithelial cells (mTECs) (36). The autoimmune regulator protein (AIRE) was first identified as the gene underlying autoimmune polyendocrinopathy-candidiasis-ectodermal dystrophy (APECED; also known as APS1) (39, 40). AIRE is highly expressed on human and mouse mTECs and is thought to play an important role in central tolerance as mice deficient in AIRE, or those lacking it specifically in the thymus, develop organ-specific autoimmune diseases presumably because they have not been rendered self-tolerant to such TSA (41). Other studies have demonstrated a role for AIRE in promoting self-Ag expression on mTECs and hence its relevance in negative selection in the thymus (42, 43). Indeed, mTECs which lack AIRE have been shown to also lack expression of a subset of TSA (37, 41). It is believed that thymic DC acquire TSA from the mTECs, process and cross present it to both $CD4^+$ and $CD8^+$ thymic T cells to ensure rigorous development of a self-tolerant repertoire of T cells (44, 45). However, some self-reactive T cells escape thymic deletion and as such central tolerance is incomplete.

1.2.2 Peripheral Tolerance

Peripheral tolerance is therefore required to ensure that tolerance is elicited to all self-antigens, developmental antigens and some food and environmental antigens which are

not present in early life. Peripheral tolerance reflects a state of antigen-specific hyporesponsiveness induced by exposure of T cells to antigen under sub-optimal activating conditions (46). There a number of proposed mechanisms of peripheral tolerance:

1.2.2.1 Ignorance of antigen

T cells can remain ignorant of their specific antigen if the antigen is not presented to the T cell. For example, antigens can be sequestered in immune-privileged sites such as the eye and so cannot be seen by circulating T cells (47).

1.2.2.2 Clonal anergy

One of the potential mechanisms of peripheral tolerance is the unresponsiveness of T cells to secondary antigenic stimulation, as a result of induction of anergy. It is well established that ligation of the TcR, upon recognition of its specific peptide in the context of MHC, in the absence of co-stimulation induces long lasting unresponsiveness (anergy) in T cells (48, 49). Several methods have been used to induce such anergy *in vitro* (50-52), including exposure to immobilised anti-CD3 in the absence of co-stimulatory signals (51, 53). Under such conditions, relative to priming conditions (TcR ligation + co-stimulation), re-stimulation with antigen leads to hugely downregulated IL-2 production and hence decreased proliferation of the T cells. This state of anergy can be reversed by the addition of exogenous IL-2 to the T cells (54).

A role for anergy in oral tolerance (a form of peripheral tolerance which is fully described in Section 1.2.3), after feeding a high dose of antigen, has also been suggested. Ovalbumin (OVA)-specific T cells have been shown to be anergic following a single feed of 20 mg OVA (55). Similarly, other studies have demonstrated that feeding a high dose of myelin basic protein (MBP) induces downregulation of IL-2 and IFNγ production and proliferation in antigen-specific T cells in response to *in vitro* re-stimulation (56, 57).

Anergy itself is an active process and during the induction of anergy, *in vitro* or after feeding *in vivo*, anergic T cells clonally expand and upregulate the activation marker CD69 (12, 58-60). However, during the maintenance phase of anergy, these T cells are unresponsive to re-stimulation with antigen *in vitro* (12, 60). As mentioned above, anergy may result from a lack of co-stimulation (CD28:CD80/86 interaction). Although resting DC and macrophages constitutively express low levels of CD86 (61-63), many studies have indicated that this default level of CD86 expression does not induce priming but rather

appears to be required for the induction of T cell tolerance and that CD80/86:CTLA-4 (cytotoxic T lymphocyte-associated antigen-4; described fully in Section 1.2.2.4) interactions may be indeed necessary for maintaining T cell tolerance (64-68). Unfortunately, as yet, there is no known specific marker for anergic T cells and definition of this unknown phenotype remains the elusive holy grail in the field of anergy.

1.2.2.3 Active suppression

1.2.2.3.1 $CD8^+$ "suppressor" T cells

Another probable mechanism of peripheral tolerance is active suppression of the immune system. Early studies indicated the involvement of $CD8^+$ "suppressor" T cells ($CD8^+$ T_{reg}) in active suppression and although the mechanisms by which those $CD8^+$ T cells exerted such effects were not fully elucidated, a role for TGF-β production by $CD8^+$ T cells was proposed (69, 70). Consistent with this, $CD8^{-/-}$ mice have been shown to exhibit deficient local supression of IgA responses in the gut after feeding Ag, indicating that $CD8^+$ T_{regs} may be important for the regulation of mucosal immune responses (71). However, systemic tolerance is unaffected in these mice, suggesting that $CD8^+$ T_{regs} exert their regulatory effects locally. Moreover, other studies in knockout mice or using neutralising Ab, have proposed a role for $CD4^+$, but not $CD8^+$ T cells in the regulation of oral tolerance (72-74).

1.2.2.3.2 $CD4^+$ T_{regs}

Indeed, active suppression is believed to be exerted by the T_{reg} population which acts to downregulate activation of $CD4^+$ T_H cells in response to antigenic stimulation (75). Several different subtypes including $CD4^+$ $CD25^+$ $Foxp3^+$ T cells, T_H3 and Tr1 cells, are thought to mediate suppression in a variety of ways (Table 1.1). It was first proposed that $CD4^+$ T cells might regulate oral tolerance via differentiation towards a T_H2 phenotype and such T_H2 cells were shown to suppress T_H1-dependent IL-2 and IFNγ production through secretion of IL-4 (76-79). However, studies in $IL4^{-/-}$ mice demonstrated that both high and low doses of Ag were able to induce oral tolerance in these mice (80, 81), suggesting that a subset of T_{regs} other than T_H2 cells may be involved in regulating oral tolerance.

Consistent with this proposal, another subset of $CD4^+$ T_{regs} has been described, which produce varying amounts of the T_H2 cytokines IL-4 and IL-10, but have been shown to be a population distinct from T_H2 cells (76). Such cells were denoted T_H3 cells (76) and Ag-specific $CD4^+$ T_H3 cells have been detected in the mesenteric lymph nodes (MLN) of DO11.10 Tg mice, after feeding multiple low doses of antigen (82, 83). In addition, it has been proposed that co-stimulation mediated by CD86, but not CD80, promotes the induction of a T_H3 phenotype (66).

$CD4^+$ T regulatory 1 (Tr1) cells were first identified, following multiple stimulations of naive T cells with Ag, in the presence of high concentrations of IL-10 *in vitro* (84). Such Tr1 cells can suppress T_H2 responses in an Ag-specific manner (84) and OVA-specific Tr1 cells have been shown to prevent inflammatory bowel disease (IBD) when they are adoptively transferred into recipient mice subsequently fed OVA (85). However, the role of Tr1 cells in oral tolerance has yet to be fully elucidated.

As stated above (Section 1.1.2.4), $CD4^+$ $CD25^+$ T_{regs} appear to be generated in the thymus (86) and certain studies have indicated that $CD4^+$ T cells bearing TcR with especially high affinity for self-Ag may be selected to become T_{regs} (87). CD25 is also upregulated on antigen-specific T cells in the periphery after feeding with tolerogenic doses of antigen (88, 89) and is thought to persist on a small subset of antigen-specific cells ($CD4^+$ $CD25^+$) which then have the capacity to suppress bystander populations of naïve T cells specific for an unrelated Ag (89, 90). Moreover, $CD4^+$ $CD25^+$ T_{regs} can suppress the cytokine production and proliferation of both $CD4^+$ and $CD8^+$ T cells *in vitro* (91, 92).

A further subset of $CD4^+$ T_{regs} has been identified according to their expression of CD45RB (93). For example, whilst transfer of $CD4^+$ $CD45RB^{hi}$ T cells into immunodeficient Scid or $Rag^{-/-}$ mice causes severe colitis (94, 95), co-transfer of $CD4^+$ $CD45RB^{low}$ T cells has been shown to inhibit this inflammation (93). This regulatory capacity of $CD4^+$ $CD45RB^{low}$ (now termed $CD45RB^+$) T cells is thought to be mediated by TGF-β (96) and/or IL-10 (97).

1.2.2.4 The role of inhibitory co-stimulatory molecules in tolerance

As described earlier, productive co-stimulation can be provided by CD28 on the T cell interacting with CD80/86 on the APC. CD28 belongs to the CD28 family of co-stimulators. CD28 family members exhibit high homology with one another and some members are known to exert inhibitory co-stimulatory effects (Figure 1.2) namely, CTLA-4

(also known as CD152) and programmed death-1 (PD-1; also known as CD279). CTLA-4, has high homology with CD28 and is expressed primarily by activated T cells. It can act as an additional receptor for CD80/86 and moreover, CTLA-4 binds to CD80/86 with more than 20-fold greater affinity than CD28 does. Ligation of CTLA-4 results in the inhibition of T cell activation and concomitant TcR signalling limits production of IL-2 and cell cycle progression (Figure 1.2c). This highlights the importance of CTLA-4 in limiting the proliferative response to T cells to their cognate antigen and hence, immune homeostasis. Indeed, deletion or blockage of CTLA-4 inhibits the induction of peripheral (67, 98) and oral (68, 88) tolerance, improves anti-tumour responses and aggravates autoimmune disorders (99, 100). Anti-CTLA-4 mAb treatment causes the promotion of cell cycle progression, expansion of antigen-specific T cells in the paracortex and follicle of draining lymph nodes and enhanced specific Ab production in the induction phase of oral tolerance (101). In addition, CTLA-4 mediated signalling also has an important regulatory role in T cell differentiation, as CTLA-4 blockade has been shown to promote differentiation of $CD4^+$ T cells into IL-4 producing T_H2 cells (102).

PD-1 is another inhibitory receptor inducibly expressed on T cells, B cells and activated monocytes (98, 103, 104). PD-1 binds to its ligands, PD-L1 (B7-H1; CD273) and PD-L2 (B7-H2; CD274). PD-L1 is constitutively expressed on T cells, B cells, DC, macrophages, mesenchymal stem cells (105) and bone marrow-derived mast cells (106) whereas, PD-L2 is inducibly expressed on DC, macrophages and bone marrow-derived mast cells (106). Co-ligation of the TcR or BcR with PD-1 results in the transduction of an inhibitory signal (Figure 1.2d). No signal is transduced when PD-1 is cross-linked alone. PD-1 and its ligands are thought to have importance in both central and peripheral tolerance and the role of PD-1 in regulating T cell tolerance and autoimmunity was first suggested by the autoimmune phenotype of PD-1-deficient (*Pdcd1*$^{-/-}$) mice (107, 108). Further evidence was provided more recently, by blockade of PD-1 and PD-L1, PD-L2 with antibodies, which demonstrated a critical role for PD-1, but not CTLA-4, in maintaining established peripheral $CD4^+$ T cell tolerance (109). Thus, whilst PD-1:PD-L1 interactions are important for sustained, long term tolerance (109), in addition, PD-L2 has been shown to have a role in oral tolerance, as PD-L2-deficient mice fed ovalbumin fail to induce tolerance in their $CD4^+$ or $CD8^+$ T cells (110).

1.2.3 Oral tolerance

Oral tolerance is the oldest and most established means of experimentally inducing peripheral tolerance. For example, it was first studied in 1911 by Wells and Osbourne who showed that systemic anaphylaxis in guinea pigs was prevented by prophylactic feeding of hen egg proteins (111). Oral tolerance models are attractive experimental systems as they have genuine physiological relevance, due to the fact that whilst a healthy individuals' intestinal immune system retains a state of unresponsiveness to food antigens throughout their lifetime, breakdown in such tolerance results in the development of diseases such as coeliac disease, where $CD4^+$ T cells respond to gliadin peptides in wheat and damage to the small intestine occurs (112), or Crohn's disease, wherein the commensal gut flora is attacked and inflammatory bowel disease (IBD) results (113).

Orally-administered antigen often stimulates a local IgA response but simultaneously induces tolerance of systemic humoral and cell-mediated immune responses (114-116). Oral tolerance is considered vital for maintaining the immunological integrity of the mucosa as it prevents inappropriate inflammatory responses. It must be noted that the ability of orally-administered antigen to induce tolerance is not absolute as co-administration of adjuvants such as cholera toxin (CT) induces productive, systemic immune responses as evidenced by antibody production and T cell responses (117-120). Although a plethora of work has been done in this field, the mechanisms which control oral tolerance have still to be fully elucidated.

1.2.3.1 Mucosal immunity

In order to investigate the mechanisms underlying oral tolerance it is essential to understand how the mucosal immune system recognises and responds to antigen. Studies have indicated that fed antigen stimulates T cells in the gut-associated lymphoid tissues (GALT) and that these activated T cells then circulate to the periphery (59, 121-123). The GALT is the name given to the lymphoid components associated with the gastrointestinal tract and contains all of the elements required to generate a productive mucosal immune response, including macrophages, DC, eosinophils, mast cells and lymphocytes. These cellular components are situated within either discrete organised or diffuse scattered lymphoid tissues. The Peyer's patches (PP) and mesenteric lymph nodes (MLN) comprise the organised tissues and the lamina propria (LP) and intraepithelial lymphocytes are examples of the scattered tissues (Figure 1.4).

1.2.3.2 Sites at which orally-acquired antigen is presented in the gut

There are several sites at which orally acquired antigen can be presented, namely the LP, PP and MLN. The induction of oral tolerance in mice lacking PP is normal (124, 125) and so the PP is thought to be superfluous for this type of tolerance induction. However, MLN were required for tolerance induction in these mice (124, 125) and the importance of MLN for the induction of oral tolerance was further demonstrated in B cell-deficient μMT mice, which lack PP and M cells (specialised epithelial cells) (126), as these mice can be tolerised as efficiently as wild-type mice (127). The MLN are believed to be the site at which the mucosal and peripheral immune systems are interlinked, as they are the draining lymph nodes for the PP and LP. Indeed, APC loaded with orally acquired antigen continually migrate from the intestine to the MLN, where they may be important for tolerance induction (128, 129).

1.2.3.3 Antigen uptake and presentation in the gut

Productive mucosal immune responses to orally acquired antigen are thought to be generated primarily in the PP. After ingestion, antigens or whole microorganisms are transported through M cells to immature DC in the sub-epithelial dome (SED) of the PP (130, 131). As these immature DC differentiate and express co-stimulatory molecules and antigen:MHC class II complexes, they migrate to the interfollicular regions (IFR). In the IFR, incoming mature DC present antigen to naïve $CD4^+$ T cells (132) or are believed to be capable of transferring their bound Ag to resident DC by a process known as cross-presentation (133-135). Such cross-presentation of Ag may perhaps provide a mechanism whereby Ag in the periphery can be presented in lymph nodes thus, inducing "cross-priming" towards transplanted tissues or "cross-tolerance" towards self-tissues. It has been suggested that the promotion of cross-priming versus cross-tolerance may reflect the maturation status of the incoming DC, with very mature (e.g. $CD86^{hi}$) DC inducing priming and immature DC inducing tolerance (133).

1.2.3.4 APC-mediated presentation of Ag to T cells in tolerance

Many different cell types have the ability to present antigen to T cells. Intra-epithelial cells (IEC) express MHC class II and can present antigen to $CD4^+$ T cells *in vitro* (136-141) but, these cells lack co-stimulatory molecules (CD80/86) and so cannot productively prime T cells. As such, IEC could be important for the induction of tolerance

as they may be capable of presenting Ag to T cells in the absence of co-stimulation, a process known to induce a state of antigenic unresponsiveness in the T cell (48, 49). However, this is thought to be unlikely as the LP contains predominantly effector/memory T cells (142, 143), which are less susceptible to tolerance induction than naïve T cells (144). Similarly, some controversy surrounds a role for B cells as APC in the induction of tolerance. Whilst decreased tolerance induction was observed in μMT mice (which lack B cells) (9), many other studies have shown that B cells are not essential for oral tolerance. For example, depletion of B cells by treating mice from birth with anti-IgM antibodies does not alter the induction of tolerance of either T_H1 or T_H2 cells by feeding high or low doses of antigen (145, 146).

DC are thought to be the major APC involved in presenting orally acquired antigen to T cells (147). In addition, DC expansion, induced by treatment with the cytokine fms-like tyrosine kinase ligand (flt3L), contributes to both priming and tolerance in response to orally-administered Ag (148, 149). In these studies, tolerance arose when soluble Ag was fed alone (148) and priming was induced when Ag was administered together with an adjuvant, such as CT (149). PP DC are known to produce IL-10 and can direct naïve T cells towards a T_H2 (150) or T_H3 (151) profile, two cell types known to have roles in the regulation of tolerance (152). In addition, LP DC are also capable of acquiring and presenting antigen (153-156) and have been reported to directly acquire antigen from the gut lumen by opening tight junctions in the epithelial layer and projecting dendrites through which to sample gut bacteria (157). DC express both MHC class II and co-stimulatory molecules (CD80/86) on their surface and so can acquire antigen and productively prime $CD4^+$ T cells. Immature DC acquire protein antigen via surface receptors e.g. Toll-like receptors (TLRs), internalise and degrade it, before presenting peptide components of the protein antigen bound to MHC class II on their surface and transporting the antigen to the draining lymph nodes where it can be presented to $CD4^+$ T cells.

1.3 T cell signalling

1.3.1 TcR-mediated signalling

1.3.1.1 Signalling proximal to the TcR

The signalling cascades initiated upon TcR ligation (Figure 1.5) govern all aspects of T cell fate and effector function. Within seconds of TcR ligation, $p56^{Lck}$ and $p59^{Fyn}$ Src family protein tyrosine kinases (PTK) are recruited to and phosphorylate immunoreceptor tyrosine-based activation motifs (ITAMs) in CD3 and TcRζ-chains (158, 159), thus enabling the recruitment of the Syk family PTK, ZAP-70, via binding of its SH2 domains to the phosphorylated ζ-chains (160). ZAP-70 can then be activated via phosphorylation by $p56^{Lck}$/$p59^{Fyn}$ and activated ZAP-70 fuels further signal transduction by recruiting and phosphorylating downstream adaptor molecules, namely SH2-domain-containing leukocyte-specific phosphoprotein of 76 kDa (SLP-76) and linker of activated T cells (LAT) and downstream kinases. Phosphorylated SLP-76 associates with the guanine nucleotide exchange factor (GEF), Vav, via its SH2 domain and also binds the Tec family PTK, IL-2 tyrosine kinase (Itk).

1.3.1.2 Role of adaptor proteins in T cell signalling

Adaptor proteins function to link antigen-receptor ligation to cellular signalling. One such adaptor protein is LAT and phosphorylated LAT binds phospholipase C-γ1 (PLC-γ1), growth factor receptor-bound protein 2 (Grb2) and the Grb2 family member, GADS. Binding to PLC-γ1 and GADS is essential for T cell activation and differentiation (161). Grb2 forms a complex with Son of Sevenless (SOS) and this complex mediates Ras activation as SOS is a GEF capable of converting Ras-GDP (inactive form) to Ras-GTP (162). In addition, GADS functions as an adaptor which binds LAT and SLP-76 following TcR ligation (163).

1.3.1.3 The PLC-γ1 pathway

Activation of PLC-**γ**1, mediated in part by LAT, results in phosphatidylinositol 4, 5-biphosphate (PIP_2) being cleaved to form inositol 1, 4, 5-triphosphate (IP_3), which increases cytosolic-free calcium, and diacylglycerol (DAG), which supports protein kinase C (PKC)

activation by binding to the cysteine-rich region (C1) of PKC, thus causing a conformational change which reduces the autoinhibition of its kinase activity (164-166). Mobilisation of Ca^{2+} leads to activation of the calcium-dependent phosphatase, calcineurin, which then de-phosphorylates nuclear factor of activated T cells (NF-AT) on specific amino acid residues revealing its nuclear localisation sequence and thus NF-AT translocates into the nucleus, where it acts in combination with activator protein 1 (AP-1) to transcribe the IL-2 gene under conditions of priming (167). AP-1 itself is a complex of c-Fos and c-Jun transcription factors. Activation of AP-1 alone is not sufficient for transcription of the IL-2 gene, as for this to occur, co-stimulation is required which initiates further signalling cascades necessary for IL-2 production (Figure 1.6).

1.3.1.4 PKC-mediated signalling in T cells

The PKC family of serine/threonine kinases act as DAG binding proteins in lymphocyte activation that can stimulate accumulation of GTP-bound (activated) Ras, independent of SOS (168). DAG can also bind the GEF Ras guanyl-releasing protein 1 (RasGRP1) through its DAG-binding domain (169). RasGRP1 also contains Ca^{2+}-binding EF hands, and following increases in the levels of intracellular Ca^{2+} and DAG, RasGRP1 is recruited to the Golgi membrane (169, 170) whereupon it converts Ras-GDP to the GTP-bound form of Ras and consequently leads to activation of downstream mitogen-activated protein (MAP) kinases such as ERK (171, 172).

1.3.1.5 MAPKinase pathways

The MAPKinases are a family of serine threonine protein kinases which are activated by a variety of extracellular stimuli and are capable of mediating an array of cellular functions, ranging from activation and proliferation to growth arrest and cell death (173). There are three different types of MAPK: the classical extracellular signal-regulated kinases (ERKs), the p38 MAPK and the c-Jun N-terminal kinases (JNK), also known as stress activated protein kinases (SAPK) (174, 175). Activation of each group is determined by different upstream MAPK kinases (MEKs) and MAPK kinase kinases (MEKKs). MAPK are activated by dual phosphorylation on tyrosine and threonine residues, located in a T-X-Y motif (176), where X is different in each group of MAPK. MAPK activation results in phosphorylation and activation of distinct downstream transcription factors, depending on the group of MAPK activated. Thus, ERK activates Elk-1 and c-Myc (177,

178), p38 activates c-Fos (179) and ATF-2 (180), and JNK activates c-Jun and ATF-2 (181). The phosphorylation and activation of these transcription factors allows the MAPK family to regulate gene expression and hence, cellular fate and effector function.

In T cells, upon TcR ligation, the TcR is linked to the Ras-ERK MAPK pathway. Ras is a membrane-bound guanine nucleotide binding protein that can be activated both at the plasma membrane (SOS-mediated; (182)) and at the Golgi membrane (RasGRP1-mediated; (171, 183, 184)), prior to recruitment to the plasma membrane. Ras-GTP recruits the serine/threonine kinase Raf-1 to the plasma membrane, where Raf-1 is activated (185). The N-terminal domain of Raf-1 is known to inhibit its kinase activity and it is the interaction of this domain with Ras that relieves the autoinhibition (186). Activated Raf-1 then phosphorylates and activates the MAPK/ERK kinase (MEK), which is unusual in that it has a dual ability to phosphorylate both threonine and tyrosine residues, required for activation of the MAPK ERK. There are many isoforms of ERK including the two major, well-characterised isoforms, ERK1 and ERK2, which differ from the other kinases such as Raf-1, in that they lack an autoinhibitory domain. Instead, as stated above, their activation is regulated by the dual phosphorylation of neighbouring threonine and tyrosine residues by MEK (187). Activated ERK homodimerises and is believed to translocate into the nucleus where it phosphorylates and activates a number of transcription factors including AP-1. ERK2 was first localised to the cytoplasm in resting cells but upon stimulation, ERK2 was also detected in the nucleus (188). Similar findings have also been reported for ERK1 (189-191).

1.3.2 Co-stimulation-dependent signalling

The signalling described thus far occurs as a result of TcR ligation. For induction of IL-2 and consequent productive priming of a T cell to occur, co-stimulation is required, as described earlier. Co-stimulation-dependent (CD28-mediated) proliferative signals, independent of ERK activation, are crucial for activation of the full range of transcription factors required for transcription of the IL-2 gene, and hence proliferation (Figure 1.6). These pro-proliferative signals include the Rho family GTPases, Rac and Cdc42 which activate p21-activated kinase (PAK), which in turn activates the dual specific kinase SAPK/ERK1 kinase (SEK1; also known as MKK4) (192). Next, the stress activated protein kinase (SAPK), c-Jun N-terminal kinase (JNK) is activated by phosphorylation of the tyrosine threonine motif residues by the dual specific SEK1 (193). Activated JNK then

phosphorylates c-Jun at serine 63/73, which contributes to the activation of AP-1 (194). It is also thought that PAK may activate other dual specific kinases such as MKK3/6 which, in turn, selectively phosphorylate p38 MAPK at both threonine and tyrosine residues. Phosphorylated p38 can activate a number of effector molecules including activating transcription factors (ATFs), a class of AP-1 dimers (172), by phosphorylation within the N-terminal domain e.g. at Thr69 and Thr71 for ATF-2 (180). Similar to ERK, p38 can also activate c-Fos via activation of ternary complex factors (TCF) within the serum response element (SRE) of c-Fos, which completes the activation of AP-1 (179). Both the ERK and p38 MAPK pathways are connected to the c-Fos promoter by members of the TCF family of E twenty-six (ETS)-domain proteins such as Elk-1 and SAP-1. The Elk-1 C-terminal domain has multiple S/T-P motifs (195) and can be phosphorylated by ERK (177, 178) and JNK *in vitro* and by MEKK *in vivo* (196). Both ERK and p38 MAPK pathways are required for optimal activation of Elk-1 and SAP-1a TCFs and hence, for transcription of c-Fos itself (179).

Phosphoinositide 3 kinase (PI3K) activation is required for optimal lymphocyte proliferation. Indeed, pharmacological inhibition of PI3K prevents IL-2 production in T cells which have been stimulated through the TcR and CD28 (197, 198). Upon engagement with their cognate ligands, CD28 and ICOS can both bind the p85 regulatory subunit of PI3K at their ^{170}YXXM (199) and ^{181}YMFM (200) signalling motifs, respectively. This can, in turn, recruit the catalytic p110 subunit of PI3K to the membrane, resulting in activation of PI3K. PI3K is then in the correct location to exert its enzymatic activity on its substrates thus, allowing production of PI3K products, namely 3-phosphoinositides. The major PI3K product is phosphatidylinositol (3,4,5)-triphosphate ($PI(3,4,5)P_3$) and this molecule is heavily involved in the co-localisation of 3'-phosphoinositide-dependent protein kinase (PDK)-1 and its substrate Akt (also known as protein kinase B (PKB)) at the plasma membrane, by binding to them via their Pleckstrin Homology (PH) domains.

Once situated correctly at the plasma membrane Akt is first phosphorylated by the mammalian target of rapamycin complex 2 (mTORC2) (201), which stimulates the subsequent phosphorylation of Akt by PDK-1, resulting in the activation of Akt. The membrane-targeting function of $PI(3,4,5)P_3$ can be reversed by specific lipid phosphatases such as the inositol 3'-phosphatase, Phosphatase and Tensin homolog deleted on chromosome 10 (PTEN) and SH2 domain-containing inositol 5'-phosphatase (SHIP). Akt activation is observed in T cells upon TcR ligation and is augmented upon co-stimulation

(202, 203). Downstream effectors of Akt are thought to include NF-κB, as expression of active Akt in T cells correlates with upregulated NF-κB function (204, 205). In addition, it has been suggested that PI3K-mediated activation of Akt plays a role in the accumulation of NF-AT in the nucleus (202, 206). Moreover, Akt has been shown to provide a co-stimulatory signal, which is indistinguishable from the co-stimulatory signal provided by CD28, for activation of the CD28 responsive element (CD28RE):AP-1 complex, known as RE/AP (205). RE/AP is one of the transcriptional elements of the IL-2 promoter and Akt is believed to synergise with PKC-θ in the induction of RE/AP (205).

PKC-θ, the PKC isoform predominantly expressed in T cells, is also known to promote NF-κB activation induced upon TcR/CD28-mediated co-stimulation (207). Moreover, T cells from PKC-θ-deficient mice exhibit impaired Ca^{2+} mobilisation and NF-AT activation, and hence decreased IL-2 production and proliferation (208). In addition, studies using T cells from PKC-θ-deficient mice have demonstrated a role for PKC-θ in the activation of NF-κB and AP-1 (209).

The involvement of PI3K in Ca^{2+} mobilisation is unclear, but it is known that PI3K activity also results in the binding of its other major group of substrates, the Tec-family kinases, whose members include Itk and Tec. Itk and Tec bind to $PI(3,4,5)P_3$ via interaction with their PH domains, and Itk is believed to contribute to TcR-dependent Ca^{2+} flux (210) as well as TcR-dependent actin polymerization (211, 212).

In summary, whilst ligation of the TcR results in activation of NF-AT and NF-κB, as well as ERK-mediated activation of c-Jun and c-Fos, these signals are not sufficient for full transcription of the IL-2 gene. For such transcription to occur, co-stimulation-dependent signals are required namely, further phosphorylation and activation of c-Jun and c-Fos by JNK and p38 MAPK respectively, as well as p38 MAPK-mediated activation of ATFs. Together, such signalling induces full transcription and hence, production, of IL-2 in T cells.

1.3.3 Lipid rafts and their role in immune signalling

In lymphocytes, as well as other cell types, many of the molecules involved in cell signalling (dually acylated src family tyrosine kinases, heterotrimeric G protein subunits, adaptor proteins, PIP_2 and lipid kinases and phosphatases) are associated with detergent-insoluble, sphingolipid- and cholesterol-rich domains in the cellular membrane, known as

lipid rafts (also termed glycolipid-enriched microdomains (GEM) or detergent-insoluble glycolipid-rich domains (DIG)). Lipid rafts can be identified via staining with a fluorescent conjugate of cholera toxin subunit B (CT_B) which binds to glycosphingolipid GM1-rich regions of the cell (213, 214). Lipid rafts are said to range in size from a few nanometers to macrodomains that are micrometers in diameter (215-218). Such lipid raft structures have been proposed to function as specialised signalling compartments in the cellular membrane (219), wherein molecules are phosphorylated and activated, and function to recruit and activate downstream signalling molecules. Indeed, lymphocyte ERK MAPK signalling is inhibited when Lck is prevented from translocating to lipid rafts by modification of its N-terminal S-acylation (220) or when the structural integrity of the lipid rafts is impaired by the removal of cholesterol (221-223). In resting T cells, the TcR/CD3 complex is thought to reside outwith lipid rafts and only upon ligation of the TcR does the TcR/CD3 complex translocate into the lipid raft assemblies whereupon its ζ chains are phosphorylated by Lck (reviewed in (224)). As described earlier, a T cell requires both Ag in the context of MHC and co-stimulation, in order for it to become productively primed. Other studies have demonstrated that co-stimulation is also necessary for actin rearrangement and lipid raft clustering at the T cell:APC interface (225, 226). This has relevance for T cell anergy which arises in the absence of co-stimulation (227). These findings suggest that a certain threshold of lipid raft assembly is required in order to achieve productive activation of TcR-mediated signalling cascades and priming of the T cell.

1.3.4 The immunological synapse

Specific molecules critical for T cell signalling are positioned at the point of contact between T cells and APC in a structured manner and this organised interface is known as the immunological synapse (228). It is believed that lipid raft macrodomains assemble to form the immunological synapse and a stable immunological synapse has been shown to be required for optimal activation and priming of T cells (Figure 1.7; (229)). The proteins and intracellular molecules present at the immunological synapse are organised into distinct spatial domains known as supramolecular activation clusters (SMACs), including the central SMAC (c-SMAC) and peripheral SMAC (p-SMAC) (Figure 1.7A; (228)). It must be noted that these structures are only observed in antigen-specific T cell:APC conjugates. The c-SMAC contains the TcR/CD3 complex and PKC-θ and hence, is thought to be the

site of TcR ligation. Within seconds of peptide-MHC engagement, the TcR initiates tyrosine phosphorylation signalling that triggers many complex signalling cascades. Minutes after T cell:APC conjugation, Lck and Fyn are also concentrated in the c-SMAC (230, 231) thus, it seems likely that signalling cascades are promoted in this domain. Initial T-cell:APC contact is accompanied by rapid re-organisation of the cytoskeleton and T-cell polarisation, possibly in response to chemokines (232). Subsequent signalling through heterotrimeric G proteins then triggers actin polymerisation and integrin activation. The p-SMAC harbours the cytoskeletal protein talin and the integrin lymphocyte associated function antigen-1 (LFA-1) and so formation of the p-SMAC and LFA-1:ICAM-1 binding is thought to promote formation of membrane protrusions with TcR-enriched tips which are likely involved in the initial scanning of peptide-MHC complexes (Figure 1.7B. ii; reviewed in (233)). Upon re-stimulation with antigen, anergic T cells fail to translocate their CD3 into the c-SMAC and assembly of the immunological synapse in human anergic T cells is arrested at the stage of the immature synapse (234).

Immunological synapse formation has predominantly been shown *in vitro* and there is considerable debate as to whether immunological synapses occur *in vivo*. However, some studies have indicated the existence of immunological synapses *in vivo* (235, 236) and recent two-photon intravital imaging has provided evidence that prolonged T cell:APC interactions are required for optimal activation and full effector function of T cells (236-242). During the early response to antigen (induction phase) both tolerised and primed $CD4^+$ T cells have contact with, and are reported to "arrest" on, DC near high endothelial venules (HEV) where they exhibit activation and proliferation (242). However, 15-20 h after the induction of tolerance or priming, primed $CD8^+$ T cells have stable, prolonged contacts with DC whereas tolerised $CD8^+$ T cells remain motile and have serial, brief encounters with multiple DC (238) although, it should be noted that these authors do not denote such T cell:DC contacts *in vivo* as immunological synapses. A recent report has suggested a new role for the immunological synapse *in vivo* in helping to coordinate asymmetric cell division (243), thus it may be important for the generation of effector and memory T cells from a single cell.

1.4 Cell cycle

Cells can only divide and proliferate if they complete a full round of the cell cycle, the set sequence of events whereby a single cell duplicates its contents before dividing into two identical daughter cells. The mammalian cell cycle comprises four distinct phases (Figure 1.8). G_1 is characterised by the cell undergoing induction of gene expression and protein synthesis, resulting in an increase in cell size and production of all the proteins required for DNA synthesis. This is the main phase of the cell cycle that is regulated primarily by extracellular signals as, after a cell exits G_1 it is generally committed to completing the cell cycle assuming no catastrophic mutations are induced during DNA replication. DNA duplication occurs in S phase (synthesis) and after chromosome replication, a second growth period, G_2, allows the cell to monitor DNA integrity and cell growth prior to M phase (mitosis) when the cell finally divides. The resulting daughter cells either immediately enter G_1, potentially to go through the full cycle again or alternatively, enter the G_0 phase (quiescence).

1.4.1 Cell cycle regulators

Cell cycle progression is mediated by a variety of signalling molecules which are crucial for optimal T cell activation and proliferation. Progression through the cell cycle is mainly driven by two regulatory components, cyclin dependent kinases (CDKs) and their cyclin partners, proteins whose levels oscillate with the cell cycle. At the G_1 checkpoint cells have to decide whether or not to commit to DNA synthesis. Here, provided the cell has received an activatory signal, Ras-mediated ERK activation and subsequent AP-1 transcription are induced, with the latter causing the upregulation of cyclin D, as c-Jun, an AP-1 constituent, activates the cyclin D1 promoter (244).

Cyclin D can then bind to CDKs 4 or 6 and the resulting complexes promote G_1/S transition by initiating the sequential phosphorylation of the retinoblastoma protein, pRb^{105}. pRb is the protein product of the tumour suppressor protein Rb (also known as Rb-1), which was originally identified as the gene mutated in retinoblastoma, a malignant tumour of the retina (245, 246), and is found to be dysfunctional in a number of other cancers (247). Together with p107 and p130 (pRb-2), it comprises a family of Pocket proteins which have bipartite pocket structures necessary for association with E2F transcription factors, interaction with viral oncoproteins (248, 249) and other biological properties including melanocyte homeostasis and neoplasia (250).

Phosphorylation of pRb is effected by the cyclin E-CDK2 complex, thus releasing the braking effect of Rb on cell cycle progression (251). For example, hypophosphorylated Rb prohibits RNA polymerase III-mediated transcription by binding to the transcription factor III B and its upstream binding factor. RNA polymerase III is required for protein synthesis and cellular growth due to its involvement in the production of transfer RNA and the small ribosomal subunit (252-256). In addition, hypophosphorylated Rb also actively blocks cell cycling by sequestering the transcription factor, E2F, thus blocking expression of genes necessary for S-phase (257). Once hyperphosphorylated by the CDK:cyclin complexes, however, E2F is released and genes required for S phase transition, including DNA polymerase-α, thymidine synthetase, cyclin D3, cyclin E and cyclin A, are transcribed (Figure 1.9) (252-256).

Cdc2 (CDK1) and CDK2 are then activated and can both associate with cyclin A at the S phase of the cell cycle. Such cdc2/CDK2:cyclin A complexes also act to further phosphorylate and inactivate Rb (Figure 1.9; (258)). Moreover, CDK2 has been suggested to play a dominant role in phosphorylation of Rb as silencing or inhibition of Cdc2 negatively regulates entry into S phase but only in the absence of CDK2 (259).

Additionally, CDK2 and CDK4 have been shown to phosphorylate cytoplasmic Smad2 and Smad3 proteins (Mothers against decapentaplegic homology 2, 3 (260-262)), which exhibit an anti-proliferative function. As a result of TGF-β signaling, Smad2 and Smad3 proteins are phosphorylated at the carboxyl terminus by the TGF-β receptor and can form complexes with Smad4. These complexes then accumulate in the nucleus where they bind to the forkhead transcription factor, FAST-1, and subsequently regulate the transcription of target genes (260, 261, 263). TGF-β inhibits cell cycle progression at the G_1 phase (264, 265) and is known to enhance T cell tolerance (266). A range of cell types from $Smad3^{-/-}$ mice are impervious to the inhibitory effects of TGF-β, suggesting that Smad3 is a key mediator of the TGF-β growth inhibitory response (267-269). Tob, a protein belonging to another anti-proliferative gene family, is a negative regulator of activation which is expressed in anergic and quiescent T cells (270). Tob exerts its effects by associating with Smad2 and Smad4 and enhancing Smad:DNA binding in the nucleus. Tob-induced downregulation of IL-2 production is mediated by enhancement of Smad binding on the -105 negative regulatory unit of the IL-2 promoter and not by the inhibition of known IL-2 transcription factors such as NF-AT, AP-1 and NF-kB (270).

Progression through cell cycle can be arrested at the G_1-S phase interface by a variety of extracellular signals resulting from stress upon, or damage to, the cell. TGF-β and IFN-α are examples of extracellular signals which can act to suppress phosphorylation of Rb through the inhibition of CDKs and recruitment of CDK inhibitors (271) in addition to effects on Smads. Two separate families of CDK inhibitors act to regulate the function of the CDK:cyclin complexes, namely the INK4 (inhibitor of CDK4; p15, p16, p18 and p19) and WAF1 (p21, p27, p57) protein families which act to block CDK activity at numerous stages of the cell cycle (Figure 1.8B). p15 (272), $p16^{INK4A}$ (273) and $p27^{kip1}$ (274, 275) have all been shown to inhibit the CDK 4/6:cyclin D complex *in vitro* whereas, $p19^{ARF}$ and $p21^{Waf1}$ are believed to interact with the tumour suppressor gene p53, thus leading to cell cycle arrest (Figure 1.8B; (276, 277)).

However, these proposals are controversial as some of the CDK inhibitors have been reported to play a role in the assembly of CDK:cyclin complexes and hence may actually be required for progression of cell cycle. Indeed, mouse embryo fibroblasts deficient in $p21^{Waf1}$, $p27^{kip1}$ or both exhibit impaired formation of CDK:cyclin D complexes (278). Also, whilst $p27^{kip1}$ can prevent recombinant CDK:cyclin D complex formation *in vitro*, it has been shown to inhibit CDK:cyclin E complexes much more effectively (279). $p27^{kip1}$ activity is regulated by its concentration, association with different cellular complexes and its phosphorylation status and subcellular localisation (271, 280-283). For example, $p27^{kip1}$ expression is highest in quiescent cells and decreases upon progression through cell cycle (284) and consistent with this, a reduction in the level of $p27^{kip1}$ is a common observation in many types of human cancer (285). $p27^{kip1}$ exerts its inhibitory effects on CDK activity when it is localised in the nucleus (286, 287) and consistent with this, ERK activation has been associated with the nuclear export of $p27^{kip1}$ (288). However, it is not clear as to how ERK accomplishes this as, ERK-mediated phosphorylation of $p27^{kip1}$ at Ser10 and Thr187 (289) has been suggested not to be essential for directing the localisation of $p27^{kip1}$ (288). Indeed, it is phosphorylation at Thr198 by p90 ribosomal protein S6 kinases (RSKs) in a Ras-Raf-MEK-ERK-dependent manner that results in cytoplasmic localization of $p27^{kip1}$ (281). Once in the cytoplasm $p27^{kip1}$ binds to the Skp1-Cullin-F-box (SCF) ubiquitin ligase family member, SCF^{Skp2}, a protein complex that targets $p27^{kip1}$ for ubiquitination and degradation (290, 291). SCF^{Skp2} components include Skp2, an F-box (cyclin F homology) protein, and Cks1 which act in conjunction to recognize $p27^{kip1}$

when it is phosphorylated at threonine 187 (290, 292). Hence, degradation of $p27^{kip1}$ in this manner attenuates its inhibitory effects on CDK activity and cell cycle can proceed.

p53 is a transcription factor with a molecular weight of 53-55,000 which is activated upon cellular stress, including DNA damage and aberrant proliferative signals, and contributes to cell cycle arrest and apoptosis. Activation of this tumour suppresser gene results in cell cycle arrest in the G_1 and G_2 phases to allow an opportunity for DNA repair to occur before replication or mitosis respectively. The final outcome of p53 activation appears to depend on the action of a variety of downstream effector genes transactivated by p53. Thus, p53-mediated G_1-S phase arrest is believed to result from p53-induced upregulation of $p21^{WAF1}$ (293) and downregulation of c-Myc (294) whereas the role of p53 in G_2-M arrest is more complex as here, it has multiple downstream targets which regulate either cell cycle (cdc2, cdc25c, cyclin B) or mitosis (e.g. topoisomerase II and MAP4) (reviewed in (295)). The protective role of p53 is highlighted by the fact that around 50% of all cancers possess an inactive form of p53, or have lost p53 all together.

1.4.2 Mechanisms of cell death

The growth and proliferation of cells is tightly regulated to prevent the production of excessive cell numbers by one of two known mechanisms of cell death; necrosis and apoptosis. Necrosis describes cellular death arising from chemical or physical injury and so is quite distinct from biologically activated apoptosis. During necrosis, chromatin condenses and organelles swell resulting in swelling of the cell until it bursts, releasing its intracellular contents which can trigger an inflammatory response. Necrotic tissue is taken up and degraded by phagocytic cells, and reflects the processes occurring during wound healing. By contrast, programmed cell death, or apoptosis, provides a mechanism for the disposal of "unwanted" cells in a coordinated manner and without the generation of inflammation. This mechanism also protects the organism by enabling the destruction of damaged or potentially harmful cells. Indeed, thymocytes which exhibit high affinity or avidity for self Ag, are removed from the T cell repertoire by apoptosis-mediated clonal deletion/negative selection in the thymus. The classical morphological features of apoptosis include the condensation of chromatin, protein and DNA fragmentation and the formation of apoptotic bodies. It is believed that the mitochondrion is the site at which apoptotic signalling pathways converge and eventually result in either caspase-dependent or – independent apoptosis (296). Most of the observed changes associated with apoptosis (i.e.

DNA/protein cleavage, nuclear shrinking, loss of cell shape) are implemented by a set of cysteine proteases, caspases (297) and as such these alterations are termed as caspase-dependent apoptosis. Caspases are mammalian homologues of the protein Ced-3, which was originally identified in *Caenorhabditis elegans* as being required for somatic cell death (298). Caspases are defined by the MEROPS database (a protease classification system) as cysteine nucleophiles with their catalytic residues in the order His, Cys that cleave proteins after aspartic acid residues. Caspases are localised in the cytosol in an inactive pro-caspase form and upon apoptotic stimuli, these pro-caspases are converted into active caspases. Caspases can be divided into two main groups: the initiator caspases (caspases 2, 8, 9 and 10), which are processed first, and the effector caspases (caspases 3, 6 and 7), which can be activated by initiator caspases to drive the ordered disassembly of the apoptotic cell.

There are two major pathways known to activate caspase-dependent apoptosis: the classical caspase pathway and the mitochondrial pathway. The classical caspase pathway, otherwise known as the extrinsic pathway, is initiated upon ligation of death receptors such as Fas/CD95 and tumour necrosis factor receptor (TNFR), which in turn recruit Fas associated protein with a death domain (FADD). FADD can convert pro-caspase 8 into caspase 8 (active form), which can then activate the effector caspase, caspase 3.

In contrast, the mitochondrial, or intrinsic, pathway involves both the opening of the mitochondrial transition pore and thus loss of mitochondrial membrane potential (MMP). The B cell lymphoma-2 (Bcl-2) family proteins are also important regulators of mitochondrial-driven apoptosis in eukaryotic cells (299). Indeed, the release of caspase-independent death factors such as apoptosis inducing factor (AIF) (300) and endonuclease G (301) is regulated by the Bcl-2 family. Interestingly, whilst two groups of Bcl-2 family members induce apoptosis, the third group promotes survival. Although members of each group contain Bcl-2 homology (BH) domains, it is the presence of different BH domains, designated BH1, BH2, BH3 and BH4, that characterizes the separate groups. Pro-survival members e.g. Bcl-2 and Bcl-x_L contain all four BH domains (BH1-4) whilst pro-apoptotic members e.g. Bax and Bak contain BH1-3 domains or just the BH3 domain alone e.g. Bid, Bik and Puma (302). Upon receipt of apoptotic stimuli, pro-apoptotic family members can form heterodimers with anti-apoptotic family members. The BH1-3 domains of Bcl-2 family members have been shown to form an elongated hydrophobic groove to which BH3 domains of other Bcl-2 family proteins can bind (303). In this way, homo- or hetero-dimers can be formed and the combined structure of these dimers determines the fate of the cell.

The amphipathic α-helical BH3 domain in pro-apoptotic family members has been demonstrated to be indispensable for pro-apoptotic and heterodimerisation functions (304).

Bcl-2 family members are regulated predominantly at the level of transcription and the balance of expression of pro-survival and pro-apoptotic Bcl-2 family proteins determines the fate of the cell (305). Post-translational modification can further regulate the dimerisation and hence effector function of Bcl-2 family members. Dimers of pro-apoptotic family proteins appear to induce apoptosis by perforating the outer mitochondrial membrane causing a decrease in MMP and release of cytochrome c which then binds to Apaf 1 and procaspase 9 forming the 'apoptosome'. Reduction in cellular MMP has other significant effects. For example, adenosine tri-phosphate (ATP) can no longer be produced and so the major function of the mitochondria, as the energy-producing powerhouse of the cell, is defunct and the production of reactive oxygen species (ROS), which are toxic to the cell, is increased.

The classical caspase and mitochondrial pathways are now believed to be two aspects of an all-encompassing apoptotic pathway rather than two distinct mechanisms of apoptosis (306-308). It is thought that once the mitochondrial transitional pore has opened, the cell has committed itself to die and that the default position, following commitment to cell death, is to die by necrosis unless this is prevented by the initiation of the caspase cascades (307) or other executioner protease systems involved in apoptosis, such as lysozomal aspartic acid and cysteine proteases e.g. cathepsins (309-311), the ubiquitin/proteosome pathway (312) or a specialized granzyme B pathway in T_H cells (313).

1.5 A review of T cell signalling in tolerance

Productively primed T cells exhibit a characteristic pattern of signalling events *in vitro* which are necessary for transcription of the IL-2 gene and subsequent clonal expansion of T cells (Figures 1.3 and 1.4) (314, 315). By contrast, and as described earlier, anergic T cells exhibit a state of antigenic unresponsiveness which can be evidenced by downregulation of IL-2 production and hence decreased proliferation. However, the differential signalling underlying such reduced IL-2 production has yet to be fully elucidated.

A number of signalling differences have been identified between T cells which have been anergised and primed *in vitro*. Anergy has been said to affect signalling events

proximal to ligation of the TcR complex and those that precede activation of PLC-γ1 in anti-CD3 Ab treated cells (316) and there is evidence to indicate that anergic T cells (induced via anti-CD3 Ab *in vitro* or superantigen (SAg) *in vivo*) can undergo only partial activation of the PLC-γ1 and ERK MAPK pathways, resulting in defective transcription factor complex formation and abrogation of IL-2–dependent clonal expansion (317, 318). Thus, it is perhaps likely that differential activation of one or all of the transcription factors required for transcription of the IL-2 gene contributes to a state of anergy in the cell.

These rather global effects may therefore reflect defects in early tyrosine kinase-dependent signalling and consistent with this, studies have shown decreased tyrosine phosphorylation of 39, 75 and 98 kDa proteins in an anergic T cell hybridoma compared with control cells (316). Moreover, other studies have similarly demonstrated reduced tyrosine phosphorylation of proteins of 38, 74 and 75 kDa in anergic T_H1 clones (319) and SAg-treated, tolerised primary T cells from Vβ8.1 Tg mice (320). In addition, a decrease in the level of $p56^{lck}$ (Lck) and an increase in the level of $p59^{fyn}$ (Fyn) in anergic T_H1 clones have been reported following anti-CD3 induced anergy *in vitro* (321-323). Furthermore, functional recovery from anergy has been shown to require restoration of Lck and Fyn expression to normal levels, indicating that reduced levels of such tyrosine kinases contribute to the maintenance of anergy (322). Indeed, the 70 kDa protein observed in anti-CD3ζ precipitates has been shown to represent ZAP-70 (324) and whilst under conditions of anergy, ZAP-70 is still capable of being recruited to the TcR:CD3 complex, its level of tyrosine phosphorylation is significantly reduced compared to control cells (325). In addition, anergy induced by oral administration of OVA has been demonstrated to cause impaired phosphorylation of TcRζ, ZAP-70, LAT and PLC-γ1 upon re-stimulation of purified splenic $CD4^+$ T cells with OVA and APC *in vitro* (326).

As described earlier, activation of LAT leads to the recruitment of Grb2, GADS, SLP-76 and PLC-γ1, and $CD4^+$ T cells, anergised either *in vitro* or *in vivo*, exhibit reduced activation of such downstream effectors due to hypophosphorylation of LAT upon re-stimulation with anti-CD3 and anti-CD28 Ab. Recruitment and localisation of LAT to the lipid raft-rich immunological synapse has also been shown to be defective in anergic T cells and such defects are believed to result from impaired palmitoylation of LAT (327). As the total protein levels of LAT were not different in anergic and control cells, it therefore

appears that anergy may be induced due to aberrant localisation of such key signalling molecules within the cell.

PKC-θ is believed to be important in the prevention of anergy by acting as a positive regulator of NF-κB (328). Indeed, as mentioned earlier, T cells from PKC-θ-deficient mice exhibit impaired Ca^{2+} mobilisation and NF-AT activation, and hence decreased IL-2 production and proliferation (208). An immediate downstream target of NF-AT is the early growth response (EGR) family of transcription factors. Expression of EGR2 and EGR3 is known to be upregulated in both *in vitro* and *in vivo* anergised T cells (329) and high levels of EGR2 have been shown to persist in anergic T cells for 2-5 days (330). EGR expression appears to be calcineurin- and PKC-dependent (329) and transduction of T cells with EGR2 or EGR3 reduces transcription of the IL-2 gene. In addition, expression of EGR2 and EGR3 also contributes to T cell anergy by upregulating expression of the E3 ligase Cbl-b (329). Together, these data suggest a role for EGR proteins in the induction of anergy.

There is increasing evidence that JNK MAPK-mediated induction of c-Fos and activation of AP-1 and NF-AT complexes may also be defective in *in vitro* and *in vivo* anergised T cells (318, 331-333). For example, it is known that NF-AT (which binds a heterotrimeric NFATp, Fos and Jun protein complex) and AP-1 (which binds Fos and Jun heterodimers) associate to enhance transcription of the IL-2 gene (181, 334, 335). As it is well established that Ca^{2+}-mediated translocation of NF-AT into the nucleus is unaffected in anergic T cells (336, 337), such data implies that the defect in AP-1 binding to NF-AT likely lies at the level of the AP-1 subunits. Indeed, Mondino *et al* demonstrated that the induction of c-Fos and JunB (constituents of AP-1) was severely impaired in anergic T_H1 cells whilst NF-AT activation was intact in these cells (336). The defect in induction of c-Fos and c-Jun appears to be secondary to downregulation of ERK and JNK MAPK activation in such anergic T cells (333, 336). Consistent with this, Fields *et al* also reported that ERK1/2 MAPK activation was decreased in anergic T cells (338) and it has been shown that the reduced ERK MAPK activation and impaired IL-2-dependent proliferation observed in anergic T cells is due to downregulation of Ras activation (331, 338).

As mentioned earlier, RasGRP1 promotes activation of Ras in a DAG-dependent manner and it has been hypothesised that defects in the RasGRP1-mediated activation of Ras may also be involved in T cell anergy as RasGRP1-deficient thymocytes exhibit

reduced Ras and ERK activation, and proliferation (339). Upon phosphorylation by diacylglycerol kinases (DGKs), DAG is converted to phosphatidic acid and consequently, DAG signalling is downregulated. Decreased DAG signalling has been observed in multiple models of T cell anergy and is believed to reduce the recruitment of RasGRP1, and hence reduce RasGRP1-mediated Ras activation (340, 341) (Figure 1.10). For example, DGKζ is thought to antagonise TcR-mediated signalling and DGKα is upregulated in anergic T cells (342-344), suggesting that DGKα may play a contributory role in the induction of anergy in T cells, following stimulation through the TcR. Supporting evidence for this hypothesis is provided by the fact that T cells from DGKα-deficient mice exhibit hyperactive DAG-dependent signalling and are resistant to anergy induction (340). Furthermore, forced expression of DGKζ has been demonstrated to selectively inhibit AP-1 activation in T cells, without affecting Ca^{2+} mobilisation (344).

The downregulation in Ras-mediated ERK activation observed in tolerised T cells is additionally thought to be regulated by the small GTPase Rap1 (also known as Kirsten-ras-reverted 1 (Krev-1) and smg p21). Rap1 was first identified based on its homology with the *Drosophila* Ras-related gene (*Dras3*) (345) and independently from its capacity to stimulate a flat phenotype in v-Ki-Ras-transformed fibroblasts (346). Subsequent studies have suggested that Rap1 mediates its inhibitory effects on ERK activation by directly antagonising Ras-Raf-1 coupling (347), whilst it has been suggested that the inability of Rap1 to activate bound Raf-1 is because it is not localised in the plasma membrane (348, 349).

Accumulation of active Rap1 has indeed been reported to play a role in the maintenance of anergy in human T cell clones (50, 347), with anergic cells displaying reduced ERK activation and IL-2 production due to recruitment of a Fyn-Cbl-CrkL-C3G-Rap1 signalling complex not found in their primed counterparts (50, 347) (Figure 1.11). Further studies have shown an inverse relationship between ERK and Rap1 activation in various T cell lines (350) and also that CD28 signalling abolished TcR-coupled Rap1 activity (351-353). Although Rap1 has also been reported to stimulate ERK via activation of B-Raf, peripheral T cells do not generally express B-Raf. Interestingly, therefore, support for Rap-1 acting to antagonise ERK activation in anergic cells has been provided by a transgenic mouse model in which ectopic expression of B-Raf within T cells prevents repression of ERK activity and anergy (354). Moreover, mice which are deficient in a

negative regulator of Rap1, the GTPase-activating protein (Rap1GAP) SPA-1, show defective ERK activation and progressive unresponsiveness or anergy of T cells (355). However, other studies have implicated positive roles for Rap1 in T cell signalling via enhanced integrin activation and adhesion (356, 357).

Although progress has therefore been made in identifying potential targets of differential signalling, the majority of work in this field has been carried out *in vitro* using T cell lines or clones, or primary T cells *ex vivo*. It is imperative that T cell signalling in anergy is examined *in vivo* as this data will better reflect the true molecular mechanisms occurring in anergic T cells *in situ*. Anergy had been induced *in vivo* using a variety of immunisation regimes including the administration of peptide (i.v.) or SAg (i.p.) (327, 358) and feeding whole protein (326), as well as exposing $CD4^-$ $CD8^-$ T cells, which express a TcR specific for 2C (the αβ Ag receptor from the cytotoxic T lymphocyte clone 2C (359)), to their specific Ag in $H\text{-}2^b$ 2C TcR Tg mice (360). Such *in vivo* induced anergy has been used to investigate T cell signalling (326, 327, 358, 360). However, as these studies used different methods for inducing tolerance than employed by *in vitro* studies, this may perhaps explain the apparently conflicting data generated from comparison of both types of experiments. Indeed, the various regimes may induce distinct "types" of "tolerance". For example, the *in vivo* studies describe a model of 'Ca^{2+}-blocked anergy' wherein there is a defect in Ca^{2+}-mediated translocation of NF-AT into the nucleus, secondary to a downregulation of PLC-γ1 activation, whilst normal activation of ERK MAPK and SAPK is observed (360). Thus, Chiodetti *et al* suggest that the discrepancies observed in *in vitro* and *in vivo* models of anergy (361) reflect that *in vitro* clonal anergy (commonly induced via treatment with anti-CD3) and *in vivo* adaptive tolerance (usually induced using Ag in protein or peptide form) are two distinct biochemical states. Both types of tolerance models result in reduced transcription of IL-2 and proliferation, but the defects in TcR-mediated signalling occur in different signalling cascades. Thus, in adaptive tolerance, T cells appear to exhibit impaired phosphorylation of ZAP-70, LAT and PLC-γ1 leading to decreased Ca^{2+} mobilisation whereas, clonal anergy appears to be predominantly mediated by defects in the Ras-ERK MAPK signalling cascade. *In vivo* tolerised T cells also display reduced ERK activation, but to a lesser extent than *in vitro* anergised T cells (361). With these discrepancies in mind, it would be beneficial to examine these signalling mechanisms *in*

vitro and *in vivo* using as similar a model of anergy as possible for both situations, in order to determine which, if any signalling processes play a general role in anergy.

1.5.1 E3 ligases and their role in tolerance

Three families of proteins with ubiquitin ligase activity have been identified namely, the HECT, RING and U-box proteins, and these are collectively termed E3 ligases. E3 ligases are thought to be involved in immune regulation by binding to proteins and thus targeting them for degradation in the proteosome (reviewed in (362)). Recent work has identified possible roles for E3 ubiquitin ligases as critical upstream factors in the effector phase of tolerance induction occurring in the absence of co-stimulation via CD28 (363-367). Such a lack of CD28-mediated co-stimulation has been associated with a partial or unbalanced calcium-dependent signalling in T cells in which TcR-mediated Ca^{2+} mobilisation predominates (368). This partial signalling can lead to prolonged and unbalanced calcineurin-mediated activation of NF-AT and the induction of a set of "anergy genes" (368), which includes negative regulators of signalling such as phosphatases, proteases and transcriptional repressors (369). These same genes are also induced *in vivo* in T cells from orally tolerised mice (368).

The resulting anergy, which can be demonstrated after re-stimulation with antigen, is known to be mediated by E3 ubiquitin ligases (e.g. Cbl, Itch, Grail). Such E3 ligases are induced during the induction phase of anergy (363, 364) and moreover, Cbl-deficient cells are resistant to induction of anergy (366). Cbl and Grail are ring finger E3s that direct E2s (ubiquitin-conjugating enzymes) to their substrate while Itch is a HECT-type E3 that accepts a ubiquitin molecule from an E2 and transfers it to substrate (363). Cbl-b is induced in the early phase (within minutes) of unresponsiveness and Grail and Itch relocate to the endosomes when anergic cells are re-stimulated with antigen (364, 365). Following calcium-mediated induction of these E3 ubiquitin ligases, there is reduced expression of the TcR signalling machinery including cell surface TcR, PLC-γ1, PKC-θ and RasGAP (370) which appears to be the result of mono-ubiquitination and targeting of these signalling elements for degradation by lysosomal proteases (364, 365). This downregulation of the TcR signalling machinery is also observed when T_H1 cells are anergised with anti-CD3 (363, 364). The precise mechanisms are unclear but the ubiquitin machinery promotes protein trafficking from the surface to the lysosomes via the endocytic pathway. Thus, Cbl may direct SMAC components to the endosomes where mono-ubiquitination by Itch/Grail

promotes lysosomal trafficking and degradation (363) preventing recycling of the signalling machinery to the immunological synapse for the sustained signalling that normally occurs when T cells are activated in the presence of co-stimulation (371-373). In addition, Cbl negatively regulates the WASP-Arp2/3 pathway that coordinates actin polymerisation and cytoskeleton remodelling at the immunological synapse. Consistent with this, Cbl-deficiency results in spontaneous receptor clustering and autoimmunity (374) and can compensate for lack of CD28 co-stimulation (367, 375). This proposed E3-dependent mechanism of anergy is efficient in that it only need target localised receptor-activated signals rather than the total cellular complement of signalling molecules (364).

1.6 Aims

Despite extensive study, the mechanisms by which the immune system can discriminate harmless and pathogenic antigens remain to be fully elucidated. The overall aim of this study was to identify the key signals regulating immunity and tolerance that might provide targets for pharmacological or immunotherapeutic intervention in inflammatory disease and vaccine development. It has been widely proposed that differential T cell signalling underlies the distinct functional outcomes of tolerance and priming but, the majority of these studies have relied upon biochemical assessment of signalling in T cell lines or clones at the population level, following polyclonal stimulation *in vitro* and this approach has yielded some conflicting data. Moreover, such data do not necessarily represent the responses of physiological frequencies of individual antigen-specific T cells within their environmental niche *in vivo*. In addition, those data represent all cell types in heterogeneous populations and do not reveal anything about the kinetics, amplitude or subcellular localisation of signals in functionally distinct groups of cells.

Therefore, the core aims of this project were to:

1. Develop and validate suitable methods with which to assess the kinetics, amplitude and subcellular localisation of signals in individual cells.
2. Develop *in vitro* and *in vivo* methods of assessing such signalling in primed and tolerised Ag-specific T cells.
3. Investigate the proposed differential T cell signalling underlying tolerance and priming, using the above methods.

Figure 1.1 Regulatory properties of B cells in immunity. B_{regs} can regulate inflammation via a variety of mechanisms. B_{regs} produce IL-10 which can act to regulate the T_H1/T_H2 balance (A.i) and downregulate inflammatory processes including IL-1 and TNF-α production by macrophages (MØ; A.ii). B_{regs} also produce TGF-β1 which induces apoptosis of effector T cells (B). $CD8^+$ and natural killer T cells (NKT) can be recruited by B_{regs} in a β2-microglobulin (β2m)-dependent manner (MHC class I (Qa-1) and CD1d) (C). Moreover, B_{regs} can downregulate $CD4^+$ T cell activation directly or by functioning as secondary APC (D). In addition, B_{regs} produce Abs (E), namely IgG and IgA, which can suppress the activation of DC through FcγRIIB:ITIM interactions (E.i), neutralise dangerous soluble factors (E.ii) and induce FcAR expression (IgA-mediated) on a subset of NKT cells, which can then secrete Ig isotype/subclass regulatory molecules (E.iii). Furthermore, such Ab production can promote clearance of apoptotic bodies (E.iv).

Figure 1.2 Activatory and inhibitory regulation of T cell activation. A T cell requires at least two signals to become fully activated, with signal 1 being the recognition of antigen (Ag) in the context of MHC and signal 2 being co-stimulation provided via the interaction of CD28 on the T cell with CD80/86 on the APC (A). Such combined signalling results in proliferation, differentiation and effector function of the T cell (A). In contrast, when a T cell encounters antigen in the context of MHC in the absence of co-stimulation, it can undergo apoptosis or become anergic (B). By contrast, if ligation of the TcR is accompanied by co-ligation of an inhibitory receptor such as CTLA-4 (C) or PD-1 (D), this results in the inhibition of T cell activation and downregulated TcR signalling which reduces the production of IL-2 and cell cycle progression.

Figure 1.3 $CD4^+$ T cell differentiation. $CD4^+$ T_H cells are activated upon recognition of their specific antigen complexed with MHC class II on an APC in the presence of co-stimulation and this activation causes the T_H cell to proliferate, and generate a clone of effector T_H cells. Either T_H1 or T_H2 effector cells are generated with each phenotype exhibiting different capabilities. T_H1 cells are generated in the presence of IL-12 and TGF-γ. Such T_H1 cells are known to express T-bet and produce IL-2, IFNγ and TNF-α. IFNγ upregulates IL-12 production by DC and macrophages and this IL-12, in turn, causes an increase in IFNγ production in T_H cells and so promotes T_H1 cell differentiation in a positive feedback loop. Moreover, IFNγ downregulates IL-4 production thus, promoting a T_H1 phenotype. Whereas, T_H2 cells, which are generated in the presence of IL-4, express GATA-3 and can produce IL-4, IL-5, IL-6, IL-10 and IL-13. Such T_H2 cells can skew adaptive immunity towards a humoral (T_H2) immune response. T_H2 cells stimulate B cells to proliferate, isotype switch and secrete IgG1 antibodies. IL-4 stimulates T_H cells to differentiate into T_H2 cells and IL-10 inhibits IL-2 and IFNγ production, as well as IL-12 production by DC and macrophages, thus directing a T_H2 profile. In addition, T_H17 cells, which are generated in the presence of TGF-β and IL-6, express RORγT and produce IL-17.

Table 1.1 Characteristics of the different regulatory T cell classes. A description of the phenotype and specificity of naturally arising $CD4^+$ $CD25^+$ T_{regs} , Tr1 and T_H3 cells is provided. Information regarding the site of induction, cytokines secreted and mechanism of suppression for each class of T_{reg} is also given.

Figure 1.4 Structure of the gut associated lymphoid tissues (GALT). The small intestine is lined with protruding villi which contain a variety of immune cells and several organised areas of leukocytes, known as Peyer's Patches (PP). The villus is enclosed by a single cell-thick layer of epithelial cells, which are generated in the crypt before migrating up through the villus and being shed from the apex of the villus. Intra-epithelial lymphocytes exist in this epithelial layer. T cells, B cells, DC and macrophages reside in the lamina propria (LP). Specialised epithelial cells, known as M cells, are responsible for the transportation of Ag across the epithelial layer. The PP are situated around such M cells. The sub-epithelial dome (SED), which contains DC and macrophages, and the thymus-dependent area (TDA), which contains T cells and B cell-rich follicles, are both positioned directly beneath M cells. The mesenteric lymph node (MLN) is the draining lymph node of the PP and LP, into which cells from those tissue traffic. This figure was adapted from (46) by kind permission.

Figure 1.5 TcR-mediated signalling. Schematic depiction of the T cell signalling cascades initiated upon ligation of the TcR. Ras-mediated signalling pathways are initiated which lead to the activation of ERK1/2 MAPK. In turn, ERK1/2 activates c-Jun and c-Fos (components of the AP-1 complex), which are required for transcription of the IL-2 gene. The classical PLC-γ1 pathway is also induced, which leads to the mobilisation of Ca^{2+} and translocation of NF-AT into the nucleus. In addition, RasGRP1 promotes the activation of Ras in a DAG-dependent manner and DAG itself mediates activation of PKC which is involved in activation of NF-κB.

Figure 1.6 Co-stimulation-dependent signalling in T cells. Schematic depiction of the additional signalling cascades induced when co-stimulation is provided. Rho-GTPase (Rac/Cdc42)-mediated signalling pathways are induced which lead to the activation of JNK and p38 MAPKs. Such MAPKs activate the remaining transcription factors (e.g. ATFs) required for transcription of the IL-2 gene and hence proliferation. PI3K is also activated, resulting mainly in the production of phosphatidylinositol (3,4,5)-triphosphate ($PI(3,4,5)P_3$). $PI(3,4,5)P_3$ plays a role in the co-localisation of PDK-1 and Akt at the plasma membrane. Such membrane targeting can be reversed by specific lipid phosphatases including PTEN and SHIP. Akt is phosphorylated first by mTORC and then by PDK-1 and is so activated. Activated Akt is believed to be involved in the activation of NF-κB and also associates with PKC-θ to induce RE/AP. Further mobilisation of Ca^{2+} is also thought to occur, in an Itk-mediated manner.

Figure 1.7 Formation of the immunological synapse. The proteins and intracellular molecules present at the immunological synapse are organised into distinct spatial domains including the central supramolecular activation cluster (cSMAC) and peripheral SMAC (pSMAC) (A). The cSMAC contains the TcR and PKC-θ and hence is thought to be the site of TcR ligation. The initial stage in formation of the immunological synapse occurs when expression of the TcR polarises towards site of potential APC contact (B. i). LFA-1 anchors the central region of the forming synapse providing support for cytoskeletal protrusions that force an outermost ring of T cell membrane into close proximity to the peptide-MHC complex. This enables the TcR to sample the peptide-MHC complex. Early signals from the TcR and CD4 stop migration of the T cell. Hence, the T cell is said to "arrest" on the APC. The next stage, the peptide-MHC transport process, requires about 5 min and is possibly mediated by actin-based transport mechanisms (B. ii). Finally, the clustered peptide-MHC complexes are fixed in place by an unknown mechanism (B. iii). Maturation of synapse is associated with sustained TcR signalling.

Figure 1.8 The cell cycle. The cell cycle is composed of several stages (A). Resting cells (G_0) enter the cell cycle at the G_1 phase, where they commence growth. When cells have completed the G_1 phase, they can undergo DNA synthesis (S phase (S)) before transiting into M phase (M), where they undergo mitosis. The cell cycle is carefully regulated at certain checkpoints which occur at the end of each growth phase (B). Progression through the cell cycle is regulated by cyclin-CDK complexes and other modulators such as p15, p16, p19, p21, p27 and p53.

Figure 1.9 Regulation of the cell cycle. Upon receiving an activatory signal, cells at G_1 phase initiate the Ras-ERK MAPK signalling cascade. Phosphorylated ERK1/2 subsequently phosphorylates the AP-1 components, c-Jun and c-Fos, thus activating the AP-1 complex. Such ERK-dependent AP-1 transcription contributes to the upregulation of cyclin D as c-Jun, an AP-1 constituent, activates the cyclin D1 promoter. CDK4, CDK6 and D-type cyclins can then associate and act to phosphorylate Rb, first by cyclin D–CDK4/6 then further by cyclin E-CDK2, thereby altering its conformation. Phosphorylated Rb (p-Rb) releases bound E2F family transcription factors which are then free to activate the genes required for entry into S phase (e.g. cyclin A and cyclin E) and hence proliferation. Cdc2 (CDK1) and CDK2 are then activated and can both associate with cyclin A at S phase where they also act to phosphorylate and inactivate Rb thus, further fuelling cell cycle progression. In addition, CDK2 and CDK4 can phosphorylate Smad2 and Smad3 proteins which exhibit an anti-proliferative function.

Figure 1.10 RasGRP1-mediated activation of Ras. Under conditions of T cell activation, RasGRP1 promotes the activation of Ras in a DAG-dependent manner (A). By contrast, when the TcR is ligated in the absence of co-stimulation, diacylglycerol kinases (DGKs) act to phosphorylate DAG (B). Phosphorylated DAG can then be converted to phosphatidic acid and subsequently, DAG signalling is downregulated. Decreased DAG signalling is believed to reduce the recruitment of RasGRP1, and hence reduce RasGRP1-mediated Ras activation.

Figure 1.11 T cell signalling in tolerance. In tolerised T cells, where the TcR has been ligated in the absence of co-stimulation, not only are the co-stimulatory signals absent, but additional inhibitory signalling pathways are initiated. For example, the small GTPase Rap1 competitively binds Raf and susbsequently, Raf is unable to bind and activate its effector, MEK1/2. Downstream effects of such Rap1 signalling include the downregulation of ERK activation and lack of AP-1 activation. Thus, production of IL-2 is also downregulated and the cell exerts a reduced ability to proliferate in response to challenge with antigen. Such anergy is likely due, in part, to the presence of a Fyn-Cbl-CrkL-C3G-Rap1 complex not observed in primed T cells.

Chapter 2

Materials and Methods

2.1 Animals

Female BALB/c (H-2^d, IgM^a) mice were purchased from Harlan Olac (Bicester, U. K.) and used from 6 to 8 weeks of age. DO11.10 TcR transgenic (Tg) mice on a BALB/c background were obtained originally from Dr. N. Lycke, University of Goteborg, Goteborg, Sweden. These Tg T cells recognise $OVA_{323-339}$ in the context of I-A^d (376). hCARΔcyt Tg mice, which express the human coxsackie/adenovirus receptor (hCAR) with a truncated cytoplasmic domain (hCARΔcyt) on their thymocytes and T lymphocytes (377), were obtained originally from Dr. R James Matthews, University of Wales College of Medicine, Cardiff, U. K. hCARΔcyt.DO11.10 mice were bred in house by crossing hCARΔcyt with DO11.10 Tg mice. All animals were maintained under specified pathogen free conditions with unrestricted access to both standard rodent pellets and water at Biological Services' Central or Veterinary Research Facilities at the University of Glasgow in accordance with Home Office regulations. Procedures were conducted under Project Licence 60/3046.

2.2 Cell culture reagents and antibodies

All cell culture reagents used were of the highest grade available and were purchased from Gibco. All other reagents were obtained from Sigma-Aldrich unless otherwise indicated. The primary Abs used are detailed in Table 2.1.

2.3 Tracking Ag-specific lymphocytes and assessing their function after induction of priming and tolerance *in vivo*

2.3.1 Preparation and purification of cell suspensions

Peripheral lymph nodes (PLN; cervical, axillary, brachial, inguinal), mesenteric lymph nodes (MLN) and spleens were removed from DO11.10 TcR Tg, hCAR Tg or hCARΔcyt.DO11.10 double Tg mice, pooled and forced through Nitex (Cadisch Precision Meshes, London, UK) to generate single cell suspensions. Alternatively, harvested tissues were fixed in 1% paraformaldehyde/PBS for 24 h then transferred into 30% sucrose/PBS for a further 48 h before being snap-frozen in liquid nitrogen in O.C.T.™ compound (Bayer, Newbury, Berkshire, England) and stored at -70^{o}C. Subsequently, tissues were defrosted, removed from O.C.T.™ and forced through Nitex to generate single cell suspensions for analysis of intracellular signalling molecule expression by FACS (Section

2.3.6). $CD4^+$ T cells were purified from freshly harvested tissue using T cell enrichment immunocolumns (Cellect™, VH Bio Ltd, Gateshead, UK) according to the manufacturer's instructions. Briefly, single cell suspensions were layered over Lympholyte®-M media and centrifuged at 1000 *g* for 20 min at room temperature. The lymphocyte layer was then carefully removed from the interface, diluted to a final volume of 10 ml in PBS, centrifuged at 1000 *g* for 5 min and re-suspended in 2-3 ml PBS. Cell Reagent (1.5 ml; supplied with kit) was added and the total volume was made up to 5-6 ml with PBS before incubation for 20 min at 4^0C. PBS (4-5 ml) was then added and the cells were centrifuged at 1000 *g* for 5 min and re-suspended in 1-1.5 ml PBS. Next, the solution was transferred to CD4 negative selection immunocolumns (supplied with kit) and PBS was added until 10 ml of eluate was collected. The eluate was centrifuged at 1000 *g* for 5 min and resuspended in an appropriate amount of buffer. The percentage of purified T cells was assessed by flow cytometry (Section 2.3.6 (378, 379)). Lymph node cells or enriched (75-85% $CD4^+$ $KJ1.26^+$ T cells) T cell suspensions were cultured in complete RPMI 1640 medium (RPMI 1640 medium supplemented with 10% foetal calf serum, 2 mM L-glutamine, 100 U/ml penicillin, 100 U/ml streptomycin and 0.05 mM β-mercaptoethanol; all obtained from Invitrogen).

2.3.2 CFSE labelling of Tg lymphocytes

Single cell suspensions were generated from PLN from DO11.10 mice as described in Section 2.3.1 before being washed twice in Hanks Balanced Salt Solution (HBSS; Sigma, Poole, UK) via centrifugation at 450 *g* for 5 min. Cells were re-suspended at 5 x 10^7/ml in RPMI 1640 medium and incubated with 5 μM 5-(and-6)-carboxyfluorescein diacetate, succinimidyl ester (5(6)-CFDA SE; CFSE; Invitrogen) for 10 min at 37^0C. Next, cells were washed once in HBSS and once in complete RPMI 1640 medium before being re-suspended at 3 x 10^6 $CD4^+$ $KJ1.26^+$ T cells per 200 μl complete RPMI 1640 medium for adoptive transfer as described in Section 2.3.3 (378, 379).

2.3.3 Adoptive transfer of antigen-specific T cells

Single cell suspensions were generated from PLN, MLN and spleens from DO11.10 mice as described in Section 2.3.1. These cells were washed in sterile RPMI 1640 medium (Gibco, Invitrogen, Paisley, UK) before being centrifuged at 450 *g* for 5 min and the supernatant discarded. The percentage of $CD4^+$ $KJ1.26^+$ DO11.10 T cells was calculated

using flow cytometry as described in section 2.3.6 and 3 x 10^6 TcR Tg T cells in 200 µl sterile RPMI 1640 medium were injected intravenously (i.v.) into age-matched, female BALB/c recipients (378, 380).

2.3.4 Administration of antigen

Twenty four hours after adoptive transfer, recipient mice were injected with $OVA_{323-339}$ (100 µg in 200 µl PBS i.v.) in the absence or presence of 1 µg LPS (*Salmonella abortus*), to induce systemic tolerance or priming respectively (161, 381-383). In addition, mice were fed 100 mg ovalbumin (OVA; Sigma) in the absence or presence of 20 µg cholera toxin (CT; Sigma), to induce oral tolerance or priming respectively (384). Alternatively, recipient mice were injected with 100 µg OVA in 100 µl PBS/50% CFA (Sigma) s.c. in the back of the neck to induce priming (384). Controls received equivalent amounts of PBS via the same routes. To elicit a secondary response, mice were challenged with $OVA_{323-339}$ (100 µg i.v.) alone or together with LPS (1 µg) in 200 µl PBS 7 or 10 days later.

2.3.5 Biotinylation of KJ1.26 Ab

The clonotypic mAb, KJ1.26, detects the Tg α/β TcR expressed by DO11.10 mice (385) and was purified from the original hybridoma (386). The KJ1.26 mAb was biotinylated using NHS-Sulfo-Biotin reagents (Pierce (387)). Briefly, solutions containing 1 mg/ml purified mAb were dialysed overnight against 50 mM Sodium Bicarbonate buffer (pH 8.5) at 4^0C and 1 ml aliquots were then mixed with 75 ng Sulfo-NHS-Biotin for 30 min at room temperature. Free biotin was then removed by dialysing overnight with PBS/0.05% NaN_3 at 4^0C. Solutions were dialysed using Slide-A-Lyzer® dialysis cassettes (Pierce) and biotinylated Ab was stored at 4^0C until use.

2.3.6 Flow cytometry

Aliquots of cells (10^6/ml) in 5 ml polystyrene tubes (Falcon, BD, UK) were washed with 200 µl cold FACS buffer (PBS, 2% FCS, 0.2% NaN_3) at 450 *g* for 5 min at 4^0C. Cells were re-suspended in 200 µl Fc receptor (FcR) blocking buffer (anti-CD16/32, clone 2.4G2, hybridoma supernatant, 10% mouse serum, 0.1% sodium azide) containing the appropriate fluorochrome-conjugated, biotinylated or purified primary Abs for 20-30 min

in the dark at 4°C. Anti-CD16/32 binds to FcγRII/III and the immunoglobulin in mouse serum binds to FcγRI, and so the FcR blocking buffer blocks non-specific binding of Ab to such FcR-bearing cells. Details of the Ab clones, their specificities and isotype controls used are provided in Table 2.1 (378). Cells were then washed with 1 ml FACS buffer as before and, where appropriate, biotinylated or purified Abs were detected following incubation with fluorochrome-conjugated streptavidin (Vector Laboratories, Burlingame, CA) or with fluorochrome-conjugated rat anti-mouse IgG1 (BD PharMingen) respectively, for 20-30 min in the dark at 4°C. For detection of intracellular signalling molecules, cells were washed with 1 ml PBS before addition of 200 µl BD Cytofix/Cytoperm™ solution (BD PharMingen) for 20 min at 4^0C and further washing with 500 µl BD Perm/Wash solution (BD PharMingen). Purified Abs were then detected following incubation with fluorochrome-conjugated anti-rabbit IgG1 (BD PharMingen) for 10 min in the dark at room temperature. Finally, cells were washed again in FACS buffer or BD Perm/Wash solution and re-suspended in 300 µl FACS flow for analysis using a FACScan and CellQuest software (BD PharMingen). Two or three-colour analysis was performed on 20,000 events as described in Figure 2.1.

2.3.7 Measurement of antigen-specific proliferation ex vivo

PLN, MLN and spleens were harvested 10 days after primary exposure to antigen and single cell suspensions were prepared as described in section 2.3.1, before being cultured *in vitro* with or without the addition of $OVA_{323-339}$ (1 µg/ml). Lymph node cells were cultured at a concentration of 4 x 10^5 cells per well (2 x 10^5 Tg T cells + 2 x 10^5 DC per well), in complete RPMI 1640 medium, in triplicate, for 72 h, in 96-well flat bottomed plates (Corning) at 37^0C in a 5% CO_2 incubator. DNA synthesis was assessed in all samples by addition of 1 µCi per well of [^{3}H] thymidine (Western Infirmary, Glasgow). Cells were then harvested onto glass fibre filter mats (Wallac, Warrington, UK) using a Betaplate 96-well harvester (Amersham Pharmacia Biotech, Turku, Finland) after an additional 16 hours. [^{3}H] thymidine incorporation was assessed using a 1205 Betaplate liquid scintillation counter (Amersham).

2.3.8 Ex vivo assessment of cytokine induction in vivo

Twelve days after primary immunisation, all groups were challenged by i.v. injection with 100 μg $OVA_{323-339}$ *in vivo* for 5 h before PLN, MLN and spleens were harvested. Single cell suspensions were prepared and stained for CD4 and KJ1.26 expression, as described in sections 2.3.1 and 2.3.6, before being fixed with 250 μl BD Cytofix/Cytoperm™ solution (Cytofix/Cytoperm™ kit; BD) per tube for 20 min at 4^0C. Samples were then washed and permeabilised with 500 μl BD Perm/Wash solution (supplied with kit) per tube via centrifugation for 5 min at 450 *g*. This step was repeated and samples were stained for intracellular IL-2 or IFNγ by incubation with phycoerythrin (PE)-conjugated anti-IL-2 or anti-IFNγ (both at 2 μg/ml) in the dark at room temperature for 30 min. Samples were washed as before, re-suspended in 250 μl FACS Flow per tube and the proportion of $CD4^+$ $KJ1.26^+$ T cells positive for IL-2 or IFNγ was determined by flow cytometry. PE-conjugated Rat IgG2b or Rat IgG1 served as isotype controls for IL-2 and IFNγ respectively.

2.3.9 Assessment of antigen-specific antibody responses

Peripheral blood was collected from the tail into heparinised capillary tubes (Hawksley & Sons Ltd., Lancing, Sussex, UK). The blood was then ejected into eppendorfs containing Serasieve (Lomb Scientific (Aust) Pty Ltd, Sydney, Australia) and left to clot at room temperature for a minimum of 2 h before serum was separated by micro-centrifugation at 12,100 *g* for 5 min and stored at -20^0C until analysis. All sera were tested for the levels of anti-OVA IgG1 and anti-OVA IgG2a Abs by ELISA. Samples were analysed in duplicate over a three-fold dilution range. Prior to analysis, Immulon-2 ELISA plates (Corning) were coated with OVA protein in PBS (20 μg/ml; 100 μl/well) overnight at 4^0C. After washing with PBS/0.05% Tween-20 (Sigma), non-specific binding sites were blocked with PBS/10% FCS for 1 h at 37^0C. Plates were then washed three times and incubated with serum samples, serially diluted (starting at 1:4 dilution of neat sample) in 100 μl PBS/0.2% FCS/0.05% Tween-20 per well, for 2 h at 37^0C. After four washes, plates were incubated with 100 μl per well of peroxidase-conjugated anti-mouse IgG1 or peroxidase-conjugated anti-mouse IgG2a (both diluted 1:8000 in PBS/0.2% FCS/0.05% Tween®-20; Southern Biotechnology Associates Inc., Birmingham, AL) for 30 min at 37^0C. Lastly, the plates were washed six times before addition of 3, 3', 5, 5'-

tetramethylbenzidine peroxidase (TMB) substrate (100 µl/well; KPL, Insight Biotechnologies, Wembley, Middlesex, UK). Plates were read at 405 nm on a Dynatech MR5000 automatic plate reader with Revelation software (both Dynex Technologies, West Sussex, UK).

2.4 Functional analysis of T cells following the induction of tolerance or priming *in vitro*.

2.4.1 Generation, maturation and antigen-loading of dendritic cells

Dendritic cells (DC) were derived from bone marrow as described previously (388). Briefly, femurs and tibiae were asceptically removed and the epiphyses of the bones were severed. The bone marrow was harvested by flushing RPMI 1640 medium through the bone using a syringe with a 23 g needle. Single cell suspensions were prepared and washed in RPMI 1640 medium. Cells were plated out at 2 x 10^5/ml in DC medium (complete RPMI 1640 medium supplemented with 10% sterile filtered supernatant from the X-63 fibroblast cell line (expressing the Granulocyte-Macrophage colony-stimulating factor (GM-CSF) gene; gift from Dr. J. Brewer, University of Glasgow, Glasgow, UK)) in 6-well tissue culture plates (Corning B.V., The Netherlands) and incubated for 9 days at 37^0C. Cells were supplemented by addition of fresh DC medium (2.5 ml per well) at days 3 and 6 before being "matured" at day 9 by culture with 1 µg/ml LPS (*Salmonella abortus*, Sigma) for 24 h. "Matured" DC were incubated with antigen (1 µg/ml $OVA_{323-339}$; Genosys, Sigma) for 3-4 h at 37^0C before unbound $OVA_{323-339}$ was removed from the culture by washing with fresh medium at 300 *g* for 5 min prior to incubation with T cells.

2.4.2 Induction of priming or anergy of T cells in vitro

Six-well plates (Corning) were coated with anti-mouse CD3ε Ab (Clone 145-2C11; 1 µg/well) in PBS (1 ml/well) and incubated for 16 h at 4^0C. Subsequently, lymph node cells or purified OVA-specific Tg T cells (1x10^6/well) were cultured in complete RPMI 1640 medium in anti-mouse CD3ε Ab-coated 6-well plates for 48 h in the presence or absence of 1 µg/ml anti-mouse CD28 Ab (Clone 37.51, BD Pharmingen, Oxford, UK) to induce priming or anergy respectively (389-391). After 48h, cells were washed twice with

RPMI 1640 medium, re-plated at a concentration of $1x10^6$ cells/ml/well and rested in complete RPMI 1640 medium for an additional 48 h.

2.4.3 Culture of T cells with DC

Following the induction of priming or anergy, primed, anergic and freshly isolated ("naïve") Tg T cells were counted by flow cytometry and re-stimulated by culturing with LPS-matured DC which had been loaded with $OVA_{323-339}$ (see section 2.4.1), at a ratio of 1:1 (5×10^5 Tg T cells + 5×10^5 DC) in complete RPMI 1640 medium (2 ml/well) in 6-well plates (Costar, Corning, NY). Alternatively, in some experiments cells, 10^5 Tg T cells + 10^5 DC, were cultured in complete RPMI 1640 medium, in 4-well chamber slides (400µl/chamber; SLS, Nottingham, UK). T cells and DC were cultured together for 1, 20 or 48 h at 37^0C in a 5% CO_2 incubator (Jencons, Leighton Buzzard, UK).

2.4.4 Assessment of antigen-specific proliferation

Naïve, anergic and primed T cells were cultured with DC ± $OVA_{323-339}$, as described in section 2.4.3, at a concentration of 4×10^5 cells per well (2×10^5 Tg T cells + 2×10^5 DC per well), in complete RPMI 1640 medium, in triplicate, for 24, 48 or 72 h, in 96-well flat bottomed plates at 37^0C in 5% CO_2. DNA synthesis was assessed in all samples by addition of 1 µCi per well of [^{3}H] thymidine (Western Infirmary, Glasgow). Cells were then harvested onto glass fibre filter mats using a Betaplate 96-well harvester after an additional 16 h. [^{3}H] thymidine incorporation was assessed using a 1205 Betaplate liquid scintillation counter. Where indicated, 10 ng/ml rIL-2 (gift from Dr D. Xu, University of Glasgow, Glasgow, UK) was added at the beginning of the proliferation assay.

2.4.5 Assessment of antigen-specific cytokine production in vitro

To detect IL-2 and IFNγ in culture supernatants, Immulon-4 plates (Costar) were coated with rat anti-mouse IL-2 or IFNγ capture Abs (1 or 1.5 µg/ml, respectively; 50 µl/well; BD Pharmingen) for 16 h at 4^0C before being blocked with 10% FCS in PBS for 1 h at 37^0C. Sample supernatants were added for 3 h at 37^0C and following washing with 0.05% Tween® 20 in PBS, were subsequently incubated with biotinylated rat anti-mouse IL-2 or IFNγ detection Abs (0.5 or 1 µg/ml, respectively; 50 µl/well; BD PharMingen) for 1 h at 37^0C. Plates were then incubated with 50 µl extravidin peroxidase per well (diluted

1:1000 in PBS/0.2% FCS/0.05% Tween®-20; Sigma-Aldrich) for 1 h at 37^0C before being treated with TMB Microwell Peroxidase Substrate. Recombinant murine IL-2 or IFNγ preparations (BD Pharmingen) were used to produce standard curves from which cytokine levels in samples were calculated.

2.4.6 Analysis of ERK1/2 expression and activation levels by Western Blotting

Primed, anergic or naïve T cells (10^6) were harvested and lysed in lysis buffer (50 mM Tris-HCl (pH 7.5) buffer containing 150 mM NaCl, 2% (v/v) Nonidet P40, 0.25% (w/v) sodium deoxycholate, 1 mM EDTA (pH 8.0), 1 mM PMSF, 10 mM Sodium orthovanadate, 10 μg/ml chymostatin, 10 μg/ml leupeptin, 10 μg/ml antipain, 10 μg/ml pepstatin A; all obtained from Sigma) for 20 min on ice. Cellular debris was removed by centrifugation at 11,000 *g* for 10 min at 4°C and the protein concentration of the soluble fraction was determined using the Micro BCA™ protein assay reagent kit (Pierce, Rockford, IL). Samples (75 μg) were mixed with an equal volume of 2 x SDS PAGE gel loading buffer (20% (v/v) Glycerol, 4% (w/v) SDS, 100 mM Tris-HCl pH 6.8, 2 μg/ml Bromophenol Blue, 5% (w/v) β- mercaptoethanol), boiled for 2 min and then separated by 10% SDS-PAGE (Bio-Rad, Hercules, CA). Proteins were then transferred to nitrocellulose membranes (Amersham, Buckinghamshire, UK) and non-specific binding sites were blocked with TBS (2 M NaCl, 20 mM Tris-HCl, pH 7.5,0.1% Tween 20), containing 5% non-fat dry milk. Immunodetection was accomplished by incubating the membranes first with primary antibodies (diluted 1:1000 in TBS, 5% non-fat dry milk) which recognise total or active ERK1 and ERK2 (rabbit anti-p44/42 MAP kinase or rabbit anti-dually-phosphorylated-p44/42 MAP kinase (anti-pERK) respectively; Cell Signalling Technology, New England Biolabs (NEB), Beverly, MA) and then with an anti-rabbit IgG HRP-conjugated secondary antibody (1:2000, Cell Signalling Technology, NEB) diluted in TBS, 5% non-fat dry milk and visualised using chemiluminescence (ECL, Amersham).

2.5 Detection of signalling in individual Ag-specific T cells *in vitro* and *in situ*

2.5.1 Detection of cell cycle progression and signalling molecules by intracellular staining of cells

To study cell cycle progression and cellular localisation of different signalling molecules and lipid raft structures, cells were cytocentrifugated onto microscope slides at 40 *g* for 4 min, using a Shandon Cytospin 3 centrifuge (Shandon Co., UK) or cultured in chamber slides (12, 392). Cells were then fixed in 4% formaldehyde in PBS for 15 min, washed in PBS and placed in 1% (w/v) blocking reagent (component D supplied with Alexa Fluor® 488 tyramide kit # T-20922; Molecular Probes, Eugene, OR) in PBS for 30 min. All antibodies were diluted in 1% blocking reagent and washing steps were carried out three times in TNT buffer (0.15 M NaCl, 0.1 M Tris-HCl, pH 7.5, 0.05% Tween 20), unless otherwise stated.

To identify OVA-specific Tg TcR T cells, cells were incubated with biotinylated anti-KJ1.26 Ab (6.4 μg/ml), for 30 min, washed and then incubated with streptavidin-HRP (diluted 1:100) for 30 min. After washing, the cells were treated with biotinylated-tyramide (diluted 1:50; TSA™ Biotin system (described in Figure 2.2A), Perkin Elmer Life Sciences, Boston, MA) for 10 min, washed and then incubated with Streptavidin-Alexa Fluor® 647 (2 μg/ml; all Alexa Fluor® dyes were purchased from Molecular Probes) for 30 min. Excess HRP was quenched using 0.1% sodium azide, 3% hydrogen peroxide, in PBS, for 10 min and this quenching step was repeated three times.

Cells were then permeabilised for 5 min in permeabilisation buffer (2% FCS, 2 mM EDTA pH 8.0, 0.1% saponin) and incubated for 15 min in 1% blocking reagent. To detect intracellular proteins, cells were incubated with antibodies against a range of signalling molecules (Table 2.1) diluted in 1% blocking reagent supplemented with 0.1% saponin for 30 min. Cells were then washed and treated with anti-rabbit IgG HRP conjugate (diluted 1:100; Cell Signalling Technology, NEB) before Alexa Fluor® 488 tyramide (diluted 1:100; described in Figure 2.2B) was added for 10 min. Cholera Toxin subunit B-Alexa Fluor® 488 (0.5 μg/ml) was used to stain the glycosphingolipid GM1-containing lipid raft structures (213, 214) and the APO-BrdU™ TUNEL assay kit containing anti-BrdU™-Alexa Fluor® 488 was used to label DNA strand breaks (393-395). Finally, cells were washed and mounted in Vectashield with DAPI (Vector Laboratories) and examined by

laser scanning cytometry (LSC; Figures 2.3 and 2.4). Biotinylated Mouse IgG2a (BD PharMingen) and Rabbit IgG (Sigma) served as isotype controls for biotinylated KJ1.26 and all antibodies against signalling molecules, respectively.

2.5.2 Preparation of tissue sections and immunofluorescence microscopy

PLN, MLN and spleens were removed at different timepoints following primary or secondary exposure to antigen and placed into 1% paraformaldehyde/PBS for 24 h then transferred into 30% sucrose/PBS for a further 48 h before being snap-frozen in liquid nitrogen in O.C.T.™ Compound and stored at -70^{o}C. Six micron sections were cut on a cryostat (ThermoShandon, Cheshire, UK) and stored at -20^{o}C. Sections were stained as described previously (392). In brief, tissue sections were fixed in acetone (analytical reagent grade; CH_3COCH_3) for 10 min and stained for KJ1.26 expression as described earlier for intracellular staining (Section 2.5.1). Next, the sections were stained with a range of anti-signalling molecule Abs or isotype controls for 16 h at 37^{0}C (Tables 2.1 and 2.2). Sections were then incubated with anti-rabbit IgG-HRP conjugate (diluted 1:100) mixed together with anti-CD45R/B220-FITC conjugate (2 μg/ml) for 30 min and then Pacific blue tyramide^{TM} (diluted 1:50; Kit # T-20940; Invitrogen; described in Figure 2.2B) was added for 10 min; both at room temperature. Finally, the sections were mounted in Vectashield (Vector Laboratories) and examined by laser scanning cytometry (LSC; Compucyte, Cambridge, MA; Figure 2.5).

2.6 Laser scanning cytometry

The fluorescence levels in individual cells were measured using a laser scanning cytometer (LSC; further explained in Chapter 3; Figures 2.3-2.5) with the spectra and laser/filter combinations shown in Table 2.2. Detector gain voltages (PMTs) were adjusted at the start of each batch of experiments to optimise fluorescence excitation (12, 392, 396, 397) with the maximum value of 75 for number of saturated pixels.

2.6.1 LSC data collection on individual cells

Appropriate data collection protocol (.PRO) and display (.DPR) files were set up to detect blue, green and long red fluorescence as follows. In the *Parameters* sub-menu of the *Instrument settings* menu, the blue, green and long red sensor boxes were checked to ensure fluorescence detected by these sensors was included in the data file. LSC detects cells using

a series of contours (Figure 2.3A) and when chamber slides or cytocentrifugated cells (cytospins) are analysed, it is common to set the primary contour, called the threshold contour, on cell nuclei (12, 392) which are identified by staining with dyes that bind to DNA, such as DAPI (398). In the *Computation* sub-menu, the threshold contour was set on blue, as this is the colour of the DAPI stain. The minimum area was then set to 5μm^2, enabling detection of DAPI stained nuclei that are sized 5μm^2 and above. This is the optimal minimum area for the T lymphocytes described hereafter. Using the LSC scan data display, the integration contour was then situated 11 pixels (1 pixel = 0.5μm (x-axis) and 0.5μm (y-axis) for 40x objective) outside the threshold contour, so as to define the outer edge of the cells already identified on the basis of their nuclear staining. The integration contour allowed calculation of the total fluorescence within each cell (fluorescence integral value) and this integration contour setting was optimal for collecting data on T lymphocytes. *Peripheral contouring* was enabled to define the peripheral area of the cell. Peripheral contours were set between the threshold contour (defined by the nucleus when contouring on DAPI) and the integration contour (defined by the edge of the cell; Fig. 2.3.A) and so the fluorescence emitted peripheral to the nucleus could be measured. Finally, two background contours measure the background fluorescence outside the cells and this value is automatically subtracted from the measured fluorescence values (Figure 2.4.A).

Using the *Scan Area* option, an area of the slide to be scanned was highlighted, which corresponded to the location of the cells on the slide. Next the Photomultiplier tube (PMT)-Voltage, Offset, and Gain settings were set to 25%, 2048, and 255, respectively, for blue; to 35%, 2048, and 255, respectively for green; and to 28%, 2048, and 255, respectively for long red. The power of the Argon laser was set to 5 mW. These settings were optimal for analysis of these samples, but were checked on each occasion when different reagents and/or cell types were used. To do this, optimal settings are indicated by the presence of dark blue lines in the upper third of the PMT scale with very little (< 75 pixels) or no saturation. If this was not the case, the PMTs were adjusted by increasing the PMTs to increase the signal, or by decreasing the PMTs to decrease saturation. Saturation occurs when the detector no longer responds to increased levels of signal.

Next, the threshold value was set to 3000 thus, ensuring all cells emitting blue fluorescence at a level ≥3000 fluorescence units were detected as events. This setting was

verified for each batch of staining and varied from 3000 to 5000 depending on the intensity of the nuclear staining. Setting the optimal threshold value for detection of cells is crucial so as to allow maximal cellular resolution and collection (Figure 2.3B and 2.4A). For example, if the threshold value is set too low then multiple cells may be detected as one cell (Figure 2.3B) and conversely, if a high threshold value is set, cells with low or medium intensity staining will not be detected at all (Figure 2.3B). Therefore, a compromise must be made when setting the threshold value so as to detect the maximum number of true single cells in a sample (Figure 2.4A). The area was then scanned and the data file saved.

2.6.2. Identifying an Ag-specific T cell population by LSC

To enable discrimination of the Ag-specific T cell population, cells were first detected via their nuclear staining as described above (Figure 2.4A), before Ag-specific T cells were identified via their Tg TcR (stained with the mAb KJ1.26 as described in section 2.5.1). As the Tg TcR is expressed on the surface of the T cell, the data derived from the integration contour (integral value) was used to distinguish the Ag-specific T cell population (Figure 2.4B). In addition, the expression level of intracellular molecules in Ag-specific T cells was quantitated by gating on the Tg TcR T cells (Figure 2.4B) and measuring the integral fluorescence value for the intracellular molecule in question (Figure 2.4C). For analysis purposes the positive gate was positioned according to the fluorescence obtained using appropriate negative/isotype controls (Figure 2.4D, E). LSC data analysis was carried out using Wincyte version 3.6 (Compucyte).

2.6.3. LSC data collection on antigen-specific Tg T cells in situ

For analysis of antigen-specific T cells in tissue sections, the primary contouring parameter was set using the long red sensor which detects the Alexa Fluor® 647-stained Tg TcR on the cell surface (Figure 2.5A), thus identifying all the antigen-specific Tg T cells in the section (Figure 2.5C) and allowing measurement of any signal expressed by these T cells *in situ* (Figure 2.5D). An advantage of using the adoptive transfer system for this analysis is that it generates a relatively low, near physiological, frequency of Ag-specific Tg T cells. This approach overcomes the usual problem encountered with cells in tissue, where they can be so densely packed to prevent setting an accurate threshold based on a cell surface marker. The optimal settings for such sporadically distributed TcR Tg T cells are as follows: threshold value: 3500; minimum area: 5 μm^2; power of Argon laser: 5mW;

PMT, offset, and gain settings: 22-32%, 2048, and 255, respectively, for blue; 30-40%, 2048, and 255, for green; and 22-32%, 2048, and 255, for long red. PMT settings varied from day to day depending on the intensity of staining in different batches of tissue.

By contrast, in order to detect the densely packed B cell follicles, phantom contours are required (Figure 2.5). Phantom contours differ from the contours described thus far in that they comprise a lattice of contours (Figure 2.5B), which is placed over the tissue section, consequently generating fluorescence values which represent the tissue section as a whole, rather than individual cells (399, 400). When phantom contours are set to detect fluorescence emitted from the B cell stain, B220-FITC, this allows the identification of B cell rich areas (Figure 2.5E), not individual B cells, and permits the generation of tissue maps on which the x- and y-position of the B cell rich areas can be plotted (Figure 2.5F). Hence, the location of pERK- or Rap1-expressing antigen-specific Tg T cells could be assessed in relation to follicular or paracortical areas within the lymph node using tissue maps (Figure 2.5F). Phantom contours were generated as follows. On the *Phantoms* tab, phantom contouring was enabled, and the *lattice* pattern and *allow overlap of events* options were selected. The radius was set to 6 μm and the minimal distance between phantom centres to 20 μm as these were the optimal settings for analysis of lymphocytes in this manner. Fluorescence images were captured using a connected 3CCD colour vision camera (regulated by a Hamamatsu and Orbit controller) and the Openlab version 3.0.9 digital imaging programme (Improvision, Warwick, UK).

2.7 Transfection of Ag-specific T cell hybridoma cells and primary T cells

2.7.1 Preparation of Luria-Bertani agar and broth

Luria-Bertani (LB) agar was prepared by dissolving 5 g Tryptone, 2.5 g Yeast Extract (both Sigma) and 2.5 g NaCl in 400 ml dH_20, and the pH adjusted to 7.5. LB Agar (7.5 g; Sigma) was added and the solution was made up to a total volume of 500 ml with dH_20 before being autoclaved. The solution was then cooled to ~55^0C on a stirrer before the appropriate antibiotic, 60 μg/ml kanamycin or 100 μg/ml ampicillin, was added. The solution was stirred for a further 20 sec before being poured into 9 cm Petri dishes (Corning) until plates were half full of LB Agar (~15 ml/plate), under sterile conditions. The plates were left to cool and set for 20 min before being stored at 4^0C.

To prepare LB broth, 10g Tryptone, 5 g Yeast Extract and 5 g NaCl were dissolved in 2 L dH_20 and the pH was adjusted to 7.5. The broth was autoclaved, cooled and supplemented with either 30 μg/ml kanamycin or 50 μg/ml ampicillin before being stored at 4^0C.

2.7.2 Transformation of chemically competent cells

One Shot® TOP10 competent *Escherichia Coli* (*E. Coli*; Invitrogen) cells were transformed with pEGFP-N1 (kanamycin-resistant (kan^r); Clontech Laboratories, Inc., Palo Alto, CA) or pcDNA3.1 (ampicillin-resistant (amp^r); Invitrogen) plasmids as per the manufacturer's instructions. Briefly, one 50 μl aliquot of One Shot® cells for each transformation was thawed, on ice, whilst the pEGFP-N1 and pcDNA3.1 plasmids were centrifuged at 12,100 *g* for 30 s before also being placed on ice. Next, 4 μl of pEGFP-N1 or pcDNA3.1 were pipetted directly into a vial of competent cells and the solution was mixed by gentle tapping. Subsequently, 0.5 M 2-mercaptoethanol was added to each vial and the vials were incubated on ice for 30 min. Following this incubation, the cells were heat-shocked at 42^0C for exactly 30 sec before being placed on ice. SOC medium (2 % tryptone, 0.5 % yeast extract, 0.4 % glucose, 10 mM NaCl, 5 mM $MgCl_2$, 5 mM $MgSO_4$, 2.5 mM KCl; 250 μl), which had been pre-warmed to room temperature, was added to each vial and the vials were shaken at 3 *g* for exactly 60 min at 37^0C in an Innova 4400 incubator shaker (New Brunswick Scientific (UK) Ltd., St. Albans, Herts, UK). Each transformation (50 μl) was then spread on separate Luria broth agar plates which were inverted and incubated at 37^0C overnight.

2.7.3 Purification and determination of yield of plasmid DNA

pEGFP-N1 (Figure 2.6) and pcDNA3.1 (Figure 2.8) plasmids were purified using HiSpeed Plasmid Maxi Kits (Qiagen, Crawley, UK) as per the manufacturer's instructions. In brief, single bacterial colonies were picked from freshly streaked plates of LB agar and used to inoculate a starter culture of 10 ml LB broth containing 30 μg/ml kanamycin or 50 μg/ml ampicillin. The cultures were incubated at 37^0C with vigorous shaking (5 *g*) for 6 h before being diluted 1:250 in LB broth containing kanamycin or ampicillin and cultured at 37^0C with vigorous shaking for 16 h. The bacterial cells were then harvested by centrifugation at 6000 *g* at 4^0C for 15 min and re-suspended in 10 ml buffer P1 (all buffers

and components supplied with kit). To lyse the cultures, 10 ml of buffer P2 was added and the cultures were mixed gently and incubated at 37^0C for 5 min. Next, 10 ml chilled P3 buffer was added to the lysate, the cultures were mixed and poured immediately into the barrels of QIAfilter cartridges and incubated at room temperature for 30 min. The plungers were then inserted into the QIAfilter cartridges and the cultures were filtered into HiSpeed tips (previously equilibrated with 10 ml buffer QBT) and the HiSpeed tips were washed with 60 ml buffer QC before the relevant DNA was eluted with 15 ml buffer QF and collected in 50 ml tubes.

DNA was then precipitated by addition of 10.5 ml isopropanol and incubation at room temperature for 5 min. This mixture was then filtered through a QIAprecipitator before the DNA was washed with 2 ml 70% ethanol. The membrane was then dried by forcing air through the QIAprecipitator and the DNA was eluted with 1 ml buffer TE and collected into a 1.5 ml tube. To ensure that the maximum amount of DNA was solubilised and recovered, the sample was eluted for a second time. DNA concentration was determined on a DU® 640 spectrophotometer (Beckman, Fullerton, CA, USA) and authentication of DNA fragments was assessed by quantitative analysis of agarose gels (1% (w/v) agarose in Tris-Acetate-EDTA (TAE) buffer with 667 ng/ml of the fluorescent DNA-intercalating dye, ethidium bromide). For example, for agarose gel analysis by electrophoresis, a double digest was performed on the pEGFP-N1 plasmid to confirm its authenticity. Restriction enzymes excised DNA immediately before and after the start and end codons for the GFP fragment, respectively (Figure 2.6). TAE buffer was poured over the gel before samples of DNA mixed with loading dye were pipetted into the wells. Electrodes were connected so that the DNA migrated towards the anode and the gel was run at 90 V for 20 min. A 1Kb DNA ladder was also run to enable analysis of DNA fragment sizes when the gel was visualised under UV light. The size of the excised DNA correlated with the expected size of the GFP fragment at ~750 bp (Figure 2.7) thus, the authenticity of this plasmid was confirmed.

2.7.4 Maintenance of DO11.10 hybridoma cells in vitro

The murine T cell hybridoma DO11.10, which recognises $OVA_{323-339}$ in the context of $I\text{-}A^d$ (from Underhill et al; (401)), was cultured in complete RPMI 1640 medium at 37^0C in 5% CO_2. Hybridoma cells were sub-passaged by diluting 1:10 in fresh complete RPMI 1640 medium every 48 h to ensure that cells remained in exponential growth phase.

2.7.5 Electroporation of plasmid DNA into the DO11.10 hybridoma or primary DO11.10 TcR Tg T cells

Briefly, 10 μg DNA was added to cuvettes and stored on ice for 10 min. Next, 1-1.5 x 10^6 DO11.10 hybridoma cells or purified primed or anergic primary DO11.10 TcR Tg $CD4^+$ T cells in 250 μl electroporation media (RPMI 1640 medium supplemented with 20% foetal calf serum) were added to each cuvette. The cuvettes were flicked gently and stored on ice for 10 min before being flicked again and the cells were then electroporated using a Bio-Rad Gene Pulser™ and Pulse Controller (Bio-Rad) set at 960 μF and 280 V. Following electroporation, cuvettes were flicked gently and stored on ice for 10 min before being seeded onto 6-well plates with complete RPMI 1640 medium. Twenty four h after electroporation, dead cells were either removed by density centrifugation using Lympholyte®-M (VH Bio Ltd, Tyne and Wear, UK) or stained with propidium iodide (PI) prior to assessment of GFP expression by Flow Cytometry.

2.8 Establishment of an Ag-specific model in which to study effects of adenovirally delivered genes on T cell responses

2.8.1 Generation of hCARΔcyt.DO11.10 mice and testing for hCAR and DO11.10 TcR Tg expression

hCARΔcyt Tg mice were crossed with DO11.10 mice at the Veterinary Research Facilities at the University of Glasgow in accordance with Home Office regulations and the first filial (F1) generations were screened for dual expression of hCAR and the Tg TcR by flow cytometry (402). Peripheral blood was withdrawn from F1 mice by superficial venepuncture and transferred to 5 ml polystyrene tubes (Falcon, BD). Following their transfer into tubes, cells were re-suspended in 100 μl FcR blocking buffer (anti-CD16/32, clone 4.G-2, hybridoma supernatant, 10 % mouse serum, 0.1 % sodium azide) containing

peridinin chlorophyll-α protein (PerCP)-conjugated anti-CD4 (0.8 µg/ml), biotinylated anti-KJ1.26 (6.4 µg/ml) and anti-CAR (4 µg/ml; clone RmcB; Upstate Biotechnologies, Dundee, UK) for 20 min in the dark at 4^0C. Cells were washed by addition of 1 ml FACS buffer (PBS, 2% FCS, 0.2% NaN_3) per tube before centrifugation at 450 *g* for 5 min. Biotinylated anti-KJ1.26 and purified anti-CAR were then detected by incubation with PE-conjugated streptavidin or fluorescein isothiocyanate (FITC)-conjugated anti-mouse IgG1 (both 5 µg/ml; both BD Pharmingen), respectively, for 10 min in the dark at 4^0C. Cells were then washed as before prior to incubation with 1 ml BD FACS™ Lysing Solution (diluted 1:10 in dH_20; BD Pharmingen) per tube for 10 min in the dark at room temperature. BD FACS™ Lysing Solution is used to lyse red blood cells following immunofluorescence staining of peripheral blood prior to flow cytometric analysis to ensure optimal detection of lymphocytes (403). PBS (1 ml) was added to each tube before washing at 300 *g* for 5 min. Cells were then re-suspended in 200 µl FACS flow and analysed with a FACScan and CellQuest software. PerCP-conjugated Rat IgG2a, biotinylated Mouse IgG2a and purified Mouse IgG1 (all BD) served as isotype controls for CD4-, KJ1.26- and CAR-specific antibodies, respectively.

2.8.2 Adenoviruses

The Ad5.UbP.GFP (404) and Ad5.CMV.GFP vectors both encode an enhanced GFP reporter gene under the control of either a human ubiquitin promoter (UbP) or CMV promoter, respectively. The Ad5.UbP.GFP was originally obtained from Dr. J. Gregori, University of Colorado Health Science Centre, Denver, CO, USA. The Ad5.CMV.GFP was a gift from Prof. A. Baker, Cardiovascular Research Centre, Glasgow, UK

2.8.3 Generation of high-titer stocks of recombinant adenovirus

High-titer stocks of recombinant adenoviruses (rAd) were produced by large scale amplification of a plaque pure stock of adenovirus in a human embryonic kidney (HEK) 293 cell line (gift from Prof. A. H. Baker, University of Glasgow, Glasgow, UK; (405, 406)). Low passage HEK 293 cells were sub-cultured in complete minimal essential medium (MEM; 10% FCS, 2 mM L-Glutamine, 100 U/ml penicillin and 100 µg/ml streptomycin (all Gibco)), in 29 x 150 cm^2 tissue culture flasks (Corning). Cells were allowed to reach 80-90% confluence before being infected with rAd (approximately 1

plaque forming unit (pfu) per cell). The medium was replaced every 3 days until the cells started to detach from the flask. Fresh medium (10 ml) was added to the flasks until this cytopathic effect was complete. Cells were harvested immediately and centrifuged at 250 *g* for 10 min at room temperature before being re-suspended in 15 ml PBS. An equal volume of Arklone P (Trichlorotrifluoroethane; ICI Ltd., Cheshire, UK) was added and the tubes were inverted for 10 s then shaken gently for 5 s. This inversion and shaking was repeated and cells were then centrifuged at 750 *g* for 10 min at room temperature. The uppermost layer, containing the rAd, was removed to a fresh tube. PBS (10 ml) was added to the remaining solvent and the extraction step was repeated. Stocks of rAd were stored at -80^{0}C until purification using CsCl density gradients.

2.8.4 Purification of recombinant adenovirus on CsCl density gradients

Freeze-thawing and extraction by Arklone P is a crude method of adenovirus extraction and stocks can be contaminated with empty viral capsids and cellular proteins which may have cytotoxic effects *in vitro* and *in vivo*. rAd stocks however, can be purified and concentrated efficiently by simple centrifugation on CsCl density gradients. First, 2 ml of CsCl with a density of 1.45 was pipetted into Ultra-Clear centrifuge tubes (Beckman Coulter (UK) Ltd., Buckinghamshire, UK) before addition of a second layer of 3 ml CsCl with a density of 1.32. A third layer of 2 ml of 40% glycerol was carefully added before addition of the crude rAd supernatant. The tubes were then placed into a Sorvall® Discovery™ 90 rotor container, inserted into a rotor (RPS4OT-859) and centrifuged at 25,000 rpm for 1.5 h at 4^{0}C. After centrifugation, a clear band of virus was visible which was situated at the interface of the 1.45 and 1.32 density bands. The virus-containing band was removed by piercing the tube immediately below the virus band with a 22 gauge needle and 1.5 ml syringe and drawn off in a minimal volume. The rAd preparation was then inserted into a Slide-A-Lyzer® dialysis cassette (MW cut off 10,000; Perbio Science UK Ltd., Northumberland, UK) and dialysed overnight against 2 L of 0.01 M Tris pH 8/0.001 M EDTA. The dialysis solution was replaced with fresh 0.01 M Tris pH 8/0.001 M EDTA and supplemented with 10% glycerol then the rAd preparation was dialysed against this solution for 2 h. Stocks of rAd were aliquoted and stored at -80^{0}C.

2.8.5 Titration of recombinant adenovirus by end-point dilution

Following purification on CsCl gradients, rAd was titered by serial dilution on HEK 293 cells. HEK 293 cells were seeded at 1 x 10^4 cells per well into 96-well plates (8 rows of 10; Corning) and incubated at 37^0C in 5% CO_2. After 24 h, when 50-60% confluence was achieved, serial dilutions (10^{-2}-10^{-11}) of CsCl-purified rAd were prepared and the medium in each well was replaced by 100 µl of appropriate adenoviral dilution or medium alone, as described in Figure 2.6. Following incubation at 37^0C in 5% CO_2 for 16-18 h, the medium in each well was replaced again with 200 µl fresh medium and the medium was then changed every 2 days for a total of 8 days.

After 8 days, the plates were examined under a microscope and the number of wells containing plaques, reflecting a cytopathic effect, were counted, and denoted as 'positive'. A plaque appears when "grape-like" clusters of cells round up and detach from the cell monolayer (407). The row in which less than 50% of the wells were positive (example Figure 2.9; row E) and the row immediately above that row, in which more than 50% were positive (example Figure 2.9; row D), were used to calculate the titer of the adenovirus. The titer was calculated in pfu/ml using the following calculation (408).

$$\text{The proportionate distance} = \frac{\text{\% positive above 50\% - 50}}{\text{\% positive above 50\% - \% positive below 50\%}}$$

and log ID_{50} (infectivity dose) =

lowest log dilution above 50% + (proportionate distance x -1)

where '% positive below 50%' is the percentage of plaque-containing wells in the row in which less than 50% of the wells were positive and '% positive above 50%' represents the percentage of plaque-containing wells in the row immediately above that row, in which greater than 50% of the wells were positive.

For example, if titration gives:- @ 10^{-4} all wells positive [10/10]
@ 10^{-6} [10/10]
@ 10^{-7} [10/10]
@ 10^{-8} [9/10]
@ 10^{-9} [3/10]
@ 10^{-10} [0/10]
@ 10^{-11} [0/10]

The proportionate distance = $\frac{90-50}{90-30} = 0.67$

$\log ID_{50} = -8 + (0.67 \times -1) = -8.67$

$ID_{50} = 10^{-8.67}$

$TCID_{50}$ (tissue culture infectivity dose 50) = $\frac{1}{10^{-8.67}}$

$TCID_{50}/100\ \mu l = 10^{8.67}$ x dilution factor (=10)

$TCID_{50}/ml = 10^{9.67} \equiv 4.67 \times 10^9\ TCID_{50}/ml$

However, 1 $TCID_{50} \simeq 0.7$ pfu

Therefore, final titer = 3.3×10^9 pfu/ml

The cells and medium from 3 wells at the highest dilution of Ad that had a visible cytopathic effect i.e. had visible plaques or EGFP expression if Ad was EGFP-containing, were harvested and stored at -80^0C. Stocks could then be used to seed further adenovirus preparations.

2.8.6 Adenoviral transduction of hCAR and hCARΔcyt.DO11.10 cells

PLN and MLN were harvested from BALB/c, hCAR Tg or hCARΔcyt.DO11.10 double Tg mice and single cell suspensions were generated as described in section 2.3.1. Live cells were counted by trypan blue exclusion and plated out at ~ 1 x 10^5/well in DMEM/10 nM Hepes in 96-well plates. Cells were infected with Ad5.CMV.GFP at

multiplicities of infection (MOI) ranging from 0-1000 and then cultured for 1 or 3 h at 37^0C in 5% CO_2. The MOI is the ratio defined by the number of infectious virus particles deposited in a well divided by the number of target cells present in that well. The following calculation was used to determine the quantity of Ad to add to each well.

$$\frac{\text{MOI x number cells/well}}{\text{Titre of Ad (pfu/ml)}}$$

For example: $\frac{1000 \times (8 \times 10^4)}{2.786 \times 10^{10}} = 2.87 \times 10^{-3} = 0.287$ µl neat Ad/well

To wash excess virus out of the culture, samples were centrifuged at 450 *g* for 5 min and re-suspended in 100 µl sterile PBS per well, before being centrifuged again. Cells were then re-suspended in 200 µl sterile CRPMI/well, immediately transferred into fresh plates and incubated for a further 24 h before being harvested and stained for CD4 expression and viability with propidium iodide (PI). Stained cells were analysed by flow cytometry to assess the percentage of live $CD4^+$ T cells that were successfully transduced with GFP (Figure 3.15).

2.9 Statistical Analysis

Results are expressed as mean ± SD or mean + range. To test significance, Student's unpaired *t* test was performed on normally distributed data with *p* values of *≤0.05, **<0.01, ***<0.001 with p≤0.05 being regarded as significant.

Figure 2.1 Analysis of antigen-specific $CD4^+$ T cells from DO11.10 Tg mice by Flow Cytometry. First, lymphocytes were distinguished via their forward scatter (FSC; size) and side scatter (SSC; granularity) properties (A; R1). Unstained lymphocytes are shown in B. PE-conjugated anti-CD4 was used to identify $CD4^+$ T cells (C) and biotinylated-KJ1.26 plus SA-FITC were used to stain the Ag-specific T cell population (D). $KJ1.26^+$ $CD4^+$ T cells were discriminated by setting appropriate gates on isotype controls, mouse IgG2a (C) and rat IgG2a (D) for KJ1.26 and anti-CD4, respectively. Sample plots are shown where the populations of Tg $CD4^+$ $KJ1.26^+$ T cells from an unimmunised mouse (E) and a mouse primed with $OVA_{323-339}$/LPS i.v. (F) were analysed.

Figure 2.2 Tyramide signal amplification. Tyramide signal amplification (TSA™) is an enzyme-based system for high density labelling of target proteins. Streptavidin-Horse radish peroxidase (HRP; A) or primary Ab-HRP (B) conjugates were used to detect the target protein. Next, biotin- (A) or fluorescent-labelled (B) tyramide (Tyr) was added and the HRP catalysed the deposition of multiple fluorescent or biotin labels in the immediate vicinity of the target protein. The biotin labels were subsequently detected by fluorescent-labelled streptavidin (SA; A). Both methods of TSA result in enhanced detection of the protein of interest.

Figure 2.3 Detection of cells by Laser Scanning Cytometry (LSC). Cells are identified by LSC using a series of contours (A). The threshold contour is set on the nuclear stain. The integration contour is set an optimal number of pixels out from the threshold contour, a value which is based on the size of the cell, to allow definition of the edge of the cell (Pixel size is 0.5µm x 0.5µm). The inner peripheral contour is set one pixel out from the threshold contour and the outer peripheral contour is set one pixel in from the integration contour, allowing definition of the periphery of the cell. A cell is discriminated if it emits nuclear fluorescence above a threshold value set by the user (B). A high threshold detects mainly individual events, whilst an intermediate threshold may detect two or more cells as one event and a low threshold will detect multiple cells as one event.

Figure 2.4 Analysis of signalling in antigen specific $CD4^+$ T cells by Laser Scanning Cytometry (LSC). The threshold contour (A; red contour) was used to detect all nucleated cells by their staining with DAPI (A; white arrows). Fluorescently-labelled KJ1.26 within the integration contour (A; green contour) was measured, thus allowing the antigen-specific ($KJ1.26^+$) Tg T cells to be identified (B; green arrows), and the signalling, pERK or Rap1, in the antigen-specific T cell population was assessed using anti-pERK or anti-Rap1 Abs respectively (C; orange). Two background contours (A; blue contours) measured the background fluorescence outside the cells and this value was automatically subtracted from the measured fluorescence values. Positive staining for KJ1.26 and pERK or Rap1 was gated relative to isotype controls (D, E).

Figure 2.5 *In situ* analysis of signalling in antigen specific CD4$^+$ T cells by Laser Scanning Cytometry (LSC). Tissue sections were stained for antigen-specific Tg T cells (KJ1.26; red), pERK or Rap1 (anti-pERK or anti-Rap1; blue) and B cells (B220; green) (A). LSC detected antigen-specific T cells using standard contours (yellow contours; A, C) and measured the levels of pERK or Rap1 inside these cells (D). B cell rich areas were identified using phantom contours (B, E) and tissue maps depicting the location of pERK- or Rap1-expressing antigen-specific Tg T cells within the lymph node with respect to B cell follicles and the paracortex (F). Mouse IgG2a, Rabbit IgG and Rat IgG2aκ isotype controls were used to set gates of positive staining for KJ1.26, pERK or Rap1 and B220, respectively. Numbers and statistics on these cells in both types of area within the lymph node can be quantified.

Figure 2.6 pEGFP-N1 plasmid map. pEGFP-N1 encodes a red-shifted mutant of wild-type GFP and so offers more intense fluorescence and expression in mammalian cells compared to wild-type GFP. This plasmid also harbours a neomycin-resistance cassette (Neo^r) which contains the SV40 early promoter, the neomycin/kanamycin resistance gene Tn5 and polyadenylation signals supplied by the Herpes simplex virus thymidine kinase (HSV-TK) gene. This cassette enables selection of stably transfected eukaryotic cells using the antibiotic G418. The presence of a pUC origin of replication in pEGFP-N1 allows propagation of this plasmid in *E.coli* and a bacterial promoter encoded upstream of the Neo^r cassette elicits resistance to the antibiotic kanamycin when pEGFP-N1 is propagated in *E.coli.* Vector map is courtesy of Clontech.

Figure 2.7 Assessment of pEGFP-N1 authenticity. The pEGFP-N1 plasmid underwent a double digest with restriction enzymes to assess its authenticity. The plasmid was cut once near the start of the GFP codon (661), with BamH1 and again, near end of GFP stop codon (1402), with Not1 for 1 h 20 min at 37^0C before quantitative analysis (as described in Section 2.7.3) on an agarose gel (1% (w/v) agarose in TAE buffer with ethidium bromide). The excised DNA (GFP fragment) appeared as expected in alignment with the 750 bp marker on the 1 kb DNA ladder.

Figure 2.8 pcDNA3.1 plasmid map. pcDNA3.1 was used as a non GFP-encoding control plasmid for transfections described in this chapter. This plasmid contains a human cytomegalovirus (CMV) promoter which permits high level expression of the gene of interest. It has multiple cloning sites in forward or reverse orientation. pcDNA3.1 also harbours a neomycin resistance (Neo^r) gene which allows stable transfection of mammalian cells using the antibiotic G418. Expression of the Neo^r gene is controlled by the SV40 early promoter and the SV40 early polyadenylation signal. The presence of a pUC origin of replication allows replication and growth in *E. Coli* and the ampicillin resistance gene enables selection of the plasmid in *E. Coli*. Vector map is courtesy of Invitrogen.

Figure 2.9 Identification of plaques in adenovirally infected cultures. Serial dilutions (10^{-2}-10^{-11}) of CsCl-purified Ad stock were prepared and added to HEK 293 cells, previously seeded into 96-well plates. After 8 days, the plates were examined under a microscope and the number of wells containing plaques was counted, and denoted as 'positive' (wells containing X). The row in which less than 50% of the wells were positive (row E; dilution 10^{-9}) and the row immediately above that row, in which more than 50% were positive (row D; dilution 10^{-8}), were used to calculate the titer of the adenovirus.

Table 2.1 Antibodies used for flow or laser scanning cytometry.

Table 2.2 Fluorescence spectra and LSC laser/filter set-up information on labels used for laser scanning cytometry.

Chapter 3

Development of technologies for examining T cell signalling *in situ*

Introduction

Current flow cytometric technology allows quantitative assessment of surface and intracellularly expressed molecules on isolated cells. However, the need to disrupt tissues prevents correlation of phenotypic expression with anatomical location. In contrast, immunohistochemistry in conjunction with conventional or confocal microscopy allows localisation of staining, but little in the way of quantitation. Laser Scanning Cytometry (LSC) allows a combination of both approaches, as it can apply quantitative flow cytometric laser technology to intact tissue.

These studies aimed to establish this technology as an effective tool for examining immunological responses *in situ* and ultimately to quantify signalling molecule expression and activation within antigen-specific T cells following induction of T cell tolerance and priming *in vivo*. This is because although, there is considerable interest in examining the intracellular signalling events which may control immune responses (318, 336), current analysis relies on techniques such as Western Blotting which identify activated signalling elements in protein extracts (409). There are a number of limitations of these methods: for example, considerable numbers of T cells are required and the signalling molecules cannot be quantified in individual cells. Furthermore, as Western blotting often dictates use of heterogeneous samples of cells, any differences observed may not be representative of the particular cell type of interest. As a result, small changes that are confined to antigen-specific cells in particular environmental niches, that may be of functional relevance, cannot be detected. By harnessing the sensitivity of flow cytometry, LSC not only allows the level of signalling molecules to be quantified, but can also be used to identify them in individual cells and in distinct tissue microenvironments (12).

In addition, LSC can identify the subcellular localisation of signalling molecules more easily than traditional subcellular fractionation and Western blotting allows. Although some of these aspects have been studied previously using flow cytometry i.e. analysis of antigen–specific transgenic (Tg) T cells isolated from lymphoid tissues *ex vivo* (383, 410), this does not allow subcellular localisation of molecules or intact tissues and anatomical relationships to be examined. Here, the adoptive transfer of trackable T cell receptor (TcR) Tg T cells (378) and the development of methods which allow efficient collection of quantitative data on the kinetics, amplitude and location of signalling within antigen-specific Tg T cells (12, 392), which can be related to the functional status of the cells, has

allowed the application of LSC technology to the study of signalling events in antigen–specific $CD4^+$ T cells *in situ* (411).

A common way to modulate gene expression in a cell is by transfecting the cells with wild type, dominant negative or constitutively active constructs of the gene of interest. Transfection is often effected by electroporation, where an electric charge is passed over the cells, porating the cell membrane thus allowing the plasmid construct to enter the cell where it travels to the nucleus and integrates into the cellular DNA. Unfortunately, this process routinely results in a high cell death rate. Primary quiescent cells are notoriously difficult to transfect and for a long time only cell lines were successfully transfected. The advent of the Amaxa Nucleofector™ technology has provided some advances, as this system offers a non-viral way to transfect primary cells as well as difficult-to-transfect cell lines. Moreover, the cells do not need to be proliferating to be transfected. However, this process of transfection activates the cells and so responses in naïve T cells can not be examined using this system. Also, when this project was being carried out, this technique had not been optimised for murine T cells thus it was not possible to take advantage of this technology at the time.

Viral transduction offers another method of gene delivery into primary cells. In particular, infection with retroviruses has been favoured as a means of gene delivery into lymphocytes (412-414) but this technique has a number of limitations. It requires cell cycle progression of the cellular host to allow viral genome integration (415), the integration site of viral genome is variable, it has limiting efficiency in that not all of the target population is transduced and detectable vector expression can be dramatically reduced over time (>1 month after transfer) *in vivo* (416-418). Also, retroviruses have a small maximum insert size (7-7.5 kb max), thus limiting the size of exogenous genes that can be packaged.

Adenoviruses have been shown to infect a wide range of cell types and offer a number of advantages over retroviruses in that they can infect both dividing and non-dividing cells (419, 420), thus allowing naïve cell responses to be examined. The vectors have a larger maximum insert size (~30 kb) and high titer stocks are easily generated (421). In addition, adenoviral transduction results in the entire cellular population being genetically modified. However, lymphocytes are not usually susceptible to adenoviral transduction due to inefficient binding to the cell surface and internalisation (422-424). Very low expression levels of the adenoviral fiber protein receptor (425, 426) together with limiting levels of α_v-containing integrins (425) on the T cell appear to be the reasons

underlying the inability of adenoviruses to enter T cells. The adenoviral fiber protein receptor, CAR (coxsackie and adenovirus receptor) has been cloned (427-429) and expression of CAR in numerous lymphocyte cell lines confers full susceptibility to adenovirus transduction (430). In addition, as this transduction does not require the cytoplasmic domain of CAR, which constitutes about one third of the protein size (431), spatial restrictions within hCAR-expressing lymphocytes are minimised (430). Recently, Hurez *et al* generated three new murine Tg lines in which thymocytes and lymphocytes express human CAR (hCAR) with a truncated cytoplasmic domain (hCARΔcyt) under direction of a CD2 mini gene (402). They also generated a double Tg hCARΔcyt.DO11.10 line and demonstrated efficient gene transfer of resting and effector antigen-specific $CD4^+$ T cells without perturbing their development (402).

Given that all of the studies conducted during the course of this project utilised DO11.10 TcR Tg mice, with such a system in place, the mechanisms underlying the signalling differences in T cell tolerance and priming could be investigated.

Aims

- To establish and validate laser scanning cytometry (LSC) detection of cell surface markers and intracellular signalling molecules in individual cells.
- To quantitate signalling in antigen-specific T cells *in vitro* and *in situ* by LSC.
- To correlate signalling with functional parameters of T cells by LSC
- To establish a suitable gene delivery system with which to dissect the mechanisms underlying the signalling differences observed in T cell tolerance and priming.

Results: Development of technologies for examining signalling *in situ*

3.1. Establishing LSC as a tool for analysing immune responses

To establish if cell surface markers and intracellular molecules could be examined in antigen-specific T cells using LSC, the functional responses of such cells to different stimuli were examined. A state of anergy or priming was induced in naïve Ag-specific TcR Tg T cells as described in Section 2.4.2. Subsequently, naïve, anergic or primed Ag-specific TcR Tg T cells were stimulated with DC alone (DC) or DC loaded with $OVA_{323-339}$ (DC + Ag) for 20 h before being harvested and analysed by flow cytometry, Western Blotting or LSC as described in Sections 2.3.6, 2.4.6 or 2.6 respectively, and Tables 2.1 and 2.2.

3.1.1. Validation of LSC analysis of functional status and signalling in vitro

3.1.1.1. Identification of antigen-specific T cells by LSC

Initially, it was investigated whether LSC was capable of efficiently distinguishing Ag-specific T cells from other cell types in a mixed population. Thus, naïve cells containing Ag-specific T cells were cultured with DC loaded with $OVA_{323-339}$ for 20 h and then cytocentrifuged onto slides before being stained with DAPI, to detect all nucleated cells in the sample, and KJ1.26 (or its isotype control) to identify the TcR Tg T cells within the population. These cells were then analysed by LSC (Figure 2.4). All cells were detected via their nuclear staining (Figure 2.4A) and the Ag-specific T cells were readily identified by positive staining with anti-KJ1.26 Ab, which recognises their Tg TcR (Figure 2.4B), using a series of contours as described in Section 2.6. A suitable analysis gate to distinguish the Ag-specific T cells was set using isotype control data (Figure 2.4D). Such analysis indicates that LSC is indeed an efficient method with which to detect Ag-specific T cells within a mixed population of cells.

3.1.1.2. Activation status of antigen-specific T cells by LSC

Next, it was investigated whether LSC could detect changes in immunologically relevant molecules, in T cells, with the same sensitivity and reproducibility as a standard flow cytometer. Thus, the expression of CD69, a glycoprotein upregulated and detectable on the surface of antigen-specific T cells within 1 hour of TcR ligation (432-434), and

which is still measurable 20 h after stimulation, was examined. To do this, naïve Ag-specific T cells that had been stimulated with DC alone or DC loaded with $OVA_{323-339}$ for 20 h, were stained with CD4, KJ1.26 and CD69 Abs for analysis by flow cytometry or with DAPI and KJ1.26 and CD69 Abs for analysis by LSC. Conventional flow cytometry showed that CD69 expression was markedly increased, as expected, in $CD4^+$ Ag-specific T cells stimulated with $OVA_{323-339}$–loaded DC (76.4 % expressed CD69 compared to 4.8 % for T cells stimulated with DC alone; Fig. 3.1A, B, F). Similarly, an increase in the proportion of antigen-stimulated cells expressing CD69 (52 % compared with 15 % for un-stimulated cells) was also observed when the samples were assessed by LSC (Fig. 3.1C-F). These data confirm that LSC is capable of detecting a similar trend in CD69 expression in these samples as that measured by flow cytometry.

3.1.1.3. Analysis of cell cycle and apoptosis by LSC

The up-regulation of CD69 expression observed in the $CD4^+$ T cells, which had been stimulated with their specific Ag in the context of MHC II, indicated that these cells had been activated. Therefore, it was hypothesised that they would be progressing through cell cycle and hence the cell cycle status of these cells was analysed to test this hypothesis. LSC has previously been shown to be a useful tool for assessing the cell cycle status of cells (12, 435-437), as it has the ability to both determine the DNA content of cells using stoichiometric fluorescent DNA–specific dyes and measure the DNA concentration utilising the Max Pixel detection parameter. By contrast, flow cytometry is unable to measure DNA concentration in such a manner and so, for example, cells at G_2 cannot be readily distinguished from those in mitosis, using this technology. In order to establish this type of LSC analysis for Ag-specific T cells, naïve T cells were treated with anti-CD3 + anti-CD28 Abs to induce priming and then re-stimulated with $OVA_{323-339}$-loaded DC for 20 h, as described in Section 2.4.3. The cells were then stained with DAPI to identify their nuclei and analysed by LSC (Figure 3.2).

By plotting Max Pixel (value of most highly fluorescent pixel within the cell) versus Integral (sum of all fluorescence within the cell) values of DAPI staining, a plot can be generated depicting the different stages of cell cycle (Figures 3.2 and 3.3A). This is because an increase in DAPI Max Pixel reflects an increase in chromatin concentration within the cell, thus allowing mitotic cells (green gate), which contain more concentrated chromatin (438, 439), to be distinguished from those cells in S phase (blue gate). Similarly, an

increase in DAPI Integral reflects an increase in the total DNA content within the cell and so cells in G_2/M (4n DNA) can be distinguished from those in G_0/G_1 (2n DNA; black gate). Newly formed daughter cells (ND; pink gate) have the same DNA content (Integral) as cells in G_0/G_1 but they still have more concentrated chromatin and so have a higher Max Pixel value. Apoptotic cells (red gate) bind less DAPI as they have fragmented DNA and contain apoptotic bodies, and as such can be readily distinguished from the cells in G_0/G_1.

When cells are scanned by LSC the cytometer records the precise x- and y-position of every event detected thus allowing these cells/events to be re-located to at a later date for the purpose of viewing and image capture. The re-location feature of LSC allowed cells at different stages of cell cycle to be directly imaged (Figures 3.2 and 3.3A). This imaging confirmed that the cells in separate gates on the scattergram were morphologically consistent with the corresponding stage of cell cycle. Apoptotic cells did not look cellular and appeared as collections of small apoptotic bodies (Figure 3.3A) with less bright and disorganised DNA staining (Figure 3.2). Cells in G_0/G_1 were fairly small (Figure 3.2 and 3.3A), consistent with them being in a resting state, whereas cells in S phase appeared to be almost double the size of the cells in G_0/G_1 (Figure 3.2 and 3.3A). This was not surprising due to cell growth and replication of DNA in preparation for mitosis. Indeed, mitotic cells were of a similar size to the cells in S phase but they were morphologically distinct in that the instigation of nuclear division was visually apparent (Figure 3.2). New daughter cells appeared as small cells with intense DAPI staining, reflecting the fact that their DNA was still temporarily condensed (Figure 3.2 and 3.3A). With this type of LSC analysis established, the cell cycle status of immunologically relevant samples could be assessed.

T cells are known to progress through cell cycle and proliferate when they are stimulated with Ag in the presence of co-stimulation (440). In order to assess the cell cycle status of Ag-specific T cells in response to stimulation with Ag by LSC, naïve Tg TcR T cells were cultured with $OVA_{323-339}$–loaded DC for 20 h before being stained with DAPI and anti-TcR Tg (KJ1.26) Ab, to distinguish the antigen-specific TcR Tg T cells. The percentage of antigen-specific T cells in each stage of cell cycle was then quantitated by LSC (Figure 3.3A, B). The highest proportion of TcR Tg T cells (52 %) were in G_0/G_1 but as expected, a large proportion (39 %) of the cells had progressed to S phase (Figure 3.3B). However, at this time following antigenic stimulation, there was little mitosis and few new daughter cells being produced, results consistent with previously published analysis by flow cytometry (441).

3.1.1.4. Further analysis of apoptosis by LSC

In addition to their distinctive DNA staining profile, apoptotic cells can also be identified by labelling the sites at which DNA fragmentation occurs. Internucleosomal DNA cleavage (fragmentation) was first identified in glucocorticoid-treated rat thymocytes (442) and is now recognised as a marker for apoptosis. The fragments of DNA, each 180-200 base pairs in length, have 3'-hydroxyl ends which can serve as starting points for terminal deoxynucleotidyl transferase (TdT), which adds deoxyribonucleotides. Addition of the deoxythymidine analogue, 5-bromo-2'-deoxyuridine 5'-triphosphate (BrdUTP) to the TdT reaction serves to label the break sites. Once incorporated into the DNA, BrdU can be detected by an Alexa Fluor® 488-labelled anti-BrdU Ab. This method of labelling DNA strand breaks is known as terminal deoxynucleotide transferase dUTP nick end labelling (TUNEL). TUNEL is a well established method of detecting apoptotic cells by LSC (393-395) and this technique was therefore established in order to expand the range of LSC analyses of Ag-specific T cell responses.

Thus, anergy or priming was induced in Ag-specific Tg TcR T cells by treatment with anti-CD3 ± anti-CD28, as described in section 2.4.2, and the anergic and primed T cells were re-stimulated with DC loaded with $OVA_{323-339}$ for 1 h, prior to staining with DAPI, anti-KJ1.26 and TUNEL. Positive and negative control human lymphoma cell lines supplied with the TUNEL kit were also stained and all samples were analysed by LSC (Figure 3.4 and Table 3.1). As expected, the positive control cells had much greater TUNEL staining, indicating a higher level of apoptosis, compared to the negative control cells (Figure 3.4A, B and Table 3.1). More apoptosis, as indicated by an increased percentage of cells staining positive for TUNEL as well a higher level of TUNEL expression (MFI), was also observed in the anergic compared with primed Ag-specific T cells that had been re-stimulated with Ag (Figure 3.4C, D and Table 3.1). These results were anticipated, as anergic cells are known to exhibit increased apoptosis compared to primed cells upon re-stimulation with Ag (49). The presence of more apoptotic cells, as evidenced by the presence of green fluorescence, in the positive control sample and the anergic T cells was confirmed by re-locating to these cells using LSC and imaging them (Figure 3.4B, C).

3.1.1.5. Detection of signalling molecules in Ag-specific T cells by LSC

Having established LSC as an efficient technique for assessing the functional status of Ag-specific T cells, the ability of LSC to quantify intracellular signals, that would usually be assessed by biochemical techniques, was next examined. The signalling molecule ERK MAPKinase was selected for study here as it is known to be important for many aspects of T cell biology including IL-2 production, cell cycle progression and proliferation (317, 443, 444). Moreover, its activation status is readily detected by specific Abs which recognise the dually phosphorylated form of ERK (pERK) and detection of ERK and pERK has been well established for Western Blotting and flow cytometry (445-447). Analysis of signalling by Western Blotting was thus conducted to validate the type of data generated by LSC (Figure 3.5A). Naïve Ag-specific T cells were cultured with DC alone (-) or DC loaded with $OVA_{323-339}$ (+) for 1, 3, 6 and 20 h before whole cell lysates were prepared for analysis of ERK activation by Western Blotting. At all timepoints examined, the level of ERK activation (pERK) was greater in the samples that had been stimulated with Ag compared to those cultured with DC alone (Figure 3.5A), this difference being most striking at 6 h. By contrast, the level of ERK activation decreased over time in the un-stimulated samples with pERK being barely detectable at 20 h. It must be noted that the ERK levels detected by Western Blotting are representative of ERK signalling in all of the cell types in the cultures and cannot be specifically attributed to the Ag-specific T cells.

Cells harvested at 20 h were also stained with DAPI and KJ1.26- and pERK-specific Abs, to measure the levels of activated ERK (pERK) in individual Ag-specific T cells by LSC (Figure 3.5B). Profiles of pERK signalling in Ag-specific T cells cultured with DC alone (DC) or DC loaded with $OVA_{323-339}$ (DC + Ag) are shown in Figure 3.5B. Here, an increase in the level of pERK expression was also observed in the Ag-stimulated cells compared with the un-stimulated cells (Figure 3.5B). However, the variation in pERK expression observed was specifically representative of the levels of ERK activation in individual Ag-specific T cells. Nevertheless, when the level of ERK activation was quantitated by LSC, the proportion of Ag-specific T cells expressing pERK (C) as well as the level of pERK expression (MFI; D) was found to be markedly increased in the Ag-stimulated population as a whole.

3.1.1.6. Detection of signalling in individual T cells throughout the cell cycle

The ability of LSC to assess the cell cycle status of Ag-stimulated, Ag-specific T cells was evidenced in Section 3.1.1.4 and efficient detection of intracellular signalling in Ag-specific T cells by LSC was demonstrated in Section 3.1.1.5. Thus, it seemed pertinent to next develop analysis of signalling in individual Ag-specific T cells at different stages of cell cycle by LSC. As described in Section 1.1.2.2, a T cell must experience both peptide in the context of MHC and co-stimulation via CD28 for it to become fully activated and undergo proliferation. Moreover, co-stimulation is known to directly regulate T cell entry into cell cycle and progression through the G_1 phase in an IL-2-independent manner by downregulating the CDK inhibitor, $p27^{kip1}$, which results in the activation of CDKs (448). Further progression into S phase is regulated by both IL-2-dependent and –independent mechanisms (448-451), evidenced by the fact that even in the absence of IL-2, some cells manage to proceed into S phase (448). Active cdc2/CDK2 is required for progression through cell cycle beyond the G_1 phase, as it is likely to be responsible for the hyperphosphorylation of Rb and hence, subsequent S phase entry (452, 453).

Thus, in order to correlate signal expression with functional outcome (i.e. cell cycle status), anergic and primed Ag-specific T cells were re-stimulated with DC loaded with $OVA_{323-339}$ for 1 h before being stained with DAPI and KJ1.26- and p-cdc2/p-CDK2-specific Abs for analysis of p-cdc2/p-CDK2 expression in TcR Tg T cells by LSC (Figure 3.6). In this case, the relationship between p-cdc2/p-CDK2 and transit through S phase was examined. This type of analysis enables observation of the range of intensities of p-cdc2/p-CDK2 expression in individual anergic and primed Ag-specific T cells at different stages of cell cycle (Figure 3.6A). LSC also allows quantitation of this data, thus, the percentage of Ag-specific T cells per stage of cell cycle expressing p-cdc2/p-CDK2 can be calculated (Figure 3.6B) and the level at which this signal is expressed in individual Ag-specific T cells in different cell cycle stages can be measured (Figure 3.6C). Expression of p-cdc2/p-CDK2 (inactive cdc2/CDK2) was expected to be higher in the anergic compared to primed T cells, as active cdc2/CDK2 is required for progression through cell cycle beyond the G_1 phase (258). Indeed, a greater proportion of the anergic compared to primed T cells in S phase were found to be expressing p-cdc2/p-CDK2 even at this early timepoint (36 % compared to 23 %; Figure 3.6B). However, rather surprisingly, the anergic T cells were found to be expressing it at a much lower level than the primed T cells in this phase of the cell cycle (Figure 3.6C). The low level of p-cdc2/p-CDK2 expression in those cells

suggests that they might progress through cell cycle thus, perhaps at this early timepoint such anergic cells had already passed the G_1 restriction point at the time of challenge with Ag but would not be able to progress to S phase after they had transited through to G_1 again. It should be noted that such cells are very low in number (Figure 3.6A). Thus, alternatively, those cells may be Ag-specific T cells in the anergic population which had themselves escaped anergy induction. As there is no definitive marker for anergy, it cannot be determined as to whether 100 % of the T cells in an anergic population have in fact been anergised.

3.1.1.7. Subcellular localisation of pERK signals in primed Ag-specific TcR Tg T cells

Another powerful feature of LSC technology is its capability to quantitate expression of intracellularly-expressed molceules in distinct subcellular locations. To enable this type of data acquisition, peripheral contours, in addition to the standard threshold and integration contours routinely used for LSC analysis, are required. The first peripheral contour was placed one pixel (one pixel = 0.5µm (x-axis) and 0.5µm (y-axis) for 40x objective) out from the threshold contour and the second peripheral contour placed one pixel inside the integration contour thus delineating the peripheral area of the cell, external to the nucleus (Figure 3.7A. ii). Data collected from within these peripheral contours can then be expressed as the peripheral fluorescence integral on a histogram (Figure 3.7A. iii). The levels of non-peripheral pERK expression can also therefore be generated by subtracting the peripheral fluorescence values from the total fluorescence values (Table 3.2). Such non-peripheral fluorescence values are not definitive, but can provide an indication of the level of signal expressed in areas distinct from the periphery of the cell, such as the nucleus.

To demonstrate this analysis, primed Ag-specific TcR Tg T cells were cultured with DC alone or DC loaded with $OVA_{323-339}$ for 20 h before being stained with DAPI and KJ1.26- and pERK-specific Abs. Subsequently, total, peripheral and non-peripheral levels of pERK expression in these Ag-specific T cells were quantitated by LSC (Figure 3.7B. ii, iii, v & vi, & Table 3.2). The proportion of cells expressing pERK increased following re-stimulation with Ag (Figure 3.7B. v cf. ii). Moreover, a greater proportion of these cells expressed pERK in their periphery upon re-stimulation with Ag (Figure 3.7B. vi). As shown in Table 3.2, pERK is detected in all parts of primed TcR Tg T cells which are cultured with DC alone and the levels of total, peripheral and non-peripheral pERK

expression were increased when these primed T cells were re-stimulated with $OVA_{323-339}$-loaded DC, indicating that T cells which receive a second signal though their TcR, via the MHC:peptide complex on the DC, express pERK at a higher level in all areas of the cell.

Using the re-location feature of LSC, representative images of primed antigen-specific T cells expressing pERK were captured (Figure 3.7C). Morphological examination showed a diffuse pattern of staining of the TcR and pERK all over the cells when they were cultured with DC alone (Figure 3.7C (DC)), whereas both molecules appear more punctate and accumulate in discrete locations near the cell surface in T cells that were re-stimulated with $OVA_{323-339}$-loaded DC (Figure 3.7C (DC+Ag)). The intensity of pERK staining in the cells which were incubated with DC alone was much lower than that in T cells re-stimulated with $OVA_{323-339}$-loaded-DC and so the pERK image shown in Figure 3.7C (DC) was over-exposed to show the distribution of the signal more clearly. This ability of LSC to reveal differences in the subcellular localisation of signalling molecules adds to its portfolio as these differences cannot be inextricably linked to corresponding quantitative data by standard techniques such as confocal microscopy or subcellular fractionation.

3.1.1.8. Quantitation of focused intracellular pERK staining in anergic and primed Ag-specific TcR Tg T cells

In addition to its ability to detect and measure the expression of immunological molecules in distinct subcellular locations, LSC has a probe spot counting feature, denoted Fluorescence *in situ* hybridisation (FISH) spot analysis in the LSC software package, which enables detection and measurement of fluorescent 'spots' (FISH spots) within the threshold contour boundary. Individual FISH spots are detected using secondary contours which are set, inside the threshold contour, to detect the fluorescent parameter of interest (Figure 3.8 A & B). FISH is a cytogenetic technique first developed for the detection of nucleic acid targets *in situ*, in *Drosophila melanogaster* (454). The nucleic acid target is detected via hybridisation of a complementary sequence, fluorescent dye-labelled nucleic acid 'probe' to the sample. Upon completion of hybridisation, the hybridised fluorescent probe spots can be visualised under a fluorescence microscope (455, 456) and quantitated by LSC (457, 458). Until now, the FISH spot analysis feature of LSC has primarily been used for chromosomal studies (459-461) with one group adapting this attribute for the phenotypic and functional analysis of individual clones from a human breast cancer cell line (462). These FISH spot analyses were designed to detect FISH spot fluorescence within the

nucleus hence, the nuclei were fluorescently stained in these studies and the threshold contour was set to detect the nuclear stain. By setting the threshold contour to detect the fluorescence emitted from a fluorescently-labelled cell surface marker (in this case, an Ag-specific Tg TcR), it was possible to develop FISH spot analysis for topographic examination of signalling molecule expression within Ag-specific T cells (Figure 3.8).

For example, anergic and primed Ag-specific TcR Tg T cells were cultured with DC alone or DC loaded with $OVA_{323-339}$ for 1 h prior to being stained with KJ1.26- and pERK-specific Abs, as described in Section 2.5.1 for LSC FISH spot analysis, as follows. The threshold contour was set to detect Ag-specific ($KJ1.26^+$) T cells via their fluorescently-labelled Tg TcR and secondary contours, demarcating FISH spots, were set to detect 'spots' of pERK fluorescence within the threshold contour boundary. The cells were then analysed by LSC and the number of $pERK^+$ FISH spots per Ag-specific T cell, as well as the pERK FISH Integral (total fluorescence emitted by all FISH spots in one cell) was quantitated (Figure 3.8). Overall, a higher percentage of primed compared to anergic Ag-specific T cells contained multiple $pERK^+$ FISH spots per cell (Figure 3.8A, B & D). Moreover, the proportion of both anergic and primed T cells containing multiple $pERK^+$ FISH spots increased upon re-stimulation with Ag and this increase was greater in the primed compared to anergic T cell population. In addition, the primed T cells which had been re-stimulated with Ag, exhibited the highest pERK FISH Integral value compared to the other samples (Figure 3.8C), which was not surprising as these cells possessed the highest number of $pERK^+$ FISH spots.

3.1.2 Translation of LSC analysis to cells in tissue in situ

Once LSC had been established as a suitable tool for analysing Ag-specific T cell responses *in vitro* it seemed pertinent to develop this technology to detect these parameters in a more physiological setting namely, in Ag-specific T cells *in situ*.

3.1.2.1 Tracking antigen-specific T cells in situ

In order to establish detection of Ag-specific T cells *in situ*, BALB/c recipients were immunised s.c. with OVA (100 µg) in 100 µl PBS/50% CFA 24 h after adoptive transfer of Ag-specific TcR Tg ($KJ1.26^+$) T cells and inguinal lymph nodes were harvested and sectioned 3 days after immunisation. Sections were stained for expression of KJ1.26, in order to detect the Ag-specific T cell population, and analysed by LSC. Previously, analysis

of cells in tissue sections has been accomplished by contouring on nuclei, but this method of detecting cells *in situ* is not ideal as not all of the nucleated cells constituting a tissue section can be identified individually due to the mathematical restrictions placed on the setting of separate contours on closely situated individual cells. The adoptive transfer system, described in Section 2.3.3, overcomes these issues as it generates an even distribution of antigen-specific TcR Tg cells throughout the thymus-dependent area (TDA) of the lymph node, which can be readily distinguished from the endogenous T cells. The threshold contour was set to detect the fluorescence emitted from the KJ1.26-labelled T cells (Figure 2.5A) thus, the Ag-specific T cell population *in situ* was identified by LSC (Figure 2.5C) and the number of Ag-specific ($KJ1.26^+$) T cells per section was quantitated by LSC (Figure 2.5C). Similar to analysis of Ag-specific T cells *in vitro*, isotype controls were used to set gates denoting $KJ1.26^+$ staining in these tissue sections, thus enabling identification of the Ag-specific T cells. As these data show, LSC is indeed capable of detecting and quantitating the number of Ag-specific T cells *in situ*.

3.1.2.2 Measuring cell division of antigen-specific Tg T cells by LSC

Having demonstrated the ability of LSC to detect clonal expansion in LNs, the differences in numbers of cell divisions *in vivo* using 5-(and-6)-carboxyfluorescein diacetate, succinimidyl ester (5(6)-CFDA SE (CFSE) was determined within normal tissue architecture, in order to determine whether such clonal expansion was due to proliferation (463, 464). CFSE permeates cellular membranes and binds spontaneously and permanently to free amine groups of cellular proteins whereupon it segregates equally between daughter cells during mitosis. This results in the sequential halving of fluorescence intensity in progeny cells and so the number of cell divisions that a cell has undergone can be measured by flow cytometry (463-466).

To do this, BALB/c recipients were immunised s.c. with OVA (100 µg) in 100 µl PBS/50% CFA 24 h after adoptive transfer of CFSE-labelled (labelling described in Section 2.3.2) antigen-specific Tg TcR ($KJ1.26^+$) T cells and inguinal lymph nodes were harvested and sectioned on days 3 and 5 after immunisation. Sections were stained with anti-TcR Tg Ab (KJ1.26), as described in Section 2.5.2, to identify the antigen-specific T cells and CFSE expression levels in these cells were imaged (Figure 3.9A) and quantitated by LSC (Figure 3.9B, C). Imaging revealed varying levels of CFSE expression by antigen-specific ($KJ1.26^+$) T cells in immunised sections (Figure 3.9A). LSC analysis showed that

these cells had undergone much more cell division at day 5 (69 % had undergone 6 or 7 divisions) than at day 3 (49 % had undergone 6 or 7 divisions; Fig. 3.9B, C and Table 3.4). To validate such LSC data, cell division, as indicated by differential CFSE expression, in these cells was also assessed on day 5 after immunisation, by flow cytometry. A similar profile of CFSE expression was observed using LSC and flow cytometry, with the majority of the cells having undergone 5 or more divisions in both cases (Figure 3.9C versus E). As expected, very little cell division was observed in the unimmunised sample (Figure 3.9D). These data demonstrate the validity and advantage of using LSC to examine cell division in this manner, as LSC is capable of detecting different levels of CFSE expression in antigen-specific T cells *in situ*.

3.1.2.3 Detection and quantitation of pERK-expressing Ag–specific Tg T cells situated in different anatomical locations by LSC

Having established that LSC could detect Ag-specific T cells *in situ* and assess their cell division status therein, the intracellular signalling profile of these Ag-specific T cells *in situ* was examined. Thus, BALB/c recipients were immunised s.c. with OVA (100 μg) in 100 μl PBS/50% CFA 24 h after adoptive transfer of antigen-specific Tg TcR ($KJ1.26^{+}$) T cells (described in Section 2.3.3) and inguinal lymph nodes were harvested and sectioned on day 3 after immunisation. Sections were stained with KJ1.26 and anti-pERK Abs, as described in Section 2.5.2, for the identification of the antigen-specific T cells and measurement of pERK expression levels in these cells by LSC. Ag-specific T cells were identified as described in Sections 2.6.3 and 3.1.2.1 and the percentage of Ag-specific T cells expressing pERK (58 %) as well as the level of pERK expression (MFI; 253511) in these cells was quantitated by LSC (Figure 3.10Aiii.). To assess Ag-specific T cell signalling in distinct anatomical locations within the lymph node, the 'tissue mapping' facility of LSC was exploited. Thus, tissue sections from the experiment described above were stained with a B220-specific Ab, to detect B cells, in addition to the KJ1.26- and pERK-specific Abs. In order to identify the densely packed B cell follicles, phantom contours were applied as described in Section 2.6.3 and Figure 2.5. The ability of LSC to generate tissue maps (described in Figure 2.5) depicting the location of B cell follicles (Figure 3.10B) and thus highlighting the paracortical region, enabled the quantitation of antigen-specific T cells in different anatomical locations within the lymph node (Figure

3.10A. ii). Moreover, the number of antigen-specific Tg T cells expressing the intracellular signalling molecule pERK, in these different locations, was also assessed (Figure 3.10A. iv and B. iii).

To quantitate these data, gates were placed onto follicular and paracortical regions of the tissue map (Figure 3.11A) and consequently statistics representative of these regions were calculated (Figure 3.11C). This analysis confirmed the visual microscopic assessment that a greater proportion of Ag-specific Tg T cells were present in the paracortical compared to follicular region of the lymph node (Figure 3.11C). Moreover, a higher percentage (93 % versus 7 %) of the Ag-specific Tg T cells expressing pERK were situated in the paracortical compared to follicular regions. However, when the level of pERK expression in Ag-specific T cells situated in the follicles and paracortex was measured, these T cells expressed a similar amount of pERK, irrespective of their location within the lymph node (Figure 3.11C). As mentioned previously, the re-location feature of LSC can be used for image capture of cells in regions of interest on a histogram or scatter plot. This facility is also available for tissue maps and a follicle of interest was imaged in this manner, to demonstrate this type of analysis (Figure 3.11B).

3.2. Development of methods for genetically modulating signals implicated in driving tolerance and priming

The above mentioned techniques allow correlation of signalling with functional parameters. To demonstrate causal relationships, methods with which to causally dissect the mechanisms underlying the signalling differences observed in T cell tolerance and priming *in situ*, were required. Therefore, a number of genetic techniques were considered and both transfection (via electroporation) and transduction (adenoviral) of primary and hybridoma Ag-specific T cells were assessed.

3.2.1. Transfection of DO11.10 hybridoma cells

Firstly, DO11.10 hybridoma cells were used in order to optimise transfection techniques before studies on primary DO11.10 T cells commenced. In order to establish whether DO11.10 hybridoma cells could be transfected successfully, such cells were electroporated with 10 or 20 μg of either pEGFP-N1 or pcDNA3.1 at 960 μF and 280 V and cultured for 24 h before being viewed using a fluorescence microscope. pEGFP-N1 was used simply to express EGFP in these cells (i.e. as a transfection marker) and

pcDNA3.1 was used as a control vector (i.e. lacking EGFP). As predicted, transfection with the control plasmid, pcDNA3.1, resulted in no green fluorescence in the cells at either concentration (Figure 3.12A, C) whereas, GFP-expressing cells were visible in the populations transfected with the pEGFP-N1 plasmid (Figure 3.12B, D). Moreover, transfection with 20 μg DNA appeared to generate a higher proportion of GFP^+ cells (Figure 3.12D). A range of electroporation conditions were then examined for the pEGFP-N1 plasmid to determine the optimal transfection conditions for DO11.10 hybridoma cells (Figure 3.12E). It was clear that optimal transfection efficiency (28 %) was achieved for the pEGFP-N1 plasmid under electroporation conditions of 960 μF and 280 V. However, it would have been preferred if this transfection rate was higher.

3.2.2. Attempted transfection of primary DO11.10 Tg T cells

Many mechanistic studies have generated information on the role of specific genes expressed in T cells. However, much of this work has involved the transfection of tumour cell lines or cell clones and as such may not be representative of the events which occur in primary T cells. For example, one report describes how the transcriptional processes that lead to production of IL-2 differ between Jurkat cells and primary human T cells (467). Some groups have successfully transfected primary T cells, but only after proliferative stimulation with IL-2 and PMA (468) or concanavalinA (ConA) (469) suggesting that naïve T cells cannot be transfected or analysed in this way. Nevertheless, other protocols, using sub-optimal concentrations of T cell stimuli, have been reported to be successful for transfecting primary naïve T cells without activating them, as indicated by IL-2 expression levels (467, 470).

In order to develop a system that could be applied to naive cells which could then be transferred to an *in vivo* model, transfection of primary antigen-specific T cells from DO11.10 Tg mice using one of the latter protocols described by Chrivia et al (470) and optimised by Cron *et al* (471) was attempted. Briefly, single cell suspensions were generated from PLN and MLN harvested from DO11.10 Tg mice and the $CD4^+$ T cells were purified. $CD4^+$ T cells were then rested or stimulated with anti-CD3 in the absence or presence of anti-CD28, to induce anergy or priming respectively, for 48 h before addition of 10 μg/ml ConA and further incubation for 20 h. Cells were then centrifuged and re-suspended in electroporation media prior to electroporation with pcDNA3.1 or pEGFP-N1.

Following electroporation, the cells were transferred to fresh media and rested for 2 h with periodic agitation before being stimulated with PMA and ionomycin for 7 h. After this time, the cells were viewed under a fluorescence microscope, at regular intervals, to check for green fluorescence which would indicate EGFP expression in the electroporated cells.

Unfortunately, although this protocol was repeated numerous times with a number of modifications, transfection of primary T cells was unsuccessful, as evidenced by no green fluorescence in these cells following the transfection procedure hence, it was necessary to develop another method for the genetic modification of primary T cells.

3.2.3. Establishment of hCAR Tg and hCARΔcyt.DO11.10 double Tg murine lines

Transduction offers a viral method of gene delivery into cells and adenovirus-mediated transduction has been demonstrated in naïve and effector primary T cells from hCARΔcyt mice whose thymocytes and lymphocytes express the human coxsackie/adenovirus receptor (hCAR) on their cell surface. In order to confirm that the hCAR Tg colony that was imported did in fact express hCAR on the surface of their T lymphocytes, a sample of their peripheral blood was taken, fluorescently stained for hCAR and CD4 expression and analysed by flow cytometry as described in Section 2.3.6. Lymphocytes were identified on the basis of their known size (forward scatter) and granularity (side scatter; Figure 3.13A) and this lymphocyte population (R1) was subsequently analysed for expression of both hCAR and CD4 (Figure 3.13B). It was found that all $CD4^+$ lymphocytes also expressed hCAR indicating that these mice carry the Tg receptor, hCAR, on their $CD4^+$ T cells.

The hCARΔcyt Tg mice were then crossed with DO11.10 Tg mice in order to generate an antigen-specific T cell system with which to study adenovirally delivered genes of interest. To confirm whether the offspring of such cross-breeding did indeed express both hCAR and DO11.10 Tg receptors on their T lymphocytes, peripheral blood was harvested from the first filial (F1) generations and fluorescently stained for expression of hCAR, CD4 and the DO11.10 Tg TcR (as detected by the monoclonal Ab KJ1.26) and analysed by flow cytometry (Figure 3.13C-E). Again, lymphocytes were identified according to their size and granularity (Figure 3.13C) and the co-expression of CD4 and KJ1.26 on the lymphocytes was assessed (Figure 3.13D). This $CD4^+$ $KJ1.26^+$ T cell population was subsequently examined for expression of hCAR and it was observed that

100% of $CD4^+$ $KJ1.26^+$ T cells in these hCARΔcyt.DO11.10 Tg mice express hCAR (Figure 3.13E).

3.2.4. Transduction of primary antigen-specific, hCAR bearing, Tg T cells

With the murine hCARΔcyt and hCARΔcyt.DO11.10 Tg lines established, some preliminary transduction experiments were performed. PLN were harvested from hCAR Tg mice and single cell suspensions were prepared, as described in Section 2.3.1. hCAR PLN cells were then infected with adenovirus (Ad5.CMV.GFP) for 1 or 3 h at a variety of multiplicities of infection (MOI) before excess Ad was washed off and the cells were subsequently incubated for 24 h with media alone, anti-CD3 alone or anti-CD3 + anti-CD28 to generate naïve, anergic or primed populations, respectively. The cells were then viewed under a fluorescence microscope to check for green fluorescence and hence GFP expression. Exemplar images of anergic and primed cells which had been successfully transfected with Ad.CMV.GFP at an MOI of 100 for 3 h are shown (Figure 3.14).

All cells were subsequently stained for CD4 expression and with propidium iodide (PI) to assess viability prior to Flow Cytometric analysis (Figure 3.15). Again, lymphocytes were identified on the basis of their known size (forward scatter) and granularity (side scatter; Figure 3.15A) and this lymphocyte population (R1) was subsequently analysed for viable cells (PI negative; R2; Figure 3.15B). Although infection with the adenoviral vector caused some cell death, a considerable proportion of the lymphocytes remained viable. These live lymphocytes were then examined for expression of CD4 (Figure 3.15C) and the level of GFP expression in these $CD4^+$ T cells was assessed (Figure 3.15D). Exemplar scattergrams are shown for uninfected (MOI: 0) and infected (MOI: 100) naïve, anergic and primed hCAR PLN cells.

Analysis of the $CD4^+$ population showed that whilst mock infection (MOI 0) resulted in no GFP-expressing $CD4^+$ cells, infection under conditions of no stimulation (naïve), anergy or priming resulted in >80% of $CD4^+$ T cells expressing GFP, with the brightest and highest proportion of GFP-expressing $CD4^+$ cells observed under conditions of priming (91.12%). In order to optimise the transduction efficiency in this system, a range of MOI's (0-1000) and two infection times (1 and 3 h), were assessed as described above (Figure 3.16). At both infection times the optimal MOI was found to be 100 and the

transduction efficiency at this MOI appeared slightly improved if the infection time was 3 h (Figure 3.16B).

Collectively, these data show that it is possible to infect naïve and activated primary hCAR Tg T cells with adenoviral constructs and moreover, indicate that transduction of hCARΔcyt.DO11.10 double Tg T cells with mutant signalling elements under conditions of tolerance and priming will likely be successful.

Discussion

The signalling mechanisms underlying lymphocyte effector function have traditionally been examined using standard biochemical techniques such as Western Blotting, and whilst such analysis has generated a plethora of information for this field of immunology, there are several limitations to using this approach. Such analysis requires a considerable amount of sample and this has previously been achieved using immortalised cell lines/clones (88, 326, 472) or large populations of purified cells, subsequently exposed to polyclonal stimulation (473). However, due to the nature of these samples, the data acquired does not necessarily reflect the responses of physiological frequencies of individual antigen-specific cells within their environmental niche within primary or secondary lymphoid tissue. Moreover, such data represents the average response of all of the cells in the sample population at any one time and hence does not provide any information on the differential kinetics, amplitude or subcellular localisation of signals generated by functionally distinct subgroups within the population.

Technologies for examining signalling in individual cells

Flow cytometry enables rapid assessment of intracellular signalling in distinct cellular sub-populations and these signalling data can be related to the functional status of the cells, in terms of activation status (CD69 expression), proliferation (CFSE expression) and cytokine production. However, flow cytometry is incapable of elucidating the subcellular localisation of such signalling molecules and cannot assess the phenotypic or functional characteristics of any cell type in its natural tissue microenvironment. With the advent of LSC technology, investigation of such parameters is now possible.

LSC essentially marries the quantitative capabilities of flow cytometric analysis of cells in suspension with the ability to analyse spatially the fluorescence of large numbers of individual cells, either in suspension or in tissue in a slide-based format. Although LSC and flow cytometry should be viewed and used as complementary quantitative technologies, LSC has the potential to provide a quantum leap in the analysis of immune function, due to the wide range of novel applications that it offers. Such applications include the detection and quantitation of immunological molecules in distinct subcellular locations. Indeed, LSC has been exploited here to analyse the proportion of Ag-specific T cells expressing the signalling molecule, pERK, and the levels of such ERK activation (pERK expression) in discrete subcellular locations such as the cell periphery, have been quantitated.

LSC also offers advantages over other similar technologies such as confocal scanning laser microscopy (CSLM), which has also been used to analyse the subcellular localisation of pERK in cells and sections of mouse lung tissue (474). For example, although CSLM offers the possibility of quantitation of cells and molecules when linked to image analysis software, it has many drawbacks when compared to LSC. Thus, whilst CSLM provides detailed structural analysis, this is limited to a small number of cells due to optical characteristics that only allow analyses of fluorescence emitted in close proximity to the focal plane. By contrast, LSC utililises a collimated laser beam which permits quantitation of all fluorescence emitted from every cell in the slide-based sample. Additionally, data collection by CSLM or fluorescence image analysis (FIA) can be very slow due to the enormous image files stored, as standard, during data acquisition. Consequently, it can take many hours to obtain the information from one tissue section, which LSC could collect in approximately five minutes. Moreover, both technologies require large amounts of computer memory to store the data generated, as individual data files can reach >1 GB in size compared to ~1-2 MB for LSC.

The relocation feature of LSC (475-477) which allows cells or a region of tissue of interest to be relocated to for further analysis, enables qualitative captured images to be indisputably linked to quantitative data. This attribute of LSC enables, for example, authentication of the scattergram analysis gates, used for the segregation of cells into different stages of cell cycle, by morphological assessment of cells collected in such gates.

Detection and quantitation of signalling in situ by LSC

Previously, analysis of tissue sections by LSC has been achieved by contouring on nuclei, involving repeat scans of the same area of tissue at different threshold levels, followed by merging all single threshold level data files into one file (478). While this method allows acquisition of data from limited numbers of individual cells within a tissue section, there are a few disadvantages. It does not detect all the cells and there is no guarantee that cells will not be counted more than once. Application of the adoptive transfer of Ag-specific T cells bearing Tg TcR eliminates these problems, as the antigen-specific TcR Tg cells are distributed sparsely throughout the thymus-dependent area (TDA) of the lymph node, and those cells can be distinguished readily from the endogenous T cells, using standard contours to detect staining of the Tg TcR.

In contrast, phantom contours were employed to locate the follicular regions of the lymph node as the individual B cells in the follicles were too densely packed together for discrimination by standard contours. Although the data collected using phantom contours were not directly representative of individual cells, they were representative of the whole section, in that the data were derived from cells expressing all levels of fluorescence. As such, the data derived from B cell-containing phantom contours was used to identify the B cell-rich follicular areas of the lymph node. Locating B cell follicles and Ag-specific Tg T cells in discrete compartments of the lymph node allows different aspects of Ag–specific T cell behaviour to be assessed directly and correlated with the anatomical localisation of the T cells. Such approaches could also be employed to assess the anatomical location of cells expressing particular cytokines, chemokines or costimulatory molecules involved in e.g. T – APC cell interactions (392, 479, 480).

Standard contours have an advantage over phantom contours in that they can generate data that are directly representative of individual cells in tissue. They have been used previously at high threshold levels, contouring on the nucleus in tissue sections, in an attempt to discriminate individual cells (481). However, this method only collects data from the nuclear compartment of the cell and also may omit a substantial proportion of the cells in the tissue, as it detects only those cells with a very high nuclear staining signal. If a high threshold level like this had been used to detect the Ag-specific Tg T cells in our work, we would have been unable to quantify the total amount of pERK expressed on a per cell basis.

Thus we have successfully established LSC as a method for detecting T cell surface markers and intracellular signalling molecules *in vitro* and *in situ*. The ability of LSC to link quantitative and qualitative data with anatomical localisation indicates its potential as a powerful tool for analysing immune responses at the cellular and molecular level *in situ*.

Methods for genetically modifying target proteins and molecules

The data described above enabled correlation of signalling with functional responses. Thus, in order to demonstrate causal relationships, methods with which to causally investigate the mechanisms underlying the signalling differences observed in tolerance and priming, were required. A variety of techniques are available with which to modulate gene expression within the cell. For instance knockout (KO) mice offer the chance to examine immune responses in the absence of specific genes. These mice have both alleles of the particular gene of interest replaced with an inactive allele and this is

usually achieved through homologous recombination. However, many KO mice are embryonic lethal and the lines are labour intensive to produce and maintain. In addition, removing one gene from the genetic repertoire may have unforseen effects on numerous pathways within the body and as such, indirect effects may influence or skew the results of studies on the pathway of interest. Reporter transgenic mice allow the expression of one gene to be tracked and studied through its fusion or bicistronic conjugation to a fluorescent marker e.g. green fluorescent protein (GFP) but again, these mice are labour intensive to produce and maintain. Another technology, utitlising small interfering RNAs (siRNAs), provides a more attractive alterative to using KO or reporter mice as it specifically knocks down the mRNA and subsequently the protein level of the targeted gene. This would have been a good technique to use for this project as it has now been shown to be successful for murine primary T cells (482) but, at the time the work described here was undertaken, there was limited evidence for its use *in vivo*. Also, the major drawback of this technology is the need to design, synthesise and test several siRNAs before an effective siRNA is identified.

Transfection offers another method of genetic modulation and is often effected by electroporation, a process which in itself results in a high level of cell death in the transfected cell population. Mutant (e.g. dominant negative, constitutively active) signalling molecules can be introduced into cells in this manner. Initial studies transfecting DO11.10 hybridoma cells were successful (28 % transfection rate) but unfortunately this technique was not transferable to primary T cells. Although Nucleofector™ technology is now available for murine T cells, the transfection efficiency is never greater than 50 %, viability after transfection is only up to 35 % and transfection still results in activation of the cells thus precluding analysis of naïve cell responses. Moreover, no publications have arisen using this technology for murine T cells at this time.

The generation of murine transgenic lines in which expression of the human coxsackie/adenovirus receptor with a truncated cytoplasmic domain is limited to T cells expressing a Tg TCR (hCARΔcyt.DO11.10) has enabled efficient gene transfer of resting (naïve) and effector antigen-specific $CD4^+$ T cells without perturbing their development, migration, activation status or functional responses (402, 419). hCARΔcyt and hCARΔcyt.DO11.10 Tg murine lines have now been established in our facility and this study has demonstrated successful transduction of naïve, anergic and primed $CD4^+$ and T cells from these mice with GFP containing adenoviral vectors. In addition, this data suggested that by varying the MOI of bicistronic-GFP vectors used, it will be possible to

analyse the effect of no, low and high expression of particular signalling elements within a single population of cells. Indeed, others have shown that an increase in MOI correlates with an increase in GFP expression in islet cells transduced with an adenoviral vector (483).

Whilst it must be noted that genetic modulation by adenoviral transduction is unlikely to be of use in a clinical setting, as there is likely to be pre-existing immunity to adenoviruses in the human population in the form of antibodies to adenoviruses from previous infection with the naturally occurring virus, hCARΔcyt.DO11.10 Tg mice most certainly provide excellent opportunities for research. In conclusion, transduction of hCARΔcyt.DO11.10 $CD4^+$ T cells with appropriate adenoviral constructs and functional analyses of such transduced Ag-specific T cells by LSC, will aid in the dissection of the mechanisms underlying the differences in T cell signalling observed in tolerance compared to priming.

Figure 3.1 Analysis of CD69 expression on antigen-specific T cells by flow cytometry and LSC. Naïve antigen-specific Tg TcR T cells were incubated with DC alone (DC; open bars) or DC loaded with $OVA_{323-339}$ (DC + Ag; closed bars) for 20 h before being stained with CD4, KJ1.26 and CD69 Abs for analysis by flow cytometry (FC; A, B, F) or with DAPI and KJ1.26 and CD69 Abs for analysis by LSC (C-F). The level of CD69 expression in Ag-specific T cells was assessed by both techniques and these data were compared (F). Isotype controls for anti-CD69 were used to set gates denoting positive CD69 expression for FC (A, B; M2) and LSC (C).

Figure 3.2 Analysis of cell cycle progression by LSC. To establish suitable gates for identifying each stage of cell cycle, primed cells (see Section 2.11) which had been incubated with LPS-matured, $OVA_{323-339}$-loaded DC for 20 h cells were cytocentrifuged onto slides and their nuclei were stained with DAPI before the cell cycle status of 1000 DAPI stained cells was assessed by LSC. A scattergram displaying Max Pixel (value of most highly fluorescent pixel within the cell) versus Integral (sum of all fluorescence within the cell) values of DAPI staining, on which the different stages of cell cycle can be defined, is shown. An increase in DAPI Max Pixel reflects an increase in chromatin concentration within the cell, thus allowing mitotic cells (green gate), which contain more condensed chromatin, to be distinguished from those cells in S phase (blue gate). Similarly, an increase in DAPI Integral reflects an increase in the total DNA content within the cell and so cells in G_2/M (4n DNA) can be distinguished from those in G_0/G_1 (2n DNA; black gate). Newly formed daughter cells (ND; pink gate) have similar DNA content (Integral) as cells in G_0/G_1 but they still have more condensed chromatin and so have a higher Max Pixel value. Apoptotic cells (red gate) bind less DAPI as they have fragmented DNA and contain apoptotic bodies, and as such can be readily distinguished from the cells in G_0/G_1. Representative images of cells in each stage of the cell cycle were captured using the re-location feature of LSC and are shown here.

Figure 3.3 Analysis of cell cycle progression of antigen-specific Tg T cells following stimulation with antigen pulsed APC by LSC. Naïve cells were stimulated with LPS-matured, $OVA_{323-339}$-loaded DC for 20 h and then cytocentrifuged onto slides before being stained with DAPI to identify the nucleus and KJ1.26 to discriminate the antigen-specific T cells. The cell cycle status of 500 antigen-specific T cells was assessed by LSC. The Max Pixel value (depicting chromatin condensation) was plotted along the x-axis and the Integral value (representing DNA content) along the y-axis of the scattergram (A). The percentages of antigen-specific TcR Tg ($KJ1.26^{+}$) T cells within the different stages of the cell cycle (G_0/G_1: black gate, S phase: blue gate, new daughter cells (ND): pink gate) and those undergoing apoptosis (AP; red gate) were quantitated by LSC (B), and representative images of antigen-specific Tg TcR cells in G_0/G_1, S phase and ND of the cell cycle and those undergoing apoptosis are also shown (A).

Figure 3.4 TUNEL analysis by LSC. Negative (A) and positive (B) control cells, supplied with the TUNEL kit, were stained with DAPI and TUNEL-Alexa Fluor® 488. Alternatively, anergic (C) and primed (D) Ag-specific T cells were re-stimulated with $OVA_{323-339}$–loaded DC for 1 h, before being cytocentrifuged onto slides and stained with DAPI, anti-KJ1.26 and TUNEL-Alexa Fluor® 488. All cells were analysed by LSC to assess the level of apoptosis, as indicated by TUNEL expression. The proportion of cells exhibiting TUNEL expression and the level of TUNEL expression was quantitated (E). TUNEL-expressing cells were discriminated by setting an appropriate gate on the negative control cells. Representative images of the cells in each sample, captured using the re-location feature of LSC, are shown (A-D).

Figure 3.5 Analysis of ERK1/2 activation by Western Blotting and LSC. Naive populations were stimulated with LPS matured DC alone (-) or DC loaded with $OVA_{323-339}$ (+) for 1, 3, 6 and 20 h. The activation levels of ERK1/2 (pERK1/2) and total ERK1/2 levels in whole cell lysates of each population were measured at each timepoint using Western Blot analysis (A). Cells were also cytocentrifuged, 20 h after culture with DC alone (DC; B:purple line) or DC loaded with $OVA_{323-339}$ (DC + Ag; B:red line), and stained with DAPI and KJ1.26 and pERK Abs as described in Section 2.4.1. Subsequently, the antigen-specific T cells were analysed for pERK expression by LSC, as described in section 2.6.2 (B). The proportion of Ag-specific T cells expressing pERK (C) and the level of pERK expression in these cells (D) was quantitated. These data are representative of at least three independent experiments.

Figure 3.6 Assessment of Ag-specific T cell signalling throughout cell cycle. Anergic (open bars) and primed (closed bars) Ag-specific T cells were re-stimulated with LPS-matured, $OVA_{323-339}$–loaded DC for 1 h before being stained with DAPI and KJ1.26 and p-cdc2/p-CDK2-specific Abs for analysis by LSC. The expression profile of p-cdc2/p-CDK2 in 250 Ag-specific ($KJ1.26^{+}$) T cells, at different stages of cell cycle, was assessed in both populations by LSC (A) and both the percentage of $KJ1.26^{+}$ T cells per stage that were expressing p-cdc2/p-CDK2 (B), and the level at which p-cdc2/p-CDK2 was expressed in these cells (C) were quantitated by LSC.

Figure 3.7 Detection of pERK in antigen-specific Tg T cells by LSC. Primed Ag-specific TcR Tg T cells were cultured with DC alone (DC) or DC loaded with $OVA_{323-339}$ (DC + Ag) for 20 h before being stained with DAPI and KJ1.26 and pERK Abs. An example three-colour image of an Ag-stimulated T cell is shown (A. i) with threshold (red), integration (green) and peripheral contours (yellow) applied (A. ii). The data collected from within the peripheral contours can be expressed as peripheral fluorescence integral (A. iii) and the total (B. ii. & v.) and peripheral (B. iii. & vi.) expression of pERK in the Ag-specific T cells (B. i. & iv) were determined. Subcellular localisation of pERK in these cells was further assessed visually by image capture using the re-location feature of LSC. Representative images of Ag-specific Tg T cells, showing the nucleus (blue), $KJ1.26^{+}$ Tg TcR (red) and pERK (green) together with a merged image are shown (C). The levels of total, peripheral and non-peripheral pERK expression (fluorescence) in each population were quantitated by LSC (D).

Figure 3.8 Quantitation of intracellular pools of signal by LSC (FISH). Anergic and primed Ag-specific TcR Tg T cells were cultured with DC alone (DC; open bars) or DC loaded with $OVA_{323-339}$ (DC + Ag; closed bars) for 1 h prior to being stained with KJ1.26 and anti-pERK Abs, as described in Section 2.5.1, for analysis by LSC. LSC FISH spot analysis was set up as follows. The threshold contour (A, B; red contour) was set to detect Ag-specific ($KJ1.26^+$) T cells via their fluorescently-labelled Tg TcR and secondary contours (A, B; white), demarcating FISH spots, were set to detect 'spots' of pERK fluorescence within the threshold contour boundary. Integration (green) and background (blue) contours are also depicted. The cells were then analysed by LSC and the number of $pERK^+$ FISH spots per Ag-specific T cell, as well as the pERK FISH Integral (C; total fluorescence emitted by all FISH spots in one cell) was quantitated (D). Exemplar histograms depicting the number of $pERK^+$ FISH spots per cell for samples re-stimulated with Ag are shown (A, B).

Figure 3.9 Measuring cell division of Ag-specific Tg T cells following antigen stimulation *in situ*. BALB/c recipients were immunised s.c. with OVA (100 μg; A-C, E, F) in 100 μl PBS/50% CFA 24 h after adoptive transfer of CFSE-labelled Ag-specific Tg TcR ($KJ1.26^+$) T cells and inguinal lymph nodes (PLN) were harvested and sectioned on days 3 and 5 after immunisation. Sections were stained with anti-KJ1.26, as described in Section 2.5.2, and exemplar colour images of a tissue section harvested at day 3 following immunisation, showing $KJ1.26^+$ T cells (red) and CFSE-labelled cells (green) are shown (A). The CFSE expression levels in this Ag-specific T cell population were measured by LSC in order to assess the number of cell divisions they had undergone 3 (B, F) and 5 (C, F) days following immunisation. Alternatively, on day 5 after immunisation, inguinal lymph nodes were harvested from unimmunised (D) and immunised (E) mice and the CFSE expression in Ag-specific $CD4^+$ T cells was assessed by flow cytometry. Control mice (unimmunised) were injected s.c. with 100 μl PBS.

Figure 3.10 Detection of pERK expression by antigen-specific T cells in different anatomical areas of the lymph node *in situ* by LSC. BALB/c recipients were immunised s.c. with OVA (100 μg) in 100 μl PBS/50% CFA 24 h after adoptive transfer of antigen-specific Tg TcR ($KJ1.26^{+}$) T cells (described in Section 2.3.3) and inguinal lymph nodes were harvested and sectioned on day 3 after immunisation. Sections were stained with B220, KJ1.26 and pERK-specific Abs, as described in Section 2.5.2, for the identification of the B cell rich follicles, antigen-specific T cells and measurement of pERK expression levels in the antigen-specific T cells by LSC. Ag-specific T cells were identified (A. i) and the percentage of Ag-specific T cells expressing pERK (A. iii.; 58 %) as well as the level of pERK expression (A. iii.; MFI; 253511) in these cells was quantitated by LSC. Tissue maps showing the location of antigen-specific Tg T cells (A. ii) which express pERK (A. iv; B. iii) and B cell follicles (B) are also shown.

Figure 3.11 Quantitation of pERK expression by antigen-specific T cells in different anatomical areas of the lymph node by LSC. A tissue map depicting the location of pERK-expressing antigen-specific T cells in relation to B cell follicles was generated, as described in Figures 2.5 and 3.10. Gates were set upon follicular (-) and paracortical (-) regions (A) and the number of antigen-specific T cells and pERK-expressing antigen-specific T cells as well as pERK MFI in pERK-expressing Ag-specific T cells, situated in each type of area was calculated (C). The re-location feature of LSC was used to capture an image of a follicle of interest (B; selected from the tissue map).

Figure 3.12 Optimisation of transfection conditions for DO11.10 hybridoma cells. DO11.10 hybridoma cells were electroporated with 10 (A, B) or 20 μg (C, D) of pcDNA3.1 (control vector) or pEFGP-N1 at 960 μF and 280 V then cultured for 24 h before being viewed on a fluorescence microscope to check for presence of green fluorescence (GFP) in the cells. GFP^+ cells were only observed in the populations transfected with the pEGFP-N1 plasmid (B, D) and a higher transfection rate was achieved when the higher concentration of DNA was used (D). DO11.10 hybridoma cells were also electroporated with 10 (open bars) or 20 μg (closed bars) pEGFP-N1 under a range of electroporation conditions to determine optimal transfection efficency. Cells were rested in culture for 24 h before treatment with Lympholyte®-M to remove the dead cells. Viable cells were then assessed for GFP expression by Flow Cytometry (E). The optimal transfection efficiency was observed using 10 μg DNA and electroporation conditions of 960 μF and 280 V.

Figure 3.13 Generation of hCARΔcyt.DO11.10 mice and testing for hCAR and DO11.10 TcR Tg expression. In order to visualise the human coxsackie/adenovirus receptor (hCAR) on founder line $CD4^+$ T cells, lymph node cultures from hCARΔcyt mice were stained with antibodies specific for CD4 (PE) and hCAR (FITC) and analysed by flow cytometry (A). Lymphocytes were identified on the basis of size and granularity (A; R1) and this population was subsequently analysed for co-expression of CD4 and hCAR (B). 20,000 events in R1 were collected using a FACScan and analysed with CellQuest software. These data confirmed that the $CD4^+$ T cells isolated from hCARΔcyt mice did indeed express hCAR. hCARΔcyt mice were then crossed with DO11.10 Tg mice and the first filial (F1) generations were screened for dual expression of hCAR and the Tg TcR by flow cytometry (C-E). Again, lymphocytes were identified on the basis of size and granularity (C; R1) and this population was subsequently analysed for co-expression of CD4 (PerCP) and KJ1.26 (PE; D). $CD4^+$ $KJ1.26^+$ T cells were then examined for expression of hCAR (FITC) and these data show that 100 % of $CD4^+$ $KJ1.26^+$ T cells also expressed hCAR indicating that the cross-breeding procedure was successful.

Figure 3.14 Transduction of anergic or primed hCARΔcyt.DO11.10 lymph node cells with a GFP-expression vector. Lymph node cultures from hCARΔcyt.DO11.10 mice were infected with Ad5.CMV.GFP, which encodes an enhanced GFP reporter gene under the control of a cytomegalovirus promoter (CMV), for 3 h at a MOI of 100. Following infection, anergy or priming was induced in the T lymphocytes, as described in Section 2.4.2, and the cells were cultured for 24 h. Cells were subsequently viewed under a fluorescence microscope, to check for the presence of green fluorescence (GFP), and brightfield and fluorescence images were captured. In these images, GFP^+ cells were clearly observed in a subpopulation of the lymph node culture, indicating that it is possible to generate anergic or primed primary $hCAR^+$ DO11.10 Tg T cells transduced with adenoviral constructs.

Figure 3.15 Analysis of transduction efficiency in hCAR Tg T cells. Lymph node cultures from hCARΔcyt.DO11.10 mice were cultured alone or infected with Ad5.UbP.GFP, which encodes an enhanced GFP reporter gene under the control of a human ubiquitin promoter (UbP), for 3 h at a MOI of 100. Following infection, anergy or priming was induced in the T lymphocytes, as described in Section 2.4.2, and the cells were cultured for a further 24 h. Subsequently, cells were stained for viability (propidium iodide exclusion) and CD4 (PerCP) expression. Lymphocytes were identified on the basis of size and granularity (A) and this population (R1) was subsequently analysed for viability (B). The viable population (R2; PI negative) was then assessed for CD4 and GFP expression (C, D) and analysis of the $CD4^+$ population showed that whilst mock infection (MOI 0) resulted in no GFP^+ $CD4^+$ cells, infection under conditions of no stimulation (naïve), anergy or priming resulted in >80 % of the $CD4^+$ T cells expressing GFP with the brightest and highest % GFP^+ $CD4^+$ cells being found under conditions of priming.

Figure 3.16 Optimisation of infection conditions for efficient transduction of hCAR Tg T cells with a GFP-expression vector. Lymph node cultures from hCARΔcyt.DO11.10 mice were cultured alone (uninfected; MOI 0) or infected with Ad5.CMV.GFP, which encodes an enhanced GFP reporter gene under the control of a human ubiquitin promoter (UbP), for 1 (A) or 3 (B) h at a MOI of 1-1000. Following infection, anergy or priming was induced in the T lymphocytes, as described in Section 2.4.2, and the cells were cultured for a further 24 h. Subsequently, lymph node cultures containing naïve (hatched bars), anergic (open bars) or primed (closed bars) hCAR-expressing Tg T cells were stained for viability (propidium iodide (PI) exclusion) and CD4 (PerCP) expression prior to flow cytometric analysis. Viable $CD4^+$ lymphocytes were identified as described in Figure 3.15 and the percentage of $CD4^+$ T cells that expressed GFP was assessed. These data indicated that optimal transduction efficiency occurred at a MOI of 100 and infection time of 3 h.

Chapter 4

Analysing the role of ERK MAPK signalling and potential cell cycle modulators in priming and tolerance of antigen-specific T cells *in vitro*.

Introduction

Peripheral tolerance is a state of antigen-specific hyporesponsiveness induced by exposure of T cells to antigen under sub-optimal activating conditions (46). Once it is induced, it can suppress many aspects of the antigen-specific immune response to subsequent challenge, including lymphocyte proliferation and cytokine production *in vitro* and *in vivo,* delayed-type hypersensitivity and antibody production (114). However, the molecular mechanisms underlying this phenomenon remain unclear (342, 484).

T lymphocyte activation requires at least two signals generated by the APC; the first of which is specific recognition of peptide-MHC by the T cell receptor (TcR; signal 1), and the second is co-stimulation provided by molecules such CD80/CD86 on the APC interacting with CD28 on the T cell (signal 2) (Figure 1.2 (485)). It is well established that TcR ligation in the absence of such co-stimulation induces long lasting unresponsiveness termed anergy of T cells *in vitro* (48, 49). Several methods have been used to induce this anergic state *in vitro* (50, 52, 486), including exposure to immobilised anti-CD3 in the absence of co-stimulatory signals (51, 487). Re-stimulation with antigen leads to a profound decrease in IL-2 production and hence reduction in proliferation, relative to that seen with cells primed with anti-CD3 + anti-CD28. Consistent with this, in T cells, the maintenance phase of anergy reflects defective activation of transcription factors, such as c-Jun/c-Fos, that are involved in formation of the AP-1 complex which is required for inducing transcription of the IL-2 gene (318, 331, 333, 336-338, 488). In turn, this appears to be determined by the differential recruitment of the signalling cascades mediated by the extracellular signal-related kinase (ERK), c-Jun-N-terminal kinase (JNK) and p38 MAPKs (333, 336, 338). Indeed, JNK-mediated induction of c-Fos expression and activation of AP-1 and NF-AT complexes are defective in T cells anergised *in vitro* and also tolerised *in vivo* (318, 331-333). Moreover, the induction of JunB has also been shown to be severely impaired in anergic T_H1 cells (336) and this defect was secondary to downregulation of ERK and JNK activation (333, 336). Consistent with this, Fields *et al* also reported that ERK1/2 activation was decreased in anergic T cells (338).

When T cells receive both antigen and co-stimulatory signals, the resulting ERK, JNK and p38 MAPK activation leads to the up-regulation of positive regulators of the cell cycle, namely cyclins and cyclin dependent kinases (CDKs) (489). This, in conjunction with the downregulation of negative regulators of cell cycle, such as CDK inhibitors (e.g. $p27^{kip1}$) and retinoblastoma protein (Rb), results in T cell proliferation (489, 490) (Figure

4.1). Activation of the Ras-Raf-MEK-ERK signalling pathway, as cells progress from G_1 to S phase of the cell cycle, has been reported to play a role in the induction of cyclin D and subsequent phosphorylation and inactivation of Rb (Figure 4.1) (491-496). Different cell types expressing constitutively active mutants of Ras or Raf have been shown to exhibit increased cyclin D1 protein levels (497, 498). Concordant with these studies, Lavoie *et al* demonstrated, in a fibroblast cell line, that dominant negative forms of MKK1 or ERK1/2 strongly inhibit expression of a reporter gene driven by the human cyclin D1 promoter, as well as cyclin D1 protein levels (494). Moreover, another reporter gene study suggested that ERK-dependent AP-1-mediated transcription contributes to the upregulation of cyclin D as c-Jun, an AP-1 constituent, activates the cyclin D1 promoter (244).

CDK4, CDK6 and D-type cyclins associate and act to phosphorylate Rb, first by cyclin D–CDK4/6 then further by cyclin E-CDK2, thereby altering its conformation (452, 453). Phosphorylated Rb (p-Rb) releases bound E2F family transcription factors which are then free to activate the genes required for entry into S phase and hence proliferation. Rb regulates proliferation by controlling progression through the restriction point within the G_1 phase of the cell cycle. Sustained, but not transient, ERK activation induces upregulation of pro-proliferative as well as downregulation of anti-proliferative signalling. Examples of such downregulated anti-proliferative molecules include JunD and Tob1. All members of the Jun family (JunD, c-Jun and JunB) are capable of forming heterodimers with Fos proteins (c-Fos, FosB, Fra-1 and Fra-2) (181) and the different permutations of such heterodimers are believed to affect AP-1 mediated cellular responses (499, 500). JunD is known to be a weaker activator of cyclin D expression than c-Jun hence, increasing the JunD:c-Jun ratio causes downregulation of cyclin D1 expression (499) and JunD-deficient immortalised 3T3 cells and Ras-transformed fibroblasts exhibit increased cyclin D1 expression (500, 501). In addition, Tob1 negatively regulates cyclin D1 expression by recruiting histone deacetylase to the cyclin D1 promoter (502).

Anergic cells are thought to arrest in the G_1 phase and this arrest is associated with up-regulation of the negative regulator $p27^{kip1}$ (326, 441, 503-505). Moreover, in anergic T cells $p27^{kip1}$ associates with the c-Jun co-activator JAB1, resulting in its cytoplasmic translocation, disruption of c-Jun association with AP-1 sites and defective transactivation of AP-1 and IL-2 transcription (441). However, controversy surrounds the role for $p27^{kip1}$ in anergy as it has also been shown not to be required for induction of anergy in certain models using $p27^{kip1}$-deficient T cells (506). In addition, other studies have demonstrated

that $p27^{kip1}$-deficient and wild type T cells exhibit similar proliferative profiles (507-509). Moreover, $p27^{kip1}$ has been shown to exert positive and negative regulatory effects on T cell proliferation during the induction and maintenance phases of anergy, respectively (510). For example, Rowell *et al* demonstrated that $p27^{kip1}$ exerts different functions within a 2-fold range of protein concentration (510), with low levels of $p27^{kip1}$ promoting cell cycle progression in activated $CD4^+$ T cells during the initial T cell proliferation associated with the induction phase of tolerance. Conversely, a higher concentration of $p27^{kip1}$ limits proliferation, downregulates effector function and promotes anergy following the peak of the response, indicative of the maintence phase of tolerance. Overall, these data suggested that the net effect of $p27^{kip1}$ on T cells is the negative regulation of their effector function.

To date, studies investigating the activation state of the various MAPK and other signalling cascades in anergy have been limited to T cell clones *in vitro*, essentially because of the limitations imposed by the large number of cells required for conventional biochemical methodology (326). However, these studies may not be representative of primary T cells in their tissue microenvironment and signalling molecules cannot be quantified in individual cells using such methodologies. Indeed, the recent ability to track antigen-specific T cells (378, 380, 511) and signal transduction events *in vivo* have shown that conclusions drawn from *in vitro* studies may not reflect what occurs under physiological conditions (383). For example, data collected from a number of *in vivo* studies suggests that *in vitro*-generated data, concerning some of the stress activated protein kinases, may not pertain to non-transformed T cells. For example, Sun *et al* demonstrated that T cells from PKC-$\theta^{-/-}$ mice displayed normal induction of JNK expression, following treatment with anti-CD3 and anti-CD28 Abs (209). These data contradicted previous findings in Jurkat T cells, which demonstrated a regulatory role for PKC-θ in the activation of JNK (512, 513). Similarly, other work conducted in JNK1-, JNK2- or JNK1/2-deficient mice has shown that whilst JNK is necessary for T cell differentiation, it is not required for T cell activation or IL-2 production (514-516). However, in other studies, T cells from JNK2-deficient mice have been shown to exhibit reduced IL-2 production (517). Furthermore, p38 MAPK but not JNK, as reported for T cell clones (336, 518), appears to be involved in the integration of signals transduced by the TcR and CD28-mediated co-stimulation, and which lead to the production of IL-2 in T cells (315).

Aims

To address these issues, laser scanning cytometry was used to quantify signalling events in individual antigen-specific primary T cells that had been primed or tolerised *in vitro*. In particular, this approach was used to investigate whether the activation patterns and subcellular distribution of the key signals ERK, cdc2/CDK2, Rb and $p27^{kip1}$ differ during the primary response and the maintenance phases of priming and tolerance following challenge of naïve, anergised and primed primary T cells with antigen loaded APC *in vitro*. Specifically, it was planned to:

- Assess ERK activation in individual primed and anergic Ag-specific T cells during the maintenance phases of tolerance and priming and compare these with primary responses.
- Examine expression of different positive (p-Rb) and negative (p-cdc2/p-CDK2 and $p27^{kip1}$) regulators of cell cycle in individual Ag-specific T cells under conditions of priming and anergy.
- Study the subcellular localisation of ERK and those cell cycle regulators in primed and anergic Ag-specific T cells.
- Investigate ERK activation and p-Rb, p-cdc2/p-CDK2 and $p27^{kip1}$ signalling throughout the cell cycle in individual primed and anergic Ag-specific T cells following antigenic challenge.

Results

4.1 Induction of priming and anergy in Ag-specific primary T cells, *in vitro*

To characterise differential signalling events in priming and anergy of antigen-specific T cells an *in vitro* system of Ag-specific priming and tolerance was developed. T cell priming or anergy was induced in primary OVA-specific TcR Tg (DO11.10) T cells by TcR engagement with or without appropriate co-stimulation as described previously (51, 487). To do this, lymph node single cell suspensions, in which typically 35-40 % of the lymphocytes were $CD4^+$ $KJ1.26^+$ T cells, were cultured for 48 h with plate-bound anti-CD3 with or without co-stimulation via anti-CD28. These cells were then washed, re-plated and rested for an additional 48 h in fresh medium, before being re-stimulated with LPS-matured DC which had been pulsed with or without $OVA_{323-339}$ (Figure 4.2).

To confirm induction of priming or anergy, naïve, primed and anergic groups of T cells were assessed for their ability to up-regulate an activation marker (CD69) and produce IL-2, as well as their proliferative capacity in response to re-stimulation with antigen-pulsed DC. T cells in the 'anergic' population showed a defect in IL-2 production upon re-stimulation with antigen relative to those from the naïve and primed DO11.10 T cell populations, which generated comparable levels of IL-2 although, as expected, most IL-2 was produced by the "primed" cells (Figure 4.3A). Once IL-2 is produced, it binds to its specific receptor complex (IL-2R) thus triggering T cell proliferation (reviewed in (519, 520)). Consistent with the IL-2 data, although the naïve T cells proliferated well in response to challenge with $OVA_{323-339}$-loaded DC, cells from the 'primed' population exhibited significantly higher levels of DNA synthesis. By contrast, cells from the 'anergic' population showed significantly reduced responses relative to either naïve or 'primed' cells (Figure 4.3B).

This proliferative unresponsiveness can be overcome by supplementing Ag-stimulated cultures with exogenous rIL-2, as this bypasses the need for co-stimulation (54, 227, 521, 522). Here, the defective proliferation was found to be partly rescued by the addition of exogenous rIL-2, as it increased the proliferation of the anergic T cells (2074 cpm) to levels equal to or greater than (16618 cpm) those reached by primed (15854 cpm) or naïve (5024 cpm) T cells stimulated with antigen in the absence of exogenous rIL-2 (Figure 4.3B and C). By contrast, when the different T cell populations were cultured with rIL-2 alone, as widely reported previously (54, 523), significant proliferation was only

detected in the primed but not naive or anergic samples (Figure 4.3C). However, these defects in IL-2 production and proliferation were not due to the failure of the anergic T cells to recognise antigen after re-stimulation as they exhibited increased expression of the early activation marker CD69 to the same extent as primed T cells (Figure 4.3D).

It was hypothesised that the lack of IL-2 production and proliferation in the anergic T cells could be due to cell death or G_1 arrest, as antigen-specific unresponsivness at the level of individual T cells has previously been shown to involve either apoptotic cell death or cell cycle arrest at the G_1-S phase transition (503). To assess the relative roles of these mechanisms quantitatively, cell cycle progression in the different T cell populations was investigated using LSC (Section 3.1.1.3). Briefly, naïve, anergic and primed Ag-specific T cells were re-stimulated with DC loaded with $OVA_{323-339}$ for 20 h, before being stained with DAPI and the KJ1.26 Ab to enable analysis of the DNA content in individual Ag-specific T cells by LSC (Figure 4.4A). Cell cycle data showed that the primed T cell population, 20 h after challenge with antigen, displayed a greater percentage of mitotic and newly formed daughter cells compared with either naïve or tolerised T cells whereas, progression into S-phase within the anergic population was reduced compared to the naïve and primed groups (Fig 4.4B). In addition, a substantial proportion of anergic T cells were apoptotic, as shown by LSC (Fig 4.4B). Apoptotic cells were rare in the primed or naïve populations. Together, these findings indicate that the different primary culture regimes induced T cell priming or anergy *in vitro* and that "anergy" reflected the induction of both growth arrest and apoptosis.

4.2 Detection of signalling in individual antigen-specific T cells

Previous studies have identified uncoupling of the ERKMAPkinase pathway as a key mechanism underlying antigen-specific unresponsiveness in anergic T cells (331, 333, 336-338, 488). However, most of these studies have been carried out using T cell clones and hence may not be representative of the situation in "normal" T cells. Therefore, the expression of pERK in individual anergic antigen-specific $CD4^+$ T cells was assessed.

To validate this approach, as outlined in Chapter 3, the profile of ERK activation in naïve, anergic and primed T cells following restimulation with antigen, was investigated firstly by classical analysis of the phosphorylation and hence activation status of ERK, in whole cell lysates from mixed cell populations by Western Blotting (Figure 4.5A), and, in parallel, in individual antigen-specific ($KJ1.26^+$) $CD4^+$ T cells in chamber slides using three

colour immunofluorescence and LSC (Figure 4.5B). Previous Western Blotting studies (Chapter 3) had for the first time, demonstrated elevated ERK activation for up to at least 20 h in the naïve population after stimulation with Ag (Figure 3.5). Here, Western Blotting analysis showed high expression of activated pERK in response to challenge with antigen in naïve and to a lesser extent primed cells at 20 h. Consistent with their activation status moreover, primed cells also showed elevated basal levels of pERK. By contrast, cells in the anergic group displayed lower basal and antigen-stimulated levels of pERK, suggesting differential signalling upstream of ERK activation during both the induction and maintenance phases of anergy compared to priming. No substantial differences were observed in ERK protein levels amongst the groups. Although Western Blotting measures the average response of the mixed population and not simply the Ag-specific response, the data collected on ERK activation in the different functional groups, generated using Western Blotting and LSC, were broadly in agreement. However, only LSC analysis allowed dissection of the different profiles of pERK expression in individual Ag-specific T cells (Figure 4.5B). For example, the naïve T cell population appears to contain two sub-populations; one expressing low levels of pERK and the other exhibiting almost double the intensity of pERK expression. Moreover, it can be seen that whilst naïve and primed groups displayed higher levels of pERK than cells in the anergic group, individual cells displayed varying levels of pERK expression, presumably reflecting their differential kinetics of response.

In order to visualise these data, colour images of the different cell populations were captured using a fluorescence microscope. All nucleated cells, including lymph node cells and bone marrow-derived DC, were imaged initially (Figure 4.6A; blue) and then the Ag-specific T cell population was identified (Figure 4.6B; red). The expression of activated ERK was also viewed (Figure 4.6C; green) and finally, these three separate images were merged (Figure 4.6D) allowing visual assessment of pERK expression in Ag-specific T cells. Such data showed that all of the primed Ag-specific T cells re-stimulated with antigen-loaded APC were expressing pERK (Figure 4.6D) whereas, the primed Ag-specific T cells exposed to APC alone exhibited little or no ERK activation (Figure 4.6E). In order to visualise sufficient numbers of anergic Ag-specific T cells, the anergic population was examined at a higher cellular concentration than the primed cells (Figure 4.6F vs. 6E). When anergic Ag-specific T cells were examined (Figure 4.6F), a much lower proportion of the Ag-specific T cells expressed pERK upon re-stimulation with antigen and those few

cells that did express pERK appeared to do so at a lower level (Figure 4.6F) than the primed cells (Figure 4.6D). These data were in agreement with the quantitative results described above.

4.3 Tolerised T cells display reduced activation of ERKMAPkinase relative to primed Ag-specific T cells

It then seemed pertinent to quantify the apparent differences in ERK activation in individual T cells from the anergic and primed populations outlined above in Section 4.2. LSC software was used to assess pERK expression in the different Ag-specific T cell populations, 20 h after re-stimulation with antigen. The analysis demonstrated that similar levels of pERK were expressed in naïve and primed T cells challenged with antigen (Figure 4.7A). However, further analysis revealed that not only was the overall level of pERK expression lower within the anergic T cell population (Fig 4.7A), but the proportion of antigen-stimulated cells expressing pERK in this group was lower than in all other groups (Fig 4.7B).

4.4 Intracellular localisation of pERK expression in primed and tolerised Ag-specific T cells

The visualisation studies (Section 4.2) suggested that pERK might be expressed predominantly at the periphery of primed Ag-specific T cells which had been re-stimulated with antigen (Figure 4.6). Analysis of cell galleries confirmed this (Figure 4.8A) and in addition, indicated that it was distributed more diffusely throughout the cell in those anergic Ag-specific T cells which expressed low levels of pERK (Figure 4.8B). The images presented depicting pERK expression in the anergic cells were over-exposed in order that the cellular distribution of this low intensity pERK be visible. Subsequently, the ability of LSC to discriminate and quantify fluorescence changes occurring at distinct intracellular compartments in individual cells (Section 3.1.1.7), was exploited to assess the localisation of pERK within the different Ag-specific T cell populations. For example, when the total and peripheral levels of pERK expression in these cells were quantified using the gating and peripheral contouring facilities of LSC, primed Ag-specific T cells not only expressed a higher level of pERK than anergic Ag-specific T cells (1 h after challenge with antigen; Figure 4.8C), but also displayed a much greater accumulation of pERK at the periphery of the cells, than anergic T cells (Figure 4.8D). Moreover, when the individual images were

merged, pERK appeared to co-localise with the TcR in the primed T cells (Figure 4.8A). Such co-localisation was not observed to the same extent in the anergic T cells (Figure 4.8B) thus, perhaps pERK and the TcR are localising to the immunological synapse for optimal activatory signalling and this may be defective in anergic T cells.

4.5 Differential association of pERK expression with lipid rafts in anergic and primed Ag-specific T cells?

As peripheral expression of pERK was associated with priming, whilst a more diffuse pERK expression correlated with anergy (Figure 4.8), these results might suggest that pERK was somehow unable to traffic to the point of T cell:APC contact in anergic T cells or alternatively, was not generated there. The cytoskeleton can traffic lipid rafts to the immunological synapse and recruit signalling molecules to enhance either the positive or negative signals generated there (524, 525) and thus, the intracellular localisation of pERK in relation to lipid rafts was examined 20 h after the cells were re-stimulated with antigen. Consistent with the idea that peripheral pERK was associated with T cell activation, pERK co-localised with lipid raft staining in primed Ag-specific T cells but such co-localisation was not observed in anergic Ag-specific T cells (Figure 4.9) suggesting that lipid raft formation or the interaction and trafficking of pERK with these structures may be defective under conditions of anergy.

4.6 ERK activation in relation to cell cycle progression of primed and tolerised Ag-specific T cells

Using the detection method described above it was also possible to examine whether differences in ERK signalling in anergic and primed T cells (441, 504, 526, 527) were associated with differential cell cycle progression, as has been suggested previously (526, 527). For example, Gauld *et al* demonstrated that a sustained cycling pattern of ERK activation correlated with cell cycle progression, cell growth and proliferation in WEHI-231 B cells (527). Here, LSC was used to analyse pERK expression in the different Ag-specific T cell populations in relation to their cell cycle status. When each stage of the cell cycle was linked to a histogram of pERK expression it was clear that the anergic Ag-specific T cells expressed much lower levels of pERK compared to primed T cells in S and mitotic phases, whilst both anergic and primed T cells in G_0/G_1 expressed very little pERK at 20 h after challenge with Ag (Figure 4.10). This type of analysis also allowed correlation

of the range of intensities of pERK expression in individual T cells in the anergic and primed populations with their cell cycle status (Figure 4.11).

Thus, naïve, anergic and primed Ag-specific T cells expressing different levels of pERK (Figure 4.11A; region 1 = lowest and 8 = highest pERK expression level) were analysed to determine their cell cycle status (Figure 4.11B-E). This type of analysis appears to indicate that naïve T cells require only basal levels of pERK expression to transit out of G_1 (Figure 4.11C), but require high levels of pERK expression to proceed through S phase and mitosis (Figure 4.11C). These trends reflect the primary response to Ag as this data was acquired 20 h after the cells had first encountered Ag. Overall, anergic T cells displayed lower levels of pERK expression than naive and primed cells and this was most apparent in the cells at G_0/G_1 phase, where hardly any pERK expression was observed (Figure 4.11D). This was perhaps not surprising as these cells are believed to arrest in G_1 thus, these data may suggest that such cell cycle arrest is likely secondary to a lack of ERK activation in these cells preventing them from achieving a threshold level necessary for cell cycle progression. A different profile again was observed in the primed T cells which had been re-stimulated with Ag (Figure 4.11E). Although, similar to the primary response to Ag (Figure 4.11C), these primed cells exhibited highest levels of activated ERK throughout the S and mitotic phases of the cell cycle, primed cells also expressed high levels of pERK expression at the G_0/G_1 phase (Figure 4.11E). This may suggest that in the secondary response to Ag, high levels of pERK maintain rapid progression through the cell cycle, at all stages (Figure 4.11E).

Next, all of the samples were further analysed to assess the proportion of Ag-specific T cells in each stage of cell cycle that were expressing pERK, as well as the mean level of pERK expression in such Ag-specific T cells at different stages of cell cycle (Figure 4.12). Consistent with the above analysis (Figure 4.11), the primed T cells expressed much higher levels of pERK compared to the anergic T cells, during each stage of cell cycle (Figure 4.12B, D) and this was true even when cells in S phase and mitosis were examined. These data, taken together with the observation that a much higher proportion of primed compared to anergic Ag-specific T cells undergoing mitosis were expressing pERK 20 h after challenge with Ag (Figure 4.12C), suggested that high levels of pERK promote cell cycle progression. Consistent with this, quantitative analysis shows that at 1 h after challenge with Ag, the bulk of both anergic (48 %) and primed (40 %) cells expressing pERK were in the G_0/G_1 phase (Figure 4.12A) but the highest levels of pERK

expression correlated with proliferating cells. By 20 h, whilst most of the anergic cells including those expressing pERK, were still in G_0/G_1 (Figure 4.12C, E), the majority of primed T cells expressing pERK (71 %) had progressed through S phase and into mitosis (Figure 4.12C) with the vast majority expressing pERK and again the level of pERK expression was highest in S phase and mitosis (Figure 4.12D).

4.7 Downregulation of p-Rb expression in tolerised T cells relative to primed T cells

Analysis of pERK expression during cell cycle progression revealed that the G_1 arrest observed in anergic T cells correlates with decreased ERK activation. Hence, ERK-dependent regulators of cell cycle were next investigated to determine if they were also differentially expressed and activated in anergy. For example, ERK activation is known to ultimately contribute to the phosphorylation and inactivation of Rb (528, 529), allowing cell cycle progression through the restriction point within G_1 (251, 452, 530). Therefore, as it was hypothesised that p-Rb expression would be down-regulated in anergic T cells, the levels of p-Rb (inactive Rb) in anergic and primed T cells were measured after re-stimulation with antigen. Consistent with this hypothesis, whilst a similar percentage of cells in all groups expressed p-Rb, and at comparable levels 1 h after challenge (Figure 4.13 A, B), by 20 h an increased proportion of the naive and primed groups were expressing p-Rb (Figure 4.13A) and those groups were expressing p-Rb at much higher levels than observed in the anergised group (Figure 4.13B).

4.8 Differential localisation of p-Rb expression in primed and tolerised T cells

It has been reported that both hypophosphorylated (active; suppressor of cell cycle progression) and hyperphosphorylated (inactive) Rb are situated in the cell nucleus (531-533) and that the hypophosphorylated form has a much higher avidity for the nuclear compartment (533). Thus, using an antibody which detects Rb when it has been hyperphosphorylated at serine 807/811, the subcellular localisation of p-Rb in anergic and primed T cells in response to challenge with antigen was analysed. Unexpectedly, p-Rb was found to be intensely localised to the periphery of anergic T cells but by contrast, exhibited diffuse, nucleus-associated staining in primed T cells. However, some bright staining at the periphery at 1 h after challenge and the rather punctate staining suggests that vesicular trafficking to or from the nucleus may be occurring (Figure 4.14A). This greater intensity of p-Rb expression at the periphery, outside of the nucleus of the anergic cells was

confirmed, quantitatively by LSC (Figure 4.14B) even when as Figure 4.13 shows, that, at this timepoint, both the anergic and primed cells exhibit similar levels of p-Rb (MFI). This suggests that the lack of p-Rb in the nucleus in anergic cells may contribute to the reduced cell cycle progression in this population.

4.9 Assessment of p-Rb expression in relation to the cell cycle status of primed and tolerised Ag-specific T cells

As p-Rb expression is widely considered to enable cell cycle progression through the restriction point within G_1, it was hypothesised that p-Rb might be most highly expressed in primed T cells at the G_0/G_1 phase to enable release of E2F to induce genes required for entry into S phase. When the p-Rb expression profile was examined in anergic compared to primed T cells, there indeed appeared to be a greater number of primed compared to anergic T cells expressing higher levels of p-Rb (1 h after challenge with antigen) in G_0/G_1, when the p-Rb expression profile was assessed in terms of cell cycle (Figure 4.15). At first sight, these results appeared to support the hypothesis for highest expression of p-Rb at the G_0/G_1 phase. However, upon re-stimulation with Ag, the majority of both anergic and primed p-Rb-expressing T cells were in G_0/G_1 at 1 h (Figure 4.16A, B) but unexpectedly, by 20 h the vast majority (69%) of these primed T cells were found in mitosis (Figure 4.16B). Moreover, 100 % of the p-Rb-expressing anergic T cells also appeared to be mitotic at this timepoint (Figure 4.16A). Although, perhaps at first sight surprising, these later data are accordant with the literature which indicates that whilst hypophosphorylated Rb is the major form present at the G_0/G_1 phase (532, 534, 535), this s807/811 hyperphosphorylated form of Rb is predominantly associated with the S and G_2/M phases (535, 536). However, the finding of a complete lack of p-Rb-expressing anergic T cells in G_0/G_1 is possibly more informative, as it suggests that, at this timepoint, p-Rb was indeed downregulated in the majority (52 %) of the anergic T cell population, which were in G_0/G_1 (Figure 4.12E).

The above data is restricted to the primed and anergic p-Rb-expressing Ag-specific T cells therefore, the proportion of the Ag-specific T cell population that was expressing p-Rb (Figure 4.17A, C), as well as the mean intensity of p-Rb expression in these cells in the different cell cycle stages (Figure 4.17B, D), were also analysed by LSC. Equivalent proportions of anergic compared with primed T cells per cell cycle stage were expressing p-Rb at 1 h and surprisingly, a higher percentage of anergic compared to primed T cells in S

phase were expressing p-Rb. However, a striking difference between the two cell types was observed at 20 h after re-stimulation with Ag (Figure 4.17C). Here, the anergic T cells in G_0/G_1 and S phase (Figure 4.12E) expressed absolutely no detectable p-Rb (Figure 4.17C), indicating that by this phase of the response, p-Rb was indeed downregulated in anergic T cells. At the 1 h timepoint, the highest levels of p-Rb expression were observed in the cells which were in G_0/G_1 or S phase, but there was no difference in the levels of p-Rb expression between the groups (Figure 4.17B). Unexpectedly, both cell types expressed p-Rb during mitosis (Figure 4.17A, C), with the anergic cells expressing a considerably lower level of p-Rb than the primed cells, at both timepoints (Figures 4.17B, D). These data were not generated from synchronised populations thus, perhaps such cells may be Ag-specific T cells in the anergic population which had themselves escaped anergy induction. As there is no definitive marker for anergy, it cannot be determined as to whether 100 % of the T cells in an anergic population have in fact been anergised. Alternatively, such cells could consitiute anergic cells that were on their way to G_1 arrest.

4.10 Examination of cdc2/CDK2 activity in primed and tolerised Ag-specific T cells

Cdc2 and CDK2 are known to be required in the S phase of cell cycle for complex formation with cyclin A and subsequent phosphorylation and inactivation of Rb. Indeed, cdc2/CDK2 is likely to be responsible for the hyperphosphorylation of Rb at serine 807/811 (537) that is maximally observed in primed mitotic cells at 20 h (Figure 4.17C). Using an antibody which detects the inactive, phosphorylated forms of cdc2 and CDK2 ($pTyr^{15}$-cdc2/p Tyr^{15}-CDK2), it was possible to assess whether the activation of this molecule in anergic and primed T cells (after challenge with antigen) also correlated with their cell cycle status. For example, as levels of hyperphosphorylated Rb were reduced, levels of inactive p-cdc2/p-CDK2 were expected to be increased under conditions of anergy. However, when the different Ag-specific T cell populations were analysed by LSC, it was clear that similar proportions of unstimulated and Ag-stimulated, anergic and primed T cells expressed p-cdc2/p-CDK2 (Figure 4.18A) and that both primed and anergic groups express p-cdc2/p-CDK2 at similar levels (Figure 4.18B). By contrast, naïve T cells, upon encountering their specific Ag for the first time, downregulated expression of p-cdc2/p-CDK2 over time, both in terms of percentage of cells expressing p-cdc2/p-CDK2 and also with respect to p-cdc2/p-CDK2 expression levels (Figure 4.18), presumably to allow subsequent clonal expansion of this population. These results suggest that deactivation of

cdc2/CDK2 is not responsible for the lack of hyperphosphorylation of Rb observed in anergic cells.

4.11 Activity of cdc2/CDK2 throughout cell cycle

Although there was no overall difference in the proportion of cells expressing p-cdc2/p-CDK2 or indeed the levels expressed between primed and anergic cells, it was possible that there may be a difference in expression when cells at different stages of the cell cycle were examined. A cell requires active (de-phosphorylated) cdc2/CDK2 to proceed into mitosis and so it was hypothesised that there may be more inactive p-cdc2/p-CDK2 in the anergic, compared to the primed cells in S phase. Thus, the expression profile of p-cdc2/p-CDK2 in primed and anergic cells at different stages of cell cycle was examined by LSC (Figure 4.19). The majority (44 % at 1 h, 42 % at 20 h) of primed cells that expressed p-cdc2/p-CDK2, after stimulation with Ag, were at the G_0/G_1 phase (Figure 4.20B) and this perhaps reflected ongoing transit of the cells, exhibiting reduced p-cdc2/p-CDK2 in mitosis, through a subsequent round of division. However, the highest proportion of p-cdc2/p-CDK2-expressing anergic T cells was observed in mitosis for both unstimulated and Ag-stimulated samples (Figure 4.20A) and it is possible that these cells may actually be arrested in G_2 immediately prior to cytokinesis.

The above data specifically examined the primed and anergic p-cdc2/p-CDK2-expressing Ag-specific T cell populations thus, it also seemed pertinent to determine the proportion of Ag-specific T cells that were expressing p-cdc2/p-CDK2 at each stage of the cell cycle. When all of the Ag-specific T cells in the different populations were analysed, a slightly higher proportion of anergic compared to primed antigen-specific T cells in S phase were expressing p-cdc2/p-CDK2 at 1 h after re-stimulation with antigen (Figure 4.21A). At 20 h after challenge with antigen, the proportion of anergic compared to primed mitotic T cells expressing p-cdc2/p-CDK2 had doubled (Figure 4.21C). Interestingly, an inverse pattern was observed in those cells in S phase at this timepoint (Figure 4.21C). There was no difference in the mean levels of p-cdc2/p-CDK2 expressed in the different populations (Figure 4.21B, D). In addition, as there was a much higher proportion of anergic (380 cells; 52 %) compared to primed (128 cells; 35 %) T cells at the G_0/G_1 phase (Figure 4.12E), the data here indicates that perhaps, whilst similar percentages of anergic and primed T cells expressed p-cdc2/p-CDK2 (Figure 4.21A, C), a considerably larger number of anergic compared to primed T cells were expressing p-cdc2/p-CDK2 at this stage. These data only

provide snap-shots, at two timepoints, of the signalling involved during cell cycle. As progression through cell cycle is dynamic, further time-course experiments examining a large range of timepoints would be required to evolve a better understanding of the signalling involved therein.

4.12 $p27^{kip1}$ expression is upregulated in tolerised T cells relative to primed T cells

As $p27^{kip1}$ negatively regulates G_1 – S phase transition by inhibiting CDK2 activity (538), this signal was also assessed, at the single cell level in the whole population of anergic or primed T cells after re-stimulation with antigen. Whilst the percentages of anergic and primed T cells expressing $p27^{kip1}$ were similar, whether re-stimulated with antigen or not at 20 h after co-culture (Figure 4.22A), there was an increase in the level of $p27^{kip1}$ expressed by the anergic T cells at this timepoint (Figure 4.22B). It should be noted here that only a low proportion of both cell types were expressing $p27^{kip1}$ (Anergic ~9-10%; Primed ~11-13%). These data suggest that it is possible that level of $p27^{kip1}$ expression, rather than the prevalence of its expression within a population, might play a role in the maintenance phase of T cell anergy.

4.13 $p27^{kip1}$ expression in tolerised T cells at different stages of cell cycle

Although no difference in the percentage of cells expressing $p27^{kip1}$ was detected between the primed and anergic populations, there was again the potential for masking the effects of anergy by assessing the total cell population. Hence, it was possible that differences in the proportion of cells expressing $p27^{kip1}$ may be observed in the primed and anergic T cells that were at the G_0/G_1 phase. As $p27^{kip1}$ is intrinsically linked to the negative regulation of cell cycle, it was important to examine this signal in anergic and primed T cells at different stages of cell cycle following challenge with antigen, as it had been expected that $p27^{kip1}$ expression would be upregulated in anergic compared to primed T cells. However, when the expression profile of $p27^{kip1}$ was examined in this way, at the single cell level, it was found to be similar for both anergic and primed Ag-specific T cells at 1 h after challenge (Figure 4.23). Moreover, when T cell-specific $p27^{kip1}$ signalling was quantitated by LSC, there was no difference in the proportion of anergic compared to primed antigen-specific T cells per stage expressing $p27^{kip1}$ at both timepoints (Figure 4.24A, C). It was also noted that the percentage of cells expressing $p27^{kip1}$ was reduced in both groups at 20 h after challenge (Figure 4.24C). In addition, LSC analysis determined

that $p27^{kip1}$ was expressed at similar levels in anergic compared to primed T cells at both timepoints (Figure 4.24B, D) and interestingly, at 1h after challenge, the intensity of $p27^{kip1}$ expression appeared to increase as cell cycle progressed, being highest during mitosis (Figure 4.24B). This latter observation was unexpected because, as $p27^{kip1}$ is thought to negatively regulate G_1-S phase transition, the opposite trend might have seemed more fitting.

4.14 Subcellular localisation of $p27^{kip1}$ under conditions of priming and tolerance

It was a little surprising that there was no difference in the proportion of anergic compared to primed T cells expressing $p27^{kip1}$. Hence, as $p27^{kip1}$ is known to exert its inhibitory effects on CDKs when it is localised in the nucleus, its subcellular localisation in anergic and primed cells was assessed with the expectation that more anergic cells would exhibit higher levels of $p27^{kip1}$ expression within their nuclei compared to primed cells. $p27^{kip1}$ appeared to localise predominantly in the nucleus in both anergic and primed T cells at 1 h after challenge (Figure 4.25A). Surprisingly, 20 h after re-stimulation with antigen, $p27^{kip1}$ redistributed somewhat to the periphery of both anergic and primed cells where, in fact, it appeared to co-localise with the polarised Tg TcR (Figure 4.25B). Upon visual examination this peripheral distribution of $p27^{kip1}$ was more apparent in the anergic cells. Moreover, when the peripheral expression of $p27^{kip1}$ was quantitated by LSC, it was found that the anergic T cells did indeed have higher expression of this molecule in their periphery (Figure 4.25C). In addition, when $p27^{kip1}$ was examined in relation to lipid rafts, peripheral $p27^{kip1}$ appeared to preferentially co-localise with the lipid rafts in both cell types, although this was even more apparent in the primed cells (Figure 4.26).

Discussion

T cells that have been tolerised or primed display different functional responses as a result of the signalling events that occur during their initial and subsequent encounters with antigen. Indeed, it has been widely proposed that both qualitative and quantitative differences in T cell signalling may underlie the differential functional outcomes of immunological tolerance and priming (525, 539). Thus, upon secondary challenge with antigen *in vitro*, productively primed T cells show a characteristic pattern of signalling resulting in the transcription of the IL-2 gene and subsequent clonal expansion of these T cells. Such signalling includes activation of the Ras-Raf-MEK-ERK MAPK cascade which leads to the activation of the transcription factor complex AP-1. PLC-γ1-dependent NF-AT translocation and activation, and PKC-mediated activation of NF-κB are also induced. In addition, CD28-mediated signalling provides JNK/p38 MAPK-mediated activation of additional transcription factors required for transcription of the IL-2 gene. In contrast, anergised T cell lines/clones display defective proliferation and an inability to produce IL-2 upon challenge (88, 472), which is associated with defective coupling of the TcR to early signalling events such as the activation of ZAP-70, ERK and JNK (525, 539). In addition, there may be upregulation of inhibitory factors such as the GTPase, Rap-1, which may act to disrupt the Ras-ERK MAPK pathway, and the cell cycle (cyclin-dependent kinase) inhibitor, $p27^{kip1}$. Interestingly, upregulation of $p27^{kip1}$ has been associated with both IL-2-dependent and –independent forms of anergy (523). Nevertheless, in all cases, these mechanisms appear to lead to G_1-S cell cycle arrest and increased apoptosis of anergised cells. However, much of this work to date has relied upon biochemical assessment of signalling in T cell lines or clones at the population level following polyclonal stimulation *in vitro* and this has often yielded conflicting results.

Here, for the first time, the signalling events underlying *in vitro* priming and tolerance of antigen-specific responses in individual primary T cells have been shown to demonstrate marked differences, in the kinetics, amplitude and localisation of the MAPkinase, ERK and a number of cell cycle regulators. Firstly, it was established that antigen-specific proliferation and IL-2 production is less in primary antigen-specific T cells that had been tolerised by pre-culture with anti-CD3 than that resulting from priming with anti-CD3 + antiCD28. In contrast, re-stimulated anergised T cells upregulated CD69 to the same extent as T cells that had been primed with anti-CD3 and anti-CD28. These results

confirm previous reports (503) and show that the defects in proliferation and IL-2 production were not the result of a failure of antigen recognition by anergised T cells. However, in contrast to some previous *in vitro* studies (503), the secondary response of such anergised T cells could be only partly restored by exogenous IL-2, recovering levels similar to those of primed cells responding to antigen alone. Nevertheless, similar findings have also been reported by others (523, 525, 539) and it seems that different forms of anergy may show differential sensitivity to IL-2-mediated reversal of tolerance. These include clonal anergy due to lack of CD28 co-stimulation, which has been proposed to be reversible by addition of exogenous IL-2, and anergy reflecting cell cycle arrest induced by CTLA-4 signalling and which is refractory to IL-2 (523). Moreover, there is also increasing evidence for induction of multiple forms of anergy (540) resulting from lack of CD28 co-stimulation in which the progression to S-phase is mediated via both IL-2 dependent and independent pathways (448, 541).

Here, using both conventional biochemical techniques and quantitative single cell analysis by laser scanning cytometry, it was shown that whilst ERK activation was elevated in all populations of T cells that were challenged with antigen, it was always lower in the anergic population. Analysis at the single cell level revealed that the proportion of antigen-stimulated cells expressing pERK was also lower in the anergic relative to the primed groups and in addition, the few anergised T cells which expressed pERK did so a lower level than primed cells. These findings were consistent with the fact that primed, but not anergic, antigen-specific T cells progressed through the cell cycle and that such progression correlated with increasing levels of pERK. In contrast, anergic T cells displayed a greater propensity to apoptose upon challenge. Collectively these results suggested that sustained ERK activation above a certain threshold level may be required for proliferation as whilst the anergic T cells in G_0/G_1 displayed pERK, albeit at low levels, they were not progressing through cell cycle. It is therefore possible that quite a high threshold of pERK expression is required for progression through cell cycle indeed, primed T cells express almost double the level of pERK compared to the anergic cells at 20 h after challenge with antigen (Figure 4.11D).

Consistent with this proposal, sustained, but not transient, activation of ERK has been shown to increase cyclin D expression (37, 41, 42) and hence promote proliferation. Moreover, Harnett *et al* have shown that periodic cycling of ERK activation is associated with the progression of B lymphoma cells through all stages of the cell cycle and that

inhibition of this sustained, but cycling ERK activation resulted in apoptosis (527). Interestingly, however, previous studies have identified opposing roles for ERK MAPkinase in regulating cell cycle progression in T cells. For example, and consistent with the above mentioned previous studies, increased ERK activation has been shown to downregulate $p27^{kip1}$ thus leading to upregulation of CDK activity followed by increased phosphorylation of Rb and subsequent S phase entry (504). By contrast, other studies using high dose anti-CD3 stimulation or a conditionally active Raf-1 mutant, showed that the resultant elevated ERK activation contributed to sustained $p27^{kip1}$ expression and hence reduced CDK2:cyclin E activity and cell cycle progression (526). These contradictory findings may be reconciled, however, if basal levels of ERK activation are required for anergy to proceed, a proposal that is consistent with the current findings that show low levels of pERK in tolerised cells. For example, completely blocking the ERK pathway using inhibitors blocks proliferation but does not induce anergy (542) and PKC-dependent activation of ERK has been shown to contribute to inhibition of IL-2 signalling (543). Perhaps it is not surprising then, that the decreased ERK activation observed in anergic relative to primed T cells at 20 h after re-stimulation with antigen correlated with an increase in the level of $p27^{kip1}$ expression in those anergic cells, although the percentage of anergic compared to primed cells expressing $p27^{kip1}$ was not increased. Previous studies (473, 504, 544, 545) have indicated that ERK activation can be associated with the nuclear export of $p27^{kip1}$ and hence linked to the downregulation of $p27^{kip1}$ CDK inhibitory function (288). Whilst ERK can phosphorylate $p27^{kip1}$ at Ser10 and Thr187 (289) the resulting alterations in conformation are not responsible for regulating localisation of $p27^{kip1}$ (288). Rather, it is phosphorylation at Thr198 by p90 ribosomal protein S6 kinases (RSKs), which are triggered in a Ras-Raf-MEK-dependent manner that results in cytoplasmic localisation of $p27^{kip1}$ (281). These findings may therefore provide an explanation for the expression of $p27^{kip1}$ by comparable levels of primed and anergic cells.

Alternatively, whilst the anergic T cells exhibit reduced ERK activation compared to primed cells, they do however express low levels of pERK. Thus, perhaps downregulation of ERK activation and/or upregulation of $p27^{kip1}$ are not sufficient for maintenance of the anergic state and hence, one or more additional negative signals are required. Such a negative signal could perhaps be provided by the downregulation of p-Rb and/or increased expression of inactive CDKs. Consistent with this, almost ten-fold fewer anergic (1.7 %) compared to primed (18.4 %) T cells were expressing p-Rb after re-

stimulation with Ag at 20 h and the anergic cells that were expressing p-Rb were expressing it at more than five-fold lower levels than primed cells (Figure 4.13B). Moreover, p-Rb localised to the periphery of anergic T cells whilst it appeared more diffuse and even vesicular, throughout the primed cells. Although hyperphosphorylated Rb (p-Rb) is known to have a lower avidity for the nuclear compartment than hypophosphorylated Rb (Rb), it is still reported to be in the nucleus (531, 532, 546). Collectively, these findings suggest that it could be the apparent lack of p-Rb in the nucleus in anergic cells that may be responsible for its reduced efficacy and susbsequent loss of cell cycle progression in this population.

Work conducted in $CDK4^{R/R}$ fibroblasts, which exhibit increased levels of Rb with a substantial fraction of Rb in its hyperphosphorylated form localised to both the nucleus and cytoplasm, has revealed that cytoplasmic mislocalisation of p-Rb in these cells is regulated by enhanced Exportin1-mediated nuclear export (547). Nuclear export of $p27^{kip1}$ is known to inhibit its negative regulatory function (548) and so Jiao *et al* hypothesised that nuclear export of p-Rb may downregulate its effector function. Indeed, they demonstrated that such translocation led to inactivation of p-Rb tumour suppressor function (547). Therefore, it may be possible that, under conditions of anergy, p-Rb rapidly (within 1 h of antigenic re-stimulation) translocates out of the nucleus via association with the nuclear export receptor, Exportin1, thereby preventing further hyperphosphorylation at serine 780 (530), 795 (529) and 807/811 required for its positive regulatory role in cell cycle progression.

Quantitation by laser scanning cytometry showed that the majority of the pERK signal appeared to be localised at the periphery of re-stimulated primed T cells, possibly in association with the TcR. In contrast, pERK was distributed more diffusely throughout those anergised T cells that expressed lower levels of pERK. These results were somewhat surprising, as it had been hypothesised not only that re-stimulation of primed cells would induce pERK to translocate to the nucleus to activate the transcription factors (549) which are required for IL-2 induction but also that this process might be defective in anergic T cells. Rather, it appeared that after priming, pERK may associate with cytoskeletal- and/or membrane-associated scaffolds such as lipid rafts (as shown in Figure 4.26) containing the TcR and other components of the proximal signalling cascade. Thus, these structures, or the association of pERK with them, may be defective in anergised T cells (Figure 4.26).

It is not clear how ERK signalling at the periphery of the cell contributes to the maintenance of T cell priming but there is increasing evidence that the cytoskeleton plays

important roles, not only in the organisation of the immunological synapse (550), but also in signal transduction (524) by its ability to recruit signalling elements to adaptor molecules in the synapse. Thus, actin scaffolds have also been postulated to promote TcR signalling by preventing degradation of signalling elements (525, 551) and by directing lipid raft trafficking to the synapse (525). Although the precise molecular details are not clear, the recent finding that ERKMAPkinase is an intermediate signal in the Vav/Rac2-mediated pathway (552) leading to nucleation of actin filaments and cytoskeleton remodelling at the immunological synapse (553) may therefore provide a molecular rationale for such TcR-associated localisation of pERK in primed T cells. Indeed, disassembly of actin scaffolds is thought to possibly contribute to the downregulation of TcR signalling in anergy (553).

Interestingly therefore, peripheral expression of $p27^{kip1}$, which was perhaps rather surprisingly found to be higher in anergic compared to primed T cells, has been implicated as having a role in the rearrangement of the cytoskeleton by its ability to negatively regulate RhoA activity (554), which is involved in the regulation of the cytoskeletal remodelling that leads to cell adhesion and migration (555). For example, in human mesangial cells Akt/PKB-mediated phosphorylation of $p27^{kip1}$ causes translocation of $p27^{kip1}$ to the cytoplasm where it binds RhoA resulting in uncoupling RhoA from the Lim kinase/cofilin pathway and leading to actin disassembly by depolymerisation (556). Further support for multiple $p27^{kip1}$ functions is apparent in a number of cancers where cytoplasmic $p27^{kip1}$ is usually concurrent with nuclear expression of $p27^{kip1}$ in tumour cells (557) and it has been suggested that such cells are able to regulate their cell cycle as well as having a decreased ability to migrate. Indeed, cytoplasmic expression of $p27^{kip1}$ is associated with a good prognosis in some cancers (557). Whilst higher levels of peripheral $p27^{kip1}$ were found in anergic compared to primed T cells, this peripheral expression predominantly co-localised with lipid rafts in both cell types indicating that perhaps $p27^{kip1}$ exerts its negative regulatory effects at this location, by preventing the cytoskeletal remodelling required for T cell activation.

In summary, the maintenance phase of anergy relative to that of priming, reflects a combination of downregulated ERK activation and differentially regulated cell cycle modulators. These data suggest that both upregulation of $p27^{kip1}$ and downregulation of nuclear p-Rb expression are necessary, together with reduced ERK MAPK signalling, for the anergic state to be maintained. Furthermore, it appears that modulation of the

subcellular localisation as well as the expression levels of such molecules is important for maintenance of the anergic phenotype.

Figure 4.1 ERK-dependent cell cycle regulation. Upon TcR ligation, in the presence of CD28-mediated co-stimulation, the Ras-ERK and p38/JNK MAPK signalling cascades are initiated and subsequently c-Fos and c-Jun are induced, and AP-1 is activated. Such ERK-dependent AP-1 transcription contributes to the upregulation of cyclin D as c-Jun, an AP-1 constituent, activates the cyclin D1 promoter. CDK4, CDK6 and D-type cyclins can then associate and act to phosphorylate Rb, first by cyclin D–cdk4/6 then further by cyclin E-cdk2, thereby altering its conformation. Hyperphosphorylated Rb (p-Rb) releases bound E2F family transcription factors which are then free to activate the genes required for entry into S phase (e.g. cyclin A and cyclin E) and hence proliferation. Cdc2 (CDK1) and CDK2 are then activated and can both associate with cyclin A at S phase where they also act to phosphorylate and inactivate Rb thus, further fuelling cell cycle progression.

Figure 4.2 Induction of priming and tolerance in Ag-specific TcR Tg T cells *in vitro*. Primary antigen-specific T cells were treated with immobilised anti-CD3 in the absence or presence of soluble anti-CD28 for 48 h, to induce anergy or priming, respectively. Excess Ab was then washed off and the cells were rested for a further 48 h. Naïve T cells were freshly isolated. Anergic, primed or naïve T cell populations were then cultured with either DC alone or $OVA_{323-339}$-loaded DC for 1 or 20 h prior to fluorescence staining and analysis by LSC.

Figure 4.3 Validation of the induction of anergy and priming in Ag-specific TcR Tg T cells *in vitro*. The functionality of anergic, primed and naïve T cells was assessed at different timepoints after stimulation with DC alone (DC) or DC loaded with $OVA_{323-339}$ (DC + Ag). Levels of IL-2 production (A) and proliferation (B, C), measured at 20 and 48 h respectively, were lower in anergic (open bars) compared with the primed (black bars) and naïve (hatched bars) T-cell populations, after re-stimulation with $OVA_{323-339}$-loaded DC. Surface expression of the early T cell activation marker, CD69, was similar in both anergic and primed T cells re-stimulated with Ag (D). The results shown (A-C) are means +/- SD of triplicate cultures and are representative of five individual experiments ($*p \leq 0.05$).

Figure 4.4 Analysis of cell cycle progression of Ag-specific T cells after re-stimulation with Ag-loaded APC by laser scanning cytometry. The cell cycle status of 1000 anergic (open bars), primed (closed bars) and naive (hatched bars) Ag-specific T-cells was analysed following staining with DAPI and the KJ1.26 Ab. The max-pixel value (depicting chromatin concentration/condensation) is plotted along the x-axis and the integral value (representing DNA content) along the y-axis (A). Apoptotic (AP) cells and cells at G_0/G_1, S phase, mitosis (M) as well as newly formed daughter cells (ND) were identified as described in Figure 3.2. The proportion of naive, anergic and primed Ag-specific T-cells at different stages of the cell cycle was determined by LSC (E). The results shown are representative of five individual experiments.

Figure 4.5 Detection of pERK by Western Blotting and LSC: a comparison. Activation levels of ERK1/2 20 h after re-stimulation with LPS matured DC alone (-) or such DC pulsed with $OVA_{323-339}$ (+) were measured using Western Blot analysis of pERK1/2 and total ERK1/2 levels in whole cell lysates of mixed cell populations (A). Cells were also cytocentrifuged 20 h after re-stimulation with $OVA_{323-339}$ pulsed DC and analysed for pERK expression in antigen-specific T cells by LSC as described in Section 2.18 (B). The data are representative of at least three independent experiments.

Figure 4.6 Visualisation of ERK activation using three colour immunofluorescence. Cells were identified by nuclear staining with the DNA dye DAPI (A; Blue) and for the transgenic TcR by staining with the clonotypic antibody (KJ1-26) (B; Red). The expression of activated ERK was then determined with an antibody specific for pERK (C; Green). Merging these images (D) allows assessment of pERK in antigen-specific T cells in the presence (D, F) or absence (E) of antigen. Primed (A-E) and anergised (F) T cells are represented. Fields of view were taken at x20 magnification, with the inset representing a single T cell-APC interaction (depicted by the square; x40 magnification). The anergic sample was examined at a higher cellular concentration in order to visualise sufficient representative numbers of Ag-specific T cells in this population.

Figure 4.7 Quantitation of antigen-specific ERK activation by laser scanning cytometry. Total cellular expression of pERK at 20 h after antigen re-stimulation of naïve, anergised and primed KJ1.26^{+} T cells is represented using the fluorescence integral value (MFI) (A). The proportion of antigen-specific KJ1.26^{+} T cells expressing pERK was also determined (B). The MFI results shown are the average of 250 KJ1.26^{+} transgenic T-cells (A). Similar results were obtained in four replicate experiments.

Figure 4.8 Intracellular localisation of pERK staining in Ag-specific T cells. KJ1.26^{+} pERK^{+} T cells from primed and anergised populations were randomly relocated by the LSC. Three representative individual primed or anergised T cells (A, B) were identified by nuclear staining with the DNA dye DAPI (A, B; Blue). Cells positive for the Tg TcR were then identified by staining with the clonotypic antibody (KJ1.26) (A, B; Red). The expression of activated ERK was then determined with an antibody specific for pERK (A, B; Green). Merging these images (A, B) allows assessment of the localisation of pERK in antigen-specific T cells in the presence of antigen. Turquoise represents a diffuse location of pERK (DAPI-Blue+ pERK-Green), whereas yellow depicts a more peripheral cytoplasmic expression (KJ1.26 -Red and pERK-Green) (C, D). Diffuse versus peripheral localisation of pERK quantitated by peripheral contouring with LSC (C). Total (C) and peripheral (D) pERK was quantified for 250 pERK^{+}, anergic and primed Ag-specific T cells.

Figure 4.9 Subcellular localisation of pERK expression in relation to lipid rafts in Ag-specific T cells. Anergic and primed antigen-specific T cells were re-stimulated with DC pulsed with $OVA_{323-339}$ for 20 h. Antigen-specific Tg T cells were identified by the clonotypic Ab KJ1.26 (blue) whereas pERK expression was detected by the relevant specific Ab (red) and lipid raft structures were identified using a Cholera Toxin subunit B-Alexa Fluor® 488 conjugate (green). $KJ1.26^+$ $pERK^+$ T cells from anergised and primed samples were randomly relocated by LSC and the localisation of pERK in relation to lipid rafts in $KJ1.26^+$ T cells was observed. Representative individual anergised and primed cells were identified and imaged as described in Chapter 3.

Figure 4.10 Profile of pERK signalling in Ag-specific T cells undergoing different stages of cell cycle. Anergic and primed T cells were re-stimulated with LPS-matured, $OVA_{323-339}$ pulsed DC for 20 h and the profile of ERK activation in Ag-specific T cells at different stages of cell cycle was assessed (1000 $KJ1.26^+$ T cells, in both populations), following staining with DAPI and anti-KJ1.26 and anti-pERK Abs and analysis by LSC.

Figure 4.11 Correlation of pERK intensity with cell cycle progression. Naïve, anergic and primed Ag-specific T cells were re-stimulated with DC loaded with $OVA_{323-339}$ for 20 h before being stained with DAPI to identify all nucleated cells, KJ1.26 Ab to detect the Ag-specific T cells (A. i) and pERK (A. ii). Each Ag-specific T cell population was analysed for its expression of pERK (A) and the cell cycle status of Ag-specific T cells expressing different intensities of pERK was assessed by LSC (B-E). Exemplar cell cycle plots are shown for naïve Ag-specific T cells expressing low (region 1), medium (region 3) and high (region 5) levels of pERK (B). The proportion of naïve (C), anergic (D) and primed (E) Ag-specific T cells, expressing different intensities of pERK expression, undergoing apoptosis (black line) and in each stage of cell cycle (G_0/G_1: blue line; S: orange line; M: green line) was examined.

Figure 4.12 Examining the expression pattern of pERK during cell cycle progression of anergic and primed T cells. Anergic (open bars) and primed (closed bars) T cells were re-stimulated with LPS-matured, $OVA_{323-339}$-loaded DC for 1 (A, B) or 20 (C, D) h and the cell cycle status of 500 pERK-expressing $KJ1.26^+$ T cells, in both populations, was analysed following staining with DAPI and anti-KJ1.26 and anti-pERK Abs by LSC (A, C). The level (MFI) at which pERK was expressed in these cells during different stages of cell cycle was also examined by LSC (B, D) and an exemplar histogram depicting the cell cycle status of the Ag-specific ($KJ1.26^+$) T cell population at 20 h is shown (E). Data are representative of four identical experiments.

Figure 4.13 Quantitation of antigen-specific p-Rb expression by laser scanning cytometry. The proportions of naïve, anergic and primed KJ1.26^{+} T cells expressing p-Rb, 1 (open bars) and 20 (closed bars) h after re-stimulation with $OVA_{323-339}$-loaded DC, were determined by LSC (A). The total cellular expression of p-Rb was also measured by LSC (B). Results shown are the average of 250 KJ1.26^{+} Tg T cells per group.

Figure 4.14 Intracellular localisation of p-Rb expression in Ag-specific T cells. Anergic and primed antigen-specific T cells were re-stimulated with $OVA_{323-339}$-loaded DC for 1 h and then stained with DAPI to identify the cells via their nucleus. Cells expressing the Tg TcR specific for $OVA_{323-339}$ were detected using the clonotypic antibody KJ1.26 (A; Red). pRb expression in these cells was detected using an antibody specific for pRb (A; Green). $KJ1.26^{+}$ pRb^{+} T cells from primed and anergised populations were randomly relocated by LSC and representative images of each population were captured (A). In addition, the peripheral pRb expression was quantitated by LSC (B).

Figure 4.15 p-Rb expression profile in T cells at different stages of cell cycle. Anergic and primed T cells were re-stimulated with LPS-matured, $OVA_{323-339}$ pulsed DC for 1 h and the expression profile of p-Rb in the different stages of cell cycle was assessed for 250 $KJ1.26^+$ T cells, in both populations, following staining with DAPI and anti-KJ1.26 and anti-p-Rb Abs by LSC.

Figure 4.16 Assessing the cell cycle status of p-Rb-expressing Ag-specific T cells. Anergic (A) and primed (B) T cells were cultured with DC alone for 1 h (hatched bars) or re-stimulated with DC loaded with $OVA_{323-339}$ for 1 (open bars) or 20 h (closed bars) and the cell cycle status of 500 p-Rb-expressing $KJ1.26^{+}$ T cells, in both populations, was analysed following staining with DAPI and anti-KJ1.26 and anti-p-Rb Abs by LSC. Thus, the cell cycle profile of the different unstimulated Ag-specific p-Rb-expressing T cell populations was compared to that of the Ag-stimulated cells over a period of time.

Figure 4.17 Proportion of Ag-specific T cells expressing p-Rb at each stage of cell cycle. Anergic (open bars) and primed (closed bars) T cells were re-stimulated with LPS-matured, $OVA_{323-339}$-loaded DC for 1 (A, B) or 20 (C, D) h and the cell cycle status of 500 p-Rb-expressing $KJ1.26^{+}$ T cells, in both populations, was analysed following staining with DAPI and anti-KJ1.26 and anti-p-Rb Abs by LSC (A, C) The level at which p-Rb was expressed in these cells during different stages of cell cycle was also examined by LSC (B, D).

Figure 4.18 Quantitation of p-cdc2/p-CDK2 expression in Ag-specific T cells by laser scanning cytometry. Naïve, anergic and primed Ag-specific T cells were cultured with DC alone for 1 h (hatched bars) or re-stimulated with LPS-matured, $OVA_{323-339}$-loaded DC for 1 (open bars) or 20 h (closed bars). Following staining with DAPI and anti-KJ1.26 and anti-p-cdc2/p-CDK2 Abs, the proportions of naïve, anergic and primed $KJ1.26^+$ T cells expressing p-cdc2 (A) as well as the level of p-cdc2/p-CDK2 expression (MFI; B) was measured by LSC. Results shown are the average of 250 $KJ1.26^+$ Tg T cells and are representative of four identical experiments.

Figure 4.19 Determining the expression profile of p-cdc2/p-CDK2 in Ag-specific T cells after challenge with antigen. Anergic and primed T cells were re-stimulated with LPS-matured, $OVA_{323-339}$ pulsed DC for 20 h and the expression profile of p-cdc2/p-CDK2 in the different stages of cell cycle was assessed for 250 $KJ1.26^+$ T cells, in both populations, following staining with DAPI and anti-KJ1.26 and anti-p-cdc2/p-CDK2 Abs by LSC.

Figure 4.20 Assessing the cell cycle status of the p-cdc2/p-CDK2-expressing Ag-specific T cells. Anergic (A) and primed (B) T cells were cultured with DC alone for 1 h (hatched bars) or re-stimulated with DC loaded with $OVA_{323-339}$ for 1 (open bars) or 20 h (closed bars) and the cell cycle status of 500 p-cdc2/p-CDK2-expressing $KJ1.26^+$ T cells, in both populations, was analysed following staining with DAPI and anti-KJ1.26 and anti- p-cdc2/p-CDK2 Abs by LSC. Thus, the cell cycle profile of the different unstimulated Ag-specific p-cdc2/p-CDK2-expressing T cell populations was compared to that of the Ag-stimulated cells over a period of time.

Figure 4.21 Proportion of Ag-specific T cells expressing p-cdc2/p-CDK2 at each stage of cell cycle. Anergic (open bars) and primed (closed bars) T cells were re-stimulated with LPS-matured, $OVA_{323-339}$-loaded DC for 1 or 20 h and the cell cycle status of 500 p-cdc2-expressing $KJ1.26^{+}$ T cells, in both populations, was analysed following staining with DAPI and anti-KJ1.26 and anti- p-cdc2 Abs by LSC (A, B). The level at which p-cdc2 was expressed in these cells during different stages of cell cycle was also examined by LSC (C, D). Data are representative of four identical experiments.

Figure 4.22 Quantitation of $p27^{kip1}$ expression in Ag-specific T cells by laser scanning cytometry. The proportions of naïve, anergic and primed $KJ1.26^{+}$ T cells expressing $p27^{kip1}$, 20 h after re-stimulation with DC alone (open bars) or $OVA_{323-339}$-loaded DC (closed bars), were determined by LSC (A). The fold increase in the level of $p27^{kip1}$ expression (MFI) in cells re-stimulated with $OVA_{323-339}$-loaded DC compared with that in cells cultured with DC alone, was also measured by LSC (B). Results shown are the average of 250 $KJ1.26^{+}$ Tg T cells. Similar results were obtained in three replicate experiments.

Figure 4.23 Determining the cell cycle profile of $p27^{kip1}$ in Ag-specific T cells. Anergic and primed T cells were re-stimulated with LPS-matured, $OVA_{323-339}$ pulsed DC for 1 h and the expression profile of $p27^{kip1}$ in the different stages of cell cycle was assessed for 250 $KJ1.26^{+}$ T cells, in both populations, following staining with DAPI and anti-KJ1.26 and anti-$p27^{kip1}$ Abs by LSC.

Figure 4.24 Proportion of Ag-specific T cells expressing $p27^{kip1}$ at each stage of cell cycle. Anergic (open bars) and primed (closed bars) T cells were re-stimulated with LPS-matured, $OVA_{323-339}$-loaded DC for 1 or 20 h and the cell cycle status of 500 $p27^{kip1}$-expressing $KJ1.26^{+}$ T cells, in both populations, was analysed following staining with DAPI and anti-KJ1.26 and anti- $p27^{kip1}$ Abs by LSC (A, B). The level at which $p27^{kip1}$ was expressed in these cells during different stages of cell cycle was also examined by LSC (C, D). Data are representative of three identical experiments.

Figure 4.25 Intracellular localisation of $p27^{kip1}$ expression in Ag-specific T cells. Anergic and primed antigen-specific T cells were re-stimulated with $OVA_{323-339}$-loaded DC for 1 (A) and 20 (B) h before being stained with the clonotypic antibody KJ1.26 in order to identify them via their Tg TcR (Blue). $p27^{kip1}$ expression in these cells was detected using an antibody specific for $p27^{kip1}$ (Red). $KJ1.26^{+}$ $p27^{kip1+}$ T cells from primed and anergised populations were randomly relocated by LSC and representative images of each population were captured (A, B). At the 20 h timepoint, the peripheral $p27^{kip1}$ expression was quantitated by LSC (C).

Figure 4.26 Subcellular localisation of $p27^{kip1}$ expression in relation to lipid rafts in Ag-specific T cells. Anergic and primed antigen-specific T cells were re-stimulated with DC pulsed with $OVA_{323-339}$ for 20 h. Antigen-specific Tg T cells were identified by the clonotypic Ab KJ1.26 (blue) whereas $p27^{kip1}$ expression was detected by the relevant specific Ab (red) and lipid raft structures were identified using a Cholera Toxin subunit B-Alexa Fluor® 488 conjugate (green). Single-, 2- (red + green) and 3-colour merged images were generated. $KJ1.26^{+}$ $p27^{kip1+}$ T cells from anergised and primed samples were randomly relocated by LSC and the localisation of $p27^{kip1}$ in relation to lipid rafts in $KJ1\text{-}26^{+}$ T cells was observed. Representative individual anergised and primed cells were identified and imaged as described in Chapter 3.

Chapter 5

Analysis of the role of Rap1 signalling in tolerance and priming

Introduction

In the previous chapter, it was reported that the distinct functional outcomes of T cell priming and tolerance are associated with marked differences in the amplitude, kinetics and cellular localisation of activated, phosphorylated ERK (pp42ERK2/ pp44ERK1) signals with primed Ag-specific T cells showing enhanced activation of ERK relative to tolerised Ag-specific cells at the single cell level (12). Consistent with this, it has previously been shown that anergised T cells exhibit a failure to transcribe IL-2 which is secondary to a lack of ERK and AP-1 activation (441). These earlier studies suggested that such defective ERK activation is accompanied by accumulation of the GTPase, Rap1 (351, 540, 558), and that such Rap1 accumulation can disrupt TcR coupling to ERK activation by sequestering Raf-1 and hence directly antagonising Ras-Raf-1-ERK signalling (347). Supporting this, accumulation of active Rap1 has been reported to play a role in the maintenance of anergy in human T cell clones (50, 347), with tolerant cells displaying reduced ERK activation due to recruitment of a Fyn-Cbl-CrkL-C3G-Rap1 signalling complex not found in their primed counterparts (347). Furthermore, an inverse relationship between ERK and Rap1 activation has been shown in various T cell lines (350) and also that CD28 signalling abolishes TcR-coupled Rap1 activity (351-353).

However, controversy surrounds the role of Rap1, as it has also been reported to play positive regulatory roles in T cell activation (356, 559). For example, studies in mice transgenic for the constitutively active mutant of Rap1, Rap1V12, have suggested that Rap1 may play a role in promoting priming of T cells (560). Moreover, other work has implicated a role for Rap1 in promoting T cell signalling via enhanced integrin activation and adhesion (356, 357). In addition, many of these events associated with Rap1 accumulation and activation in anergised T cells appear to be downstream consequences of, as yet, poorly defined defects in events proximal to TcR signalling and have mainly been characterised using *in vitro* models that may not reflect the responses of primary Ag–specific $CD4^+$ T cells *in vivo*. As a result the role(s) of Rap1 in the primary molecular processes that distinguish tolerised and primed T cells in intact lymphoid tissues remain uncertain.

Aims

In order to investigate the potential role of Rap1 in mediating the differences previously observed in ERK signalling under conditions of tolerance and priming (Chapter 4) in a physiological setting, the expression and subcellular localisation of Rap1 in tolerised compared to primed Ag-specific T cells both *in vitro* and *in vivo* was investigated using laser scanning cytometry. Specifically, it was planned to:

- Assess Rap1 expression in individual anergic and primed antigen-specific T cells during the induction and maintenance phases of tolerance and priming *in vitro*.
- Examine the subcellular localisation of Rap1 in anergic and primed antigen-specific T cells.
- Investigate Rap1 expression throughout the cell cycle in individual primed and anergic Ag-specific T cells following antigenic challenge.
- Study ERK activation and Rap1 expression in individual tolerised and primed Ag-specific T cells following challenge with Ag *in vivo*.
- Examine ERK activation and Rap1 expression in individual Ag-specific T cells following induction of tolerance and priming *in vivo*.
- Investigate the expression of Rap1 in *in vivo* tolerised and primed antigen-specific T cells situated in distinct areas of the lymph node.

Results

5.1 Rap1 expression is higher in tolerised than in primed Ag-specific CD4$^+$ T cells *in vitro*

Priming or anergy was induced in primary Ag-specific TcR Tg T cells by activation of the TcR in the presence or absence of appropriate co-stimulation using plate-bound anti-CD3 and soluble anti-CD28 as described previously (Section 4.1; (12, 51, 53)). These conditions induced functional priming or unresponsiveness by the criteria illustrated in Section 4.1 (12, 51, 487) and as evidenced here by the analysis of IL-2 production. Thus, upon re-stimulation with Ag, primed T cells produced significantly higher levels of IL-2 than naïve cells whilst anergic T cells produced no IL-2 whatsoever (Figure 5.1A).

To investigate the potential role(s) of Rap1 in the induction and effector phases of such tolerance induction *in vitro*, Rap1 expression in naïve, primed or anergic groups of T cells was examined by LSC (Figures 5.1B-D) 20 h after these T cells had been stimulated in the absence or presence of Ag. As expected and consistent with the IL-2 production data (Figure 5.1A), such LSC analysis confirmed that the *in vitro* priming and tolerance regimes produced a larger population of antigen-specific (KJ1.26$^+$) T cells in the primed relative to the anergic groups (Figure 5.1B). When challenged with LPS-matured DC in the absence of Ag, a similar percentage of anergic and primed Tg T cells expressed Rap1 and this was higher than that observed for naïve cells cultured with DC alone (Figure 5.1B & C), suggesting it was unlikely that Rap1 played an essential role in the induction phase of anergy. Upon re-stimulation with Ag, however, there was a sharp decrease in the percentage of primed Ag-specific T cells expressing Rap1. Conversely, there was a substantial increase in the percentage of anergic Ag-specific T cells expressing Rap1 (Figure 5.1B & C), suggesting that Rap1 expression may be associated with the maintenance phase of tolerance. Moreover, the finding that Rap1 expression is downregulated in naïve and primed T cells challenged with Ag in the presence of co-stimulation (as provided by LPS-matured DC pulsed with Ag) is consistent with previous reports that CD28-signalling downregulates Rap1 (50, 351-353) and perhaps also suggests that Rap1 expression may play a role in preventing inappropriate activation of naive T cells. Quantitation of the Rap1 signal in Rap1$^+$ Ag-specific T cells revealed that, when expressed, Rap1 was expressed at similar levels in all groups, regardless of whether they had been re-stimulated with Ag or not (Figures 5.1B & D).

5.2 Differential intracellular localisation of Rap1 expression in anergic and primed Ag-specific T cells

As was shown previously (Section 4.2; (12)), primed T cells expressed higher levels of activated ERK (pERK) relative to anergic T cells after challenge with Ag and this pERK was localised primarily at the cell periphery. Conversely, the lower levels of pERK expressed by anergic T cells exhibited a more diffuse cellular distribution (Figure 5.2A). To investigate whether the lack of focused, peripheral pERK expression reflected membrane localisation of Rap1, sequestration of Raf-1 and hence disruption of recruitment and activation of ERK, the intracellular localisation of Rap1 was examined in anergic and primed Ag-specific T cells. Rap1 was indeed found to display an inverse pattern of cellular localisation to that of pERK, being concentrated at the periphery of anergic T cells, and showing a more diffuse, punctate, pattern of expression in primed T cells. Interestingly, although some foci of Rap1 staining could be seen at the periphery of primed cells, it appeared to be excluded from the vicinity of the TcR (Figure 5.2A). In accordance with such punctate Rap1 expression, there is evidence in the literature that Rap1 may localise to vesicular compartments in certain instances. For example, nerve growth factor-induced activation of Rap1 has been shown to occur in neuronal early endosomes (561) and exposure of FRTL-5 (rat thyroid cell line) to forskolin results in the recruitment of B-Raf to a vesicular compartment where it co-localises with Rap1 (562). In addition, tuberin-associated microsomes in 293 T cells have been shown to be enriched with Rap1 (563).

To quantify the subcellular localisation of Rap1 by LSC, peripheral contour analysis methods established previously (Section 4.4; (12, 392)), were utilised (Figure 5.2B, C). These confirmed that, in addition to a greater percentage of anergic relative to primed cells expressing Rap1 following challenge with Ag, a higher proportion of anergic T cells expressed Rap1 peripherally (Figure 5.2D). Moreover, although the integral levels of such peripheral Rap1 expression appeared similar in both groups of T cells following antigenic challenge (Figure 5.2E), this showed a more focused pattern of expression in anergic T cells, as indicated by increased intensity (max pixel) of signal (Figure 5.2F). This peripheral localisation of Rap1 in anergic cells is again inverse to that of pERK, which was found previously to be expressed at much lower levels in the periphery of anergic T cells compared with primed T cells (Figure 4.8; (12)).

5.3 Relationship of ERK and Rap1 localisation to lipid rafts in primed and anergic Ag-specific T cells.

As organised recruitment of the TcR and signalling molecules in lipid rafts to the immunological synapse is one of the principal features of T cell activation and this is reported to be defective in anergic cells (524, 539, 564, 565), the intracellular localisation of pERK and Rap1 in relation to lipid rafts was examined, 20 h after the cells were re-stimulated with Ag. Consistent with the idea that peripheral pERK was associated with T cell activation, pERK co-localised with lipid raft staining in primed Ag-specific T cells (Figure 4.9 and 5.2G). Such co-localisation was not observed in anergic Ag-specific T cells, suggesting that lipid rafts, or the interaction of pERK with these structures, is defective under conditions of tolerance. Conversely, there was marked co-localisation of Rap1 with lipid rafts in anergic, but not primed, Ag-specific T cells following re-stimulation with Ag (Figure 5.2G), perhaps suggesting that within lipid raft regions of the immunological synapse of anergic cells, Rap1 is activated to antagonise ERK recruitment and activation.

5.4 Cell cycle progression of Rap1-expressing Ag-specific T cells

In Chapter 4, cell cycle progression was investigated in naïve, primed and anergised T cell populations, following challenge with Ag, using LSC (566-568) and in addition, the activation status of ERK at each stage of the cell cycle was assessed at the single cell level (Section 4.6). As mentioned previously, Ag-specific unresponsiveness can result in cell cycle arrest at the transition from G_1-S phase in individual T cells (444, 540) and consistent with this, these studies showed that primed T cells exhibited a higher percentage of mitotic and newly formed daughter cells compared to anergic T cells, whilst anergic T cells showed downregulated progression through S phase and higher levels of apoptosis compared to primed T cells (Figure 4.12, (12)). Associated with this, we found that the enhanced ERK activation, observed in primed relative to anergic cells correlated with increased ERK activation at all stages of cell cycle progression but not in cells arrested in G_0/G_1 or undergoing apoptosis. Hence, it was hypothesised that the highest percentage of Rap1 expressing anergic T cells might be observed in the G_0/G_1 phase.

The cell cycle status of the anergic and primed Rap1-expressing Ag-specific ($KJ1.26^+$ $Rap1^+$) T cell populations was therefore assessed at 1 and 20 h after re-stimulation with LPS-matured DC pulsed, or not, with Ag. The 1 h timepoint was chosen to assess

early effects of Ag on cell cycle progression and the 20 h timepoint was selected mainly to examine S phase transition as effective stimulation has been shown to promote entry of naïve primary T cells into cell cycle within this time scale (441). After 1 h, the majority of both primed and anergic T cells expressing Rap1 were found to be in G_0/G_1 phase whether they have been re-stimulated with Ag (Figure 5.3C) or not (Figure 5.3A). No obvious differences were observed in the remaining cell cycle stages between the groups. By 20 h both primed and anergic Rap1 expressing T cells appear to be progressing through cell cycle regardless of re-stimulation status (Figure 5.3B, D), but these percentage data do not provide any information as to the relative rates of progression or numbers of cycles undergone by the individual groups. For further clarification, this data was then interpreted as the number of Rap1-expressing Ag-specific T cells expressed as the percentage of all of the Ag-specific T cells in each stage but again, this analysis did not highlight any clear differences between primed and tolerised cells or indeed, any correlation of Rap1 with arrest or cell cycle progression (data not shown).

Similarly, the mean fluorescence intensity (MFI) of Rap1 expressed by Ag-specific T cells in different stages of cell cycle was next examined. At the 1 h timepoint Rap1 appears to be expressed at similar levels in both anergic and primed T cells except during mitosis, when anergic T cells have been re-stimulated with Ag (Figure 5.4C). Here, the intensity of Rap1 expression is 2-fold greater than in T cells in any other stage of cell cycle. By 20 h, the anergic T cells which had progressed into mitosis were expressing a higher level of Rap1 compared to the primed T cells in this stage (Figure 5.4B, D). It should be noted that, at 20 h, Rap1 expression in primed cells was highest in those in G_0/G_1 (Figure 5.4D) and, according to the previous figure (Figure 5.3D), such cells constituted a small proportion of the Ag-specific T cell population. Conversely, Rap1 expression was highest in mitotic anergic cells (Figure 5.4D) and such cells composed a high proportion of the Ag-specific T cell population (Figure 5.3D). It is possible that such $Rap1^{hi}$ anergic cells may be arrested at the G_2/M phase and are therefore unable to further progress through cell cycle. Furthermore, the primed T cells which were in G_0/G_1 exhibited higher levels of Rap1 expression than the anergic G_0/G_1 cells (Figure 5.4C, D). It may be that the high level of Rap1 expression observed in such primed T cells is preventing these cells from proceeding through another round of cell division. However, for this to be proven, later timepoints would need to be examined to assess whether this was the case. Indeed, these data only provide a snapshot, at two timepoints, of Rap1 signalling in relation to cell cycle status of T

cells. In order for this relationship to be fully investigated, extensive kinetic studies would be required in which regular, frequent timepoints from 0 to at least 48 h following co-culture of T cells with APC, were assessed. Such analysis would be necessary to investigate the possible differential kinetics of the responses elicited by anergic versus primed T cells. For example, the rate of cell cycle progression may be different in these two cell types thus, kinetic studies should enable a more informed interpretation of the signalling profiles within these different cellular populations.

5.5 Role for Rap1 in the maintenance of tolerance *in vivo?*

To investigate whether similar inverse patterns of Rap1 and pERK accumulation are found during tolerance and priming *in vivo*, Rap1 expression was examined in Ag-specific $CD4^+$ T cells taken from a systemic model of Ag-specific priming and tolerance (89, 378, 382, 383). Thus, 24 h after adoptive transfer of Ag-specific TcR Tg T cells, recipient mice received $OVA_{323-339}$ peptide i.v., either alone or together with LPS to induce systemic tolerance or priming respectively. The efficacy of these regimes was confirmed by assessing the clonal expansion (Figure 5.5) and follicular migration (Figure 5.6) of Ag-specific $CD4^+$ T cells in the peripheral lymph nodes (PLN), mesenteric lymph nodes (MLN) and spleen, 0, 3, 5 and 10 days after primary exposure to Ag ± LPS. In addition, the proliferative (Figure 5.7A) and cytokine (Figure 5.7B) recall responses of such Ag-specific $CD4^+$ T cells from peripheral lymph nodes were assessed *ex vivo*.

The peak of Ag-specific clonal expansion of each of the PLN, MLN and splenocyte populations (Figure 5.5A, B and C, respectively) was observed, as previously reported (378, 382, 569), at D3 after immunisation in both the tolerised and primed groups. Moreover, and, as also shown previously (378, 384), at all times after primary immunisation there was significantly higher clonal expansion in the tissues harvested from primed compared to tolerised mice. In addition, quantitation of the percentage of Ag-specific T cells in follicular and paracortical areas of the PLN at D3 after primary immunisation indicated that the proportion of Ag-specific T cells present in the follicular areas of these tissues was significantly lower in the tolerised compared to primed groups (Figure 5.6), suggesting that fewer tolerised than primed Ag-specific $CD4^+$ T cells had migrated into the B cell-rich follicles of these PLN. These latter results are consistent with previous findings that during the primary response to Ag, anergic Ag-specific T cells are defective in their ability to migrate to B cell follicles and hence, provide B cell help (378,

384). Similar results were obtained when the MLN and spleen were examined (data not shown). Furthermore, after re-stimulation with $OVA_{323-339}$ *in vitro*, tolerised T cells from PLN also showed reduced proliferation (Figure 5.7A) and IFNγ production (Figure 5.7B) relative to cells from primed mice. PLN cells from naïve mice proliferated significantly more than the tolerised group but less than the primed group. Finally, tolerised mice showed considerably lower serum OVA-specific IgG1 antibody responses after challenge with Ag *in vivo* than primed mice (Figure 5.7C). Collectively, these data show that i.v. administration of OVA with or without LPS as an adjuvant, induced priming and tolerance respectively *in vivo*.

5.6 Investigation of the role(s) of pERK and Rap1 signalling in the maintenance phase of systemic priming and tolerance *in vivo*.

The experiments investigating the role(s) of pERK (Section 4.2) and Rap1 (Section 5.1) in the induction and maintenance of tolerance *in vitro* suggested that these molecules may play a role in the effector, but not induction phase, of priming and tolerance respectively. To determine whether this was also the case *in vivo*, mice were immunised, 24 h after adoptive transfer of Ag-specific TcR Tg T cells, with $OVA_{323-339}$ peptide i.v., either alone or together with LPS to induce systemic tolerance or priming respectively. Seven days after the primary immunisation, recipient mice were challenged with $OVA_{323-339}$/LPS i.v. in order to examine the maintenance phase of tolerance. Following antigenic challenge (24 h), the expression of both pERK and Rap1 in Ag-specific T cells in the PLN was examined *in situ* by LSC, as described in Section 2.6.3.

In situ analysis of Ag-specific T cells primed or tolerised *in vivo*, corroborated the *in vitro* findings in that a significantly lower percentage of *in vivo* tolerised compared to primed T cells expressed pERK (Figure 5.8B, C). However, the level of ERK activation did not differ significantly between the groups at this time (Figure 5.8D). Moreover, and also in agreement with the *in vitro* data, a significantly higher percentage of Ag-specific T cells in PLN from the tolerised group expressed Rap1 compared to those from the primed group (Figure 5.8F, G). Furthermore, when the levels at which Rap1 was being expressed in these PLN cells *in situ* were measured, the tolerised Ag-specific T cells were found to be expressing Rap1 at significantly higher levels than the primed Ag-specific T cells (Figure 5.8H). In addition, when splenic tissue was examined, a significantly higher percentage of tolerised compared to primed Ag-specific T cells were expressing Rap1 and the pERK-

expressing tolerised T cells exhibited significantly lower levels of ERK activation than the primed T cells (data not shown). From these data, it seems possible that the increased Rap1 expression observed in the *in vivo* tolerised T cells *in situ*, may correlate with the downregulation of ERK activation detected in these cells *in vivo*.

5.7 Does Rap1 also have a role in the maintenance of oral tolerance *in vivo*?

To determine whether elevated Rap1 expression is generally associated with the maintenance of tolerance *in vivo*, or restricted to that induced systemically, the pattern of pERK and Rap1 expression in a more physiologically relevant model of oral tolerance (58, 384) was examined. Mice were thus fed soluble OVA to induce tolerance or immunised subcutaneously with OVA/CFA to induce priming. The efficacy of this immunisation regime to induce priming and oral tolerance has previously been demonstrated (58). For example, Smith *et al* showed that animals tolerised in this manner generated a significantly lower Ag-specific delayed type hypersensitivity (DTH) response, less clonal expansion and fewer divisions of the Ag-specific T cells in the MLN than the primed animals (58), significantly reduced serum Ab production, a defect in follicular migration during the primary response to Ag and an inability to provide B cell help after challenge with Ag (384). In summary, this oral tolerising regime has been shown to be highly effective at inducing a state of tolerance *in vivo*.

Ten days after primary immunisation, mice were challenged with $OVA_{323-339}$ i.v. and 1 h later the expression of pERK and Rap1 in Ag-specific Tg T cells was examined in the inguinal PLN. In agreement with the *in vitro* and *in vivo* systemic models of tolerance, a significantly lower percentage of tolerised compared to primed Ag-specific T cells expressed pERK, after challenge with Ag (Figure 5.9B, C). Moreover, there did appear to be a trend indicating that the primed T cells were expressing higher levels of ERK activation, however this was not significantly different between the groups (Figure 5.9D), although it is possible that if more tissue sections per group were analysed, this apparent trend would be substantiated. By contrast, when Rap1 expression was assessed in these samples, a significantly higher proportion of tolerised compared to primed Ag-specific T cells expressed Rap1 (Figure 5.9F, G). In addition, and in agreement with the *in vitro* data, the tolerised Ag-specific T cells expressed Rap1 at significantly higher levels than the primed Ag-specific T cells (Figure 5.9F). Collectively, these data demonstrate that pERK and Rap1 exhibit inverse patterns of expression in both systemic and oral models of

tolerance and priming, which lends further support for the potential contributory role of Rap1 in the downregulation of ERK activation observed in tolerised T cells *in vivo*.

5.8 Assessing the migratory capacity of Rap1 expressing Ag-specific T cells

As described above, Ag-specific T cells tolerised *in vivo* do not enter B cell follicles. However, when re-challenged with a priming antigenic signal *in vivo*, such tolerised T cells are able to enter B cell follicles but they remain unresponsive as evidenced by their inability to provide B cell help (384). To investigate whether such unresponsiveness of follicular-located T cells reflects Rap1 expression, the percentage of Ag-specific T cells expressing Rap1 in distinct areas of the PLN was quantitated *in situ* by LSC, as described in Section 2.6.3. Consistent with the finding that re-challenge with priming Ag abrogates the block in follicular migration of tolerised T cells, there was no difference in the percentage of Ag-specific T cells expressing Rap1 in the B cell follicles or paracortex between groups, when this was measured as a percentage of the total number of Rap1-expressing Ag-specific T cells in the whole tissue (Figure 5.10C). However, the follicular tolerised Ag-specific T cells expressing Rap1 were found to express Rap1 at a significantly higher level than follicular primed Ag-specific T cells in the PLN (Figure 5.10D). Interestingly, when the number of Ag-specific T cells expressing Rap1 was expressed as a percentage of the total number of Ag-specific T cells in the follicle or paracortex, there was a significantly higher percentage of tolerised compared to primed Ag-specific T cells expressing Rap1 in the follicles and this also appeared to apply to paracortical cells in the PLN where a significant difference was detected (Figure 5.10E).

Although tolerised T cells regain migratory capacity following antigenic challenge, they have been shown to be defective in their ability to provide B cell help (384). As Rap1 may be involved in the disruption of MAPK signalling in tolerised T cells after challenge with Ag *in vivo*, the upregulated expression of Rap1 detected in tolerised compared to primed follicular Ag-specific T cells could therefore potentially implicate a role for Rap1 in incapacitating T cells from providing B cell help.

5.9 Examining Rap1 expression in Ag-specific T cells situated in distinct tissue locations during the maintenance phase of oral tolerance

The microenvironment location of Ag-specific T cells following oral induction of tolerance was also assessed to determine whether such localisation reflected the level of

Rap1 expression in these cells. Again, tissue was processed for analysis by LSC as described earlier for Figure 5.10 and the percentage of Ag-specific T cells expressing Rap1 as well as the intensity of Rap1 expression in these cells was quantitated in distinct areas of the lymph node *in situ* (Figure 5.11). There was no significant difference in the number of Ag-specific T cells expressing Rap1 in the B cell follicles or paracortex between groups, when this was measured as a percentage of the total number of Rap1-expressing Ag-specific T cells, in the PLN (Figure 5.11A). However, the follicular tolerised Ag-specific T cells expressing Rap1 were found to express Rap1 at a significantly higher level than follicular primed Ag-specific T cells (Figure 5.11B). In addition, no difference was observed, between the primed and tolerised T cells, when the number of Ag-specific T cells expressing Rap1 was expressed as a percentage of the total number of Ag-specific T cells in the follicle or paracortex (Figure 5.11C).

5.10 Preliminary investigation of the role(s) of pERK and Rap1 signalling in the induction phase of systemic priming and tolerance *in vivo*.

As described previously, the data generated from the *in vitro* studies indicated that pERK and Rap1 play roles in the maintenance but not induction phases of priming and tolerance. To investigate whether these molecules played roles in the induction phase of tolerance *in vivo*, pERK and Rap1 expression was assessed *in situ* in tolerised and primed Ag-specific T cells following primary exposure to Ag *in vivo*. Thus, 24 h after adoptive transfer of Ag-specific TcR Tg T cells, recipient mice were immunised with $OVA_{323-339}$ peptide i.v., either alone or together with LPS to induce systemic tolerance or priming respectively. At 0, 4, 8, 12, 24 and 72 h following immunisation, PLN were harvested and the clonal expansion of the Ag-specific TcR Tg ($CD4^+$ $KJ1.26^+$) T cell population in each group was analysed by flow cytometry, as described in Sections 2.3.1 and 2.3.6. As expected and shown earlier (Figure 5.5), the peak of clonal expansion was observed 72 h after immunisation in both the tolerised and primed groups (Figure 5.12A). However, no clonal expansion was observed prior to this timepoint in any of the groups examined (Figure 5.12A).

Due to the lack of Ag-specific T cell clonal expansion at any of the timepoints examined except 72 h, the frequency of Ag-specific T cells per tissue section was inadequate for quantitative analysis of pERK and Rap1 expression in these cells by LSC. Instead, frozen archived tissues from each group were thawed and processed for detection

of CD4, KJ1.26 and pERK or Rap1 expression by flow cytometry as described in Sections 2.3.1 and 2.3.6. When the proportion of Ag-specific T cells expressing pERK was assessed, a significantly higher percentage of primed (22 %) compared to tolerised (12 %) T cells were found to exhibit ERK activation at 12 h (Figure 5.12B). However, an inverse pattern was observed at 24 h, when significantly more tolerised (47 %) than primed (6 %) T cells expressed pERK. A negligible percentage of naive T cells expressed pERK at all of the timepoints examined. A more detailed kinetic study of pERK expression at, and between, these timepoints may shed further light on the possible role of these differential kinetics of ERK activation during this part of the induction phase of tolerance.

By contrast, Ag-specific T cells displayed similar kinetics of Rap1 expression during the induction of priming and tolerance and a higher proportion of both tolerised and primed groups expressed Rap1 compared with naïve T cells at 4, 8, 12 and 24 h after immunisation (Figure 5.12C). Such data indicates that elevated percentages of Rap1-expressing T cells are required for induction of both tolerance and priming. When the levels of both pERK and Rap1 expression in the different Ag-specific T cell populations were measured, no differences were detected between the groups, suggesting that the levels of ERK activation or Rap1 expression did not play a determining role in the induction phase of tolerance or priming (Figure 5.12D, E).

Discussion

It was shown in the previous chapter that marked differences in the kinetics, amplitude and localisation of pERK signals were found in individual naïve, primed and tolerised primary Ag-specific T cells responding to Ag *in vitro* (Chapter 4; (12)). In particular, it was shown that primed T cells display higher levels of phosphorylation and activation of ERK, upon challenge, than tolerised T cells. In addition, the low levels of pERK found in tolerised T cells were distributed diffusely throughout the cell, whereas in primed T cells, pERK appeared to be targeted to the same regions of the cell as the TcR (Chapter 4; (12)). These studies have now been extended to physiological *in vivo* models of Ag-specific priming and tolerance and have shown that a higher percentage of primed, relative to naïve or tolerised Ag-specific T cells *in situ* exhibit pERK expression following re-challenge with Ag indicating that sustained ERK signalling *in vivo* correlates with productive T cell responses whilst defective ERK signalling is associated with the maintenance of tolerance. The precise mechanisms underlying such differential ERK signalling remain unclear but the data provided in this chapter show that the GTPase Rap1, which has previously been reported to accumulate and antagonise signals upstream of ERK activation under tolerogenic conditions *in vitro* (50, 347), is expressed in a significantly higher percentage of tolerised Ag-specific T cells, and at significantly higher levels, compared with primed T cells following challenge with Ag, both *in vitro* and *in vivo*. It is important to emphasise that, in accordance with the *in vitro* experiments, the inverse relationship between the accumulation of Rap1 and antagonism of ERK activation was also observed during the maintenance of tolerance *in vivo*. Moreover, as such a relationship was also observed in an oral tolerance model *in vivo*, these findings may have potential implications for clinical application, as oral tolerance has been suggested as a therapy for inflammatory disorders (570) and also because oral administration of compounds offers a more attractive route for drug delivery in humans.

The finding that Rap1 expression is downregulated in naïve and primed T cells after activation in the presence of costimulation is consistent with previous reports that CD28-signalling downregulates Rap1 (351-353). Moreover, the pattern of expression of Rap1 in such cells is the inverse to that of pERK thus, in anergic T cells, Rap1 shows a highly focused, peripheral expression that mirrors that of the TcR and is reminiscent of the formation of an immunological synapse, whereas in primed T cells, despite still forming foci at the periphery, expression of Rap1 is less polarised to the periphery and more diffuse

throughout the cell. The finding that Rap1 could be localised to the periphery of both primed and anergic T cells suggested that localisation alone was not sufficient to disrupt the peripheral recruitment and activation of pERK necessary for priming and that Rap1 activation and/or complex formation with other signal transducers may be required.

In this respect, it should be noted that the association between pERK and Rap1 and lipid rafts in re-stimulated, primed and tolerised cells also revealed an inverse relationship, with pERK being localised within such membrane microdomains in primed but not tolerised cells and Rap1 being targeted to lipid rafts in tolerised Ag-specific T cells. Collectively, these data suggest that Rap1 may be up-regulated and recruited to the immune synapse upon stimulation of tolerised T cells with Ag and that this may result in downregulation of ERK recruitment and activation, possibly as a result of Raf-1 sequestration. This would lead to the uncoupling of the RasERKMAPkinase pathway from the TcR as has been observed in tolerant cells (571-573).

As mentioned previously, Ag-specific unresponsiveness can result in cell cycle arrest at the transition from G_1-S phase and associated with this, enhanced ERK activation observed in primed relative to anergic T cells correlated with increased ERK activation at all stages of cell cycle progression but not in cells arrested in G_1 or undergoing apoptosis (Figures 4.9-4.11). It therefore seemed possible that the highest proportion of Rap1-expressing anergic T cells would be detected in G_0/G_1. However, when Rap1 expression was assessed in such cells at different stages of cell cycle, no differences were observed between the groups (Figure 5.3). Such data may also reflect the dual roles of Rap1, as Rap1 may be fulfilling a positive regulatory role in primed $Rap1^{hi}$ Ag-specific T cells. Moreover, the current data only provide a snapshot, at two timepoints, of Rap1 signalling in relation to cell cycle status of T cells and in order for this relationship to be fully investigated, extensive kinetic studies would be required in which regular, frequent timepoints from 0 to at least 48 h following co-culture of T cells with APC, need to be assessed. Such analysis would be necessary to investigate the possibly differential kinetics of the responses elicited by anergic versus primed T cells. For example, the rate of cell cycle progression may be different in these two cell types thus, kinetic studies should enable a more informed interpretation of the signalling profiles within these different cellular populations.

Integrins are known to play a role in the migration and localisation of T cells (574, 575) and Rap1 has received recent attention for its role in enhancing the function of a variety of integrins including LFA-1 & VLA-4 (576, 577). Consistent with this, Rap1A-

deficient T cells have been shown to exhibit impaired integrin-mediated cellular adhesion (578) and Rap1-dependent adhesion via different integrin subsets is known to facilitate T cell migration and augment Ag-dependent T cell activation (560, 577). Thus, further to the differential expression of Rap1 observed in *in vivo* tolerised and primed T cells, Rap1 signalling was examined in Ag-specific T cells which were situated in distinct areas of the lymph node. Although tolerised T cells regain their ability to migrate into the B cell-rich follicles following antigenic challenge, they have been shown to be defective in their ability to provide B cell help (384). As Rap1 may be involved in the disruption of MAPK signalling in tolerised T cells after challenge with Ag *in vivo*, the upregulated expression of Rap1 detected in tolerised compared to primed follicular Ag-specific T cells in this work could potentially implicate a role for Rap1 in incapacitating T cells from providing B cell help.

Rap1 has long been implicated in the desensitisation of ERK and the consequent defective IL-2 production found in tolerised T cells (50, 352, 354, 579). Moreover, recent studies by Boussiotis and coworkers (580) have directly demonstrated that $CD4^+$ T cells from Tg mice expressing a constitutively active Rap1 mutant, Rap1E63, exhibit defective ERK activation, IL-2 production and proliferation when primed *in vivo* and re-stimulated with specific Ag *in vitro*. These results were interpreted as showing that the expression of Rap1E63 may be responsible for maintaining the anergic state. Interestingly, Rap1E63-Tg mice also exhibit increased numbers of $CD4^+$ $CD103^+$ T cells with regulatory function (581) and other recent work shows that $CD4^+$ $CD25^+$ T_{regs}, from human cord blood display sustained Rap1, but impaired ERK, signalling in response to challenge with Ag, resulting in defective IL-2 production, cell cycle arrest and apoptosis (581). Together these results suggest a central role for Rap1 in T cell hyporesponsiveness in general rather than simply being restricted to T cell anergy.

Indeed, the mechanisms responsible for the tolerance observed in the present studies have not been fully elucidated, as this is an area of considerable uncertainty in the field in general and with tolerant T cells *in vivo* in particular. The anti-CD3 treatment regime has classically been used to induce “anergy” in T cells *in vitro* (53, 582, 583) and in the current studies, the behaviour of such treated cells was entirely consistent with this definition, as they do not proliferate or produce IL-2 when restimulated with antigen (12). Similarly, the T cell proliferation (clonal expansion) observed during the induction phase of tolerance *in vivo*, followed by failure to proliferate or make effector cytokines on restimulation, is

entirely consistent with this form of tolerance (13-18). Nevertheless, in the absence of specific markers of anergy, it is difficult to prove that the T cells studied here *in vivo* are truly "anergic". Moreover, such T cell proliferation during the induction phase of tolerance with consequent failure to expand in response to a secondary antigenic challenge is an almost universal feature of all models of peripheral tolerance. Therefore, cells have simply been described as "tolerised" as it is possible that more than one form of T cell unresponsiveness could be present (12, 582).

Despite Rap1 upregulation being widely associated with tolerance, the precise role(s) of Rap1 in T cell biology has become increasingly controversial. Indeed, mice transgenic for a different constitutively active mutant of Rap1, Rap1V12, showed normal T cell proliferation and ERK activation in response to anti-CD3 stimulation (560). Other studies have also implicated a positive role for Rap1 in T cell signalling (356, 357), possibly mediated by the adhesion and degranulation-promoting protein (ADAP) (584, 585) which plays a key role in cytoskeletal rearrangement and in the regulation of synapse formation following TcR activation (586). It is not known how the TcR and Rap1 might connect to ADAP signalling, but it is likely to involve Fyn and SLP-76 (584, 585) activating Rap1 via PLCε, which contains a Ras-Rap-binding domain (RBD) and can act as a guanine nucleotide exchange factor (GEF) for Rap1 (587, 588). Consistent with this, there is evidence that Rap1 activation after antigen-specific triggering of lymphocytes requires PLC activation and consequent calcium mobilisation and DAG generation (560, 589, 590).

At first sight it might appear difficult to reconcile such opposing models of Rap1 signalling. However, it is possible that Rap1 may play distinct roles depending on the context of the signal and/or on stage of priming and tolerance. Indeed, it has been shown here that Rap1 expression is up-regulated during the induction phases of both priming and tolerance, relative to the levels seen in naïve cells. Thus, in the early stages of T cell activation common to the induction of both priming and tolerance, Rap1 may act to promote TcR signalling via integrin-mediated inside-out signalling. However, once priming or tolerance is established, it is possible that "rewiring" of Rap1 signalling occurs, reflecting differential levels/kinetics of Rap1 expression. Consistent with a role for signal strength in directing these processes, Boussiotis *et al* (580) suggested that the differential responses of the Rap1V12- and Rap1E63-Tg mice might reflect the finding that the Rap1E63 mutant exhibits 5x the biological activity of Rap1V12 (591) being insensitive to the negative regulator of Rap1, Rap1GAP (592). This proposal is supported by recent

studies showing that mice which are deficient in the Rap1GAP, SPA-1, exhibit defective ERK activation and progressive unresponsiveness or tolerance of T cells (355).

Alternatively, rewiring of Rap1 signalling may reflect compartmentalisation mediated by the Fyn-Cbl-CrkL-C3G-Rap1 complex which is generated selectively in tolerant T cells (50). Consistent with this latter idea, the preferential expression of Rap1 in tolerised cells showed an inverse pattern of expression to that of pERK, with Rap1 expression being localized within lipid rafts at the plasma membrane of tolerised cells (12). The mechanisms involved in such temporal and spatial segregation are not clear but may reflect the functional sequestration of Fyn (within lipid rafts) from Lck in the absence of productive priming (593). Defective partitioning of Lck and Fyn has been postulated to be an early negative signal in the induction of T cell anergy (594) and may contribute to the reduced phosphorylation and lipid raft recruitment of LAT (327), with the consequent uncoupling of downstream signals such as PLCγ, PKC and ERK (225, 595) observed in tolerised T cells. Such decreased PLC-γ1 and PKC-θ signalling, and the subsequent decrease in LFA-1 function, have in turn been suggested as being responsible for the defective translocation of TcR, PKC-θ and lipid rafts into the immunological synapse in tolerised T cells (564, 565). However, the inverse localisation of pERK staining within plasma membrane lipid rafts in primed but not tolerised cells might suggest that Rap1 antagonism of ERK activation could also reflect disruption and termination of productive synapse formation and signalling. Consistent with this, recent reports have indicated that ERK is an intermediate signal in the Vav/Rac2-mediated pathway (552) leading to nucleation of actin filaments and cytoskeleton remodelling at the immunological synapse (553). Thus, partitioning of Fyn and Lck and the consequent generation of the negative regulatory complex comprising Fyn, PAG and Csk (596, 597), might be required for compartmentalisation and rewiring of Rap1 signalling via the assembly of the Fyn-Cbl-CrkL-C3G-Rap1 complex (322, 323, 598), that is found to be selectively expressed in tolerised cells (50).

In summary, these data show that the defective ERK signalling observed in tolerised Ag-specific $CD4^+$ T cells (12) correlates with up-regulation of Rap1 in tolerised, relative to primed, cells following subsequent stimulation with Ag *in vitro* and in both systemic and oral tolerance models *in vivo*. Importantly, they demonstrate for the first time, a physiologically relevant, inverse relationship between endogeneous Rap1 and pERK

expression and signalling, *in situ*, in individual antigen-specific $CD4^+$ T cells that have been primed or tolerised *in vivo*. As this occurs after the induction of both systemic and oral routes of tolerance, these data suggest that Rap1 antagonism of pERK signalling may play an important and general role in the maintenance of antigen-specific $CD4^+$ T cell tolerance.

Figure 5.1 Quantitation of Rap1 expression in primed and tolerised Ag-specific T cells at the single cell level by LSC. Naïve T cells were freshly isolated from resting mice whilst tolerised or primed Tg Ag-specific T cells were generated *in vitro* using anti-CD3 ± anti-CD28, as described in Chapter 2. The cells were then re-stimulated with DC alone (open bars) or DC + $OVA_{323-339}$ (closed bars) for 20 h. In panel A, IL-2 production was determined by analysis of culture supernatants by ELISA and the ELISA results shown are the mean ± SD of triplicate cultures. In panel B, exemplar LSC histograms showing cells re-stimulated with DC alone (i) or DC + $OVA_{323-339}$ (ii) depict how cells were gated upon for analysis. From these it was clear that whilst the level of Rap1 expression was similar in all groups, the percentage of anergic $KJ1.26^+$ T cells expressing Rap1 was greater compared with naïve and primed $KJ1.26^+$ T cells upon re-stimulation with Ag (panel B. ii.). All data are representative of at least three individual experiments with quantitative population statistical analysis being performed on at least 200 $KJ1.26^+$ T cells in each group. The proportion of Ag-specific ($KJ1\text{-}26^+$) T cells expressing Rap1 (panel C) and the total cellular level of Rap1 expression (panel D) in $Rap1^+$ Ag-specific ($KJ1\text{-}26^+$) T cells was determined by LSC analysis (panel B).

Figure 5.2 Intracellular localisation of Rap1 expression in Ag-specific Tg T cells. Anergic and primed Ag-specific Tg T cells were generated *in vitro* using anti-CD3 ± anti-CD28, as described in the Methods section, and re-stimulated with DC alone (open bars) or DC + $OVA_{323-339}$ (closed bars) for 20 h. Cells were treated with DAPI to stain the nuclei (blue) and the clonotypic Ab KJ1-26 to visualise the Tg TcR (red). Rap1 or pERK expression was detected using specific Abs (green). KJ1-26^+ $Rap1^+$ T cells from anergic and primed samples were randomly relocated by LSC. Representative individual anergic and primed cells were identified and imaged as described previously ((12); panel A) showing the relative levels of expression of Rap1 and pERK in primed and anergic cell populations. pERK expression in anergic cells was also imaged using a higher exposure time to demonstrate better the distribution of signal within these cells (pERK*, panel A). Panel B shows an example of 3-colour merged images depicting a $Rap1^+$ (green staining) KJ1-26^+ (red staining) T cell (panel i) with threshold (red), integral (green) and peripheral (yellow) contours applied (panel ii). Peripheral contours discriminate the periphery of the cell, external to the nucleus, and the fluorescence detected therein was plotted as histograms (panel C). In panel D, the percentage of KJ1-26^+ T cells expressing Rap1 at their periphery was therefore quantitated by peripheral contouring using LSC. Similarly, the peripheral MFI of Rap1 is shown in Panel E, while Panel F shows the intensity (Max Pixel value) of Rap1 expression within the periphery, calculated as the difference between the Max Pixel of cells cultured with DC alone and those stimulated with DC + $OVA_{323-339}$. Rap1 expression was assessed in 200 anergic (open bars) and primed (closed bars) $Rap1^+$ KJ1-26^+ T cells per samples and results are representative of three replicate experiments. In panel G, anergic and primed Ag-specific T cells were induced and re-stimulated with DC + Ag for 20 h. Ag-specific Tg T cells were identified by the clonotypic Ab KJ1-26 (blue) whereas Rap1 or pERK expression was detected by the relevant specific Abs (red) and lipid raft structures were identified using a Cholera Toxin subunit B-Alexa Fluor® 488 conjugate (green). KJ1-26^+ $pERK^+$ and KJ1-26^+ $Rap1^+$ T cells from anergic and primed samples were randomly relocated by LSC and the localisation of pERK and Rap1 in KJ1.26^+ T cells was determined in relation to lipid rafts (KJ1-26 staining not shown). Yellow indicates co-localisation of signal with lipid rafts. Representative individual anergic and primed cells were identified and imaged as described previously (12).

Figure 5.3 Analysis of cell cycle progression of Rap1 expressing Ag-specific primary T cells after stimulation with Ag-pulsed or unpulsed APCs by LSC. Anergic (open bars) and primed (closed bars) Ag-specific T cells were re-stimulated with DC alone (A, B) or DC loaded with $OVA_{323-339}$ (C, D), for 1 (A, C) or 20 h (B, D). Ag-specific TcR Tg T cells were identified by staining with the clonotypic Ab KJ1-26 and Rap1 was detected using an appropriate Ab. All cell nuclei were stained with DAPI and the cell cycle status of the Rap1-expressing Ag-specific T cell population was analysed by LSC as described in Sections 2.5.1 and 4.5. The percentage of Ag-specific T cells expressing Rap1 following incubation with DC alone or DC loaded with $OVA_{323-339}$ in each stage of cell cycle was calculated. The number of Ag-specific T cells in each stage of cell cycle was also measured by LSC (E).

Figure 5.4 Measurement of Rap1 expression levels in Ag-specific primary T cells in different stages of cell cycle by LSC. Anergic and primed Ag-specific T cells were re-stimulated with DC alone or DC loaded with $OVA_{323-339,}$ for 1 or 20 h. Ag-specific TcR Tg T cells were identified by staining with the clonotypic Ab KJ1-26 and Rap1 was detected using an appropriate Ab. All cell nuclei were stained with DAPI and the cell cycle status of $KJ1.26^{+}$ $Rap1^{+}$ T cells was analysed by LSC as described in Chapters 2-4. The level of Rap1 expression in anergic (open bars) and primed (closed bars) $KJ1.26^{+}$ $Rap1^{+}$ T cells was assessed for each stage of the cell cycle. Such analysis was performed following incubation with DC alone (A, B) or DC loaded with $OVA_{323-339}$ (C, D) for 1 (A, C) or 20 h (B, D).

Figure 5.5 Clonal expansion of Ag-specific CD4$^+$ T cells *in vivo*. Ag-specific TcR Tg T cells were adoptively transferred into naïve recipients 24 h prior to i.v. injection with $OVA_{323-339}$ + LPS (primed; closed squares), $OVA_{323-339}$ alone (tolerised; open squares) or sterile PBS (naïve; triangles). At D0, 3, 5 and 10 after immunisation, PLN (A), MLN (B) and spleens (C) were harvested, single cell suspensions were prepared and stained for expression of CD4 and KJ1.26 as described in Section 2.1.7. Subsequently, the percentage of CD4$^+$ Ag-specific Tg T cells in each tissue was assessed by flow cytometry. Data represent mean ± SD for three mice per group *$p<0.05$, **$p<0.01$.

Figure 5.6 Analysis of T cell migration into B cell follicles. Ag-specific TcR Tg T cells were adoptively transferred into naïve recipients 24 h prior to i.v. injection with $OVA_{323-339}$ + LPS (primed), $OVA_{323-339}$ alone (tolerised) or sterile PBS (naïve). At D3 after immunisation, PLN were harvested, and the percentage of Ag-specific Tg T cells present in follicular and paracortical areas of this tissue was determined by LSC (392, 479, 480). LSC histograms depicting how $B220^+$ B cells (A) and KJ1-26^+ T cells (B) were gated are shown, together with a sample tissue map which illustrates how KJ1-26^+ T cells situated in follicular and paracortical areas of the lymph node were quantitated (C). The proportions of naïve, tolerised and primed Ag-specific T cells situated in follicular (open bars) and paracortical (closed bars) areas of the lymph node were quantitated by LSC (D). The data represent mean ± SD for three mice per group *$p<0.05$.

Figure 5.7 Functional analysis of T cells tolerised or primed *in vivo*. Ag-specific TcR Tg T cells were adoptively transferred into naïve recipients 24 h prior to i.v. injection with $OVA_{323-339}$ + LPS (primed), $OVA_{323-339}$ alone (tolerised) or sterile PBS (naive). At D10 after immunisation, PLN were harvested and single cell suspensions were re-stimulated *in vitro* with or without Ag to assess proliferation (A) and IFNγ production (B). Proliferation was assayed by [^{3}H] thymidine uptake at 72 h and the level of IFNγ in culture supernatants was detected by ELISA at 48 h after re-stimulation *in vitro*. Both proliferation and IFNγ data are expressed as fold increase in signal from samples re-stimulated in the presence of Ag compared with the signal from those re-stimulated with media alone. Ova-specific IgG1 antibody levels in serum, of mice challenged with OVA/CFA 7 days after the induction of priming or tolerance with $OVA_{323-339}$ ± LPS, were also measured (C). Data represent mean ± SD for three mice per group and each animal sample was performed in triplicate. *$p<0.05$, **$p<0.01$.

Figure 5.8 Quantitation of Ag-specific pERK and Rap1 expression in primed and tolerised Ag-specific T cells in PLNs *in situ* by LSC. Following induction of systemic priming or tolerance of adoptively transferred Tg TcR T cells *in vivo*, all groups were challenged with 100 μg $OVA_{323-339}$/1 μg LPS 7 days after primary immunisation. Inguinal lymph nodes (PLN) were harvested 24 h after challenge, sectioned and stained using the appropriate specific Abs, for TcR Tg T cells (KJ1-26; red), B cells (B220; green) and pERK or Rap1 (blue). Sample stained tissue sections from tolerised and primed animals are shown (A, E). LSC analysis (as described previously (1); B, F) were used to determine the proportion of Ag-specific T cells expressing pERK (C) and Rap1 (G) as well as the total cellular levels of pERK (D) and Rap1 expression (H) *in situ*. Representative LSC histograms depicting the pERK and Rap1 signalling profiles in tolerised and primed T cells, *in situ,* are shown in panels B & F. Results presented in panels C, D, G & H are mean values ± SD of three animals per group. *$p<0.05$, **/*$p<0.01$.

Figure 5.9 Quantitation of Ag-specific pERK and Rap1 expression in primed and orally tolerised Ag-specific T cells in PLNs *in situ* by LSC. Following induction of priming or tolerance of adoptively transferred Tg TcR T cells *in vivo*, all groups were challenged with 100 μg $OVA_{323-339}$ 10 days after primary immunisation. Inguinal lymph nodes were harvested 1 h after secondary challenge and stained using the appropriate specific Abs, for TcR Tg T cells (KJ1-26; red), B cells (B220; green) and pERK or Rap1 (blue). Sample stained tissue sections from orally tolerised and primed animals are shown (A, E). Analysis by LSC (as described previously (1); B, F) were used to determine the proportion of Ag-specific T cells expressing pERK (C) and Rap1 (G) as well as the total cellular levels of pERK (D) and Rap1 expression (H) *in situ*. Representative LSC histograms depicting the pERK and Rap1 signalling profiles in tolerised and primed T cells, *in situ,* are shown in panels B & F. The results shown in C, D, G & H are expressed as mean section values ± SD where sections were derived from three animals per group. *$p<0.05$, **$p<0.01$.

Figure 5.10 Detection of Rap1 expression by Ag-specific T cells in different tissue locations *ex vivo* by LSC. Following induction of priming or tolerance of adoptively transferred Tg TcR T cells *in vivo*, all groups were challenged with 100 μg $OVA_{323-339}$/1 μg LPS 7 days after primary immunisation. Inguinal lymph nodes were harvested 24 h after challenge, sectioned and stained using the appropriate specific Abs, for TcR Tg T cells (KJ1-26; red), B cells (B220; green) and pERK or Rap1 (blue). A sample stained tissue section from a primed animal is shown (A). The location of the Ag-specific Tg T cells and B cell follicles within the lymph node sections was determined by LSC, as described in Figures 3.10 and 3.11 (B). Gates were placed on all follicular and paracortical regions depicted on a tissue map (B) and statistics from these gates were used to calculate the proportion of Ag-specific T cells expressing Rap1 (C) and the level at which they were expressing Rap1 (D) in different locations within the lymph node *in situ*. The number of Ag-specific, Rap1-expressing T cells in the follicles and paracortex was also expressed as the percentage of total Ag-specific T cells in the follicles or paracortex (E). Data represent mean ± SD for three mice per group *$p<0.05$, **$p<0.01$.

Figure 5.11 Detection of Rap1 expression by orally tolerised Ag-specific T cells in different tissue locations *ex vivo* by LSC. Following induction of priming or oral tolerance of adoptively transferred Tg TcR T cells *in vivo*, all groups were challenged with 100 μg $OVA_{323-339}$ 10 days after primary immunisation. Inguinal lymph nodes were harvested 1 h after challenge and stained as described in Figure 5.10 legend. The location of the Ag-specific Tg T cells and B cell follicles within the lymph node sections was determined by LSC as described in Figure 5.10 legend. All follicular and paracortical regions were gated upon using tissue maps and statistics from these gates were used to calculate the proportion of Ag-specific T cells expressing Rap1 (A) and the level at which they were expressing Rap1 (B) in different locations within the lymph node *in situ*. The number of Rap1-expressing Ag-specific T cells was also expressed as a percentage of the total number of Ag-specific T cells in the follicular or paracortical areas (C). Data represent mean ± SD for three mice per group *$p<0.05$.

Figure 5.12 Quantitation of Ag-specific pERK and Rap1 expression in the induction phase of tolerance *in vivo*. Twenty four h after adoptive transfer of Ag-specific TcR Tg T cells, recipient mice were immunised with $OVA_{323-339}$ peptide i.v., either alone or together with LPS to induce systemic tolerance (blue triangles) or priming (red triangles) respectively. Control mice received sterile PBS i.v. and are denoted "Naïve" (black squares). Zero, 4, 8, 12, 24 and 72 h following immunisation, PLN were harvested and processed for detection of CD4, KJ1.26 and pERK or Rap1 expression by flow cytometry, as described in Sections 2.3.1 and 2.3.6. Clonal expansion of the Ag-specific TcR Tg T cell population was assessed for each group (A) and the percentage of Ag-specific TcR Tg T cells expressing pERK (B) or Rap1 (C) as well as the level at which these molecules are expressed in these cells (D, E) are also shown here. These data are representative of three animals per group. *$p<0.05$, **$p<0.01$.

Chapter 6

General Discussion

6. General discussion

The immune system in a healthy individual is capable of distinguishing self, or harmless, from harmful non-self antigens. This discriminatory capacity enables the body to both elicit a productive primed immune response against invasive pathogens and generate a state of antigen-specific hyporesponsiveness towards self components (30) or harmless food antigens. This state of antigen-specific hyporesponsiveness, known as peripheral tolerance, is induced when T cells are exposed to antigen under sub-optimal activating conditions (46). Once it is induced, it can suppress many aspects of the antigen-specific immune response to subsequent antigenic challenge, including lymphocyte proliferation, cytokine production, delayed-type hypersensitivity and antibody production (114). A breakdown in tolerance within an individual can result in the development of a variety of autoimmune disorders e.g. Type 1 diabetes, rheumatoid arthritis, systemic lupus erythematosus and inflammatory bowel disease (IBD). Despite a plethora of work in this field, however, the mechanisms by which the immune system can discriminate harmless and pathogenic antigens remain to be fully elucidated. If these mechanisms are further understood, hopefully this information could be exploited to help develop better therapies for autoimmune diseases, improve the rate of successful transplantations and increase the efficacy of vaccines.

6.1 Development of a quantitative imaging technology for examining signalling *in situ*

It has been widely proposed that both qualitative and quantitative differences in T cell signalling may underlie the differential functional outcomes of tolerance and priming (525, 539). However, the majority of these studies have relied upon biochemical assessment of signalling in T cell lines or clones, at the population level following polyclonal stimulation *in vitro,* leading to conflicting data. Moreover, these data do not necessarily reflect the responses of physiological frequencies of individual antigen-specific T cells within their environmental niche within primary or secondary lymphoid tissue. In addition, such data represents the responses of all of the cell types in the sample population at any one time and hence does not provide any information on the differential kinetics, amplitude or subcellular localisation of signals generated by functionally distinct subgroups within the population.

Flow cytometry offers the rapid assessment of intracellular signalling in such distinct cell sub-populations and these signalling data can be directly related to the

functional status of the cells, in terms of activation status, proliferative capacity and cytokine production. However, a newer technology, laser scanning cytometry (LSC), offers further possibilities as it essentially marries the quantitative capabilities of flow cytometric analysis of cells in suspension with the ability to analyse spatially the fluorescence of large numbers of individual cells, either in suspension or in tissue in a slide-based format. Although LSC and flow cytometry should be viewed and used as complementary quantitative technologies, LSC has the potential to provide a quantum leap in the analysis of immune function, due to the wide range of novel applications that it offers and have been described in Chapter 3.

Previously, such *in situ* analysis of cells in tissue sections by LSC has been achieved by contouring on nuclei. Due to the close proximity of cells in tissue, this work necessitates multiple repeat scans of the same area of tissue at different threshold levels, followed by merging of single threshold level data files into one file (478). Whilst informative, this type of *in situ* analysis does not detect all of the cells in the sample and there is also the possibility of detecting false positives, as it is likely that certain cells will be counted more than once. Thus, the limited adoptive transfer system involving TcR Tg T cells (569) provides an attractive means of studying antigen-specific responses occurring at physiological frequencies *in situ*, as it generates an even distribution of antigen-specific TcR Tg T cells throughout the thymus-dependent area of the lymph node. Such antigen-specific T cells can be readily distinguished from the endogenous T cells by LSC, following fluorescent staining of their Tg TcR, as they are sparsely situated amongst the endogenous T cell population within the lymph node. The studies reported in Chapter 3 describe how use of the adoptive transfer system, in combination with LSC analysis, has enabled the development of a quantitative imaging technology with which to study T cell signalling in individual antigen-specific T cells *in vitro* and *in situ*.

6.2 Differential TcR-mediated signalling in tolerance versus priming *in vitro* and *in vivo*

In T cells, the maintenance phase of anergy has been reported to reflect defective activation of transcription factors, such as c-Jun/c-Fos, that are involved in formation of the AP-1 complex which is required for inducing transcription of the IL-2 gene and optimal activation and effector function of T cells (318, 331, 333, 336-338, 488). In turn, this appears to be determined by the lack of recruitment of the ERK, JNK and p38 MAPK

signalling cascades (333, 336, 338). In addition, Rap1 has long been implicated in such desensitisation of ERK, and the consequent reduced IL-2 production, observed in tolerised T cells (50, 352, 354, 579). However, as described earlier, the majority of these findings were obtained from *in vitro* studies of T cell lines or clones and as such are not necessarily representative of physiological responses of primary Ag-specific T cells *in situ*.

The studies in Chapters 4 and 5 therefore describe, for the first time, an inverse relationship between ERK activation and Rap1 expression in individual primary Ag-specific T cells during the maintenance phases of tolerance and priming, both *in vitro* and *in vivo* (Figures 6.1 and 6.2). Thus, the signalling events underlying antigen-specific responses in individual primary T cells were shown to demonstrate marked differences in the kinetics, amplitude and localisation of the MAPkinase pERK in priming versus anergy (Chapter 4). In accordance with the traditional biochemical studies in the literature, this work demonstrated that whilst ERK activation was elevated in all populations of T cells that were challenged with Ag, it was always lower in the anergic relative to primed populations. Analysis at the single cell level further revealed that the proportion of Ag-stimulated cells expressing pERK was also lower in the anergic relative to primed groups and the few anergised T cells expressing pERK did so at a lower level than the primed cells. Moreover, when these studies were extended to physiological *in vivo* models of Ag-specific priming and tolerance, it was shown that a significantly greater proportion of primed, relative to naïve or tolerised Ag-specific T cells *in situ* exhibited pERK expression following re-challenge with Ag, further indicating that elevated ERK signalling *in vivo* correlates with productive T cell responses whilst reduced ERK signalling is associated with the maintenance phase of tolerance.

In contrast, the data presented in Chapter 5 demonstrated that Rap1 was expressed in a greater proportion of anergic Ag-specific T cells, and at considerably higher levels, compared with primed T cells following re-stimulation with Ag *in vitro*. This inverse trend of Rap1 expression was also observed in tolerised Ag-specific T cells *in situ*, when *in vivo* models of priming and tolerance were examined. It is important to note that the inverse relationship between the accumulation of Rap1 and antagonism of ERK activation was observed during the maintenance phases of both systemic and oral tolerance *in vivo*, suggesting that such Rap1 signals play a general role in T cell hyporesponsiveness. As this type of tolerance induction has been proposed as a potential therapy for autoimmune

disorders (570) and, oral administration of compounds offers a more attractive route for drug delivery in humans, these findings may have potential clinical applications.

6.3 Differential T cell signalling during the induction and maintenance phases of tolerance

Strikingly, correlation of increased Rap1 expression with decreased ERK activation in tolerised T cells was only observed during the maintenance phase of tolerance both *in vitro* and *in vivo*. Indeed, similar patterns of Rap1 expression and ERK activation were observed in Ag-specific T cells during the induction phases of tolerance and priming both *in vitro* and *in vivo*. This was not necessarily surprising, as tolerised T cells are known to up-regulate expression of the early activation marker, CD69, to similar levels as detected for primed T cells and it is known that these T cells can clonally expand in response to primary immunisation *in vivo,* albeit to a significantly lower level than primed T cells. Therefore, such tolerised T cells exert some level of response upon initial encounter with Ag or Ab-mediated stimulation through the TcR.

The increased proportions of Rap1-expressing Ag-specific T cells observed in both the anergic and primed populations compared to the naïve population *in vitro* suggested that such increased percentages of Rap1-expressing T cells were required for the induction of both tolerance and priming. This hypothesis may fit with the reported positive regulatory role for Rap1 in T cell activation (356, 357, 560). In these studies, Sebzda *et al* generated mice in which constitutively active expression of Rap1A, V12Rap1A, was restricted to the T cell lineage and demonstrated that Rap1A activation was sufficient to induce considerable activation of the β1 and β2 integrins and hence T cell activation through avidity modulation (560). No evidence for a negative regulatory role for Rap1 in T cells was observed in these mice. However, although they did not display defective T cell activation *in vitro*, these studies did not extend to examine the effects of V12Rap1A on the induction or maintenance of tolerance *in vitro* or *in vivo.* Therefore, it seems possible that Rap1 may play distinct roles depending on the context of the signal and/or the stage of priming or tolerance. For example, in the early stages of T cell activation common to the induction of both priming and tolerance, Rap1 may act to promote TcR signalling via integrin-mediated inside-out signalling. In contrast, once priming or tolerance is established it is possible that “rewiring” of Rap1 signalling occurs, reflecting differential levels/kinetics of Rap1 expression.

6.4 Inverse subcellular localisation of pERK and Rap1 in tolerance

The inverse subcellular localisation of pERK and Rap1 found in tolerised versus primed Ag-specific T cells indicates that perhaps, compartmentalisation of at least these two molecules in addition to their differential expression levels is responsible for the downstream effects of tolerance, namely decreased IL-2 production, cell cycle progression and proliferation. Indeed, the subcellular positioning of these molecules may also play a role in maintaining a tolerogenic or primed state in T cells. Quantitation by LSC showed that the majority of the pERK signal appeared to be localised at the periphery of re-stimulated primed T cells, possibly in association with the TcR, *in vitro*. In contrast, pERK was distributed more diffusely throughout the anergic cells that expressed lower levels of pERK. These results were somewhat surprising, as it had been hypothesised that re-stimulation of primed cells would cause the translocation of pERK into the nucleus where it would activate the transcription factors required for IL-2 production (549) and that this process would be defective in anergic T cells. Rather, it appeared that after priming, pERK may associate with cytoskeletal- and/or membrane-associated scaffolds such as lipid rafts which contain the TcR and other proximal signalling molecules. Thus, these structures, or the association of pERK with them, may be defective in anergic T cells.

Here again, an inverse relationship was observed between pERK and Rap1, this time with respect to their subcellular localisation. Thus, in anergic T cells, Rap1 exhibited a highly focused peripheral expression that mirrored that of the TcR and was reminiscent of the formation of an immunological synapse. In contrast, whilst Rap1 still formed foci at the periphery in primed T cells, the expression of Rap1 in these cells was less polarised to the periphery and appeared more diffuse throughout the cell. The finding that Rap1 could be localised to the periphery of both primed and anergic T cells suggested that localisation alone was not sufficient to disrupt the peripheral recruitment and activation of pERK necessary for priming and that Rap1 activation and/or complex formation with other signal transducers may be required. Moreover, whilst pERK appeared to co-localise with lipid raft structures in primed but not anergic T cells, Rap1, conversely, appeared to be targeted to lipid rafts in anergic but not primed T cells. Collectively, these data suggest that Rap1 may be up-regulated and recruited to the immunological synapse upon re-stimulation with Ag in anergic T cells and that such Rap1 localisation and expression may contribute to the downregulation of ERK recruitment and activation in these cells. It is possible that Rap1 may achieve this by sequestering the Ras effector, Raf-1, which would lead to the

previously reported uncoupling of the Ras-Raf-MEK-ERK signalling cascade in tolerised T cells (571-573).

It seems likely that Raf-1 would be expressed at the periphery of both tolerised and primed T cells as this is where it may act to activate MEKK-ERK signalling thus, time permitting, the above hypothesis that Rap1 may exert its negative regulatory effects on T cell activation by competitively binding and sequestering Raf-1, would have been tested by assessing the localisation/co-localisation of Ras and Raf-1 or Rap1 and Raf-1 in tolerised and primed T cells. This could be achieved using fluorescence resonance energy transfer (FRET), a distance-dependent interaction between the electronic excited states of two fluorescent molecules (each with a different emission wavelength) in which excitation is transferred from a donor molecule to an acceptor molecule. The donor molecule would be attached to the GTPase (Ras /Rap1) and the acceptor molecule would be bound to Raf-1 thus, any co-localisation of Ras and Raf-1 or Rap1 and Raf-1 would be indicated by fluorescence emitted from the acceptor molecule. In addition, the localisation of scaffolds and other molecules indicated as having roles in Ras-mediated ERK activation, could be assessed in tolerised relative to primed cells. For example, the adaptor molecule CrkL and the guanidine nucleotide-releasing factor C3G, reported to be constituents of a Fyn-Cbl-CrkL-C3G-Rap1 signalling complex found in tolerised but not primed T cells (50, 347), could be assessed for their proximity to Rap1 in tolerised relative to primed T cells.

6.5 Do lipid rafts exist *in vivo*?

Lipid raft structures have been proposed to function as specialised signalling compartments in the cellular membrane (219) wherein molecules are phosphorylated and activated, and subsequently act to recruit and activate downstream signalling molecules. Consistent with the idea that peripheral pERK was associated with T cell activation, pERK co-localised with lipid raft staining in primed Ag-specific T cells and such co-localisation was not observed in anergic Ag-specific T cells (Figure 4.9) suggesting that lipid raft formation or the interaction and trafficking of pERK with these structures is defective under conditions of anergy.

However, the very existence of lipid rafts *in vivo* is a topic of great controversy and indeed, direct evidence for lipid rafts occurring *in vivo* is sparse. Moreover, there are two schools of thought regarding the nature of lipid rafts: one being that they are large micron-sized cholesterol- and sphingolipid-rich structures which likely contain high concentrations

of proteins (219, 599) and the other being that they are small (nanometer-sized), dynamic associations wherein lipid-associated molecules reside (600). The location and prevalence of the latter type is thought to be a result of the presence of large protein complexes in the plasma membrane (600). Whilst large micron-sized lipid rafts have been readily observed in artificial membranes (601), studies utilising fluorescence microscopy and conventional electron microscopy have failed to detect such large scale lipid rafts in living cells (602, 603), suggesting that lipid rafts of this size do not occur *in vivo*. By contrast, recent work by Sharma *et al* has revealed a nanometer scale organisation of lipid rafts *in vivo* (217) as indicated by FRET analysis of lipid-dependent organisation of glyosylphosphatidylinositol-anchored proteins (GPI-APs) in living cells. Further support and explanation for the existence of such small scale lipid rafts *in vivo* has very recently been provided by Yethiraj and Weisshaar (604). They suggest that integral membrane proteins attached to the cytoskeleton act as obstacles that limit the size of lipid rafts in the plasma membrane. Such large obstacles are not present in artificial membranes hence large scale lipid rafts are free to assemble. In conclusion, it appears that lipid rafts may indeed exist *in vivo* but on a much smaller scale than was previously imagined.

6.6 Regulation of cell cycle progression by ERK and cell cycle regulators in anergy

Primed, but not anergic, T cells progress through cell cycle and this study has shown that such cell cycle progression correlated with increasing levels of pERK (Figure 6.3). From these data, it was hypothesised that sustained ERK activation above a certain threshold level may be required for proliferation, as whilst anergic T cells in G_0/G_1 exhibited low levels of pERK, they did not progress through cell cycle. Consistent with this, sustained, but not transient, ERK activation has been shown to increase cyclin D expression (501, 504, 544). Anergic T cells are believed to arrest in the G_1 phase of the cell cycle and such arrest has previously been associated with the up-regulation of $p27^{kip1}$ (326, 441, 503-505). Consistent with such earlier studies (473, 504, 544), the current data shows that the decreased ERK activation observed in anergic relative to primed T cells correlated with an increase in the level of $p27^{kip1}$ expression in those anergic T cells. Perhaps such upregulation of $p27^{kip1}$ and/or decreased activation of CDKs is required, in addition to reduced ERK activation and consequent cyclin D induction, to prevent cell cycle progression in anergy. Indeed, the proportion of anergic, compared to primed, T cells expressing inactive forms of cdc2/CDK2 doubled upon re-stimulation with Ag at 20 h and

this change was not observed in the primed population. Moreover, almost ten-fold fewer of those anergic compared to primed T cells were expressing p-Rb and those anergic T cells that expressed Rb were expressing it at much lower levels. Together these findings suggest that it could be that up-regulation of $p27^{kip1}$ resulting in inactivation of cdc2/CDK2 with consequent downregulation of nuclear p-Rb expression is necessary, together with reduced ERK MAPK signalling, for the anergic state to be maintained (Figure 6.4).

In Chapter 4, the possibility that, under conditions of anergy, p-Rb rapidly (within 1 h of antigen re-stimulation) translocates out of the nucleus via association with the nuclear export receptor, Exportin1, was suggested. Such nuclear export may prevent further hyperphosphorylation of p-Rb at serine 780 (251), 795 (529) and 807/811, which is required for its positive regulatory role in cell cycle progression. Therefore, time permitting, it would have been interesting to assess the phosphorylation of Rb at all of these different sites, in tolerised and primed Ag-specific T cells at different stages of cell cycle. Perhaps such investigation may reveal at which phosphorylation site and/or cell cycle stage, the downregulation of hyperphosphorylated Rb occurs, in anergy.

Moreover, it would have been informative to simultaneously assess the expression and activation of CDK4/6 and CDK2 in such cells. For example, it is known that Rb is first phosphorylated by CDK4 at serine 780 (452), but requires further phosphorylation by CDK2 at serine 807/811 (452, 530) for hyperphosphorylation to occur, and which ultimately results in E2F release and progression through S phase. Furthermore, it has been shown that mutation of serine 807/811 does not abolish the regulation of E2F binding (605), suggesting that phosphorylation of Rb, at multiple sites, is indeed required for release of E2F and cell cycle progression. Therefore, such studies may identify defects in CDK-mediated phosphorylation(s) of Rb in anergy.

6.7 Dissecting the mechanisms underlying the differential T cell signalling observed in tolerance and priming

In Chapters 4 & 5, the defective ERK signalling observed in tolerised versus primed antigen-specific T cells was shown to correlate with increased Rap1 expression in tolerised compared to primed T cells after challenge with antigen *in vitro* and *in vivo* (12, 13). Whilst these data potentially indicate a key role for Rap1 in inducing the dowregulation of ERK activation observed in tolerised T cells, they only provide circumstantial evidence for Rap1 directing maintenance of T cell tolerance. Therefore, to assess the causal relationships

underlying the differences in ERK activation and Rap1 expression in antigen-specific T cells observed under conditions of tolerance and priming, an adenoviral gene delivery system has now been developed (Chapter 3).

Thus, the generation of murine transgenic lines in which expression of the human coxsackie/adenovirus receptor with a truncated cytoplasmic domain is limited to T cells expressing a Tg TCR (hCARΔcyt.DO11.10) has enabled efficient gene transfer of resting (naïve) and effector antigen-specific $CD4^+$ T cells without perturbing their development, migration, activation status or functional responses (402, 419). hCARΔcyt and hCARΔcyt.DO11.10 Tg murine lines have now been established in this facility and this current study has demonstrated successful transduction of naïve, anergic and primed $CD4^+$ and Ag-specific $CD4^+$ T cells from these mice with GFP-containing adenoviral vectors (Chapter 3), indicating the feasibility of dissecting causal functional signalling relationships in these differential effector cells. In addition, these data suggested that by varying the MOI of bicistronic-GFP vectors used, it will be possible to analyse the effect of no, low and high expression of particular signalling elements within a single population of cells (483). For example, if time had permitted, a range of adenoviral Ras- and Rap1-GFP constructs could have been generated and their effects on naïve, tolerised and primed Ag-specific primary T cells *in vitro* and *in vivo* assessed (Figure 6.5).

Thus, for example, the effect of sustained activation of ERK in tolerised antigen-specific T cells could be investigated. The reduced ERK activation in tolerised T cells relative to primed T cell populations, suggests that defective ERK signalling may play a role in maintaining tolerance. Therefore, it would have been interesting to investigate as to whether ectopic expression of active RasV12-GFP bicistronic constructs following induction of anergy *in vitro* could break tolerance to subsequent antigen challenge as assessed by cell cycle progression, proliferation and cytokine production (12, 392). Moreover, the effects of the constitutively active parent RasV12 mutant that can signal to both Raf and PI3K, as well as two related constructs, RasV12S35-GFP which can couple to ERK via Raf and MEK but not PI3K signalling, and RasV12C40-GFP which can couple to PI3K but not to the Raf/MEK/ERK cascade, could be assessed. Likewise, it would have been ascertained as to whether expression of the dominant negative construct, RasN17-GFP or the constitutively active construct, Rap1V12, following induction of priming, converts antigen-specific T cells to a tolerised phenotype. Adenoviral vectors expressing GFP alone would have been used as controls for the adenoviral gene transfer procedure.

Such mutant naïve, primed and tolerised cells could also be transferred to recipient BALB/c mice to assess the effects of these constructs on the induction and maintenance phases of systemic and oral tolerance and priming *in vivo*. For example, to specifically address the role of ERK activation in the induction of tolerance and/or priming, these mutants could be expressed in hCARΔcyt.DO11.10 T cells prior to the induction of tolerance or priming to determine whether reduced ERK activation plays a role in the induction of tolerance. The effects of these constructs on the early interactions between T cells and APCs (duration, cluster size etc) and how these processes correlate with induction of priming and tolerance could be assessed by 2-photon microscopy (606), as it is known that primed T cells form larger and longer-lived clusters within mucosal and peripheral lymph nodes than tolerised T cells (606). As the expression levels of the Ras/Rap1 mutants could be quantified by LSC/flow cytometric analysis of GFP expression, this approach allows both the relative behaviour of wild type and Ras/Rap1 mutant-expressing Ag-specific T cells, as well as the effect of differential signal strengths, to be assessed. Indeed, signal strength has been suggested as having a role in directing differential functional processes (580). For example, the differential responses of Rap1V12- and Rap1E63-Tg mice may reflect the finding that the Rap1E63 mutant exhibits 5x the biological activity of Rap1V12.

In addition, Ras and interacting chimeric unit (Raichu) probes, which are GFP-based FRET probes that allow direct and non-destructive monitoring of the activation status of Ras and Rho proteins, could be used to investigate Ras and Rap1 regulation in primed and tolerised T cells. Indeed, Raichu probes have already been utilised to examine the spatio-temporal regulation of Ras and Rho proteins in living cells (607, 608) and in some cases such probes were cloned into adenoviral vectors prior to use (607). Thus, such probes could easily be introduced to the hCARΔcyt.DO11.10 system described above. The FRET efficiency of a Raichu probe correlates with the GTP/GDP ratio of the GTPase in question. Hence, the activities of Ras and Rap1 could be estimated in such a manner. Furthermore, such probes can be modified in order to detect Ras/Rap1 activation in different subcellular locations e.g. plasma membrane, endomembranes, lipid rafts and non-raft domains (609). Such modified probes would provide a means to examine the spatial regulation of Rap1 and this may help in dissecting the mechanisms underlying the differential subcellular localisation of Rap1 observed in tolerised versus primed T cells.

6.8 Potential role for Rap1 in mediating T cell-dependent B cell help?

The inability of T cells to migrate into B cell-rich follicles following the induction of tolerance *in vivo* has been established (378, 384) and although tolerised T cells regain such migratory capacity upon antigenic challenge, they are known to be ineffectual at providing B cell help (384). The work described in this study indicates that Rap1 may be involved in the disruption of MAPK signalling in tolerised T cells after challenge with Ag *in vivo*. Thus, the upregulated expression of Rap1 observed in tolerised compared to primed follicular Ag-specific T cells could also potentially implicate a role for Rap1 in incapacitating T cells from providing B cell help (Figure 6.6). At least, these data provide an interesting starting point for further investigation. Thus, if time had allowed, Ag-specific T cells could then be adenovirally transduced with a dominant negative Rap1 mutant (Rap1N17) before being adoptively transferred into recipients in which tolerance and priming would then have been induced. The ability of such Rap1-deficient T cells to provide Ag-specific B cell help could be investigated following antigenic challenge *in vivo* by measuring serum Ab production. The hypothesis would be that such Rap1-deficient T cells would indeed, be able to provide B cell help (Figure 6.6H), that would perhaps be evidenced by increased serum Ab production relative to that detected in normally tolerised animals. In addition, as Rap1 has been shown to have a possible role in the induction phases of both priming and tolerance, such Rap1-deficient T cells may exhibit a reduced ability to migrate into the B cell follicles during the induction phase of priming (Figure 6.6E) relative to normal T cells (Figure 6.6A).

6.9 Summary

In summary, defective ERK signalling correlates with the up-regulation of Rap1 expression in tolerised relative to primed Ag-specific $CD4^+$ T cells during the maintenance phases of tolerance *in vitro* and *in vivo*. As this association occurs after the induction of both systemic and oral routes of tolerance, these data suggest that Rap1 antagonism of pERK signalling may play an important and general role in the maintenance of antigen-specific $CD4^+$ T cell tolerance. By advancing our knowledge of these key signals in regulating tolerance and priming at the single cell level *in vitro* and *in vivo*, we will increase our understanding of an important physiological process at the molecular level, ultimately leading to identification of potential targets for enhancing or inhibiting immunity and tolerance.

Figure 6.1 Activatory T cell signalling. Schematic depiction of the T cell signalling cascades initiated upon ligation of the TcR in combination with co-stimulation. Under such conditions of priming, both Ras- and Rho-GTPase-mediated signalling pathways are induced which lead to the activation of ERK, SAPK and p38 MAPKs. In turn, each of these MAPK activates one or more of the transcription factors required for transcription of the IL-2 gene. Upon activation of all of the necessary transcription factors, IL-2 is produced followed by cell cycle progression and proliferation. Subsequently the primed T cell can exert full effector function.

Figure 6.2 Inhibitory T cell signalling. Tolerance can be induced in T cells when the TcR is ligated in the absence of co-stimulation. Consequently, not only are the co-stimulatory signals absent, additional inhibitory signalling pathways are initiated. Under such conditions, the small GTPase Rap1 competitively binds the known Ras effector, Raf, and susbsequently Raf is unable to bind and activate its effector, MEK1/2. In its unactivated state, MEK1/2 cannot bind and activate ERK1/2 hence the AP-1 transcription factor complex cannot be activated. In the absence of AP-1 activation, IL-2 cannot be transcribed. In summary, such tolerogenic signalling results in a state of antigenic unresponsiveness, known as anergy, in the T cell. Anergy/tolerance is evidenced by the downregulation of IL-2 production and G1 cell cycle arrest, and the consequent decrease in proliferation. Such tolerised T cells are incapable of mounting a productive immunological response to antigenic challenge.

Figure 6.3 Cell cycle progression in primed T cells. Upon TcR ligation in the presence of CD28-mediated co-stimulation, the Ras-ERK and p38/JNK MAPK signalling cascades are initiated and subsequently, AP-1 is activated following induction of c-Jun/c-Fos. Such ERK-dependent AP-1 transcription contributes to the upregulation of cyclin D as c-Jun, an AP-1 constituent, activates the cyclin D1 promoter. CDK4, CDK6 and D-type cyclins can then associate and act to phosphorylate Rb, first by cyclin D–CDK4/6 then further by cyclin E-cdk2, thereby altering its conformation. Phosphorylated Rb (p-Rb) releases bound E2F family transcription factors which are then free to activate the genes required for entry into S phase (e.g. cyclin A and cyclin E) and hence proliferation. Cdc2 (CDK1) and CDK2 are then activated and can both associate with cyclin A at S phase where they also act to hyperphosphorylate and inactivate Rb thus, further fuelling cell cycle progression.

Figure 6.4 Induction of G_1 arrest in anergic T cells. Ligation of the TcR in the absence of co-stimulation can result in a state of anergy. Anergy is believed to occur as a result of reduced activation of the Ras-Raf-MEK-ERK signalling cascade, which in turn leads to reduced IL-2 production, cell cycle progression and proliferation. It is believed that Rap1 is involved in the uncoupling of the Ras-ERK cascade via competitive binding and sequestration of Raf. It seems likely that this downregulation in ERK activation would lead to reduced phosphorylation and activation of the AP-1 complex, which in turn would result in decreased cyclin D activation and complex formation with CDK4/6. Consequently, there may be a reduction in CDK4/6-mediated phosphorylation of Rb. Moreover, upregulation of $p27^{kip1}$, which is also observed in anergy, may cause downregulation of CDK1/2-mediated phosphorylation of Rb. Such downregulation in the phosphorylation of Rb would reduce E2F release and transit into S phase thus, cell cycle arrest at the G_1 phase would likely result. In summary, it is possible that up-regulation of $p27^{kip1}$ (B) and downregulation of nuclear p-Rb expression (C) is necessary, together with reduced ERK MAPK signalling (A), for the anergic state to be maintained.

Figure 6.5 Genetic modulation of ERK activation in primed and tolerised T cells. Hypothesised effects of a range of adenoviral constructs on tolerised (A) and primed Ag-specific primary T cells. Transduction of Ag-specific T cells, following induction of anergy, with a constitutively active parent RasV12-GFP mutant (A. ii) that can signal to both Raf and PI3K, or the related construct, RasV12S35-GFP (A. iii) which can couple to ERK via Raf and MEK but not PI3K signalling, may break tolerance in these cells. This break in tolerance would be evidenced by increased IL-2 production, cell cycle progression and proliferation, relative to anergic T cells that had been transduced with the empty vector. Alternatively, transduction with RasV12C40-GFP (A. iv) which can couple to PI3K but not to the Raf/MEK/ERK cascade, would perhaps result in no detectable difference in ERK activation relative to control anergic cells (A. i). Adenoviral vectors expressing GFP alone (empty vectors) would have been used as controls for the adenoviral gene transfer procedure (A. i, B. i). Transduction of Ag-specific T cells, following induction of priming, with the dominant negative form of Ras (RasN17-GFP; B. ii) or the constitutively active form of Rap1 (Rap1V12; B. iii) would perhaps convert such Ag-specific T cells to a tolerised phenotype, as evidenced by reduced IL-2 production, cell cycle progression and proliferation, relative to primed T cells that had been transduced with the empty vector.

Figure 6.6 Potential role for Rap1 in mediating T cell-dependent B cell help. Schematic diagram depicting the differential migration and capacity to provide B cell help of Ag-specific T cells in response to antigenic stimulation during the induction (A, B) and maintenance (C, D) phases of tolerance (B, D) and priming (A, C) *in vivo*. The up-regulated expression of Rap1 detected in tolerised compared to primed follicular Ag-specific T cells in response to challenge with Ag *in vivo* indicates a potential role for Rap1 in incapacitating T cells from providing B cell help which may contribute to the downregulation of Ab production observed during the maintenance phase of tolerance *in vivo* (D). Such Rap1-expressing tolerised follicular Ag-specific T cells are denoted as $Rap1^{hi}$ here. Time permitting, Ag-specific T cells would have been adenovirally transduced with a dominant negative Rap1 mutant (Rap1N17), here termed $Rap1^{lo}$ cells, before being adoptively transferred into recipients, in which tolerance and priming would then have been induced. As Rap1 has been shown to have a possible role in the induction phases of both priming and tolerance, it is hypothesised that $Rap1^{lo}$ T cells may exhibit a reduced ability to migrate into the B cell follicles during the induction phase of priming (E), relative to normal T cells (A). This proposed reduced migration would perhaps result in decreased serum Ab production in these animals. The ability of these Rap1-deficient T cells to provide Ag-specific B cell help would also have been investigated following antigenic challenge *in vivo* by measuring such serum Ab production. The hypothesis would be that tolerised Rap1-deficient T cells would indeed, be able to provide B cell help, following challenge with Ag (H). Such "restored" B cell help would perhaps be evidenced by increased serum Ab production relative to that detected in control tolerised animals (B).

References

1. Fillatreau, S., C. H. Sweenie, M. J. McGeachy, D. Gray, and S. M. Anderton. 2002. B cells regulate autoimmunity by provision of IL-10. *Nature immunology* 3:944-950.
2. Mizoguchi, A., E. Mizoguchi, H. Takedatsu, R. S. Blumberg, and A. K. Bhan. 2002. Chronic intestinal inflammatory condition generates IL-10-producing regulatory B cell subset characterized by CD1d upregulation. *Immunity* 16:219-230.
3. Evans, J. G., K. A. Chavez-Rueda, A. Eddaoudi, A. Meyer-Bahlburg, D. J. Rawlings, M. R. Ehrenstein, and C. Mauri. 2007. Novel suppressive function of transitional 2 B cells in experimental arthritis. *J Immunol* 178:7868-7878.
4. Fiorentino, D. F., A. Zlotnik, T. R. Mosmann, M. Howard, and A. O'Garra. 1991. IL-10 inhibits cytokine production by activated macrophages. *J Immunol* 147:3815-3822.
5. Grunig, G., D. B. Corry, M. W. Leach, B. W. Seymour, V. P. Kurup, and D. M. Rennick. 1997. Interleukin-10 is a natural suppressor of cytokine production and inflammation in a murine model of allergic bronchopulmonary aspergillosis. *The Journal of experimental medicine* 185:1089-1099.
6. O'Farrell, A. M., Y. Liu, K. W. Moore, and A. L. Mui. 1998. IL-10 inhibits macrophage activation and proliferation by distinct signaling mechanisms: evidence for Stat3-dependent and -independent pathways. *The EMBO journal* 17:1006-1018.
7. Pestka, S., C. D. Krause, D. Sarkar, M. R. Walter, Y. Shi, and P. B. Fisher. 2004. Interleukin-10 and related cytokines and receptors. *Annu Rev Immunol* 22:929-979.
8. Wolf, S. D., B. N. Dittel, F. Hardardottir, and C. A. Janeway, Jr. 1996. Experimental autoimmune encephalomyelitis induction in genetically B cell-deficient mice. *The Journal of experimental medicine* 184:2271-2278.
9. Gonnella, P. A., H. P. Waldner, and H. L. Weiner. 2001. B cell-deficient (mu MT) mice have alterations in the cytokine microenvironment of the gut-associated lymphoid tissue (GALT) and a defect in the low dose mechanism of oral tolerance. *J Immunol* 166:4456-4464.
10. Parekh, V. V., D. V. Prasad, P. P. Banerjee, B. N. Joshi, A. Kumar, and G. C. Mishra. 2003. B cells activated by lipopolysaccharide, but not by anti-Ig and anti-

CD40 antibody, induce anergy in CD8+ T cells: role of TGF-beta 1. *J Immunol* 170:5897-5911.

11. Tian, J., D. Zekzer, L. Hanssen, Y. Lu, A. Olcott, and D. L. Kaufman. 2001. Lipopolysaccharide-activated B cells down-regulate Th1 immunity and prevent autoimmune diabetes in nonobese diabetic mice. *J Immunol* 167:1081-1089.
12. Adams, C. L., A. M. Grierson, A. M. Mowat, M. M. Harnett, and P. Garside. 2004. Differences in the kinetics, amplitude, and localization of ERK activation in anergy and priming revealed at the level of individual primary T cells by laser scanning cytometry. *J Immunol* 173:1579-1586.
13. Morton, A. M., B. McManus, P. Garside, A. M. Mowat, and M. M. Harnett. 2007. Inverse Rap1 and Phospho-ERK Expression Discriminate the Maintenance Phase of Tolerance and Priming of Antigen-Specific CD4+ T Cells In Vitro and In Vivo. *J Immunol* 179:8026-8034.
14. Coyle, A. J., and J. C. Gutierrez-Ramos. 2001. The expanding B7 superfamily: increasing complexity in costimulatory signals regulating T cell function. *Nature immunology* 2:203-209.
15. Coyle, A., S. Lehar, C. Lloyd, J. Tian, T. Delaney, S. Manning, T. Nguyen, T. Burwell, H. Schneider, J. Gonzalo, M. Gosselin, O. L, C. Rudd, and J. Gutierrez-Ramos. 2000. The CD28-Related Molecule ICOS Is Required for Effective T Cell-dependent Immune Responses. *Immunity* 13:95-105.
16. Hutloff, A., A. M. Dittrich, K. C. Beier, B. Eljaschewitsch, R. Kraft, I. Anagnostopoulos, and R. A. Kroczek. 1999. ICOS is an inducible T-cell co-stimulator structurally and functionally related to CD28. *Nature* 397:263-266.
17. McAdam, A. J., T. T. Chang, A. E. Lumelsky, E. A. Greenfield, V. A. Boussiotis, J. S. Duke-Cohan, T. Chernova, N. Malenkovich, C. Jabs, V. K. Kuchroo, V. Ling, M. Collins, A. H. Sharpe, and G. J. Freeman. 2000. Mouse inducible costimulatory molecule (ICOS) expression is enhanced by CD28 costimulation and regulates differentiation of CD4+ T cells. *J Immunol* 165:5035-5040.
18. Smith, K. M., J. M. Brewer, P. Webb, A. J. Coyle, C. Gutierrez-Ramos, and P. Garside. 2003. Inducible costimulatory molecule-B7-related protein 1 interactions are important for the clonal expansion and B cell helper functions of naive, Th1, and Th2 T cells. *J Immunol* 170:2310-2315.

19. Szabo, S. J., S. T. Kim, G. L. Costa, X. Zhang, C. G. Fathman, and L. H. Glimcher. 2000. A novel transcription factor, T-bet, directs Th1 lineage commitment. *Cell* 100:655-669.
20. So, E. Y., H. H. Park, and C. E. Lee. 2000. IFN-gamma and IFN-alpha posttranscriptionally down-regulate the IL-4-induced IL-4 receptor gene expression. *J Immunol* 165:5472-5479.
21. Ma, J., T. Chen, J. Mandelin, A. Ceponis, N. E. Miller, M. Hukkanen, G. F. Ma, and Y. T. Konttinen. 2003. Regulation of macrophage activation. *Cell Mol Life Sci* 60:2334-2346.
22. Zheng, W., and R. A. Flavell. 1997. The transcription factor GATA-3 is necessary and sufficient for Th2 cytokine gene expression in CD4 T cells. *Cell* 89:587-596.
23. Ivanov, II, B. S. McKenzie, L. Zhou, C. E. Tadokoro, A. Lepelley, J. J. Lafaille, D. J. Cua, and D. R. Littman. 2006. The orphan nuclear receptor RORgammat directs the differentiation program of proinflammatory IL-17+ T helper cells. *Cell* 126:1121-1133.
24. Harrington, L. E., P. R. Mangan, and C. T. Weaver. 2006. Expanding the effector CD4 T-cell repertoire: the Th17 lineage. *Current opinion in immunology* 18:349-356.
25. Weaver, C. T., L. E. Harrington, P. R. Mangan, M. Gavrieli, and K. M. Murphy. 2006. Th17: an effector CD4 T cell lineage with regulatory T cell ties. *Immunity* 24:677-688.
26. McGeachy, M. J., and D. J. Cua. 2007. T cells doing it for themselves: TGF-beta regulation of Th1 and Th17 cells. *Immunity* 26:547-549.
27. Chatenoud, L., B. Salomon, and J. A. Bluestone. 2001. Suppressor T cells--they're back and critical for regulation of autoimmunity! *Immunological reviews* 182:149-163.
28. Bluestone, J. A., and A. K. Abbas. 2003. Natural versus adaptive regulatory T cells. *Nat Rev Immunol* 3:253-257.
29. Fu, S., N. Zhang, A. C. Yopp, D. Chen, M. Mao, D. Chen, H. Zhang, Y. Ding, and J. S. Bromberg. 2004. TGF-beta induces Foxp3 + T-regulatory cells from CD4 + CD25 - precursors. *Am J Transplant* 4:1614-1627.
30. Matzinger, P. 1994. Tolerance, danger, and the extended family. *Annu Rev Immunol* 12:991-1045.

31. Shortman, K., and L. Wu. 1996. Early T lymphocyte progenitors. *Annu Rev Immunol* 14:29-47.
32. Zuniga-Pflucker, J. C., and M. J. Lenardo. 1996. Regulation of thymocyte development from immature progenitors. *Current opinion in immunology* 8:215-224.
33. Dudley, E. C., H. T. Petrie, L. M. Shah, M. J. Owen, and A. C. Hayday. 1994. T cell receptor beta chain gene rearrangement and selection during thymocyte development in adult mice. *Immunity* 1:83-93.
34. von Boehmer, H., I. Aifantis, J. Feinberg, O. Lechner, C. Saint-Ruf, U. Walter, J. Buer, and O. Azogui. 1999. Pleiotropic changes controlled by the pre-T-cell receptor. *Current opinion in immunology* 11:135-142.
35. Sebzda, E., S. Mariathasan, T. Ohteki, R. Jones, M. F. Bachmann, and P. S. Ohashi. 1999. Selection of the T cell repertoire. *Annu Rev Immunol* 17:829-874.
36. Kyewski, B., and J. Derbinski. 2004. Self-representation in the thymus: an extended view. *Nat Rev Immunol* 4:688-698.
37. Derbinski, J., J. Gabler, B. Brors, S. Tierling, S. Jonnakuty, M. Hergenhahn, L. Peltonen, J. Walter, and B. Kyewski. 2005. Promiscuous gene expression in thymic epithelial cells is regulated at multiple levels. *The Journal of experimental medicine* 202:33-45.
38. Smith, K. M., D. C. Olson, R. Hirose, and D. Hanahan. 1997. Pancreatic gene expression in rare cells of thymic medulla: evidence for functional contribution to T cell tolerance. *International immunology* 9:1355-1365.
39. 1997. An autoimmune disease, APECED, caused by mutations in a novel gene featuring two PHD-type zinc-finger domains. *Nature genetics* 17:399-403.
40. Nagamine, K., P. Peterson, H. S. Scott, J. Kudoh, S. Minoshima, M. Heino, K. J. Krohn, M. D. Lalioti, P. E. Mullis, S. E. Antonarakis, K. Kawasaki, S. Asakawa, F. Ito, and N. Shimizu. 1997. Positional cloning of the APECED gene. *Nature genetics* 17:393-398.
41. Anderson, M. S., E. S. Venanzi, L. Klein, Z. Chen, S. P. Berzins, S. J. Turley, H. von Boehmer, R. Bronson, A. Dierich, C. Benoist, and D. Mathis. 2002. Projection of an immunological self shadow within the thymus by the aire protein. *Science (New York, N.Y* 298:1395-1401.

42. Anderson, M. S., E. S. Venanzi, Z. Chen, S. P. Berzins, C. Benoist, and D. Mathis. 2005. The cellular mechanism of Aire control of T cell tolerance. *Immunity* 23:227-239.
43. Liston, A., S. Lesage, J. Wilson, L. Peltonen, and C. C. Goodnow. 2003. Aire regulates negative selection of organ-specific T cells. *Nature immunology* 4:350-354.
44. Dillon, S. R., S. C. Jameson, and P. J. Fink. 1994. V beta 5+ T cell receptors skew toward OVA+H-2Kb recognition. *J Immunol* 152:1790-1801.
45. Gallegos, A. M., and M. J. Bevan. 2004. Central tolerance to tissue-specific antigens mediated by direct and indirect antigen presentation. *The Journal of experimental medicine* 200:1039-1049.
46. Mowat, A. M. 2003. Anatomical basis of tolerance and immunity to intestinal antigens. *Nat Rev Immunol* 3:331-341.
47. Rocha, G., M. G. Baines, and J. Deschenes. 1992. The immunology of the eye and its systemic interactions. *Critical reviews in immunology* 12:81-100.
48. Alegre, M. L., K. A. Frauwirth, and C. B. Thompson. 2001. T-cell regulation by CD28 and CTLA-4. *Nat Rev Immunol* 1:220-228.
49. Lechler, R., J. G. Chai, F. Marelli-Berg, and G. Lombardi. 2001. T-cell anergy and peripheral T-cell tolerance. *Philos Trans R Soc Lond B Biol Sci* 356:625-637.
50. Boussiotis, V. A., G. J. Freeman, A. Berezovskaya, D. L. Barber, and L. M. Nadler. 1997. Maintenance of human T cell anergy: blocking of IL-2 gene transcription by activated Rap1. *Science (New York, N.Y* 278:124-128.
51. Jenkins, M. K., C. A. Chen, G. Jung, D. L. Mueller, and R. H. Schwartz. 1990. Inhibition of antigen-specific proliferation of type 1 murine T cell clones after stimulation with immobilized anti-CD3 monoclonal antibody. *J Immunol* 144:16-22.
52. Quill, H., and R. H. Schwartz. 1987. Stimulation of normal inducer T cell clones with antigen presented by purified Ia molecules in planar lipid membranes: specific induction of a long-lived state of proliferative nonresponsiveness. *J Immunol* 138:3704-3712.
53. Chai, J. G., and R. I. Lechler. 1997. Immobilized anti-CD3 mAb induces anergy in murine naive and memory CD4+ T cells in vitro. *International immunology* 9:935-944.

54. DeSilva, D. R., K. B. Urdahl, and M. K. Jenkins. 1991. Clonal anergy is induced in vitro by T cell receptor occupancy in the absence of proliferation. *J Immunol* 147:3261-3267.
55. Melamed, D., and A. Friedman. 1993. Direct evidence for anergy in T lymphocytes tolerized by oral administration of ovalbumin. *European journal of immunology* 23:935-942.
56. Jewell, S. D., I. E. Gienapp, K. L. Cox, and C. C. Whitacre. 1998. Oral tolerance as therapy for experimental autoimmune encephalomyelitis and multiple sclerosis: demonstration of T cell anergy. *Immunol Cell Biol* 76:74-82.
57. Whitacre, C. C., I. E. Gienapp, C. G. Orosz, and D. M. Bitar. 1991. Oral tolerance in experimental autoimmune encephalomyelitis. III. Evidence for clonal anergy. *J Immunol* 147:2155-2163.
58. Smith, K. M., J. M. Davidson, and P. Garside. 2002. T-cell activation occurs simultaneously in local and peripheral lymphoid tissue following oral administration of a range of doses of immunogenic or tolerogenic antigen although tolerized T cells display a defect in cell division. *Immunology* 106:144-158.
59. Sun, J., B. Dirden-Kramer, K. Ito, P. B. Ernst, and N. Van Houten. 1999. Antigen-specific T cell activation and proliferation during oral tolerance induction. *J Immunol* 162:5868-5875.
60. Van Houten, N., and S. F. Blake. 1996. Direct measurement of anergy of antigen-specific T cells following oral tolerance induction. *J Immunol* 157:1337-1341.
61. Hathcock, K. S., G. Laszlo, C. Pucillo, P. Linsley, and R. J. Hodes. 1994. Comparative analysis of B7-1 and B7-2 costimulatory ligands: expression and function. *The Journal of experimental medicine* 180:631-640.
62. Inaba, K., M. Witmer-Pack, M. Inaba, K. S. Hathcock, H. Sakuta, M. Azuma, H. Yagita, K. Okumura, P. S. Linsley, S. Ikehara, S. Muramatsu, R. J. Hodes, and R. M. Steinman. 1994. The tissue distribution of the B7-2 costimulator in mice: abundant expression on dendritic cells in situ and during maturation in vitro. *The Journal of experimental medicine* 180:1849-1860.
63. Kawamura, T., and M. Furue. 1995. Comparative analysis of B7-1 and B7-2 expression in Langerhans cells: differential regulation by T helper type 1 and T helper type 2 cytokines. *European journal of immunology* 25:1913-1917.

64. Bluestone, J. A. 1997. Is CTLA-4 a master switch for peripheral T cell tolerance? *J Immunol* 158:1989-1993.
65. Lane, P., C. Haller, and F. McConnell. 1996. Evidence that induction of tolerance in vivo involves active signaling via a B7 ligand-dependent mechanism: CTLA4-Ig protects V beta 8+ T cells from tolerance induction by the superantigen staphylococcal enterotoxin B. *European journal of immunology* 26:858-862.
66. Liu, L., V. K. Kuchroo, and H. L. Weiner. 1999. B7.2 (CD86) but not B7.1 (CD80) costimulation is required for the induction of low dose oral tolerance. *J Immunol* 163:2284-2290.
67. Perez, V. L., L. Van Parijs, A. Biuckians, X. X. Zheng, T. B. Strom, and A. K. Abbas. 1997. Induction of peripheral T cell tolerance in vivo requires CTLA-4 engagement. *Immunity* 6:411-417.
68. Samoilova, E. B., J. L. Horton, H. Zhang, S. J. Khoury, H. L. Weiner, and Y. Chen. 1998. CTLA-4 is required for the induction of high dose oral tolerance. *International immunology* 10:491-498.
69. Lider, O., L. M. Santos, C. S. Lee, P. J. Higgins, and H. L. Weiner. 1989. Suppression of experimental autoimmune encephalomyelitis by oral administration of myelin basic protein. II. Suppression of disease and in vitro immune responses is mediated by antigen-specific CD8+ T lymphocytes. *J Immunol* 142:748-752.
70. Miller, A., O. Lider, A. B. Roberts, M. B. Sporn, and H. L. Weiner. 1992. Suppressor T cells generated by oral tolerization to myelin basic protein suppress both in vitro and in vivo immune responses by the release of transforming growth factor beta after antigen-specific triggering. *Proceedings of the National Academy of Sciences of the United States of America* 89:421-425.
71. Grdic, D., E. Hornquist, M. Kjerrulf, and N. Y. Lycke. 1998. Lack of local suppression in orally tolerant CD8-deficient mice reveals a critical regulatory role of CD8+ T cells in the normal gut mucosa. *J Immunol* 160:754-762.
72. Barone, K. S., S. L. Jain, and J. G. Michael. 1995. Effect of in vivo depletion of CD4+ and CD8+ cells on the induction and maintenance of oral tolerance. *Cellular immunology* 163:19-29.
73. Desvignes, C., H. Bour, J. F. Nicolas, and D. Kaiserlian. 1996. Lack of oral tolerance but oral priming for contact sensitivity to dinitrofluorobenzene in major

histocompatibility complex class II-deficient mice and in CD4+ T cell-depleted mice. *European journal of immunology* 26:1756-1761.

74. Garside, P., M. Steel, F. Y. Liew, and A. M. Mowat. 1995. CD4+ but not CD8+ T cells are required for the induction of oral tolerance. *International immunology* 7:501-504.
75. Benacerraf, B., and R. N. Germain. 1981. A single major pathway of T-lymphocyte interactions in antigen-specific immune suppression. *Scand J Immunol* 13:1-10.
76. Chen, Y., V. K. Kuchroo, J. Inobe, D. A. Hafler, and H. L. Weiner. 1994. Regulatory T cell clones induced by oral tolerance: suppression of autoimmune encephalomyelitis. *Science (New York, N.Y* 265:1237-1240.
77. Fishman-Lobell, J., A. Friedman, and H. L. Weiner. 1994. Different kinetic patterns of cytokine gene expression in vivo in orally tolerant mice. *European journal of immunology* 24:2720-2724.
78. Khoury, S. J., W. W. Hancock, and H. L. Weiner. 1992. Oral tolerance to myelin basic protein and natural recovery from experimental autoimmune encephalomyelitis are associated with downregulation of inflammatory cytokines and differential upregulation of transforming growth factor beta, interleukin 4, and prostaglandin E expression in the brain. *The Journal of experimental medicine* 176:1355-1364.
79. Melamed, D., J. Fishman-Lovell, Z. Uni, H. L. Weiner, and A. Friedman. 1996. Peripheral tolerance of Th2 lymphocytes induced by continuous feeding of ovalbumin. *International immunology* 8:717-724.
80. Garside, P., M. Steel, E. A. Worthey, A. Satoskar, J. Alexander, H. Bluethmann, F. Y. Liew, and A. M. Mowat. 1995. T helper 2 cells are subject to high dose oral tolerance and are not essential for its induction. *J Immunol* 154:5649-5655.
81. Wolvers, D. A., M. J. van der Cammen, and G. Kraal. 1997. Mucosal tolerance is associated with, but independent of, up-regulation Th2 responses. *Immunology* 92:328-333.
82. Chen, Y., J. Inobe, and H. L. Weiner. 1997. Inductive events in oral tolerance in the TCR transgenic adoptive transfer model. *Cellular immunology* 178:62-68.
83. Gonnella, P. A., Y. Chen, J. Inobe, Y. Komagata, M. Quartulli, and H. L. Weiner. 1998. In situ immune response in gut-associated lymphoid tissue (GALT) following oral antigen in TCR-transgenic mice. *J Immunol* 160:4708-4718.

84. Groux, H., A. O'Garra, M. Bigler, M. Rouleau, S. Antonenko, J. E. de Vries, and M. G. Roncarolo. 1997. A CD4+ T-cell subset inhibits antigen-specific T-cell responses and prevents colitis. *Nature* 389:737-742.

85. Cottrez, F., S. D. Hurst, R. L. Coffman, and H. Groux. 2000. T regulatory cells 1 inhibit a Th2-specific response in vivo. *J Immunol* 165:4848-4853.

86. Itoh, M., T. Takahashi, N. Sakaguchi, Y. Kuniyasu, J. Shimizu, F. Otsuka, and S. Sakaguchi. 1999. Thymus and autoimmunity: production of CD25+CD4+ naturally anergic and suppressive T cells as a key function of the thymus in maintaining immunologic self-tolerance. *J Immunol* 162:5317-5326.

87. Jordan, M. S., A. Boesteanu, A. J. Reed, A. L. Petrone, A. E. Holenbeck, M. A. Lerman, A. Naji, and A. J. Caton. 2001. Thymic selection of CD4+CD25+ regulatory T cells induced by an agonist self-peptide. *Nature immunology* 2:301-306.

88. Fowler, S., and F. Powrie. 2002. CTLA-4 expression on antigen-specific cells but not IL-10 secretion is required for oral tolerance. *European journal of immunology* 32:2997-3006.

89. Thorstenson, K. M., and A. Khoruts. 2001. Generation of anergic and potentially immunoregulatory CD25+CD4 T cells in vivo after induction of peripheral tolerance with intravenous or oral antigen. *J Immunol* 167:188-195.

90. Zhang, X., L. Izikson, L. Liu, and H. L. Weiner. 2001. Activation of CD25(+)CD4(+) regulatory T cells by oral antigen administration. *J Immunol* 167:4245-4253.

91. Piccirillo, C. A., and E. M. Shevach. 2001. Cutting edge: control of CD8+ T cell activation by CD4+CD25+ immunoregulatory cells. *J Immunol* 167:1137-1140.

92. Takahashi, T., Y. Kuniyasu, M. Toda, N. Sakaguchi, M. Itoh, M. Iwata, J. Shimizu, and S. Sakaguchi. 1998. Immunologic self-tolerance maintained by CD25+CD4+ naturally anergic and suppressive T cells: induction of autoimmune disease by breaking their anergic/suppressive state. *International immunology* 10:1969-1980.

93. Powrie, F., M. W. Leach, S. Mauze, L. B. Caddle, and R. L. Coffman. 1993. Phenotypically distinct subsets of CD4+ T cells induce or protect from chronic intestinal inflammation in C. B-17 scid mice. *International immunology* 5:1461-1471.

94. Aranda, R., B. C. Sydora, P. L. McAllister, S. W. Binder, H. Y. Yang, S. R. Targan, and M. Kronenberg. 1997. Analysis of intestinal lymphocytes in mouse colitis mediated by transfer of CD4+, CD45RBhigh T cells to SCID recipients. *J Immunol* 158:3464-3473.

95. Powrie, F., M. W. Leach, S. Mauze, S. Menon, L. B. Caddle, and R. L. Coffman. 1994. Inhibition of Th1 responses prevents inflammatory bowel disease in scid mice reconstituted with CD45RBhi CD4+ T cells. *Immunity* 1:553-562.

96. Powrie, F., J. Carlino, M. W. Leach, S. Mauze, and R. L. Coffman. 1996. A critical role for transforming growth factor-beta but not interleukin 4 in the suppression of T helper type 1-mediated colitis by CD45RB(low) CD4+ T cells. *The Journal of experimental medicine* 183:2669-2674.

97. Asseman, C., S. Mauze, M. W. Leach, R. L. Coffman, and F. Powrie. 1999. An essential role for interleukin 10 in the function of regulatory T cells that inhibit intestinal inflammation. *The Journal of experimental medicine* 190:995-1004.

98. Greenwald, R. J., V. A. Boussiotis, R. B. Lorsbach, A. K. Abbas, and A. H. Sharpe. 2001. CTLA-4 regulates induction of anergy in vivo. *Immunity* 14:145-155.

99. Karandikar, N. J., C. L. Vanderlugt, T. L. Walunas, S. D. Miller, and J. A. Bluestone. 1996. CTLA-4: a negative regulator of autoimmune disease. *The Journal of experimental medicine* 184:783-788.

100. Perrin, P. J., D. Scott, L. Quigley, P. S. Albert, O. Feder, G. S. Gray, R. Abe, C. H. June, and M. K. Racke. 1995. Role of B7:CD28/CTLA-4 in the induction of chronic relapsing experimental allergic encephalomyelitis. *J Immunol* 154:1481-1490.

101. Chen, Y., Y. Ma, and Y. Chen. 2002. Roles of cytotoxic T-lymphocyte-associated antigen-4 in the inductive phase of oral tolerance. *Immunology* 105:171-180.

102. Walunas, T. L., and J. A. Bluestone. 1998. CTLA-4 regulates tolerance induction and T cell differentiation in vivo. *J Immunol* 160:3855-3860.

103. Chen, L. 2004. Co-inhibitory molecules of the B7-CD28 family in the control of T-cell immunity. *Nat Rev Immunol* 4:336-347.

104. Okazaki, T., and T. Honjo. 2006. The PD-1-PD-L pathway in immunological tolerance. *Trends in immunology* 27:195-201.

105. Augello, A., R. Tasso, S. M. Negrini, A. Amateis, F. Indiveri, R. Cancedda, and G. Pennesi. 2005. Bone marrow mesenchymal progenitor cells inhibit lymphocyte

proliferation by activation of the programmed death 1 pathway. *European journal of immunology* 35:1482-1490.

106. Nakae, S., H. Suto, M. Iikura, M. Kakurai, J. D. Sedgwick, M. Tsai, and S. J. Galli. 2006. Mast cells enhance T cell activation: importance of mast cell costimulatory molecules and secreted TNF. *J Immunol* 176:2238-2248.

107. Nishimura, H., M. Nose, H. Hiai, N. Minato, and T. Honjo. 1999. Development of lupus-like autoimmune diseases by disruption of the PD-1 gene encoding an ITIM motif-carrying immunoreceptor. *Immunity* 11:141-151.

108. Nishimura, H., T. Okazaki, Y. Tanaka, K. Nakatani, M. Hara, A. Matsumori, S. Sasayama, A. Mizoguchi, H. Hiai, N. Minato, and T. Honjo. 2001. Autoimmune dilated cardiomyopathy in PD-1 receptor-deficient mice. *Science (New York, N.Y* 291:319-322.

109. Fife, B. T., I. Guleria, M. Gubbels Bupp, T. N. Eagar, Q. Tang, H. Bour-Jordan, H. Yagita, M. Azuma, M. H. Sayegh, and J. A. Bluestone. 2006. Insulin-induced remission in new-onset NOD mice is maintained by the PD-1-PD-L1 pathway. *The Journal of experimental medicine* 203:2737-2747.

110. Zhang, Y., Y. Chung, C. Bishop, B. Daugherty, H. Chute, P. Holst, C. Kurahara, F. Lott, N. Sun, A. A. Welcher, and C. Dong. 2006. Regulation of T cell activation and tolerance by PDL2. *Proceedings of the National Academy of Sciences of the United States of America* 103:11695-11700.

111. Wells, H., and T. Osbourne. 1911. The biological reactions of the vegetable proteins. *I. Anaphylaxis. J Infect. Dis.* 8:66-124.

112. Sollid, L. M. 2002. Coeliac disease: dissecting a complex inflammatory disorder. *Nat Rev Immunol* 2:647-655.

113. Mowat, A., and H. Weiner. 1999. Oral Tolerance: physiological basis and clinical applications. In *Mucosal Immunity*. P. Ogra, J. Mestecky, M. Lamm, W. Strober, J. Bienenstock, and J. McGhee, eds. Academic Press, San Diego, CA. 587-617.

114. Garside, P., and A. M. Mowat. 2001. Oral tolerance. *Seminars in immunology* 13:177-185.

115. Nagler-Anderson, C. 2000. Tolerance and immunity in the intestinal immune system. *Critical reviews in immunology* 20:103-120.

116. Weiner, H. L., A. Friedman, A. Miller, S. J. Khoury, A. al-Sabbagh, L. Santos, M. Sayegh, R. B. Nussenblatt, D. E. Trentham, and D. A. Hafler. 1994. Oral tolerance:

immunologic mechanisms and treatment of animal and human organ-specific autoimmune diseases by oral administration of autoantigens. *Annu Rev Immunol* 12:809-837.

117. Elson, C. O., and W. Ealding. 1984. Cholera toxin feeding did not induce oral tolerance in mice and abrogated oral tolerance to an unrelated protein antigen. *J Immunol* 133:2892-2897.

118. Elson, C. O., and W. Ealding. 1984. Generalized systemic and mucosal immunity in mice after mucosal stimulation with cholera toxin. *J Immunol* 132:2736-2741.

119. Lycke, N., and J. Holmgren. 1986. Strong adjuvant properties of cholera toxin on gut mucosal immune responses to orally presented antigens. *Immunology* 59:301-308.

120. Van der Heijden, P. J., A. T. Bianchi, M. Dol, J. W. Pals, W. Stok, and B. A. Bokhout. 1991. Manipulation of intestinal immune responses against ovalbumin by cholera toxin and its B subunit in mice. *Immunology* 72:89-93.

121. Bilsborough, J., and J. L. Viney. 2002. Getting to the guts of immune regulation. *Immunology* 106:139-143.

122. Blanas, E., G. M. Davey, F. R. Carbone, and W. R. Heath. 2000. A bone marrow-derived APC in the gut-associated lymphoid tissue captures oral antigens and presents them to both CD4+ and CD8+ T cells. *J Immunol* 164:2890-2896.

123. Williamson, E., J. M. O'Malley, and J. L. Viney. 1999. Visualizing the T-cell response elicited by oral administration of soluble protein antigen. *Immunology* 97:565-572.

124. Spahn, T. W., A. Fontana, A. M. Faria, A. J. Slavin, H. P. Eugster, X. Zhang, P. A. Koni, N. H. Ruddle, R. A. Flavell, P. D. Rennert, and H. L. Weiner. 2001. Induction of oral tolerance to cellular immune responses in the absence of Peyer's patches. *European journal of immunology* 31:1278-1287.

125. Spahn, T. W., H. L. Weiner, P. D. Rennert, N. Lugering, A. Fontana, W. Domschke, and T. Kucharzik. 2002. Mesenteric lymph nodes are critical for the induction of high-dose oral tolerance in the absence of Peyer's patches. *European journal of immunology* 32:1109-1113.

126. Golovkina, T. V., M. Shlomchik, L. Hannum, and A. Chervonsky. 1999. Organogenic role of B lymphocytes in mucosal immunity. *Science (New York, N.Y* 286:1965-1968.

127. Alpan, O., G. Rudomen, and P. Matzinger. 2001. The role of dendritic cells, B cells, and M cells in gut-oriented immune responses. *J Immunol* 166:4843-4852.
128. Huang, F. P., N. Platt, M. Wykes, J. R. Major, T. J. Powell, C. D. Jenkins, and G. G. MacPherson. 2000. A discrete subpopulation of dendritic cells transports apoptotic intestinal epithelial cells to T cell areas of mesenteric lymph nodes. *The Journal of experimental medicine* 191:435-444.
129. Liu, L. M., and G. G. MacPherson. 1993. Antigen acquisition by dendritic cells: intestinal dendritic cells acquire antigen administered orally and can prime naive T cells in vivo. *The Journal of experimental medicine* 177:1299-1307.
130. Keren, D. F. 1992. Antigen processing in the mucosal immune system. *Seminars in immunology* 4:217-226.
131. Trier, J. S. 1991. Structure and function of intestinal M cells. *Gastroenterol Clin North Am* 20:531-547.
132. Kelsall, B. L., and W. Strober. 1996. The role of dendritic cells in antigen processing in the Peyer's patch. *Ann N Y Acad Sci* 778:47-54.
133. Inaba, K., S. Turley, F. Yamaide, T. Iyoda, K. Mahnke, M. Inaba, M. Pack, M. Subklewe, B. Sauter, D. Sheff, M. Albert, N. Bhardwaj, I. Mellman, and R. M. Steinman. 1998. Efficient presentation of phagocytosed cellular fragments on the major histocompatibility complex class II products of dendritic cells. *The Journal of experimental medicine* 188:2163-2173.
134. Pierre, P., S. J. Turley, E. Gatti, M. Hull, J. Meltzer, A. Mirza, K. Inaba, R. M. Steinman, and I. Mellman. 1997. Developmental regulation of MHC class II transport in mouse dendritic cells. *Nature* 388:787-792.
135. Randolph, G. J., K. Inaba, D. F. Robbiani, R. M. Steinman, and W. A. Muller. 1999. Differentiation of phagocytic monocytes into lymph node dendritic cells in vivo. *Immunity* 11:753-761.
136. Bland, P. W., and L. G. Warren. 1986. Antigen presentation by epithelial cells of the rat small intestine. II. Selective induction of suppressor T cells. *Immunology* 58:9-14.
137. Bland, P. W., and L. G. Warren. 1986. Antigen presentation by epithelial cells of the rat small intestine. I. Kinetics, antigen specificity and blocking by anti-Ia antisera. *Immunology* 58:1-7.

138. Bland, P. W., and C. V. Whiting. 1992. Induction of MHC class II gene products in rat intestinal epithelium during graft-versus-host disease and effects on the immune function of the epithelium. *Immunology* 75:366-371.
139. Hershberg, R. M., and L. F. Mayer. 2000. Antigen processing and presentation by intestinal epithelial cells - polarity and complexity. *Immunol Today* 21:123-128.
140. Mayer, L., D. Eisenhardt, P. Salomon, W. Bauer, R. Plous, and L. Piccinini. 1991. Expression of class II molecules on intestinal epithelial cells in humans. Differences between normal and inflammatory bowel disease. *Gastroenterology* 100:3-12.
141. Mayer, L., and R. Shlien. 1987. Evidence for function of Ia molecules on gut epithelial cells in man. *The Journal of experimental medicine* 166:1471-1483.
142. Schieferdecker, H. L., R. Ullrich, H. Hirseland, and M. Zeitz. 1992. T cell differentiation antigens on lymphocytes in the human intestinal lamina propria. *J Immunol* 149:2816-2822.
143. Senju, M., K. C. Wu, Y. R. Mahida, and D. P. Jewell. 1991. Two-color immunofluorescence and flow cytometric analysis of lamina propria lymphocyte subsets in ulcerative colitis and Crohn's disease. *Dig Dis Sci* 36:1453-1458.
144. Chung, Y., S. Y. Chang, and C. Y. Kang. 1999. Kinetic analysis of oral tolerance: memory lymphocytes are refractory to oral tolerance. *J Immunol* 163:3692-3698.
145. Peng, H. J., Z. N. Chang, S. W. Kuo, C. C. Lee, and Y. Y. Tzau. 2000. Resting B cells are not antigen-presenting cells in the induction of oral tolerance of specific Th2 immune responses in mice. *Int Arch Allergy Immunol* 122:174-181.
146. Peng, H. J., Z. N. Chang, C. C. Lee, and S. W. Kuo. 2000. B-cell depletion fails to abrogate the induction of oral tolerance of specific Th1 immune responses in mice. *Scand J Immunol* 51:454-460.
147. Mowat, A. M. 2005. Dendritic cells and immune responses to orally administered antigens. *Vaccine* 23:1797-1799.
148. Viney, J. L., A. M. Mowat, J. M. O'Malley, E. Williamson, and N. A. Fanger. 1998. Expanding dendritic cells in vivo enhances the induction of oral tolerance. *J Immunol* 160:5815-5825.
149. Williamson, E., G. M. Westrich, and J. L. Viney. 1999. Modulating dendritic cells to optimize mucosal immunization protocols. *J Immunol* 163:3668-3675.
150. Daynes, R. A., B. A. Araneo, T. A. Dowell, K. Huang, and D. Dudley. 1990. Regulation of murine lymphokine production in vivo. III. The lymphoid tissue

microenvironment exerts regulatory influences over T helper cell function. *The Journal of experimental medicine* 171:979-996.

151. Chen, Y., J. Inobe, R. Marks, P. Gonnella, V. K. Kuchroo, and H. L. Weiner. 1995. Peripheral deletion of antigen-reactive T cells in oral tolerance. *Nature* 376:177-180.

152. Iwasaki, A., and B. L. Kelsall. 1999. Freshly isolated Peyer's patch, but not spleen, dendritic cells produce interleukin 10 and induce the differentiation of T helper type 2 cells. *The Journal of experimental medicine* 190:229-239.

153. Liu, L. M., and G. G. MacPherson. 1995. Rat intestinal dendritic cells: immunostimulatory potency and phenotypic characterization. *Immunology* 85:88-93.

154. Mayrhofer, G., C. W. Pugh, and A. N. Barclay. 1983. The distribution, ontogeny and origin in the rat of Ia-positive cells with dendritic morphology and of Ia antigen in epithelia, with special reference to the intestine. *European journal of immunology* 13:112-122.

155. Pavli, P., D. A. Hume, E. Van De Pol, and W. F. Doe. 1993. Dendritic cells, the major antigen-presenting cells of the human colonic lamina propria. *Immunology* 78:132-141.

156. Pavli, P., C. E. Woodhams, W. F. Doe, and D. A. Hume. 1990. Isolation and characterization of antigen-presenting dendritic cells from the mouse intestinal lamina propria. *Immunology* 70:40-47.

157. Rescigno, M., G. Rotta, B. Valzasina, and P. Ricciardi-Castagnoli. 2001. Dendritic cells shuttle microbes across gut epithelial monolayers. *Immunobiology* 204:572-581.

158. Straus, D. B., and A. Weiss. 1992. Genetic evidence for the involvement of the lck tyrosine kinase in signal transduction through the T cell antigen receptor. *Cell* 70:585-593.

159. van Oers, N. S., N. Killeen, and A. Weiss. 1996. Lck regulates the tyrosine phosphorylation of the T cell receptor subunits and ZAP-70 in murine thymocytes. *The Journal of experimental medicine* 183:1053-1062.

160. Chan, A. C., M. Iwashima, C. W. Turck, and A. Weiss. 1992. ZAP-70: a 70 kd protein-tyrosine kinase that associates with the TCR zeta chain. *Cell* 71:649-662.

161. Sommers, C. L., R. K. Menon, A. Grinberg, W. Zhang, L. E. Samelson, and P. E. Love. 2001. Knock-in mutation of the distal four tyrosines of linker for activation of T cells blocks murine T cell development. *The Journal of experimental medicine* 194:135-142.

162. Buday, L., S. E. Egan, P. Rodriguez Viciana, D. A. Cantrell, and J. Downward. 1994. A complex of Grb2 adaptor protein, Sos exchange factor, and a 36-kDa membrane-bound tyrosine phosphoprotein is implicated in ras activation in T cells. *The Journal of biological chemistry* 269:9019-9023.

163. Liu, S. K., N. Fang, G. A. Koretzky, and C. J. McGlade. 1999. The hematopoietic-specific adaptor protein gads functions in T-cell signaling via interactions with the SLP-76 and LAT adaptors. *Curr Biol* 9:67-75.

164. Kurosaki, T., A. Maeda, M. Ishiai, A. Hashimoto, K. Inabe, and M. Takata. 2000. Regulation of the phospholipase C-gamma2 pathway in B cells. *Immunological reviews* 176:19-29.

165. Marshall, A. J., H. Niiro, T. J. Yun, and E. A. Clark. 2000. Regulation of B-cell activation and differentiation by the phosphatidylinositol 3-kinase and phospholipase Cgamma pathway. *Immunological reviews* 176:30-46.

166. Wange, R. L. 2000. LAT, the linker for activation of T cells: a bridge between T cell-specific and general signaling pathways. *Sci STKE* 2000:RE1.

167. Chen, L., J. N. Glover, P. G. Hogan, A. Rao, and S. C. Harrison. 1998. Structure of the DNA-binding domains from NFAT, Fos and Jun bound specifically to DNA. *Nature* 392:42-48.

168. Guerrero, C., L. Pesce, E. Lecuona, K. M. Ridge, and J. I. Sznajder. 2002. Dopamine activates ERKs in alveolar epithelial cells via Ras-PKC-dependent and Grb2/Sos-independent mechanisms. *American journal of physiology* 282:L1099-1107.

169. Ebinu, J. O., D. A. Bottorff, E. Y. Chan, S. L. Stang, R. J. Dunn, and J. C. Stone. 1998. RasGRP, a Ras guanyl nucleotide- releasing protein with calcium- and diacylglycerol-binding motifs. *Science (New York, N.Y* 280:1082-1086.

170. Cullen, P. J., and P. J. Lockyer. 2002. Integration of calcium and Ras signalling. *Nature reviews* 3:339-348.

171. Bivona, T. G., I. Perez De Castro, I. M. Ahearn, T. M. Grana, V. K. Chiu, P. J. Lockyer, P. J. Cullen, A. Pellicer, A. D. Cox, and M. R. Philips. 2003.

Phospholipase Cgamma activates Ras on the Golgi apparatus by means of RasGRP1. *Nature* 424:694-698.

172. Ebinu, J. O., S. L. Stang, C. Teixeira, D. A. Bottorff, J. Hooton, P. M. Blumberg, M. Barry, R. C. Bleakley, H. L. Ostergaard, and J. C. Stone. 2000. RasGRP links T-cell receptor signaling to Ras. *Blood* 95:3199-3203.
173. Mor, A., and M. R. Philips. 2006. Compartmentalized Ras/MAPK signaling. *Annu Rev Immunol* 24:771-800.
174. Dhanasekaran, N., and E. Premkumar Reddy. 1998. Signaling by dual specificity kinases. *Oncogene* 17:1447-1455.
175. Elion, E. A. 1998. Routing MAP kinase cascades. *Science (New York, N.Y* 281:1625-1626.
176. Ward, Y., S. Gupta, P. Jensen, M. Wartmann, R. J. Davis, and K. Kelly. 1994. Control of MAP kinase activation by the mitogen-induced threonine/tyrosine phosphatase PAC1. *Nature* 367:651-654.
177. Gille, H., M. Kortenjann, O. Thomae, C. Moomaw, C. Slaughter, M. H. Cobb, and P. E. Shaw. 1995. ERK phosphorylation potentiates Elk-1-mediated ternary complex formation and transactivation. *The EMBO journal* 14:951-962.
178. Gille, H., A. D. Sharrocks, and P. E. Shaw. 1992. Phosphorylation of transcription factor p62TCF by MAP kinase stimulates ternary complex formation at c-fos promoter. *Nature* 358:414-417.
179. Price, M., F. Cruzalegui, II, and R. Treisman. 1996. The p38 and ERK MAP kinase pathways cooperate to activate ternary complex factors and c-fos transcription in response to UV light. *The EMBO journal* 15.
180. Raingeaud, J., S. Gupta, J. Rogers, M. Dickens, J. Ilan, R. Ulevitch, and R. Davis. 1995. Pro-inflammatory cytokines and environmental stress cause p38 mitogen-activated protein kinase activation by dual phosphorylation on tyrosine and threonine. *The Journal of biological chemistry* 270.
181. Angel, P., and M. Karin. 1991. The role of Jun, Fos and the AP-1 complex in cell-proliferation and transformation. *Biochimica et biophysica acta* 1072:129-157.
182. Zhao, C., G. Du, K. Skowronek, M. A. Frohman, and D. Bar-Sagi. 2007. Phospholipase D2-generated phosphatidic acid couples EGFR stimulation to Ras activation by Sos. *Nature cell biology* 9:706-712.

183. Caloca, M. J., J. L. Zugaza, and X. R. Bustelo. 2003. Exchange factors of the RasGRP family mediate Ras activation in the Golgi. *The Journal of biological chemistry* 278:33465-33473.

184. Perez de Castro, I., T. G. Bivona, M. R. Philips, and A. Pellicer. 2004. Ras activation in Jurkat T cells following low-grade stimulation of the T-cell receptor is specific to N-Ras and occurs only on the Golgi apparatus. *Molecular and cellular biology* 24:3485-3496.

185. Marais, R., Y. Light, H. F. Paterson, and C. J. Marshall. 1995. Ras recruits Raf-1 to the plasma membrane for activation by tyrosine phosphorylation. *The EMBO journal* 14:3136-3145.

186. Tran, N. H., and J. A. Frost. 2003. Phosphorylation of Raf-1 by p21-activated kinase 1 and Src regulates Raf-1 autoinhibition. *The Journal of biological chemistry* 278:11221-11226.

187. Owens, D. M., and S. M. Keyse. 2007. Differential regulation of MAP kinase signalling by dual-specificity protein phosphatases. *Oncogene* 26:3203-3213.

188. Chen, R. H., C. Sarnecki, and J. Blenis. 1992. Nuclear localization and regulation of erk- and rsk-encoded protein kinases. *Molecular and cellular biology* 12:915-927.

189. Brunet, A., D. Roux, P. Lenormand, S. Dowd, S. Keyse, and J. Pouyssegur. 1999. Nuclear translocation of p42/p44 mitogen-activated protein kinase is required for growth factor-induced gene expression and cell cycle entry. *The EMBO journal* 18:664-674.

190. Gonzalez, F. A., A. Seth, D. L. Raden, D. S. Bowman, F. S. Fay, and R. J. Davis. 1993. Serum-induced translocation of mitogen-activated protein kinase to the cell surface ruffling membrane and the nucleus. *The Journal of cell biology* 122:1089-1101.

191. Lenormand, P., C. Sardet, G. Pages, G. L'Allemain, A. Brunet, and J. Pouyssegur. 1993. Growth factors induce nuclear translocation of MAP kinases (p42mapk and p44mapk) but not of their activator MAP kinase kinase (p45mapkk) in fibroblasts. *The Journal of cell biology* 122:1079-1088.

192. Mor, A., M. L. Dustin, and M. R. Philips. 2007. Small GTPases and LFA-1 reciprocally modulate adhesion and signaling. *Immunological reviews* 218:114-125.

193. Lin, A., A. Minden, H. Martinetto, F. Claret, C. Lange-Carter, F. Mercurio, G. Johnson, and M. Karin. 1995. Identification of a dual specificity kinase that activates the Jun kinases and p38-Mpk2. *Science (New York, N.Y* 268:286-290.

194. Minden, A., A. Lin, T. Smeal, B. Derijard, M. Cobb, R. Davis, and M. Karin. 1994. c-Jun N-terminal phosphorylation correlates with activation of the JNK subgroup but not the ERK subgroup of mitogen-activated protein kinases. *Molecular and cellular biology* 14:6683-6688.

195. Dalton, S., and R. Treisman. 1992. Characterization of SAP-1, a protein recruited by serum response factor to the c-fos serum response element. *Cell* 68.

196. Janknecht, R., W. H. Ernst, V. Pingoud, and A. Nordheim. 1993. Activation of ternary complex factor Elk-1 by MAP kinases. *The EMBO journal* 12:5097-5104.

197. Fruman, D. A., S. B. Snapper, C. M. Yballe, L. Davidson, J. Y. Yu, F. W. Alt, and L. C. Cantley. 1999. Impaired B cell development and proliferation in absence of phosphoinositide 3-kinase p85alpha. *Science (New York, N.Y* 283:393-397.

198. Ueda, Y., B. L. Levine, M. L. Huang, G. J. Freeman, L. M. Nadler, C. H. June, and S. G. Ward. 1995. Both CD28 ligands CD80 (B7-1) and CD86 (B7-2) activate phosphatidylinositol 3-kinase, and wortmannin reveals heterogeneity in the regulation of T cell IL-2 secretion. *International immunology* 7:957-966.

199. Ward, S. G. 1996. CD28: a signalling perspective. *The Biochemical journal* 318 (Pt 2):361-377.

200. Parry, R. V., C. A. Rumbley, L. H. Vandenberghe, C. H. June, and J. L. Riley. 2003. CD28 and inducible costimulatory protein Src homology 2 binding domains show distinct regulation of phosphatidylinositol 3-kinase, Bcl-xL, and IL-2 expression in primary human CD4 T lymphocytes. *J Immunol* 171:166-174.

201. Frias, M. A., C. C. Thoreen, J. D. Jaffe, W. Schroder, T. Sculley, S. A. Carr, and D. M. Sabatini. 2006. mSin1 is necessary for Akt/PKB phosphorylation, and its isoforms define three distinct mTORC2s. *Curr Biol* 16:1865-1870.

202. Cantrell, D. 2002. Protein kinase B (Akt) regulation and function in T lymphocytes. *Seminars in immunology* 14:19-26.

203. Otero, D. C., S. A. Omori, and R. C. Rickert. 2001. Cd19-dependent activation of Akt kinase in B-lymphocytes. *The Journal of biological chemistry* 276:1474-1478.

204. Jones, R. G., M. Parsons, M. Bonnard, V. S. Chan, W. C. Yeh, J. R. Woodgett, and P. S. Ohashi. 2000. Protein kinase B regulates T lymphocyte survival, nuclear factor

kappaB activation, and Bcl-X(L) levels in vivo. *The Journal of experimental medicine* 191:1721-1734.

205. Kane, L. P., P. G. Andres, K. C. Howland, A. K. Abbas, and A. Weiss. 2001. Akt provides the CD28 costimulatory signal for up-regulation of IL-2 and IFN-gamma but not TH2 cytokines. *Nature immunology* 2:37-44.

206. Kane, L. P., and A. Weiss. 2003. The PI-3 kinase/Akt pathway and T cell activation: pleiotropic pathways downstream of PIP3. *Immunological reviews* 192:7-20.

207. Coudronniere, N., M. Villalba, N. Englund, and A. Altman. 2000. NF-kappa B activation induced by T cell receptor/CD28 costimulation is mediated by protein kinase C-theta. *Proceedings of the National Academy of Sciences of the United States of America* 97:3394-3399.

208. Pfeifhofer, C., K. Kofler, T. Gruber, N. G. Tabrizi, C. Lutz, K. Maly, M. Leitges, and G. Baier. 2003. Protein kinase C theta affects Ca2+ mobilization and NFAT cell activation in primary mouse T cells. *The Journal of experimental medicine* 197:1525-1535.

209. Sun, Z., C. W. Arendt, W. Ellmeier, E. M. Schaeffer, M. J. Sunshine, L. Gandhi, J. Annes, D. Petrzilka, A. Kupfer, P. L. Schwartzberg, and D. R. Littman. 2000. PKC-theta is required for TCR-induced NF-kappaB activation in mature but not immature T lymphocytes. *Nature* 404:402-407.

210. Schaeffer, E. M., and P. L. Schwartzberg. 2000. Tec family kinases in lymphocyte signaling and function. *Current opinion in immunology* 12:282-288.

211. Grasis, J. A., C. D. Browne, and C. D. Tsoukas. 2003. Inducible T cell tyrosine kinase regulates actin-dependent cytoskeletal events induced by the T cell antigen receptor. *J Immunol* 170:3971-3976.

212. Labno, C. M., C. M. Lewis, D. You, D. W. Leung, A. Takesono, N. Kamberos, A. Seth, L. D. Finkelstein, M. K. Rosen, P. L. Schwartzberg, and J. K. Burkhardt. 2003. Itk functions to control actin polymerization at the immune synapse through localized activation of Cdc42 and WASP. *Curr Biol* 13:1619-1624.

213. Dietrich, C., Z. N. Volovyk, M. Levi, N. L. Thompson, and K. Jacobson. 2001. Partitioning of Thy-1, GM1, and cross-linked phospholipid analogs into lipid rafts reconstituted in supported model membrane monolayers. *Proceedings of the National Academy of Sciences of the United States of America* 98:10642-10647.

214. Gupta, N., and A. L. DeFranco. 2003. Visualizing lipid raft dynamics and early signaling events during antigen receptor-mediated B-lymphocyte activation. *Molecular biology of the cell* 14:432-444.
215. Prior, I. A., C. Muncke, R. G. Parton, and J. F. Hancock. 2003. Direct visualization of Ras proteins in spatially distinct cell surface microdomains. *The Journal of cell biology* 160:165-170.
216. Rodgers, W., and J. Zavzavadjian. 2001. Glycolipid-enriched membrane domains are assembled into membrane patches by associating with the actin cytoskeleton. *Experimental cell research* 267:173-183.
217. Sharma, P., R. Varma, R. C. Sarasij, Ira, K. Gousset, G. Krishnamoorthy, M. Rao, and S. Mayor. 2004. Nanoscale organization of multiple GPI-anchored proteins in living cell membranes. *Cell* 116:577-589.
218. Wilson, B. S., S. L. Steinberg, K. Liederman, J. R. Pfeiffer, Z. Surviladze, J. Zhang, L. E. Samelson, L. H. Yang, P. G. Kotula, and J. M. Oliver. 2004. Markers for detergent-resistant lipid rafts occupy distinct and dynamic domains in native membranes. *Molecular biology of the cell* 15:2580-2592.
219. Simons, K., and D. Toomre. 2000. Lipid rafts and signal transduction. *Nature reviews* 1:31-39.
220. Kabouridis, P. S., A. I. Magee, and S. C. Ley. 1997. S-acylation of LCK protein tyrosine kinase is essential for its signalling function in T lymphocytes. *The EMBO journal* 16:4983-4998.
221. Chen, X., and M. D. Resh. 2001. Activation of mitogen-activated protein kinase by membrane-targeted Raf chimeras is independent of raft localization. *The Journal of biological chemistry* 276:34617-34623.
222. Furuchi, T., and R. G. Anderson. 1998. Cholesterol depletion of caveolae causes hyperactivation of extracellular signal-related kinase (ERK). *The Journal of biological chemistry* 273:21099-21104.
223. Kabouridis, P. S., J. Janzen, A. L. Magee, and S. C. Ley. 2000. Cholesterol depletion disrupts lipid rafts and modulates the activity of multiple signaling pathways in T lymphocytes. *European journal of immunology* 30:954-963.
224. Horejsi, V. 2003. The roles of membrane microdomains (rafts) in T cell activation. *Immunological reviews* 191:148-164.

225. Viola, A., S. Schroeder, Y. Sakakibara, and A. Lanzavecchia. 1999. T lymphocyte costimulation mediated by reorganization of membrane microdomains. *Science (New York, N.Y* 283:680-682.

226. Wulfing, C., and M. M. Davis. 1998. A receptor/cytoskeletal movement triggered by costimulation during T cell activation. *Science (New York, N.Y* 282:2266-2269.

227. Schwartz, R. H. 1990. A cell culture model for T lymphocyte clonal anergy. *Science (New York, N.Y* 248:1349-1356.

228. Monks, C. R., B. A. Freiberg, H. Kupfer, N. Sciaky, and A. Kupfer. 1998. Three-dimensional segregation of supramolecular activation clusters in T cells. *Nature* 395:82-86.

229. Lee, K. H., A. D. Holdorf, M. L. Dustin, A. C. Chan, P. M. Allen, and A. S. Shaw. 2002. T cell receptor signaling precedes immunological synapse formation. *Science (New York, N.Y* 295:1539-1542.

230. Freiberg, B. A., H. Kupfer, W. Maslanik, J. Delli, J. Kappler, D. M. Zaller, and A. Kupfer. 2002. Staging and resetting T cell activation in SMACs. *Nature immunology* 3:911-917.

231. Stone, J. D., L. A. Conroy, K. F. Byth, R. A. Hederer, S. Howlett, Y. Takemoto, N. Holmes, and D. R. Alexander. 1997. Aberrant TCR-mediated signaling in CD45-null thymocytes involves dysfunctional regulation of Lck, Fyn, TCR-zeta, and ZAP-70. *J Immunol* 158:5773-5782.

232. Sanchez-Madrid, F., and M. A. del Pozo. 1999. Leukocyte polarization in cell migration and immune interactions. *The EMBO journal* 18:501-511.

233. Dustin, M. L., and J. A. Cooper. 2000. The immunological synapse and the actin cytoskeleton: molecular hardware for T cell signaling. *Nature immunology* 1:23-29.

234. Carlin, L. M., K. Yanagi, A. Verhoef, E. N. Nolte-'t Hoen, J. Yates, L. Gardner, J. Lamb, G. Lombardi, M. J. Dallman, and D. M. Davis. 2005. Secretion of IFN-gamma and not IL-2 by anergic human T cells correlates with assembly of an immature immune synapse. *Blood* 106:3874-3879.

235. Reichert, P., R. L. Reinhardt, E. Ingulli, and M. K. Jenkins. 2001. Cutting edge: in vivo identification of TCR redistribution and polarized IL-2 production by naive CD4 T cells. *J Immunol* 166:4278-4281.

236. Stoll, S., J. Delon, T. M. Brotz, and R. N. Germain. 2002. Dynamic imaging of T cell-dendritic cell interactions in lymph nodes. *Science (New York, N.Y* 296:1873-1876.

237. Bousso, P., and E. Robey. 2003. Dynamics of CD8+ T cell priming by dendritic cells in intact lymph nodes. *Nature immunology* 4:579-585.

238. Hugues, S., L. Fetler, L. Bonifaz, J. Helft, F. Amblard, and S. Amigorena. 2004. Distinct T cell dynamics in lymph nodes during the induction of tolerance and immunity. *Nature immunology* 5:1235-1242.

239. Mempel, T. R., S. E. Henrickson, and U. H. Von Andrian. 2004. T-cell priming by dendritic cells in lymph nodes occurs in three distinct phases. *Nature* 427:154-159.

240. Miller, M. J., O. Safrina, I. Parker, and M. D. Cahalan. 2004. Imaging the single cell dynamics of CD4+ T cell activation by dendritic cells in lymph nodes. *The Journal of experimental medicine* 200:847-856.

241. Miller, M. J., S. H. Wei, I. Parker, and M. D. Cahalan. 2002. Two-photon imaging of lymphocyte motility and antigen response in intact lymph node. *Science (New York, N.Y* 296:1869-1873.

242. Shakhar, G., R. L. Lindquist, D. Skokos, D. Dudziak, J. H. Huang, M. C. Nussenzweig, and M. L. Dustin. 2005. Stable T cell-dendritic cell interactions precede the development of both tolerance and immunity in vivo. *Nature immunology* 6:707-714.

243. Chang, J. T., V. R. Palanivel, I. Kinjyo, F. Schambach, A. M. Intlekofer, A. Banerjee, S. A. Longworth, K. E. Vinup, P. Mrass, J. Oliaro, N. Killeen, J. S. Orange, S. M. Russell, W. Weninger, and S. L. Reiner. 2007. Asymmetric T lymphocyte division in the initiation of adaptive immune responses. *Science (New York, N.Y* 315:1687-1691.

244. Albanese, C., J. Johnson, G. Watanabe, N. Eklund, D. Vu, A. Arnold, and R. G. Pestell. 1995. Transforming p21ras mutants and c-Ets-2 activate the cyclin D1 promoter through distinguishable regions. *The Journal of biological chemistry* 270:23589-23597.

245. Friend, S. H., R. Bernards, S. Rogelj, R. A. Weinberg, J. M. Rapaport, D. M. Albert, and T. P. Dryja. 1986. A human DNA segment with properties of the gene that predisposes to retinoblastoma and osteosarcoma. *Nature* 323:643-646.

246. Lee, W. H., R. Bookstein, F. Hong, L. J. Young, J. Y. Shew, and E. Y. Lee. 1987. Human retinoblastoma susceptibility gene: cloning, identification, and sequence. *Science (New York, N.Y* 235:1394-1399.

247. Murphree, A. L., and W. F. Benedict. 1984. Retinoblastoma: clues to human oncogenesis. *Science (New York, N.Y* 223:1028-1033.

248. Felsani, A., A. M. Mileo, and M. G. Paggi. 2006. Retinoblastoma family proteins as key targets of the small DNA virus oncoproteins. *Oncogene* 25:5277-5285.

249. White, M. K., and K. Khalili. 2006. Interaction of retinoblastoma protein family members with large T-antigen of primate polyomaviruses. *Oncogene* 25:5286-5293.

250. Tonks, I. D., N. K. Hayward, and G. F. Kay. 2006. Pocket protein function in melanocyte homeostasis and neoplasia. *Pigment cell research / sponsored by the European Society for Pigment Cell Research and the International Pigment Cell Society* 19:260-283.

251. Harbour, J. W., R. X. Luo, A. Dei Santi, A. A. Postigo, and D. C. Dean. 1999. Cdk phosphorylation triggers sequential intramolecular interactions that progressively block Rb functions as cells move through G1. *Cell* 98:859-869.

252. Bras, A., A. Ruiz-Vela, G. Gonzalez de Buitrago, and A. C. Martinez. 1999. Caspase activation by BCR cross-linking in immature B cells: differential effects on growth arrest and apoptosis. *Faseb J* 13:931-944.

253. D'Abaco, G. M., S. Hooper, H. Paterson, and C. J. Marshall. 2002. Loss of Rb overrides the requirement for ERK activity for cell proliferation. *J Cell Sci* 115:4607-4616.

254. Lam, E. W., M. S. Choi, J. van der Sman, S. A. Burbidge, and G. G. Klaus. 1998. Modulation of E2F activity via signaling through surface IgM and CD40 receptors in WEHI-231 B lymphoma cells. *The Journal of biological chemistry* 273:10051-10057.

255. Levine, A. J. 1997. p53, the cellular gatekeeper for growth and division. *Cell* 88:323-331.

256. Ma, Y., J. Yuan, M. Huang, R. Jove, and W. D. Cress. 2003. Regulation of the cyclin D3 promoter by E2F1. *The Journal of biological chemistry* 278:16770-16776.

257. Dyson, N. 1998. The regulation of E2F by pRB-family proteins. *Genes & development* 12:2245-2262.

258. Kim, D. M., K. Yang, and B. S. Yang. 2003. Biochemical characterizations reveal different properties between CDK4/cyclin D1 and CDK2/cyclin A. *Experimental & molecular medicine* 35:421-430.

259. Aleem, E., H. Kiyokawa, and P. Kaldis. 2005. Cdc2-cyclin E complexes regulate the G1/S phase transition. *Nature cell biology* 7:831-836.

260. Attisano, L., and J. L. Wrana. 1996. Signal transduction by members of the transforming growth factor-beta superfamily. *Cytokine Growth Factor Rev* 7:327-339.

261. Baker, J. C., and R. M. Harland. 1997. From receptor to nucleus: the Smad pathway. *Curr Opin Genet Dev* 7:467-473.

262. Matsuura, I., N. G. Denissova, G. Wang, D. He, J. Long, and F. Liu. 2004. Cyclin-dependent kinases regulate the antiproliferative function of Smads. *Nature* 430:226-231.

263. Liu, F., C. Pouponnot, and J. Massague. 1997. Dual role of the Smad4/DPC4 tumor suppressor in TGFbeta-inducible transcriptional complexes. *Genes & development* 11:3157-3167.

264. Derynck, R., R. J. Akhurst, and A. Balmain. 2001. TGF-beta signaling in tumor suppression and cancer progression. *Nature genetics* 29:117-129.

265. Massague, J., S. W. Blain, and R. S. Lo. 2000. TGFbeta signaling in growth control, cancer, and heritable disorders. *Cell* 103:295-309.

266. Ando, T., K. Hatsushika, M. Wako, T. Ohba, K. Koyama, Y. Ohnuma, R. Katoh, H. Ogawa, K. Okumura, J. Luo, T. Wyss-Coray, and A. Nakao. 2007. Orally administered TGF-beta is biologically active in the intestinal mucosa and enhances oral tolerance. *J Allergy Clin Immunol*.

267. Datto, M. B., J. P. Frederick, L. Pan, A. J. Borton, Y. Zhuang, and X. F. Wang. 1999. Targeted disruption of Smad3 reveals an essential role in transforming growth factor beta-mediated signal transduction. *Molecular and cellular biology* 19:2495-2504.

268. Rich, J. N., M. Zhang, M. B. Datto, D. D. Bigner, and X. F. Wang. 1999. Transforming growth factor-beta-mediated p15(INK4B) induction and growth inhibition in astrocytes is SMAD3-dependent and a pathway prominently altered in human glioma cell lines. *The Journal of biological chemistry* 274:35053-35058.

269. Yang, X., J. J. Letterio, R. J. Lechleider, L. Chen, R. Hayman, H. Gu, A. B. Roberts, and C. Deng. 1999. Targeted disruption of SMAD3 results in impaired mucosal immunity and diminished T cell responsiveness to TGF-beta. *The EMBO journal* 18:1280-1291.

270. Tzachanis, D., G. J. Freeman, N. Hirano, A. A. van Puijenbroek, M. W. Delfs, A. Berezovskaya, L. M. Nadler, and V. A. Boussiotis. 2001. Tob is a negative regulator of activation that is expressed in anergic and quiescent T cells. *Nature immunology* 2:1174-1182.

271. Sherr, C. J., and J. M. Roberts. 1999. CDK inhibitors: positive and negative regulators of G1-phase progression. *Genes Dev* 13:1501-1512.

272. Hannon, G. J., and D. Beach. 1994. p15INK4B is a potential effector of TGF-beta-induced cell cycle arrest. *Nature* 371:257-261.

273. Lukas, J., D. Parry, L. Aagaard, D. J. Mann, J. Bartkova, M. Strauss, G. Peters, and J. Bartek. 1995. Retinoblastoma-protein-dependent cell-cycle inhibition by the tumour suppressor p16. *Nature* 375:503-506.

274. Polyak, K., J. Y. Kato, M. J. Solomon, C. J. Sherr, J. Massague, J. M. Roberts, and A. Koff. 1994. p27Kip1, a cyclin-Cdk inhibitor, links transforming growth factor-beta and contact inhibition to cell cycle arrest. *Genes & development* 8:9-22.

275. Reynisdottir, I., K. Polyak, A. Iavarone, and J. Massague. 1995. Kip/Cip and Ink4 Cdk inhibitors cooperate to induce cell cycle arrest in response to TGF-beta. *Genes & development* 9:1831-1845.

276. Groth, A., J. D. Weber, B. M. Willumsen, C. J. Sherr, and M. F. Roussel. 2000. Oncogenic Ras induces p19ARF and growth arrest in mouse embryo fibroblasts lacking p21Cip1 and p27Kip1 without activating cyclin D-dependent kinases. *The Journal of biological chemistry* 275:27473-27480.

277. Sugihara, T., S. C. Kaul, J. Kato, R. R. Reddel, H. Nomura, and R. Wadhwa. 2001. Pex19p dampens the p19ARF-p53-p21WAF1 tumor suppressor pathway. *The Journal of biological chemistry* 276:18649-18652.

278. Cheng, M., P. Olivier, J. A. Diehl, M. Fero, M. F. Roussel, J. M. Roberts, and C. J. Sherr. 1999. The p21(Cip1) and p27(Kip1) CDK 'inhibitors' are essential activators of cyclin D-dependent kinases in murine fibroblasts. *The EMBO journal* 18:1571-1583.

279. Toyoshima, H., and T. Hunter. 1994. p27, a novel inhibitor of G1 cyclin-Cdk protein kinase activity, is related to p21. *Cell* 78:67-74.
280. Fujita, N., S. Sato, K. Katayama, and T. Tsuruo. 2002. Akt-dependent phosphorylation of p27Kip1 promotes binding to 14-3-3 and cytoplasmic localization. *The Journal of biological chemistry* 277:28706-28713.
281. Fujita, N., S. Sato, and T. Tsuruo. 2003. Phosphorylation of p27Kip1 at threonine 198 by p90 ribosomal protein S6 kinases promotes its binding to 14-3-3 and cytoplasmic localization. *The Journal of biological chemistry* 278:49254-49260.
282. Ishida, N., T. Hara, T. Kamura, M. Yoshida, K. Nakayama, and K. I. Nakayama. 2002. Phosphorylation of p27Kip1 on serine 10 is required for its binding to CRM1 and nuclear export. *The Journal of biological chemistry* 277:14355-14358.
283. Shin, I., F. M. Yakes, F. Rojo, N. Y. Shin, A. V. Bakin, J. Baselga, and C. L. Arteaga. 2002. PKB/Akt mediates cell-cycle progression by phosphorylation of p27(Kip1) at threonine 157 and modulation of its cellular localization. *Nat Med* 8:1145-1152.
284. Hengst, L., and S. I. Reed. 1996. Translational control of p27Kip1 accumulation during the cell cycle. *Science (New York, N.Y* 271:1861-1864.
285. Slingerland, J., and M. Pagano. 2000. Regulation of the cdk inhibitor p27 and its deregulation in cancer. *J Cell Physiol* 183:10-17.
286. Muller, D., K. Thieke, A. Burgin, A. Dickmanns, and M. Eilers. 2000. Cyclin E-mediated elimination of p27 requires its interaction with the nuclear pore-associated protein mNPAP60. *The EMBO journal* 19:2168-2180.
287. Zeng, Y., K. Hirano, M. Hirano, J. Nishimura, and H. Kanaide. 2000. Minimal requirements for the nuclear localization of p27(Kip1), a cyclin-dependent kinase inhibitor. *Biochemical and biophysical research communications* 274:37-42.
288. Delmas, C., N. Aragou, S. Poussard, P. Cottin, J. M. Darbon, and S. Manenti. 2003. MAP kinase-dependent degradation of p27Kip1 by calpains in choroidal melanoma cells. Requirement of p27Kip1 nuclear export. *The Journal of biological chemistry* 278:12443-12451.
289. Kawada, M., S. Yamagoe, Y. Murakami, K. Suzuki, S. Mizuno, and Y. Uehara. 1997. Induction of p27Kip1 degradation and anchorage independence by Ras through the MAP kinase signaling pathway. *Oncogene* 15:629-637.

290. Carrano, A. C., E. Eytan, A. Hershko, and M. Pagano. 1999. SKP2 is required for ubiquitin-mediated degradation of the CDK inhibitor p27. *Nature cell biology* 1:193-199.

291. Sutterluty, H., E. Chatelain, A. Marti, C. Wirbelauer, M. Senften, U. Muller, and W. Krek. 1999. p45SKP2 promotes p27Kip1 degradation and induces S phase in quiescent cells. *Nature cell biology* 1:207-214.

292. Tsvetkov, L. M., K. H. Yeh, S. J. Lee, H. Sun, and H. Zhang. 1999. p27(Kip1) ubiquitination and degradation is regulated by the SCF(Skp2) complex through phosphorylated Thr187 in p27. *Curr Biol* 9:661-664.

293. Waldman, T., K. W. Kinzler, and B. Vogelstein. 1995. p21 is necessary for the p53-mediated G1 arrest in human cancer cells. *Cancer research* 55:5187-5190.

294. Ho, J. S., W. Ma, D. Y. Mao, and S. Benchimol. 2005. p53-Dependent transcriptional repression of c-myc is required for G1 cell cycle arrest. *Molecular and cellular biology* 25:7423-7431.

295. Taylor, W. R., and G. R. Stark. 2001. Regulation of the G2/M transition by p53. *Oncogene* 20:1803-1815.

296. Wang, X. 2001. The expanding role of mitochondria in apoptosis. *Genes & development* 15:2922-2933.

297. Thornberry, N. A., and Y. Lazebnik. 1998. Caspases: enemies within. *Science (New York, N.Y* 281:1312-1316.

298. Ellis, H. M., and H. R. Horvitz. 1986. Genetic control of programmed cell death in the nematode C. elegans. *Cell* 44:817-829.

299. Borner, C., and L. Monney. 1999. Apoptosis without caspases: an inefficient molecular guillotine? *Cell death and differentiation* 6:497-507.

300. Susin, S. A., H. K. Lorenzo, N. Zamzami, I. Marzo, B. E. Snow, G. M. Brothers, J. Mangion, E. Jacotot, P. Costantini, M. Loeffler, N. Larochette, D. R. Goodlett, R. Aebersold, D. P. Siderovski, J. M. Penninger, and G. Kroemer. 1999. Molecular characterization of mitochondrial apoptosis-inducing factor. *Nature* 397:441-446.

301. Li, L. Y., X. Luo, and X. Wang. 2001. Endonuclease G is an apoptotic DNase when released from mitochondria. *Nature* 412:95-99.

302. Huang, D. C., and A. Strasser. 2000. BH3-Only proteins-essential initiators of apoptotic cell death. *Cell* 103:839-842.

303. Sattler, M., H. Liang, D. Nettesheim, R. P. Meadows, J. E. Harlan, M. Eberstadt, H. S. Yoon, S. B. Shuker, B. S. Chang, A. J. Minn, C. B. Thompson, and S. W. Fesik. 1997. Structure of Bcl-xL-Bak peptide complex: recognition between regulators of apoptosis. *Science (New York, N.Y* 275:983-986.

304. Opferman, J. T., and S. J. Korsmeyer. 2003. Apoptosis in the development and maintenance of the immune system. *Nature immunology* 4:410-415.

305. Hengartner, M. O. 2000. The biochemistry of apoptosis. *Nature* 407:770-776.

306. Conradt, B. 2002. With a little help from your friends: cells don't die alone. *Nature cell biology* 4:E139-143.

307. Green, D., and G. Kroemer. 1998. The central executioners of apoptosis: caspases or mitochondria? *Trends in cell biology* 8:267-271.

308. Leist, M., and M. Jaattela. 2001. Four deaths and a funeral: from caspases to alternative mechanisms. *Nature reviews* 2:589-598.

309. Foghsgaard, L., D. Wissing, D. Mauch, U. Lademann, L. Bastholm, M. Boes, F. Elling, M. Leist, and M. Jaattela. 2001. Cathepsin B acts as a dominant execution protease in tumor cell apoptosis induced by tumor necrosis factor. *The Journal of cell biology* 153:999-1010.

310. Isahara, K., Y. Ohsawa, S. Kanamori, M. Shibata, S. Waguri, N. Sato, T. Gotow, T. Watanabe, T. Momoi, K. Urase, E. Kominami, and Y. Uchiyama. 1999. Regulation of a novel pathway for cell death by lysosomal aspartic and cysteine proteinases. *Neuroscience* 91:233-249.

311. Katz, E., M. R. Deehan, S. Seatter, C. Lord, R. D. Sturrock, and M. M. Harnett. 2001. B cell receptor-stimulated mitochondrial phospholipase A2 activation and resultant disruption of mitochondrial membrane potential correlate with the induction of apoptosis in WEHI-231 B cells. *J Immunol* 166:137-147.

312. Palaga, T., and B. Osborne. 2002. The 3D's of apoptosis: death, degradation and DIAPs. *Nature cell biology* 4:E149-151.

313. Stoka, V., B. Turk, S. L. Schendel, T. H. Kim, T. Cirman, S. J. Snipas, L. M. Ellerby, D. Bredesen, H. Freeze, M. Abrahamson, D. Bromme, S. Krajewski, J. C. Reed, X. M. Yin, V. Turk, and G. S. Salvesen. 2001. Lysosomal protease pathways to apoptosis. Cleavage of bid, not pro-caspases, is the most likely route. *The Journal of biological chemistry* 276:3149-3157.

314. Alberola-Ila, J., S. Takaki, J. D. Kerner, and R. M. Perlmutter. 1997. Differential signaling by lymphocyte antigen receptors. *Annu Rev Immunol* 15:125-154.
315. Zhang, J., K. V. Salojin, J. X. Gao, M. J. Cameron, I. Bergerot, and T. L. Delovitch. 1999. p38 mitogen-activated protein kinase mediates signal integration of TCR/CD28 costimulation in primary murine T cells. *J Immunol* 162:3819-3829.
316. Dubois, P. M., F. Andris, R. A. Shapiro, L. K. Gilliland, M. Kaufman, J. Urbain, J. A. Ledbetter, and O. Leo. 1994. T cell long-term hyporesponsiveness follows antigen receptor engagement and results from defective signal transduction. *European journal of immunology* 24:348-354.
317. Schwartz, R. H. 1997. T cell clonal anergy. *Current opinion in immunology* 9:351-357.
318. Sundstedt, A., and M. Dohlsten. 1998. In vivo anergized CD4+ T cells have defective expression and function of the activating protein-1 transcription factor. *J Immunol* 161:5930-5936.
319. Cho, E. A., M. P. Riley, A. L. Sillman, and H. Quill. 1993. Altered protein tyrosine phosphorylation in anergic Th1 cells. *J Immunol* 151:20-28.
320. Bhandoola, A., E. A. Cho, K. Yui, H. U. Saragovi, M. I. Greene, and H. Quill. 1993. Reduced CD3-mediated protein tyrosine phosphorylation in anergic CD4+ and CD8+ T cells. *J Immunol* 151:2355-2367.
321. Yu, S. C., and B. Nag. 1997. Differential expression of protein tyrosine kinases and their phosphorylation in murine Th1 cells anergized with class II MHC-peptide complexes. *Immunol Cell Biol* 75:295-302.
322. Quill, H., M. P. Riley, E. A. Cho, J. E. Casnellie, J. C. Reed, and T. Torigoe. 1992. Anergic Th1 cells express altered levels of the protein tyrosine kinases p56lck and p59fyn. *J Immunol* 149:2887-2893.
323. Gajewski, T. F., D. Qian, P. Fields, and F. W. Fitch. 1994. Anergic T-lymphocyte clones have altered inositol phosphate, calcium, and tyrosine kinase signaling pathways. *Proceedings of the National Academy of Sciences of the United States of America* 91:38-42.
324. Straus, D. B., and A. Weiss. 1993. The CD3 chains of the T cell antigen receptor associate with the ZAP-70 tyrosine kinase and are tyrosine phosphorylated after receptor stimulation. *The Journal of experimental medicine* 178:1523-1530.

325. Smith, J. A., J. Y. Tso, M. R. Clark, M. S. Cole, and J. A. Bluestone. 1997. Nonmitogenic anti-CD3 monoclonal antibodies deliver a partial T cell receptor signal and induce clonal anergy. *The Journal of experimental medicine* 185:1413-1422.

326. Asai, K., S. Hachimura, M. Kimura, T. Toraya, M. Yamashita, T. Nakayama, and S. Kaminogawa. 2002. T cell hyporesponsiveness induced by oral administration of ovalbumin is associated with impaired NFAT nuclear translocation and p27kip1 degradation. *J Immunol* 169:4723-4731.

327. Hundt, M., H. Tabata, M. S. Jeon, K. Hayashi, Y. Tanaka, R. Krishna, L. De Giorgio, Y. C. Liu, M. Fukata, and A. Altman. 2006. Impaired activation and localization of LAT in anergic T cells as a consequence of a selective palmitoylation defect. *Immunity* 24:513-522.

328. Berg-Brown, N. N., M. A. Gronski, R. G. Jones, A. R. Elford, E. K. Deenick, B. Odermatt, D. R. Littman, and P. S. Ohashi. 2004. PKCtheta signals activation versus tolerance in vivo. *The Journal of experimental medicine* 199:743-752.

329. Safford, M., S. Collins, M. A. Lutz, A. Allen, C. T. Huang, J. Kowalski, A. Blackford, M. R. Horton, C. Drake, R. H. Schwartz, and J. D. Powell. 2005. Egr-2 and Egr-3 are negative regulators of T cell activation. *Nature immunology* 6:472-480.

330. Harris, J. E., K. D. Bishop, N. E. Phillips, J. P. Mordes, D. L. Greiner, A. A. Rossini, and M. P. Czech. 2004. Early growth response gene-2, a zinc-finger transcription factor, is required for full induction of clonal anergy in CD4+ T cells. *J Immunol* 173:7331-7338.

331. Kang, S. M., B. Beverly, A. C. Tran, K. Brorson, R. H. Schwartz, and M. J. Lenardo. 1992. Transactivation by AP-1 is a molecular target of T cell clonal anergy. *Science (New York, N.Y* 257:1134-1138.

332. Chou, Y. K., I. Robey, C. N. Woody, W. Li, H. Offner, A. A. Vandenbark, and M. P. Davey. 1998. Induction of T cell anergy by high concentrations of immunodominant native peptide is accompanied by IL-10 production and a block in JNK activity. *Cellular immunology* 188:125-136.

333. DeSilva, D. R., W. S. Feeser, E. J. Tancula, and P. A. Scherle. 1996. Anergic T cells are defective in both jun NH2-terminal kinase and mitogen-activated protein kinase signaling pathways. *The Journal of experimental medicine* 183:2017-2023.

334. Jain, J., P. G. McCaffrey, V. E. Valge-Archer, and A. Rao. 1992. Nuclear factor of activated T cells contains Fos and Jun. *Nature* 356:801-804.

335. Jain, J., V. E. Valge-Archer, and A. Rao. 1992. Analysis of the AP-1 sites in the IL-2 promoter. *J Immunol* 148:1240-1250.

336. Li, W., C. D. Whaley, A. Mondino, and D. L. Mueller. 1996. Blocked signal transduction to the ERK and JNK protein kinases in anergic CD4+ T cells. *Science (New York, N.Y* 271:1272-1276.

337. Mondino, A., C. D. Whaley, D. R. DeSilva, W. Li, M. K. Jenkins, and D. L. Mueller. 1996. Defective transcription of the IL-2 gene is associated with impaired expression of c-Fos, FosB, and JunB in anergic T helper 1 cells. *J Immunol* 157:2048-2057.

338. Fields, P. E., T. F. Gajewski, and F. W. Fitch. 1996. Blocked Ras activation in anergic CD4+ T cells. *Science (New York, N.Y* 271:1276-1278.

339. Dower, N. A., S. L. Stang, D. A. Bottorff, J. O. Ebinu, P. Dickie, H. L. Ostergaard, and J. C. Stone. 2000. RasGRP is essential for mouse thymocyte differentiation and TCR signaling. *Nature immunology* 1:317-321.

340. Olenchock, B. A., R. Guo, J. H. Carpenter, M. Jordan, M. K. Topham, G. A. Koretzky, and X. P. Zhong. 2006. Disruption of diacylglycerol metabolism impairs the induction of T cell anergy. *Nature immunology* 7:1174-1181.

341. Zha, Y., R. Marks, A. W. Ho, A. C. Peterson, S. Janardhan, I. Brown, K. Praveen, S. Stang, J. C. Stone, and T. F. Gajewski. 2006. T cell anergy is reversed by active Ras and is regulated by diacylglycerol kinase-alpha. *Nature immunology* 7:1166-1173.

342. Macian, F., F. Garcia-Cozar, S. H. Im, H. F. Horton, M. C. Byrne, and A. Rao. 2002. Transcriptional mechanisms underlying lymphocyte tolerance. *Cell* 109:719-731.

343. Zhong, X. P., E. A. Hainey, B. A. Olenchock, M. S. Jordan, J. S. Maltzman, K. E. Nichols, H. Shen, and G. A. Koretzky. 2003. Enhanced T cell responses due to diacylglycerol kinase zeta deficiency. *Nature immunology* 4:882-890.

344. Zhong, X. P., E. A. Hainey, B. A. Olenchock, H. Zhao, M. K. Topham, and G. A. Koretzky. 2002. Regulation of T cell receptor-induced activation of the Ras-ERK pathway by diacylglycerol kinase zeta. *The Journal of biological chemistry* 277:31089-31098.

345. Pizon, V., P. Chardin, I. Lerosey, B. Olofsson, and A. Tavitian. 1988. Human cDNAs rap1 and rap2 homologous to the Drosophila gene Dras3 encode proteins closely related to ras in the 'effector' region. *Oncogene* 3:201-204.

346. Kitayama, H., Y. Sugimoto, T. Matsuzaki, Y. Ikawa, and M. Noda. 1989. A ras-related gene with transformation suppressor activity. *Cell* 56:77-84.

347. Abraham, R. T. 2002. Antigen receptors rap to integrin receptors. *Nature immunology* 3:212-213.

348. Frech, M., J. John, V. Pizon, P. Chardin, A. Tavitian, R. Clark, F. McCormick, and A. Wittinghofer. 1990. Inhibition of GTPase activating protein stimulation of Ras-p21 GTPase by the Krev-1 gene product. *Science (New York, N.Y* 249:169-171.

349. Hata, Y., A. Kikuchi, T. Sasaki, M. D. Schaber, J. B. Gibbs, and Y. Takai. 1990. Inhibition of the ras p21 GTPase-activating protein-stimulated GTPase activity of c-Ha-ras p21 by smg p21 having the same putative effector domain as ras p21s. *The Journal of biological chemistry* 265:7104-7107.

350. Czyzyk, J., D. Leitenberg, T. Taylor, and K. Bottomly. 2000. Combinatorial effect of T-cell receptor ligation and CD45 isoform expression on the signaling contribution of the small GTPases Ras and Rap1. *Molecular and cellular biology* 20:8740-8747.

351. Appleman, L. J., and V. A. Boussiotis. 2003. T cell anergy and costimulation. *Immunological reviews* 192:161-180.

352. Carey, K. D., T. J. Dillon, J. M. Schmitt, A. M. Baird, A. D. Holdorf, D. B. Straus, A. S. Shaw, and P. J. Stork. 2000. CD28 and the tyrosine kinase lck stimulate mitogen-activated protein kinase activity in T cells via inhibition of the small G protein Rap1. *Molecular and cellular biology* 20:8409-8419.

353. Reedquist, K. A., and J. L. Bos. 1998. Costimulation through CD28 suppresses T cell receptor-dependent activation of the Ras-like small GTPase Rap1 in human T lymphocytes. *The Journal of biological chemistry* 273:4944-4949.

354. Dillon, T. J., V. Karpitski, S. A. Wetzel, D. C. Parker, A. S. Shaw, and P. J. Stork. 2003. Ectopic B-Raf expression enhances extracellular signal-regulated kinase (ERK) signaling in T cells and prevents antigen-presenting cell-induced anergy. *The Journal of biological chemistry* 278:35940-35949.

355. Kometani, K., D. Ishida, M. Hattori, and N. Minato. 2004. Rap1 and SPA-1 in hematologic malignancy. *Trends in molecular medicine* 10:401-408.

356. Bos, J. L., J. de Rooij, and K. A. Reedquist. 2001. Rap1 signalling: adhering to new models. *Nature reviews* 2:369-377.

357. de Bruyn, K. M., S. Rangarajan, K. A. Reedquist, C. G. Figdor, and J. L. Bos. 2002. The small GTPase Rap1 is required for Mn(2+)- and antibody-induced LFA-1- and VLA-4-mediated cell adhesion. *The Journal of biological chemistry* 277:29468-29476.

358. Kimura, M., M. Yamashita, M. Kubo, M. Iwashima, C. Shimizu, K. Tokoyoda, J. Chiba, M. Taniguchi, M. Katsumata, and T. Nakayama. 2000. Impaired Ca/calcineurin pathway in in vivo anergized CD4 T cells. *International immunology* 12:817-824.

359. Saito, H., D. M. Kranz, Y. Takagaki, A. C. Hayday, H. N. Eisen, and S. Tonegawa. 1984. A third rearranged and expressed gene in a clone of cytotoxic T lymphocytes. *Nature* 312:36-40.

360. Utting, O., S. J. Teh, and H. S. Teh. 2000. A population of in vivo anergized T cells with a lower activation threshold for the induction of CD25 exhibit differential requirements in mobilization of intracellular calcium and mitogen-activated protein kinase activation. *J Immunol* 164:2881-2889.

361. Chiodetti, L., S. Choi, D. L. Barber, and R. H. Schwartz. 2006. Adaptive tolerance and clonal anergy are distinct biochemical states. *J Immunol* 176:2279-2291.

362. Weissman, A. M. 2001. Themes and variations on ubiquitylation. *Nature reviews* 2:169-178.

363. Davis, M., and Y. Ben-Neriah. 2004. Behind the scenes of anergy: a tale of three E3s. *Nat Immunol* 5.

364. Heissmeyer, V., F. Macian, S.-H. Im, R. Varma, S. Feske, K. Venuprasad, H. Gu, Y.-C. Liu, M. L. Dustin, and A. Rao. 2004. Calcineurin imposes T cell unresponsiveness through targeted proteolysis of signaling proteins. *Nat Immunol* 5.

365. Heissmeyer, V., and A. Rao. 2004. E3 ligases in T cell anergy--turning immune responses into tolerance. *Sci STKE* 2004.

366. Jeon, M.-S., A. Atfield, K. Venuprasad, C. Krawczyk, R. Sarao, C. Elly, C. Yang, S. Arya, K. Bachmaier, L. Su, D. Bouchard, R. Jones, M. Gronski, P. Ohashi, T. Wada, D. Bloom, C. G. Fathman, Y.-C. Liu, and J. M. Penninger. 2004. Essential role of the E3 ubiquitin ligase Cbl-b in T cell anergy induction. *Immunity* 21.

367. Naramura, M., I.-K. Jang, H. Kole, F. Huang, D. Haines, and H. Gu. 2002. c-Cbl and Cbl-b regulate T cell responsiveness by promoting ligand-induced TCR down-modulation. *Nat Immunol* 3.

368. Macian, F., F. Garcia-Cozar, S.-H. Im, H. F. Horton, M. C. Byrne, and A. Rao. 2002. Transcriptional mechanisms underlying lymphocyte tolerance. *Cell* 109.

369. Macian, F., S.-H. Im, F. J. Garcia-Cozar, and A. Rao. 2004. T-cell anergy. *Curr Opin Immunol* 16.

370. Mueller, D. L. 2004. E3 ubiquitin ligases as T cell anergy factors. *Nat Immunol* 5.

371. Grakoui, A., S. K. Bromley, C. Sumen, M. M. Davis, A. S. Shaw, P. M. Allen, and M. L. Dustin. 1999. The immunological synapse: a molecular machine controlling T cell activation. *Science* 285.

372. Huppa, J. B., M. Gleimer, C. Sumen, and M. M. Davis. 2003. Continuous T cell receptor signaling required for synapse maintenance and full effector potential. *Nat Immunol* 4.

373. Monks, C. R., B. A. Freiberg, H. Kupfer, N. Sciaky, and A. Kupfer. 1998. Three-dimensional segregation of supramolecular activation clusters in T cells. *Nature* 395.

374. Krawczyk, C., and J. M. Penninger. 2001. Molecular controls of antigen receptor clustering and autoimmunity. *Trends Cell Biol* 11.

375. Chiang, Y. J., H. K. Kole, K. Brown, M. Naramura, S. Fukuhara, R. J. Hu, I. K. Jang, J. S. Gutkind, E. Shevach, and H. Gu. 2000. Cbl-b regulates the CD28 dependence of T-cell activation. *Nature* 403.

376. Murphy, K. M., A. B. Heimberger, and D. Y. Loh. 1990. Induction by antigen of intrathymic apoptosis of CD4+CD8+TCRlo thymocytes in vivo. *Science* 250.

377. Hurez, V., R. Dzialo-Hatton, J. Oliver, R. J. Matthews, and C. T. Weaver. 2002. Efficient adenovirus-mediated gene transfer into primary T cells and thymocytes in a new coxsackie/adenovirus receptor transgenic model. *BMC Immunol* 3:4.

378. Kearney, E. R., K. A. Pape, D. Y. Loh, and M. K. Jenkins. 1994. Visualization of peptide-specific T cell immunity and peripheral tolerance induction in vivo. *Immunity* 1:327-339.

379. Garside, P., E. Ingulli, R. R. Merica, J. G. Johnson, R. J. Noelle, and M. K. Jenkins. 1998. Visualization of specific B and T lymphocyte interactions in the lymph node. *Science* 281.

380. Garside, P., E. Ingulli, R. Merica, J. Johnson, R. Noelle, and M. Jenkins. 1998. Visualization of specific B and T lymphocyte interactions in the lymph node. *Science (New York, N.Y* 281.

381. Pape, K. A., R. Merica, A. Mondino, A. Khoruts, and M. K. Jenkins. 1998. Direct evidence that functionally impaired CD4+ T cells persist in vivo following induction of peripheral tolerance. *J Immunol* 160:4719-4729.

382. Reinhardt, R. L., A. Khoruts, R. Merica, T. Zell, and M. K. Jenkins. 2001. Visualizing the generation of memory CD4 T cells in the whole body. *Nature* 410:101-105.

383. Zell, T., A. Khoruts, E. Ingulli, J. L. Bonnevier, D. L. Mueller, and M. K. Jenkins. 2001. Single-cell analysis of signal transduction in CD4 T cells stimulated by antigen in vivo. *Proceedings of the National Academy of Sciences of the United States of America* 98:10805-10810.

384. Smith, K. M., F. McAskill, and P. Garside. 2002. Orally tolerized T cells are only able to enter B cell follicles following challenge with antigen in adjuvant, but they remain unable to provide B cell help. *J Immunol* 168:4318-4325.

385. Haskins, K., R. Kubo, J. White, M. Pigeon, J. Kappler, and P. Marrack. 1983. The major histocompatibility complex-restricted antigen receptor on T cells. I. Isolation with a monoclonal antibody. *J Exp Med* 157.

386. Haskins, K., R. Kubo, J. White, M. Pigeon, J. Kappler, and P. Marrack. 1983. The major histocompatibility complex-restricted antigen receptor on T cells. I. Isolation with a monoclonal antibody. *The Journal of experimental medicine* 157:1149-1169.

387. Altin, J. G., and E. B. Pagler. 1995. A one-step procedure for biotinylation and chemical cross-linking of lymphocyte surface and intracellular membrane-associated molecules. *Analytical biochemistry* 224:382-389.

388. Lutz, M. B., N. Kukutsch, A. L. Ogilvie, S. Rossner, F. Koch, N. Romani, and G. Schuler. 1999. An advanced culture method for generating large quantities of highly pure dendritic cells from mouse bone marrow. *J Immunol Methods* 223.

389. Williams, M. E., C. M. Shea, A. H. Lichtman, and A. K. Abbas. 1992. Antigen receptor-mediated anergy in resting T lymphocytes and T cell clones. Correlation with lymphokine secretion patterns. *J Immunol* 149:1921-1926.

390. Chai, J. G., and R. I. Lechler. 1997. Immobilized anti-CD3 mAb induces anergy in murine naive and memory CD4+ T cells in vitro. *Int Immunol* 9.

391. Jenkins, M. K., C. A. Chen, G. Jung, D. L. Mueller, and R. H. Schwartz. 1990. Inhibition of antigen-specific proliferation of type 1 murine T cell clones after stimulation with immobilized anti-CD3 monoclonal antibody. *J Immunol* 144.

392. Grierson, A. M., P. Mitchell, C. L. Adams, A. M. Mowat, J. M. Brewer, M. M. Harnett, and P. Garside. 2005. Direct quantitation of T cell signaling by laser scanning cytometry. *Journal of immunological methods* 301:140-153.

393. Agar, A., S. S. Yip, M. A. Hill, and M. T. Coroneo. 2000. Pressure related apoptosis in neuronal cell lines. *Journal of neuroscience research* 60:495-503.

394. Gorczyca, W., E. Bedner, P. Burfeind, Z. Darzynkiewicz, and M. R. Melamed. 1998. Analysis of apoptosis in solid tumors by laser-scanning cytometry. *Mod Pathol* 11:1052-1058.

395. Szodoray, P., S. Jellestad, B. Nakken, J. G. Brun, and R. Jonsson. 2003. Programmed cell death in rheumatoid arthritis peripheral blood T-cell subpopulations determined by laser scanning cytometry. *Laboratory investigation; a journal of technical methods and pathology* 83:1839-1848.

396. Kamentsky, L. A. 2001. Laser scanning cytometry. *Methods Cell Biol* 63.

397. Darzymkiewicz, Z., E. Bedner, X. Li, W. Gorczyca, and M. Melamed. 1999. Laser-Scanning cytometry: a new instrumentation with many applications. *Experimental Cell Research* 249:1-12.

398. Kapuscinski, J. 1995. DAPI: a DNA-specific fluorescent probe. *Biotech Histochem* 70:220-233.

399. Grierson, A. M., P. Mitchell, C. L. Adams, A. M. Mowat, J. M. Brewer, M. M. Harnett, and P. Garside. 2005. Direct quantitation of T cell signaling by laser scanning cytometry. *J Immunol Methods*.

400. Dong, W. K., M. L. Andres, G. M. Miller, J. D. Cao, L. M. Green, A. L. B. Seynhaeve, T. L. M. Ten Hagen, and D. S. Gridley. 2002. Immunohistochemical analysis of immune cell infiltration of a human colon xenograft after treatment with Stealth liposome-encapsulated tumour necrosis factor-α and radiation. *International Journal of Oncology* 21:973-979.

401. Underhill, D. M., M. Bassetti, A. Rudensky, and A. Aderem. 1999. Dynamic interactions of macrophages with T cells during antigen presentation. *The Journal of experimental medicine* 190:1909-1914.

402. Hurez, V., R. Dzialo-Hatton, J. Oliver, R. J. Matthews, and C. T. Weaver. 2002. Efficient adenovirus-mediated gene transfer into primary T cells and thymocytes in a new coxsackie/adenovirus receptor transgenic model. *BMC immunology* 3:4.

403. Renzi, P., and L. C. Ginns. 1987. Analysis of T cell subsets in normal adults. Comparison of whole blood lysis technique to Ficoll-Hypaque separation by flow cytometry. *Journal of immunological methods* 98:53-56.

404. Schorpp, M., R. Jager, K. Schellander, J. Schenkel, E. F. Wagner, H. Weiher, and P. Angel. 1996. The human ubiquitin C promoter directs high ubiquitous expression of transgenes in mice. *Nucleic Acids Res* 24:1787-1788.

405. Graham, F. L., J. Smiley, W. C. Russell, and R. Nairn. 1977. Characteristics of a human cell line transformed by DNA from human adenovirus type 5. *J Gen Virol* 36:59-74.

406. Nicklin, S. A., Baker, A. H. 1999. Simple Methods for Preparing Recombinant Adenoviruses for High-Efficiency Transduction of Vascular Cells. In *Methods in Molecular Medicine, Vascular Disease: Molecular Biology and Gene Therapy Protocols*. A. H. Baker, ed. Humana Press Inc. 271-282.

407. Nicklin, S., and A. Baker. 1999. Simple Methods for Preparing Recombinant Adenoviruses for High-Efficiency Transduction of Vascular Cells. In *Vascular Disease:Molecular Biology and Gene Therapy Protocols*. A. Baker, ed. Humana Press Inc., Totowa, NJ. 271-283`.

408. Maheshwari, G., R. Jannat, L. McCormick, and D. Hsu. 2004. Thermal inactivation of adenovirus type 5. *Journal of virological methods* 118:141-146.

409. Hunter, T. 2000. Signaling--2000 and beyond. *Cell* 100:113-127.

410. Zell, T., and M. K. Jenkins. 2002. Flow cytometric analysis of T cell receptor signal transduction. *Sci STKE* 2002:PL5.

411. Adams, C. L., N. Kobets, G. R. Meiklejohn, O. R. Millington, A. M. Morton, C. M. Rush, K. M. Smith, and P. Garside. 2004. Tracking lymphocytes in vivo. *Arch Immunol Ther Exp (Warsz)* 52:173-187.

412. Hagani, A. B., I. Riviere, C. Tan, A. Krause, and M. Sadelain. 1999. Activation conditions determine susceptibility of murine primary T-lymphocytes to retroviral infection. *J Gene Med* 1:341-351.

413. Karapetian, O., A. N. Shakhov, J. P. Kraehenbuhl, and H. Acha-Orbea. 1994. Retroviral infection of neonatal Peyer's patch lymphocytes: the mouse mammary tumor virus model. *The Journal of experimental medicine* 180:1511-1516.

414. Nakagawa, R., S. M. Mason, and A. M. Michie. 2006. Determining the role of specific signaling molecules during lymphocyte development in vivo: instant transgenesis. *Nat Protoc* 1:1185-1193.

415. Miller, D. G., M. A. Adam, and A. D. Miller. 1990. Gene transfer by retrovirus vectors occurs only in cells that are actively replicating at the time of infection. *Molecular and cellular biology* 10:4239-4242.

416. Dai, Y., M. Roman, R. K. Naviaux, and I. M. Verma. 1992. Gene therapy via primary myoblasts: long-term expression of factor IX protein following transplantation in vivo. *Proceedings of the National Academy of Sciences of the United States of America* 89:10892-10895.

417. Palmer, T. D., G. J. Rosman, W. R. Osborne, and A. D. Miller. 1991. Genetically modified skin fibroblasts persist long after transplantation but gradually inactivate introduced genes. *Proceedings of the National Academy of Sciences of the United States of America* 88:1330-1334.

418. St Louis, D., and I. M. Verma. 1988. An alternative approach to somatic cell gene therapy. *Proceedings of the National Academy of Sciences of the United States of America* 85:3150-3154.

419. Hurez, V., R. D. Hautton, J. Oliver, R. J. Matthews, and C. K. Weaver. 2002. Gene delivery into primary T cells: overview and characterization of a transgenic model for efficient adenoviral transduction. *Immunol Res* 26:131-141.

420. Wan, Y. Y., R. P. Leon, R. Marks, C. M. Cham, J. Schaack, T. F. Gajewski, and J. DeGregori. 2000. Transgenic expression of the coxsackie/adenovirus receptor enables adenoviral-mediated gene delivery in naive T cells. *Proceedings of the National Academy of Sciences of the United States of America* 97:13784-13789.

421. Nevins, J. R., J. DeGregori, L. Jakoi, and G. Leone. 1997. Functional analysis of E2F transcription factor. *Methods Enzymol* 283:205-219.

422. Chu, Y., K. Sperber, L. Mayer, and M. T. Hsu. 1992. Persistent infection of human adenovirus type 5 in human monocyte cell lines. *Virology* 188:793-800.

423. DeMatteo, R. P., S. E. Raper, M. Ahn, K. J. Fisher, C. Burke, A. Radu, G. Widera, B. R. Claytor, C. F. Barker, and J. F. Markmann. 1995. Gene transfer to the thymus.

A means of abrogating the immune response to recombinant adenovirus. *Ann Surg* 222:229-239; discussion 239-242.

424. Neering, S. J., S. F. Hardy, D. Minamoto, S. K. Spratt, and C. T. Jordan. 1996. Transduction of primitive human hematopoietic cells with recombinant adenovirus vectors. *Blood* 88:1147-1155.

425. Huang, S., R. I. Endo, and G. R. Nemerow. 1995. Upregulation of integrins alpha v beta 3 and alpha v beta 5 on human monocytes and T lymphocytes facilitates adenovirus-mediated gene delivery. *J Virol* 69:2257-2263.

426. Huang, S., T. Kamata, Y. Takada, Z. M. Ruggeri, and G. R. Nemerow. 1996. Adenovirus interaction with distinct integrins mediates separate events in cell entry and gene delivery to hematopoietic cells. *J Virol* 70:4502-4508.

427. Bergelson, J. M., J. A. Cunningham, G. Droguett, E. A. Kurt-Jones, A. Krithivas, J. S. Hong, M. S. Horwitz, R. L. Crowell, and R. W. Finberg. 1997. Isolation of a common receptor for Coxsackie B viruses and adenoviruses 2 and 5. *Science (New York, N.Y* 275:1320-1323.

428. Bergelson, J. M., A. Krithivas, L. Celi, G. Droguett, M. S. Horwitz, T. Wickham, R. L. Crowell, and R. W. Finberg. 1998. The murine CAR homolog is a receptor for coxsackie B viruses and adenoviruses. *J Virol* 72:415-419.

429. Tomko, R. P., R. Xu, and L. Philipson. 1997. HCAR and MCAR: the human and mouse cellular receptors for subgroup C adenoviruses and group B coxsackieviruses. *Proceedings of the National Academy of Sciences of the United States of America* 94:3352-3356.

430. Leon, R. P., T. Hedlund, S. J. Meech, S. Li, J. Schaack, S. P. Hunger, R. C. Duke, and J. DeGregori. 1998. Adenoviral-mediated gene transfer in lymphocytes. *Proceedings of the National Academy of Sciences of the United States of America* 95:13159-13164.

431. Carson, S. D. 2001. Receptor for the group B coxsackieviruses and adenoviruses: CAR. *Reviews in medical virology* 11:219-226.

432. Cebrian, M., E. Yague, M. Rincon, M. Lopez-Botet, M. O. de Landazuri, and F. Sanchez-Madrid. 1988. Triggering of T cell proliferation through AIM, an activation inducer molecule expressed on activated human lymphocytes. *The Journal of experimental medicine* 168:1621-1637.

433. Testi, R., J. H. Phillips, and L. L. Lanier. 1988. Constitutive expression of a phosphorylated activation antigen (Leu 23) by CD3bright human thymocytes. *J Immunol* 141:2557-2563.

434. Ziegler, S. F., F. Ramsdell, and M. R. Alderson. 1994. The activation antigen CD69. *Stem Cells* 12:456-465.

435. Kawasaki, M., K. Sasaki, T. Satoh, A. Kurose, T. Kamada, T. Furuya, T. Murakami, and T. Todoroki. 1997. Laser scanning cytometry (LCS) allows detailed analysis of the cell cycle in PI stained human fibroblasts (TIG-7). *Cell Prolif* 30:139-147.

436. Luther, E., and L. A. Kamentsky. 1996. Resolution of mitotic cells using laser scanning cytometry. *Cytometry* 23:272-278.

437. Bedner, E., X. Li, W. Gorczyca, M. R. Melamed, and Z. Darzynkiewicz. 1999. Analysis of apoptosis by laser scanning cytometry. *Cytometry* 35:181-195.

438. Cameron, I. L., R. L. Sparks, K. L. Horn, and N. R. Smith. 1977. Concentration of elements in mitotic chromatin as measured by x-ray microanalysis. *The Journal of cell biology* 73:193-199.

439. Labhart, P., T. Koller, and H. Wunderli. 1982. Involvement of higher order chromatin structures in metaphase chromosome organization. *Cell* 30:115-121.

440. Croft, M., and C. Dubey. 1997. Accessory molecule and costimulation requirements for CD4 T cell response. *Critical reviews in immunology* 17:89-118.

441. Boussiotis, V., G. Freeman, P. Taylor, A. Berezovskaya, I. Grass, B. Blazar, and L. Nadler. 2000. $p27^{kip1}$ functions as an anergy factor inhibiting interleukin 2 transcription and clonal expansion of alloreactive human and mouse helper T lymphocytes. *Nature Medicine* 6:290-297.

442. Wyllie, A. H. 1980. Glucocorticoid-induced thymocyte apoptosis is associated with endogenous endonuclease activation. *Nature* 284:555-556.

443. Alberola-Ila, J., and G. Hernandez-Hoyos. 2003. The Ras/MAPK cascade and the control of positive selection. *Immunological reviews* 191:79-96.

444. Fields, P., F. W. Fitch, and T. F. Gajewski. 1996. Control of T lymphocyte signal transduction through clonal anergy. *Journal of molecular medicine (Berlin, Germany)* 74:673-683.

445. Altan-Bonnet, G., and R. N. Germain. 2005. Modeling T cell antigen discrimination based on feedback control of digital ERK responses. *PLoS biology* 3:e356.

446. Crellin, N. K., R. V. Garcia, and M. K. Levings. 2007. Flow cytometry-based methods for studying signaling in human CD4+CD25+FOXP3+ T regulatory cells. *Journal of immunological methods* 324:92-104.

447. Garcia-Garcia, E., and C. Rosales. 2007. Nuclear factor activation by FcgammaR in human peripheral blood neutrophils detected by a novel flow cytometry-based method. *Journal of immunological methods* 320:104-118.

448. Appleman, L. J., A. Berezovskaya, I. Grass, and V. A. Boussiotis. 2000. CD28 costimulation mediates T cell expansion via IL-2-independent and IL-2-dependent regulation of cell cycle progression. *J Immunol* 164:144-151.

449. Schorle, H., T. Holtschke, T. Hunig, A. Schimpl, and I. Horak. 1991. Development and function of T cells in mice rendered interleukin-2 deficient by gene targeting. *Nature* 352:621-624.

450. Shahinian, A., K. Pfeffer, K. P. Lee, T. M. Kundig, K. Kishihara, A. Wakeham, K. Kawai, P. S. Ohashi, C. B. Thompson, and T. W. Mak. 1993. Differential T cell costimulatory requirements in CD28-deficient mice. *Science (New York, N.Y* 261:609-612.

451. Thompson, C. B., T. Lindsten, J. A. Ledbetter, S. L. Kunkel, H. A. Young, S. G. Emerson, J. M. Leiden, and C. H. June. 1989. CD28 activation pathway regulates the production of multiple T-cell-derived lymphokines/cytokines. *Proceedings of the National Academy of Sciences of the United States of America* 86:1333-1337.

452. Lundberg, A. S., and R. A. Weinberg. 1998. Functional inactivation of the retinoblastoma protein requires sequential modification by at least two distinct cyclin-cdk complexes. *Molecular and cellular biology* 18:753-761.

453. Takaki, T., K. Fukasawa, I. Suzuki-Takahashi, K. Semba, M. Kitagawa, Y. Taya, and H. Hirai. 2005. Preferences for phosphorylation sites in the retinoblastoma protein of D-type cyclin-dependent kinases, Cdk4 and Cdk6, in vitro. *J Biochem (Tokyo)* 137:381-386.

454. Bauman, J. G., J. Wiegant, P. Van Duijn, N. H. Lubsen, P. J. Sondermeijer, W. Hennig, and E. Kubli. 1981. Rapid and high resolution detection of in situ hybridisation to polytene chromosomes using fluorochrome-labeled RNA. *Chromosoma* 84:1-18.

455. Adams, B. S., K. Leung, P. S. Meltzer, K. A. Lewis, C. Wagner-McPherson, G. A. Evans, and G. J. Nabel. 1992. Localization of the gene encoding R kappa B

(NFRKB), a tissue-specific DNA binding protein, to chromosome 11q24-q25. *Genomics* 14:270-274.

456. Lawrence, J. B., L. M. Marselle, K. S. Byron, C. V. Johnson, J. L. Sullivan, and R. H. Singer. 1990. Subcellular localization of low-abundance human immunodeficiency virus nucleic acid sequences visualized by fluorescence in situ hybridization. *Proceedings of the National Academy of Sciences of the United States of America* 87:5420-5424.

457. Kozubek, M., S. Kozubek, E. Lukasova, A. Mareckova, E. Bartova, M. Skalnikova, and A. Jergova. 1999. High-resolution cytometry of FISH dots in interphase cell nuclei. *Cytometry* 36:279-293.

458. Darzynkiewicz, Z., E. Bedner, X. Li, W. Gorczyca, and M. R. Melamed. 1999. Laser-scanning cytometry: A new instrumentation with many applications. *Experimental cell research* 249:1-12.

459. Ishidate, M., Jr., K. F. Miura, and T. Sofuni. 1998. Chromosome aberration assays in genetic toxicology testing in vitro. *Mutation research* 404:167-172.

460. Numa, Y., K. Matsudaira, H. Tsukazaki, K. Kawamoto, T. Sato, and Y. kiyomatsu. 1996. [Analysis of cell nuclei and the quantity of chromosomal DNA by laser scanning cytometer (LSC)]. *Hum Cell* 9:237-243.

461. Smolewski, P., Q. Ruan, L. Vellon, and Z. Darzynkiewicz. 2001. Micronuclei assay by laser scanning cytometry. *Cytometry* 45:19-26.

462. Bedner, E., Q. Ruan, S. Chen, L. A. Kamentsky, and Z. Darzynkiewicz. 2000. Multiparameter analysis of progeny of individual cells by laser scanning cytometry. *Cytometry* 40:271-279.

463. Lyons, A. B., and C. R. Parish. 1994. Determination of lymphocyte division by flow cytometry. *Journal of immunological methods* 171:131-137.

464. Weston, S. A., and C. R. Parish. 1990. New fluorescent dyes for lymphocyte migration studies. Analysis by flow cytometry and fluorescence microscopy. *Journal of immunological methods* 133:87-97.

465. Mintern, J., M. Li, G. M. Davey, E. Blanas, C. Kurts, F. R. Carbone, and W. R. Heath. 1999. The use of carboxyfluorescein diacetate succinimidyl ester to determine the site, duration and cell type responsible for antigen presentation in vivo. *Immunol Cell Biol* 77:539-543.

466. Adler, A. J., C. T. Huang, G. S. Yochum, D. W. Marsh, and D. M. Pardoll. 2000. In vivo CD4+ T cell tolerance induction versus priming is independent of the rate and number of cell divisions. *J Immunol* 164:649-655.

467. Hughes, C. C., and J. S. Pober. 1996. Transcriptional regulation of the interleukin-2 gene in normal human peripheral blood T cells. Convergence of costimulatory signals and differences from transformed T cells. *The Journal of biological chemistry* 271:5369-5377.

468. Cann, A., Y. Koyanagi, and I. Chen. 1998. High efficiency transfection of primary human lymphocytes and studies of gene expression. . *Oncogene* 3.

469. Novak, T. J., F. K. Yoshimura, and E. V. Rothenberg. 1992. In vitro transfection of fresh thymocytes and T cells shows subset-specific expression of viral promoters. *Molecular and cellular biology* 12:1515-1527.

470. Chrivia, J. C., T. Wedrychowicz, H. A. Young, and K. J. Hardy. 1990. A model of human cytokine regulation based on transfection of gamma interferon gene fragments directly into isolated peripheral blood T lymphocytes. *The Journal of experimental medicine* 172:661-664.

471. Cron, R. Q., L. A. Schubert, D. B. Lewis, and C. C. Hughes. 1997. Consistent transient transfection of DNA into non-transformed human and murine T-lymphocytes. *Journal of immunological methods* 205:145-150.

472. Maier, C. C., A. Bhandoola, W. Borden, K. Yui, K. Hayakawa, and M. I. Greene. 1998. Unique molecular surface features of in vivo tolerized T cells. *Proceedings of the National Academy of Sciences of the United States of America* 95.

473. Wells, A. D., M. C. Walsh, D. Sankaran, and L. A. Turka. 2000. T cell effector function and anergy avoidance are quantitatively linked to cell division. *J Immunol* 165:2432-2443.

474. Buder-Hoffmann, S., C. Palmer, P. Vacek, D. Taatjes, and B. Mossman. 2001. Different accumulation of activated extracellular signal-regulated kinases (ERK 1/2) and role in cell-cycle alterations by epidermal growth factor, hydrogen peroxide, or asbestos in pulmonary epithelial cells. *Am J Respir Cell Mol Biol* 24:405-413.

475. Clatch, R. J., and J. L. Walloch. 1998. Multiparameter immunophenotypic analysis by laser scanning cytometry. *Acta Cytologica* 41:109-122.

476. Clatch, R. J., J. R. Foreman, and J. L. Walloch. 1998. Simplified Immunophenotypic Analysis by Laser Scanning Cytometry. *Cytometry (Communications in Clinical Cytometry)* 34:3-16.

477. Gerstner, A., W. Laffers, F. Bootz, and A. Tarnok. 2000. Immunophenotyping of peripheral blood leucocytes by laser scanning cytometry. *Journal of immunological methods* 246:175-185.

478. Tarnok, A., A. Gerstner, D. Lenz, P. Osmancik, P. Schneider, C. Trumpfheller, P. Racz, and K. Tenner-Racz. 2002. Multicolor immunophenotyping of tissue sections by Laser Scanning Cytometry (LSC). *Proceedings of the SPIE* 4622:229-239.

479. Smith, K. M., J. M. Brewer, C. M. Rush, J. Riley, and P. Garside. 2004. In vivo generated Th1 cells can migrate to B cell follicles to support B cell responses. *J Immunol* 173:1640-1646.

480. Marshall, F. A., A. M. Grierson, P. Garside, W. Harnett, and M. M. Harnett. 2005. ES-62, an immunomodulator secreted by filarial nematodes, suppresses clonal expansion and modifies effector function of heterologous antigen-specific T cells in vivo. *J Immunol* 175:5817-5826.

481. Grace, M. J., L. Xie, M. L. Musco, S. Cui, M. Gurnani, R. DiGiacomo, A. Chang, S. Indelicato, J. Syed, R. Johnson, and L. L. Nielsen. 1999. The use of laser scanning cytometry to assess depth of penetration of adenovirus p53 gene therapy in human xenograft biopsies. *Am J Pathol* 155:1869-1878.

482. Chan, S. M., J. A. Olson, and P. J. Utz. 2006. Single-cell analysis of siRNA-mediated gene silencing using multiparameter flow cytometry. *Cytometry A* 69:59-65.

483. Cheng, K., D. Fraga, C. Zhang, M. Kotb, A. O. Gaber, R. V. Guntaka, and R. I. Mahato. 2004. Adenovirus-based vascular endothelial growth factor gene delivery to human pancreatic islets. *Gene Ther* 11:1105-1116.

484. Sebille, F., B. Vanhove, and J. P. Soulillou. 2001. Mechanisms of tolerance induction: blockade of co-stimulation. *Philos Trans R Soc Lond B Biol Sci* 356.

485. Harding, F. A., J. G. McArthur, J. A. Gross, D. H. Raulet, and J. P. Allison. 1992. CD28-mediated signalling co-stimulates murine T cells and prevents induction of anergy in T-cell clones. *Nature* 356:607-609.

486. Jenkins, M. K., and R. H. Schwartz. 1987. Antigen presentation by chemically modified splenocytes induces antigen-specific T cell unresponsiveness in vitro and in vivo. *The Journal of experimental medicine* 165.

487. Chai, J., and R. Lechler. 1997. Immobilized anti-CD3 mAb induces anergy in murine naive and memory $CD4^+$ T cells *in vitro*. *International immunology* 9:935-944.

488. Li, W., C. D. Whaley, J. L. Bonnevier, A. Mondino, M. E. Martin, K. M. Aagaard-Tillery, and D. L. Mueller. 2001. CD28 signaling augments Elk-1-dependent transcription at the c-fos gene during antigen stimulation. *J Immunol* 167:827-835.

489. Vidal, A., and A. Koff. 2000. Cell-cycle inhibitors: three families united by a common cause. *Gene* 247:1-15.

490. Morgan, D. O. 1995. Principles of CDK regulation. *Nature* 374:131-134.

491. Coleman, M. L., C. J. Marshall, and M. F. Olson. 2004. RAS and RHO GTPases in G1-phase cell-cycle regulation. *Nature reviews* 5:355-366.

492. Downward, J. 2003. Targeting RAS signalling pathways in cancer therapy. *Nat Rev Cancer* 3:11-22.

493. Kerkhoff, E., and U. R. Rapp. 1998. Cell cycle targets of Ras/Raf signalling. *Oncogene* 17:1457-1462.

494. Lavoie, J. N., G. L'Allemain, A. Brunet, R. Muller, and J. Pouyssegur. 1996. Cyclin D1 expression is regulated positively by the p42/p44MAPK and negatively by the p38/HOGMAPK pathway. *The Journal of biological chemistry* 271:20608-20616.

495. Massague, J. 2004. G1 cell-cycle control and cancer. *Nature* 432:298-306.

496. Sears, R. C., and J. R. Nevins. 2002. Signaling networks that link cell proliferation and cell fate. *The Journal of biological chemistry* 277:11617-11620.

497. Filmus, J., A. I. Robles, W. Shi, M. J. Wong, L. L. Colombo, and C. J. Conti. 1994. Induction of cyclin D1 overexpression by activated ras. *Oncogene* 9:3627-3633.

498. Liu, J. J., J. R. Chao, M. C. Jiang, S. Y. Ng, J. J. Yen, and H. F. Yang-Yen. 1995. Ras transformation results in an elevated level of cyclin D1 and acceleration of G1 progression in NIH 3T3 cells. *Molecular and cellular biology* 15:3654-3663.

499. Bakiri, L., D. Lallemand, E. Bossy-Wetzel, and M. Yaniv. 2000. Cell cycle-dependent variations in c-Jun and JunB phosphorylation: a role in the control of cyclin D1 expression. *The EMBO journal* 19:2056-2068.

500. Mechta, F., D. Lallemand, C. M. Pfarr, and M. Yaniv. 1997. Transformation by ras modifies AP1 composition and activity. *Oncogene* 14:837-847.

501. Weitzman, J. B., L. Fiette, K. Matsuo, and M. Yaniv. 2000. JunD protects cells from p53-dependent senescence and apoptosis. *Mol Cell* 6:1109-1119.

502. Yoshida, Y., T. Nakamura, M. Komoda, H. Satoh, T. Suzuki, J. K. Tsuzuku, T. Miyasaka, E. H. Yoshida, H. Umemori, R. K. Kunisaki, K. Tani, S. Ishii, S. Mori, M. Suganuma, T. Noda, and T. Yamamoto. 2003. Mice lacking a transcriptional corepressor Tob are predisposed to cancer. *Genes & development* 17:1201-1206.

503. Kubsch, S., E. Graulich, J. Knop, and K. Steinbrink. 2003. Suppressor activity of anergic T cells induced by IL-10-treated human dendritic cells: association with IL-2- and CTLA-4-dependent G1 arrest of the cell cycle regulated by p27Kip1. *European journal of immunology* 33.

504. Jackson, S., A. DeLoose, and K. Gilbert. 2001. Induction of Anergy in Th1 Cells Associated with Increased Levels of Cyclin-Dependent Kinase Inhibitors $p21^{Cip1}$ and $p27^{kip11}$. *The Journal of Immunology* 166:952-958.

505. Kudo, H., T. Matsuoka, H. Mitsuya, Y. Nishimura, and S. Matsushita. 2002. Cross-linking HLA-DR molecules on Th1 cells induces anergy in association with increased level of cyclin-dependent kinase inhibitor p27(Kip1). *Immunol Lett* 81:149-155.

506. Powell, J. D., D. Bruniquel, and R. H. Schwartz. 2001. TCR engagement in the absence of cell cycle progression leads to T cell anergy independent of p27(Kip1). *European journal of immunology* 31:3737-3746.

507. Fero, M. L., M. Rivkin, M. Tasch, P. Porter, C. E. Carow, E. Firpo, K. Polyak, L. H. Tsai, V. Broudy, R. M. Perlmutter, K. Kaushansky, and J. M. Roberts. 1996. A syndrome of multiorgan hyperplasia with features of gigantism, tumorigenesis, and female sterility in p27(Kip1)-deficient mice. *Cell* 85:733-744.

508. Huleatt, J. W., J. Cresswell, K. Bottomly, and I. N. Crispe. 2003. P27kip1 regulates the cell cycle arrest and survival of activated T lymphocytes in response to interleukin-2 withdrawal. *Immunology* 108:493-501.

509. Zhang, S., V. A. Lawless, and M. H. Kaplan. 2000. Cytokine-stimulated T lymphocyte proliferation is regulated by p27Kip1. *J Immunol* 165:6270-6277.

510. Rowell, E. A., M. C. Walsh, and A. D. Wells. 2005. Opposing roles for the cyclin-dependent kinase inhibitor p27kip1 in the control of CD4+ T cell proliferation and effector function. *J Immunol* 174:3359-3368.

511. Pape, K., E. Kearney, A. Khoruts, A. Mondino, R. Merica, Z. Chen, E. Ingulli, J. White, J. Johnson, and M. K. Jenkins. 1997. Use of adoptive transfer of T-cell-antigen-receptor-transgenic T cells for the study of T-cell activatin in vivo. *Immunological reviews* 156:67-78.

512. Ghaffari-Tabrizi, N., B. Bauer, A. Villunger, G. Baier-Bitterlich, A. Altman, G. Utermann, F. Uberall, and G. Baier. 1999. Protein kinase Ctheta, a selective upstream regulator of JNK/SAPK and IL-2 promoter activation in Jurkat T cells. *European journal of immunology* 29:132-142.

513. Werlen, G., E. Jacinto, Y. Xia, and M. Karin. 1998. Calcineurin preferentially synergizes with PKC-theta to activate JNK and IL-2 promoter in T lymphocytes. *The EMBO journal* 17:3101-3111.

514. Dong, C., D. D. Yang, C. Tournier, A. J. Whitmarsh, J. Xu, R. J. Davis, and R. A. Flavell. 2000. JNK is required for effector T-cell function but not for T-cell activation. *Nature* 405:91-94.

515. Dong, C., D. D. Yang, M. Wysk, A. J. Whitmarsh, R. J. Davis, and R. A. Flavell. 1998. Defective T cell differentiation in the absence of Jnk1. *Science (New York, N.Y* 282:2092-2095.

516. Yang, D. D., D. Conze, A. J. Whitmarsh, T. Barrett, R. J. Davis, M. Rincon, and R. A. Flavell. 1998. Differentiation of CD4+ T cells to Th1 cells requires MAP kinase JNK2. *Immunity* 9:575-585.

517. Sabapathy, K., Y. Hu, T. Kallunki, M. Schreiber, J. P. David, W. Jochum, E. F. Wagner, and M. Karin. 1999. JNK2 is required for efficient T-cell activation and apoptosis but not for normal lymphocyte development. *Curr Biol* 9:116-125.

518. Su, B., E. Jacinto, M. Hibi, T. Kallunki, M. Karin, and Y. Ben-Neriah. 1994. JNK is involved in signal integration during costimulation of T lymphocytes. *Cell* 77:727-736.

519. Greene, W. C., and W. J. Leonard. 1986. The human interleukin-2 receptor. *Annu Rev Immunol* 4:69-95.

520. Minami, Y., T. Kono, T. Miyazaki, and T. Taniguchi. 1993. The IL-2 receptor complex: its structure, function, and target genes. *Annu Rev Immunol* 11:245-268.

521. Eriksson, K., I. Nordstrom, C. Czerkinsky, and J. Holmgren. 2000. Differential effect of cholera toxin on CD45RA+ and CD45RO+ T cells: specific inhibition of cytokine production but not proliferation of human naive T cells. *Clinical and experimental immunology* 121:283-288.

522. Janeway, C. A., Jr., and K. Bottomly. 1994. Signals and signs for lymphocyte responses. *Cell* 76:275-285.

523. Wells, A. D., M. C. Walsh, J. A. Bluestone, and L. A. Turka. 2001. Signaling through CD28 and CTLA-4 controls two distinct forms of T cell anergy. *J Clin Invest* 108.

524. Delon, J., N. Bercovici, R. Liblau, and A. Trautmann. 1998. Imaging antigen recognition by naive CD4+ T cells: compulsory cytoskeletal alterations for the triggering of an intracellular calcium response. *European journal of immunology* 28:716-729.

525. Nel, A. E. 2002. T-cell activation through the antigen receptor. Part 1: signaling components, signaling pathways, and signal integration at the T-cell antigen receptor synapse. *J Allergy Clin Immunol* 109.

526. Chen, D., V. Heath, A. O'Garra, J. Johnston, and M. McMahon. 1999. Sustained activation of the raf-MEK-ERK pathway elicits cytokine unresponsiveness in T cells. *J Immunol* 163.

527. Gauld, S. B., D. Blair, C. A. Moss, S. D. Reid, and M. M. Harnett. 2002. Differential roles for extracellularly regulated kinase-mitogen-activated protein kinase in B cell antigen receptor-induced apoptosis and CD40-mediated rescue of WEHI-231 immature B cells. *J Immunol* 168.

528. Guo, J., G. Sheng, and B. W. Warner. 2005. Epidermal growth factor-induced rapid retinoblastoma phosphorylation at Ser780 and Ser795 is mediated by ERK1/2 in small intestine epithelial cells. *The Journal of biological chemistry* 280:35992-35998.

529. Garnovskaya, M. N., Y. V. Mukhin, T. M. Vlasova, J. S. Grewal, M. E. Ullian, B. G. Tholanikunnel, and J. R. Raymond. 2004. Mitogen-induced rapid phosphorylation of serine 795 of the retinoblastoma gene product in vascular smooth muscle cells involves ERK activation. *The Journal of biological chemistry* 279:24899-24905.

530. Kitagawa, M., H. Higashi, H. K. Jung, I. Suzuki-Takahashi, M. Ikeda, K. Tamai, J. Kato, K. Segawa, E. Yoshida, S. Nishimura, and Y. Taya. 1996. The consensus motif for phosphorylation by cyclin D1-Cdk4 is different from that for phosphorylation by cyclin A/E-Cdk2. *The EMBO journal* 15:7060-7069.

531. Avni, D., H. Yang, F. Martelli, F. Hofmann, W. M. ElShamy, S. Ganesan, R. Scully, and D. M. Livingston. 2003. Active localization of the retinoblastoma protein in chromatin and its response to S phase DNA damage. *Mol Cell* 12:735-746.

532. DeCaprio, J. A., Y. Furukawa, F. Ajchenbaum, J. D. Griffin, and D. M. Livingston. 1992. The retinoblastoma-susceptibility gene product becomes phosphorylated in multiple stages during cell cycle entry and progression. *Proceedings of the National Academy of Sciences of the United States of America* 89:1795-1798.

533. Mittnacht, S., H. Paterson, M. F. Olson, and C. J. Marshall. 1997. Ras signalling is required for inactivation of the tumour suppressor pRb cell-cycle control protein. *Curr Biol* 7:219-221.

534. Mihara, K., X. R. Cao, A. Yen, S. Chandler, B. Driscoll, A. L. Murphree, A. T'Ang, and Y. K. Fung. 1989. Cell cycle-dependent regulation of phosphorylation of the human retinoblastoma gene product. *Science (New York, N.Y* 246:1300-1303.

535. Chen, P. L., P. Scully, J. Y. Shew, J. Y. Wang, and W. H. Lee. 1989. Phosphorylation of the retinoblastoma gene product is modulated during the cell cycle and cellular differentiation. *Cell* 58:1193-1198.

536. Chao, R., W. Khan, and Y. A. Hannun. 1992. Retinoblastoma protein dephosphorylation induced by D-erythro-sphingosine. *The Journal of biological chemistry* 267:23459-23462.

537. Takemura, M., T. Yamamoto, M. Kitagawa, Y. Taya, T. Akiyama, H. Asahara, S. Linn, S. Suzuki, K. Tamai, and S. Yoshida. 2001. Stimulation of DNA polymerase alpha activity by cdk2-phosphorylated Rb protein. *Biochemical and biophysical research communications* 282:984-990.

538. Li, L., Y. Iwamoto, A. Berezovskaya, and V. A. Boussiotis. 2006. A pathway regulated by cell cycle inhibitor p27Kip1 and checkpoint inhibitor Smad3 is involved in the induction of T cell tolerance. *Nature immunology* 7:1157-1165.

539. Nel, A. E., and N. Slaughter. 2002. T-cell activation through the antigen receptor. Part 2: role of signaling cascades in T-cell differentiation, anergy, immune

senescence, and development of immunotherapy. *J Allergy Clin Immunol* 109:901-915.

540. Schwartz, R. H. 2003. T cell anergy. *Annu Rev Immunol* 21.

541. Colombetti, S., F. Benigni, V. Basso, and A. Mondino. 2002. Clonal anergy is maintained independently of T cell proliferation. *J Immunol* 169.

542. DeSilva, D. R., E. A. Jones, M. F. Favata, B. D. Jaffee, R. L. Magolda, J. M. Trzaskos, and P. A. Scherle. 1998. Inhibition of mitogen-activated protein kinase kinase blocks T cell proliferation but does not induce or prevent anergy. *J Immunol* 160.

543. Lee, I. H., W. P. Li, K. B. Hisert, and L. B. Ivashkiv. 1999. Inhibition of interleukin 2 signaling and signal transducer and activator of transcription (STAT)5 activation during T cell receptor-mediated feedback inhibition of T cell expansion. *The Journal of experimental medicine* 190.

544. Boussiotis, V. A., G. J. Freeman, P. A. Taylor, A. Berezovskaya, I. Grass, B. R. Blazar, and L. M. Nadler. 2000. p27kip1 functions as an anergy factor inhibiting interleukin 2 transcription and clonal expansion of alloreactive human and mouse helper T lymphocytes. *Nat Med* 6:290-297.

545. Jackson, S. K., A. DeLoose, and K. M. Gilbert. 2001. Induction of anergy in Th1 cells associated with increased levels of cyclin-dependent kinase inhibitors p21Cip1 and p27Kip1. *J Immunol* 166:952-958.

546. Mittnacht, S. 2005. The retinoblastoma protein--from bench to bedside. *Eur J Cell Biol* 84:97-107.

547. Jiao, W., J. Datta, H. M. Lin, M. Dundr, and S. G. Rane. 2006. Nucleocytoplasmic shuttling of the retinoblastoma tumor suppressor protein via Cdk phosphorylation-dependent nuclear export. *The Journal of biological chemistry* 281:38098-38108.

548. Blain, S. W., and J. Massague. 2002. Breast cancer banishes p27 from nucleus. *Nat Med* 8:1076-1078.

549. Davis, R. J. 1993. The mitogen-activated protein kinase signal transduction pathway. *The Journal of biological chemistry* 268.

550. Kaga, S., S. Ragg, K. A. Rogers, and A. Ochi. 1998. Stimulation of CD28 with B7-2 promotes focal adhesion-like cell contacts where Rho family small G proteins accumulate in T cells. *J Immunol* 160.

551. Valitutti, S., S. Muller, M. Salio, and A. Lanzavecchia. 1997. Degradation of T cell receptor (TCR)-CD3-zeta complexes after antigenic stimulation. *The Journal of experimental medicine* 185.

552. Yu, H., D. Leitenberg, B. Li, and R. A. Flavell. 2001. Deficiency of small GTPase Rac2 affects T cell activation. *The Journal of experimental medicine* 194:915-926.

553. Sechi, A. S., J. Buer, J. Wehland, and M. Probst-Kepper. 2002. Changes in actin dynamics at the T-cell/APC interface: implications for T-cell anergy? *Immunological reviews* 189:98-110.

554. Besson, A., M. Gurian-West, A. Schmidt, A. Hall, and J. M. Roberts. 2004. p27Kip1 modulates cell migration through the regulation of RhoA activation. *Genes & development* 18:862-876.

555. Ridley, A. J., M. A. Schwartz, K. Burridge, R. A. Firtel, M. H. Ginsberg, G. Borisy, J. T. Parsons, and A. R. Horwitz. 2003. Cell migration: integrating signals from front to back. *Science (New York, N.Y* 302:1704-1709.

556. Crean, J. K., F. Furlong, D. Mitchell, E. McArdle, C. Godson, and F. Martin. 2006. Connective tissue growth factor/CCN2 stimulates actin disassembly through Akt/protein kinase B-mediated phosphorylation and cytoplasmic translocation of p27(Kip-1). *Faseb J* 20:1712-1714.

557. Watson, N. F., L. G. Durrant, J. H. Scholefield, Z. Madjd, D. Scrimgeour, I. Spendlove, I. O. Ellis, and P. M. Patel. 2006. Cytoplasmic expression of p27(kip1) is associated with a favourable prognosis in colorectal cancer patients. *World J Gastroenterol* 12:6299-6304.

558. Mueller, D. L. 2004. E3 ubiquitin ligases as T cell anergy factors. *Nature immunology* 5:883-890.

559. Stork, P. J., and T. J. Dillon. 2005. Multiple roles of Rap1 in hematopoietic cells: complementary versus antagonistic functions. *Blood* 106:2952-2961.

560. Sebzda, E., M. Bracke, T. Tugal, N. Hogg, and D. A. Cantrell. 2002. Rap1A positively regulates T cells via integrin activation rather than inhibiting lymphocyte signaling. *Nature immunology* 3:251-258.

561. Delcroix, J. D., J. Valletta, C. Wu, C. L. Howe, C. F. Lai, J. D. Cooper, P. V. Belichenko, A. Salehi, and W. C. Mobley. 2004. Trafficking the NGF signal: implications for normal and degenerating neurons. *Progress in brain research* 146:3-23.

562. Iacovelli, L., L. Capobianco, L. Salvatore, M. Sallese, G. M. D'Ancona, and A. De Blasi. 2001. Thyrotropin activates mitogen-activated protein kinase pathway in FRTL-5 by a cAMP-dependent protein kinase A-independent mechanism. *Molecular pharmacology* 60:924-933.

563. Yamamoto, Y., K. A. Jones, B. C. Mak, A. Muehlenbachs, and R. S. Yeung. 2002. Multicompartmental distribution of the tuberous sclerosis gene products, hamartin and tuberin. *Archives of biochemistry and biophysics* 404:210-217.

564. Heissmeyer, V., F. Macian, S. H. Im, R. Varma, S. Feske, K. Venuprasad, H. Gu, Y. C. Liu, M. L. Dustin, and A. Rao. 2004. Calcineurin imposes T cell unresponsiveness through targeted proteolysis of signaling proteins. *Nature immunology* 5:255-265.

565. Ise, W., K. Nakamura, N. Shimizu, H. Goto, K. Fujimoto, S. Kaminogawa, and S. Hachimura. 2005. Orally tolerized T cells can form conjugates with APCs but are defective in immunological synapse formation. *J Immunol* 175:829-838.

566. Darzynkiewicz, Z., X. Li, and E. Bedner. 2001. Use of Flow and Laser-Scanning Cytometry in Analysis of Cell Death. In *Methods in Cell Biology*. Academic Press. 69-109.

567. Darzynkiewicz, Z., P. Smolewski, and E. Bedner. 2001. Use of flow and laser scanning cytometry to study mechanisms regulating cell cycle and controlling cell death. *Clin Lab Med* 21.

568. Deptala, A., X. Li, E. Bedner, W. Cheng, F. Traganos, and Z. Darzynkiewicz. 1999. Differences in induction of p53, p21WAF1 and apoptosis in relation to cell cycle phase of MCF-7 cells treated with camptothecin. *Int J Oncol* 15.

569. Pape, K. A., E. R. Kearney, A. Khoruts, A. Mondino, R. Merica, Z. M. Chen, E. Ingulli, J. White, J. G. Johnson, and M. K. Jenkins. 1997. Use of adoptive transfer of T-cell-antigen-receptor-transgenic T cell for the study of T-cell activation in vivo. *Immunological reviews* 156.

570. Mowat, A. M. 1999. Basic mechanisms and clinical implications of oral tolerance. *Current opinion in gastroenterology* 15:546-556.

571. Carey, K. D., R. T. Watson, J. E. Pessin, and P. J. Stork. 2003. The requirement of specific membrane domains for Raf-1 phosphorylation and activation. *The Journal of biological chemistry* 278:3185-3196.

572. Cook, S. J., B. Rubinfeld, I. Albert, and F. McCormick. 1993. RapV12 antagonizes Ras-dependent activation of ERK1 and ERK2 by LPA and EGF in Rat-1 fibroblasts. *The EMBO journal* 12:3475-3485.

573. Schmitt, J. M., and P. J. Stork. 2001. Cyclic AMP-mediated inhibition of cell growth requires the small G protein Rap1. *Molecular and cellular biology* 21:3671-3683.

574. Takagi, J., and T. A. Springer. 2002. Integrin activation and structural rearrangement. *Immunological reviews* 186:141-163.

575. Hogg, N., R. Henderson, B. Leitinger, A. McDowall, J. Porter, and P. Stanley. 2002. Mechanisms contributing to the activity of integrins on leukocytes. *Immunological reviews* 186:164-171.

576. Katagiri, K., M. Hattori, N. Minato, S. Irie, K. Takatsu, and T. Kinashi. 2000. Rap1 is a potent activation signal for leukocyte function-associated antigen 1 distinct from protein kinase C and phosphatidylinositol-3-OH kinase. *Molecular and cellular biology* 20:1956-1969.

577. Reedquist, K. A., E. Ross, E. A. Koop, R. M. Wolthuis, F. J. Zwartkruis, Y. van Kooyk, M. Salmon, C. D. Buckley, and J. L. Bos. 2000. The small GTPase, Rap1, mediates CD31-induced integrin adhesion. *The Journal of cell biology* 148:1151-1158.

578. Duchniewicz, M., T. Zemojtel, M. Kolanczyk, S. Grossmann, J. S. Scheele, and F. J. Zwartkruis. 2006. Rap1A-deficient T and B cells show impaired integrin-mediated cell adhesion. *Molecular and cellular biology* 26:643-653.

579. Katagiri, K., M. Hattori, N. Minato, and T. Kinashi. 2002. Rap1 functions as a key regulator of T-cell and antigen-presenting cell interactions and modulates T-cell responses. *Molecular and cellular biology* 22:1001-1015.

580. Li, L., R. J. Greenwald, E. M. Lafuente, D. Tzachanis, A. Berezovskaya, G. J. Freeman, A. H. Sharpe, and V. A. Boussiotis. 2005. Rap1-GTP is a negative regulator of Th cell function and promotes the generation of CD4+CD103+ regulatory T cells in vivo. *J Immunol* 175:3133-3139.

581. Li, L., W. R. Godfrey, S. B. Porter, Y. Ge, C. H. June, B. R. Blazar, and V. A. Boussiotis. 2005. CD4+CD25+ regulatory T-cell lines from human cord blood have functional and molecular properties of T-cell anergy. *Blood* 106:3068-3073.

582. Fathman, C. G., and N. B. Lineberry. 2007. Molecular mechanisms of CD4+ T-cell anergy. *Nat Rev Immunol* 7:599-609.

583. Hayashi, R. J., D. Y. Loh, O. Kanagawa, and F. Wang. 1998. Differences between responses of naive and activated T cells to anergy induction. *J Immunol* 160:33-38.

584. Peterson, E. J., M. L. Woods, S. A. Dmowski, G. Derimanov, M. S. Jordan, J. N. Wu, P. S. Myung, Q. H. Liu, J. T. Pribila, B. D. Freedman, Y. Shimizu, and G. A. Koretzky. 2001. Coupling of the TCR to integrin activation by Slap-130/Fyb. *Science (New York, N.Y* 293:2263-2265.

585. Griffiths, E. K., C. Krawczyk, Y. Y. Kong, M. Raab, S. J. Hyduk, D. Bouchard, V. S. Chan, I. Kozieradzki, A. J. Oliveira-Dos-Santos, A. Wakeham, P. S. Ohashi, M. I. Cybulsky, C. E. Rudd, and J. M. Penninger. 2001. Positive regulation of T cell activation and integrin adhesion by the adapter Fyb/Slap. *Science (New York, N.Y* 293:2260-2263.

586. Wang, H., F. E. McCann, J. D. Gordan, X. Wu, M. Raab, T. H. Malik, D. M. Davis, and C. E. Rudd. 2004. ADAP-SLP-76 binding differentially regulates supramolecular activation cluster (SMAC) formation relative to T cell-APC conjugation. *The Journal of experimental medicine* 200:1063-1074.

587. Jin, T. G., T. Satoh, Y. Liao, C. Song, X. Gao, K. Kariya, C. D. Hu, and T. Kataoka. 2001. Role of the CDC25 homology domain of phospholipase Cepsilon in amplification of Rap1-dependent signaling. *The Journal of biological chemistry* 276:30301-30307.

588. Mochizuki, N., S. Yamashita, K. Kurokawa, Y. Ohba, T. Nagai, A. Miyawaki, and M. Matsuda. 2001. Spatio-temporal images of growth-factor-induced activation of Ras and Rap1. *Nature* 411:1065-1068.

589. McLeod, S. J., R. J. Ingham, J. L. Bos, T. Kurosaki, and M. R. Gold. 1998. Activation of the Rap1 GTPase by the B cell antigen receptor. *The Journal of biological chemistry* 273:29218-29223.

590. McLeod, S. J., and M. R. Gold. 2001. Activation and function of the Rap1 GTPase in B lymphocytes. *International reviews of immunology* 20:763-789.

591. Kitayama, H., T. Matsuzaki, Y. Ikawa, and M. Noda. 1990. Genetic analysis of the Kirsten-ras-revertant 1 gene: potentiation of its tumor suppressor activity by specific point mutations. *Proceedings of the National Academy of Sciences of the United States of America* 87:4284-4288.

592. Brinkmann, T., O. Daumke, U. Herbrand, D. Kuhlmann, P. Stege, M. R. Ahmadian, and A. Wittinghofer. 2002. Rap-specific GTPase activating protein follows an alternative mechanism. *The Journal of biological chemistry* 277:12525-12531.

593. Filipp, D., and M. Julius. 2004. Lipid rafts: resolution of the "fyn problem"? *Molecular immunology* 41:645-656.

594. Thomas, S., R. Kumar, A. Preda-Pais, S. Casares, and T. D. Brumeanu. 2003. A model for antigen-specific T-cell anergy: displacement of CD4-p56(lck) signalosome from the lipid rafts by a soluble, dimeric peptide-MHC class II chimera. *J Immunol* 170:5981-5992.

595. Bi, K., Y. Tanaka, N. Coudronniere, K. Sugie, S. Hong, M. J. van Stipdonk, and A. Altman. 2001. Antigen-induced translocation of PKC-theta to membrane rafts is required for T cell activation. *Nature immunology* 2:556-563.

596. Yasuda, K., M. Nagafuku, T. Shima, M. Okada, T. Yagi, T. Yamada, Y. Minaki, A. Kato, S. Tani-Ichi, T. Hamaoka, and A. Kosugi. 2002. Cutting edge: Fyn is essential for tyrosine phosphorylation of Csk-binding protein/phosphoprotein associated with glycolipid-enriched microdomains in lipid rafts in resting T cells. *J Immunol* 169:2813-2817.

597. Shimada, Y., M. Inomata, H. Suzuki, M. Hayashi, A. Abdul Waheed, and Y. Ohno-Iwashita. 2005. Separation of a cholesterol-enriched microdomain involved in T-cell signal transduction. *The FEBS journal* 272:5454-5463.

598. Gajewski, T. F., P. Fields, and F. W. Fitch. 1995. Induction of the increased Fyn kinase activity in anergic T helper type 1 clones requires calcium and protein synthesis and is sensitive to cyclosporin A. *European journal of immunology* 25:1836-1842.

599. Simons, K., and E. Ikonen. 1997. Functional rafts in cell membranes. *Nature* 387:569-572.

600. Anderson, R. G., and K. Jacobson. 2002. A role for lipid shells in targeting proteins to caveolae, rafts, and other lipid domains. *Science (New York, N.Y* 296:1821-1825.

601. Baumgart, T., S. T. Hess, and W. W. Webb. 2003. Imaging coexisting fluid domains in biomembrane models coupling curvature and line tension. *Nature* 425:821-824.

602. Hao, M., S. Mukherjee, and F. R. Maxfield. 2001. Cholesterol depletion induces large scale domain segregation in living cell membranes. *Proceedings of the National Academy of Sciences of the United States of America* 98:13072-13077.

603. Mayor, S., K. G. Rothberg, and F. R. Maxfield. 1994. Sequestration of GPI-anchored proteins in caveolae triggered by cross-linking. *Science (New York, N.Y* 264:1948-1951.

604. Yethiraj, A., and J. C. Weisshaar. 2007. Why are lipid rafts not observed in vivo? *Biophys J.*

605. Knudsen, E. S., and J. Y. Wang. 1996. Differential regulation of retinoblastoma protein function by specific Cdk phosphorylation sites. *The Journal of biological chemistry* 271:8313-8320.

606. Zinselmeyer, B. H., J. Dempster, A. M. Gurney, D. Wokosin, M. Miller, H. Ho, O. R. Millington, K. M. Smith, C. M. Rush, I. Parker, M. Cahalan, J. M. Brewer, and P. Garside. 2005. In situ characterization of CD4+ T cell behavior in mucosal and systemic lymphoid tissues during the induction of oral priming and tolerance. *The Journal of experimental medicine* 201:1815-1823.

607. Itoh, R. E., K. Kurokawa, Y. Ohba, H. Yoshizaki, N. Mochizuki, and M. Matsuda. 2002. Activation of rac and cdc42 video imaged by fluorescent resonance energy transfer-based single-molecule probes in the membrane of living cells. *Molecular and cellular biology* 22:6582-6591.

608. Nakamura, T., K. Aoki, and M. Matsuda. 2005. Monitoring spatio-temporal regulation of Ras and Rho GTPase with GFP-based FRET probes. *Methods (San Diego, Calif* 37:146-153.

609. Fukano, T., A. Sawano, Y. Ohba, M. Matsuda, and A. Miyawaki. 2007. Differential Ras activation between caveolae/raft and non-raft microdomains. *Cell structure and function* 32:9-15.

Publications

1. Claire L. Adams, Natalie Kobets, Gordon R. Meiklejohn, Owain R. Millington, **Angela M. Grierson**, Catherine M. Rush, Karen M. Smith and Paul Garside. Tracking lymphocytes *in vivo.*
   Arch Immunol Ther Exp (Warsz). 2004 May-Jun;52(3):173-87 Review

2. Claire L. Adams, **Angela M. Grierson**, Allan McI Mowat, Margaret M. Harnett and Paul Garside. Differences in the Kinetics, Amplitude and Localisation of ERK Activation in Anergy and Priming Revealed at the Level of Individual Primary T cells by Laser Scanning Cytometry.
   J Immunol. 2004 Aug 1;173(3):1579-86

3. **Angela M. Grierson**, Paul Mitchell, Claire L. Adams, Allan McI Mowat, James M. Brewer, Margaret M. Harnett and Paul Garside. Direct quantitation of T-cell signalling by Laser Scanning Cytometry.
   Journal of Immunol Methods. 2005 Jun;301(1-2):140-53

4. Fraser A. Marshall, **Angela M. Grierson**, Paul Garside, William Harnett and Margaret M. Harnett. ES-62, an Immunomodulator Secreted by Filarial Nematodes, Suppresses Clonal Expansion and Modifies Effector Function of Heterologous Antigen-Specific T cells *In Vivo*.
   J Immunol. 2005 Nov 1 175(9): 5817-5826

5. **Angela M. Morton**, Barbara McManus, Paul Garside, Allan McI Mowat and Margaret M. Harnett. Analysing the role of Rap1 signalling in tolerance and priming of antigen-specific T cells at the single cell level *in vitro* and *in vivo*.
   J. Immunol. 2007 Dec 15; 179(12):8026-34

Figure 1.1

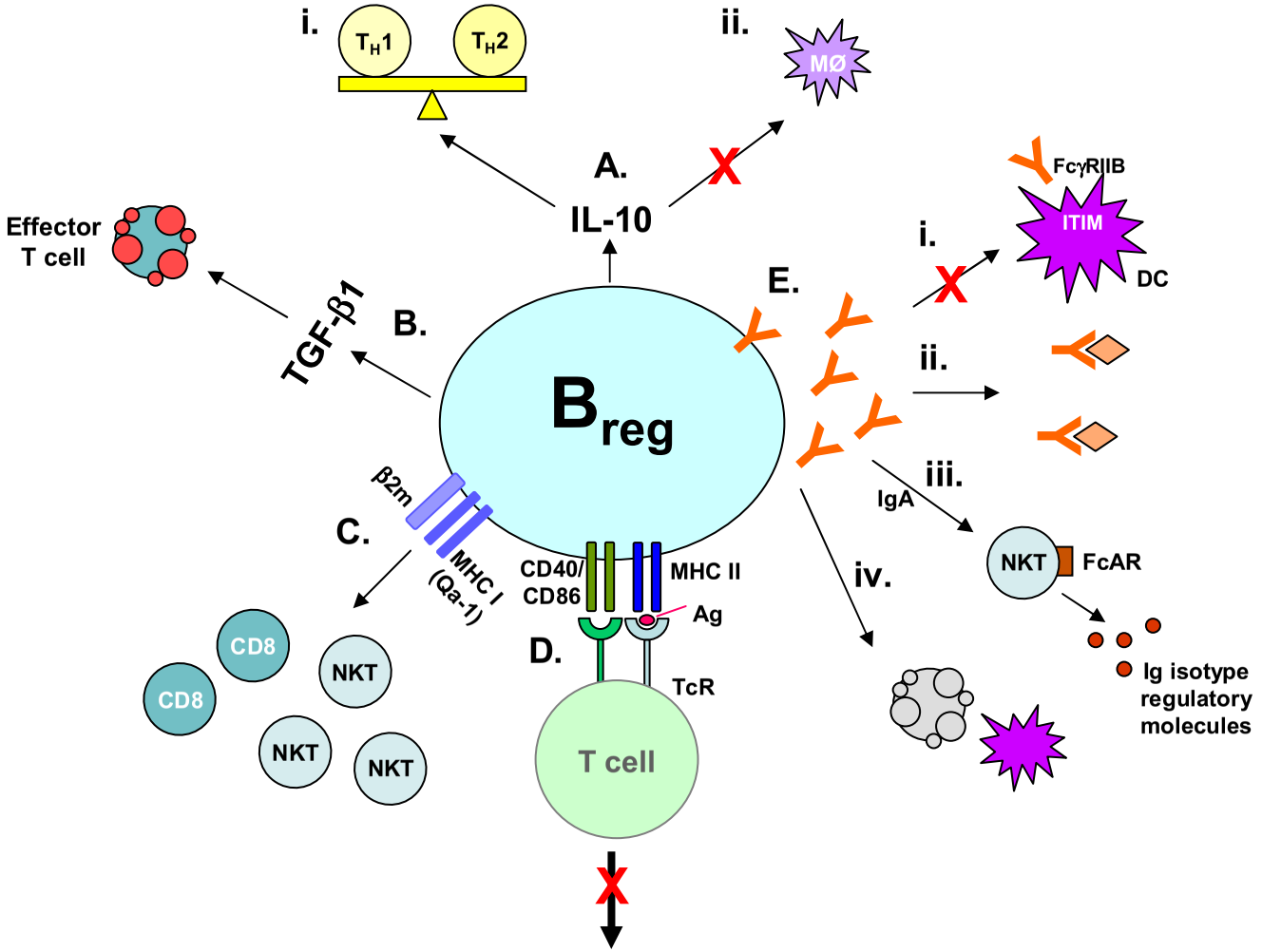
i.
T_H1
T_H2
ii.
MØ
A.
IL-10
X
Effector
T cell
TGF-β1
B.
B_{reg}
E.
i.
X
FcγRIIB
ITIM
DC
ii.
iii.
IgA
NKT
FcAR
Ig isotype
regulatory
molecules
iv.
β2m
C.
MHC I
(Qa-1)
CD40/
CD86
MHC II
Ag
D.
TcR
T cell
CD8
CD8
NKT
NKT
NKT
X

Figure 1.2

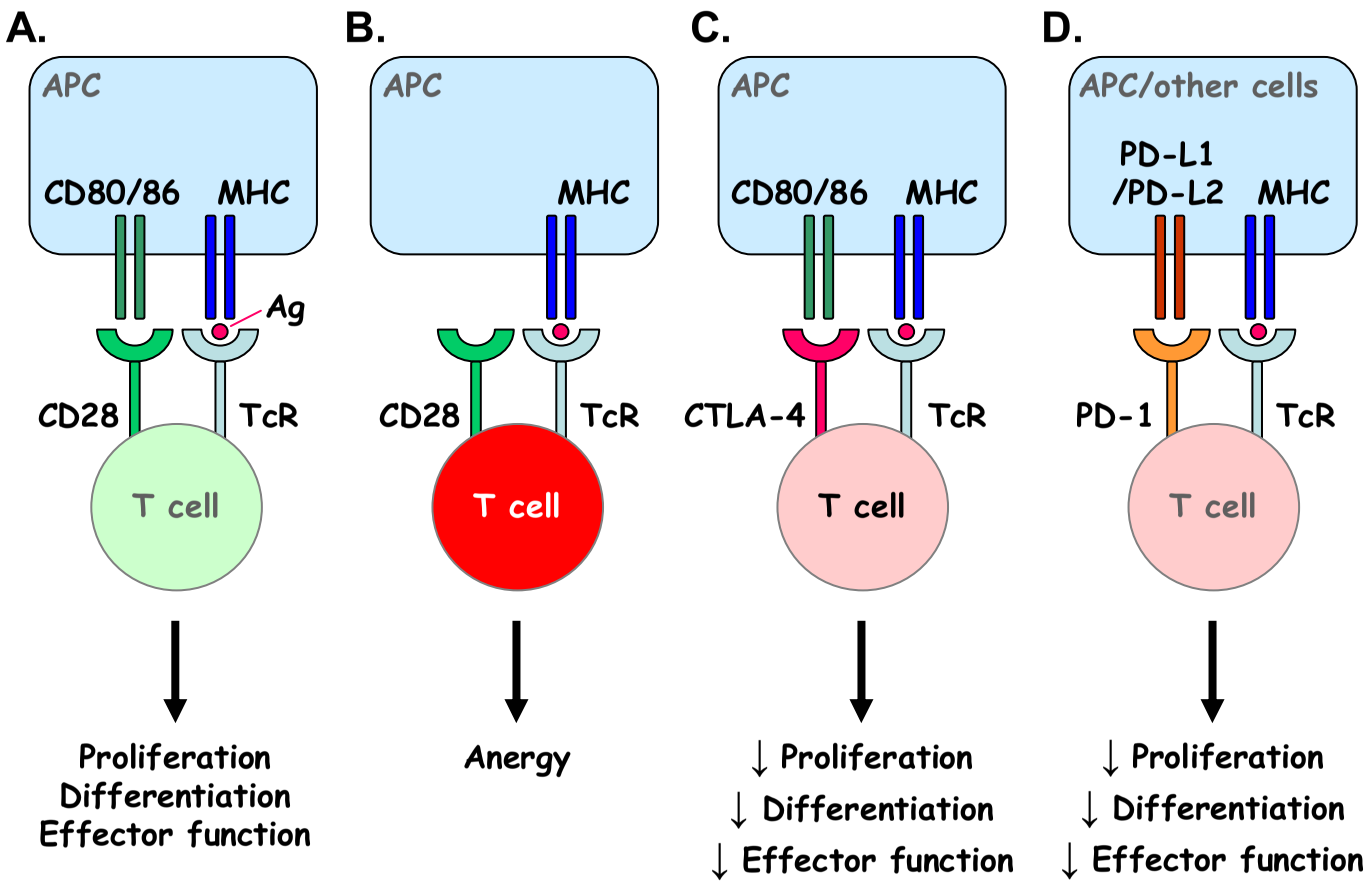
A.
APC
CD80/86
MHC
Ag
CD28
TcR
T cell
Proliferation
Differentiation
Effector function
B.
APC
MHC
CD28
TcR
T cell
Anergy
C.
APC
CD80/86
MHC
CTLA-4
TcR
T cell
↓ Proliferation
↓ Differentiation
↓ Effector function
D.
APC/other cells
PD-L1
/PD-L2
MHC
PD-1
TcR
T cell
↓ Proliferation
↓ Differentiation
↓ Effector function

Figure 1.3

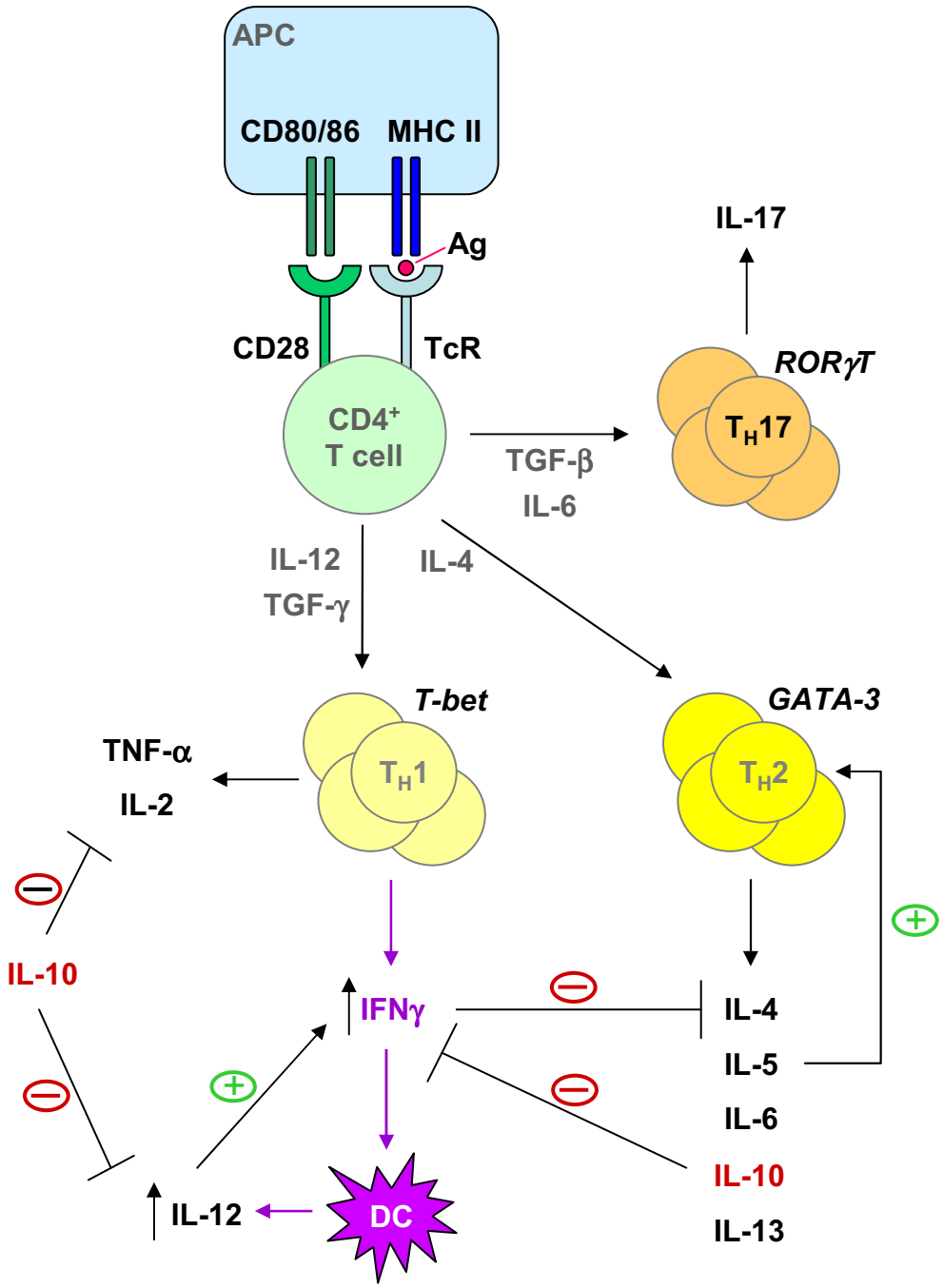
APC
CD80/86
MHC II
Ag
CD28
TcR
CD4+
T cell
TGF-β
IL-6
IL-17
RORγT
TH17
IL-12
TGF-γ
IL-4
T-bet
TH1
TNF-α
IL-2
GATA-3
TH2
IL-10
IFNγ
IL-4
IL-5
IL-6
IL-10
IL-13
IL-12
DC

	$CD4^+$ $CD25^+$ natural T_{regs}	Tr1 cells	T_H3 cells
Phenotype	$CD25^+$, $Foxp3^+$, $CD45RB^{lo}$, $CTLA\text{-}4^+$, $GITR^{+/-}$, $CD103^{+/-}$	$CD25^{+/-}$, Foxp3?	$CD25^{+/-}$, Foxp3?, $CTLA\text{-}4^+$
Specificity	Self-Ag in the thymus, Foreign Ag?	Tissue specific Ag Foreign Ag	Tissue specific Ag?
Site of induction	Thymus	Periphery	Periphery
Cytokines secreted	$IL10^{+/-}$, $TGF\text{-}\beta^{+/-}$	Predominantly IL-10	Predominantly TGF-β
Mechanism of suppression	Direct cell:cell contact, Secreted cytokines?	Secreted IL-10	Secreted TGF-β

Table 1.1. Characteristics of the different regulatory T cell classes

Figure 1.4

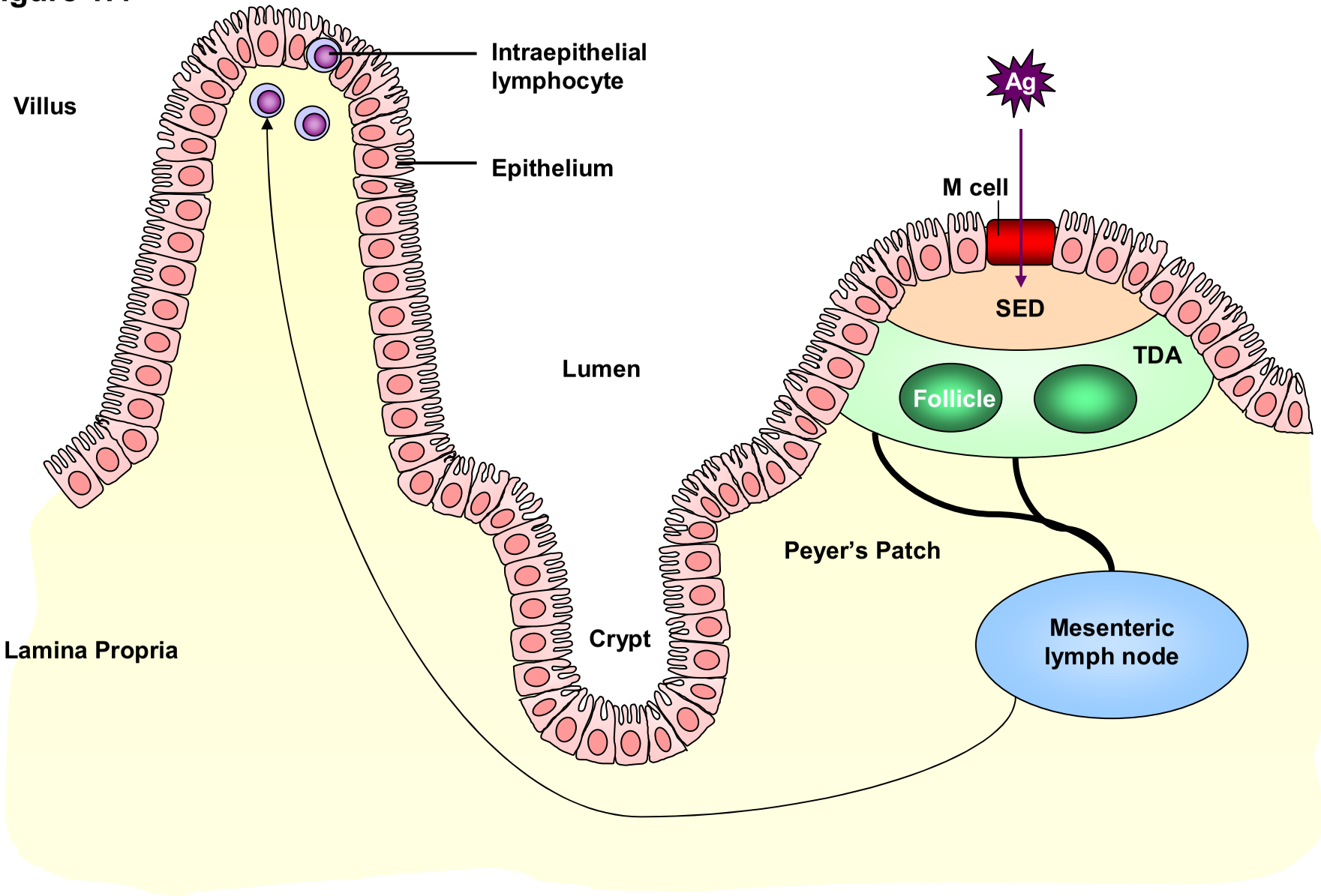
Intraepithelial lymphocyte
Villus
Epithelium
Ag
M cell
SED
TDA
Follicle
Lumen
Peyer's Patch
Crypt
Lamina Propria
Mesenteric lymph node

Figure 1.5

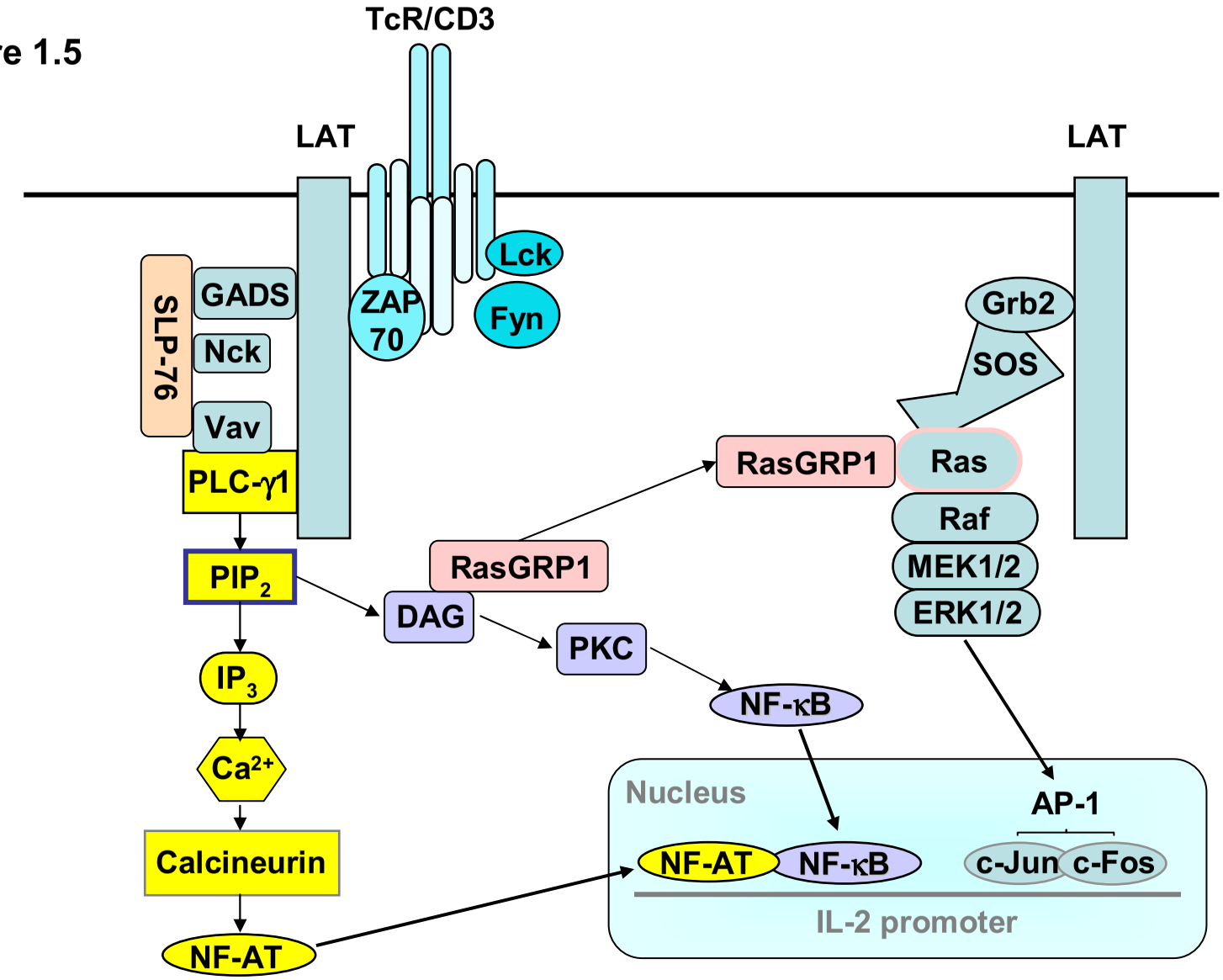
TcR/CD3
LAT
LAT
Lck
Fyn
ZAP 70
SLP-76
GADS
Nck
Vav
PLC-γ1
PIP2
IP3
Ca2+
Calcineurin
NF-AT
DAG
RasGRP1
RasGRP1
PKC
NF-κB
Grb2
SOS
Ras
Raf
MEK1/2
ERK1/2
Nucleus
AP-1
NF-AT
NF-κB
c-Jun
c-Fos
IL-2 promoter

Figure 1.6

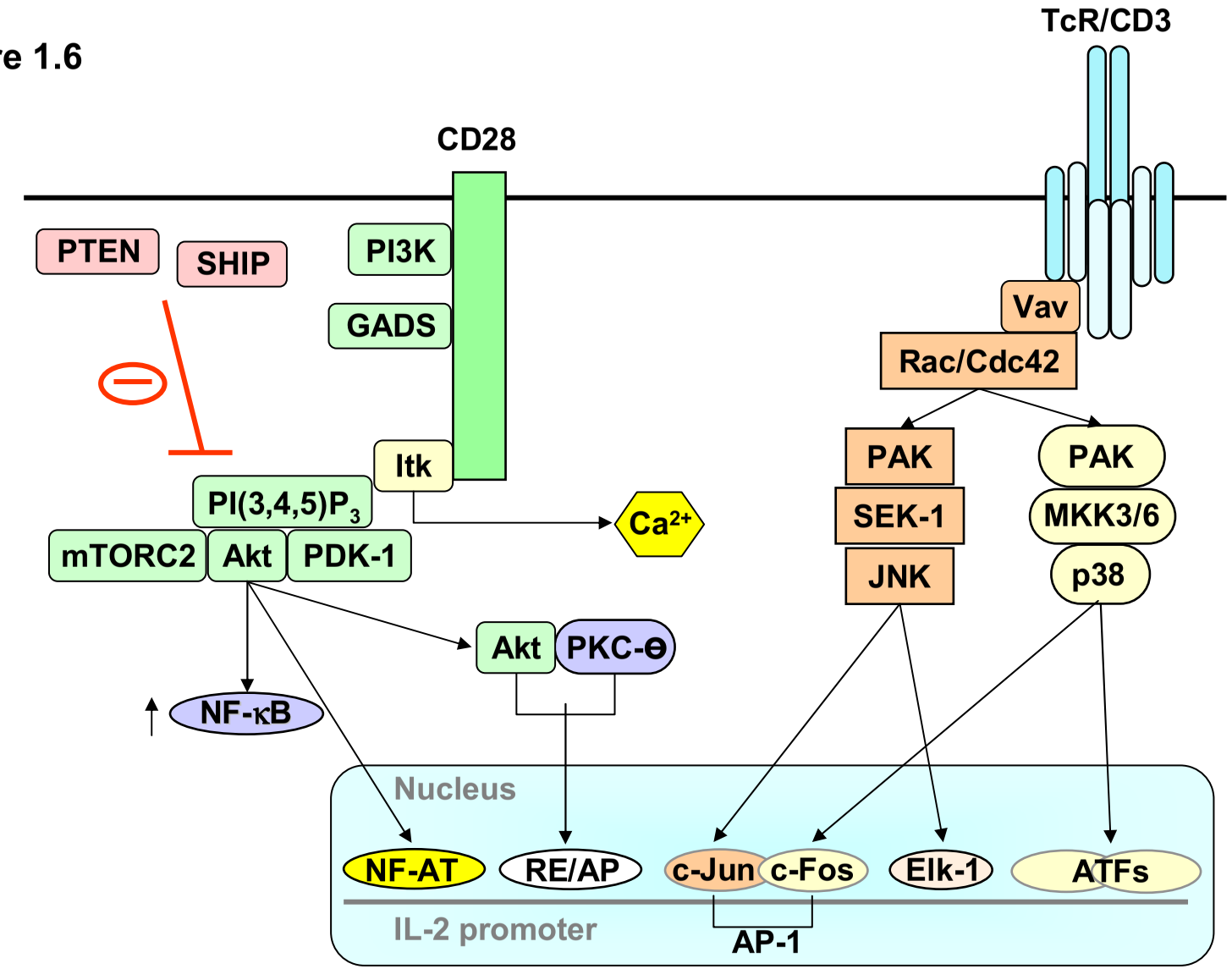
TcR/CD3
CD28
PTEN
SHIP
PI3K
GADS
Vav
Rac/Cdc42
PAK
SEK-1
JNK
PAK
MKK3/6
p38
Itk
PI(3,4,5)P3
Ca2+
mTORC2
Akt
PDK-1
Akt
PKC-θ
NF-κB
Nucleus
NF-AT
RE/AP
c-Jun
c-Fos
Elk-1
ATFs
IL-2 promoter
AP-1

Figure 1.7

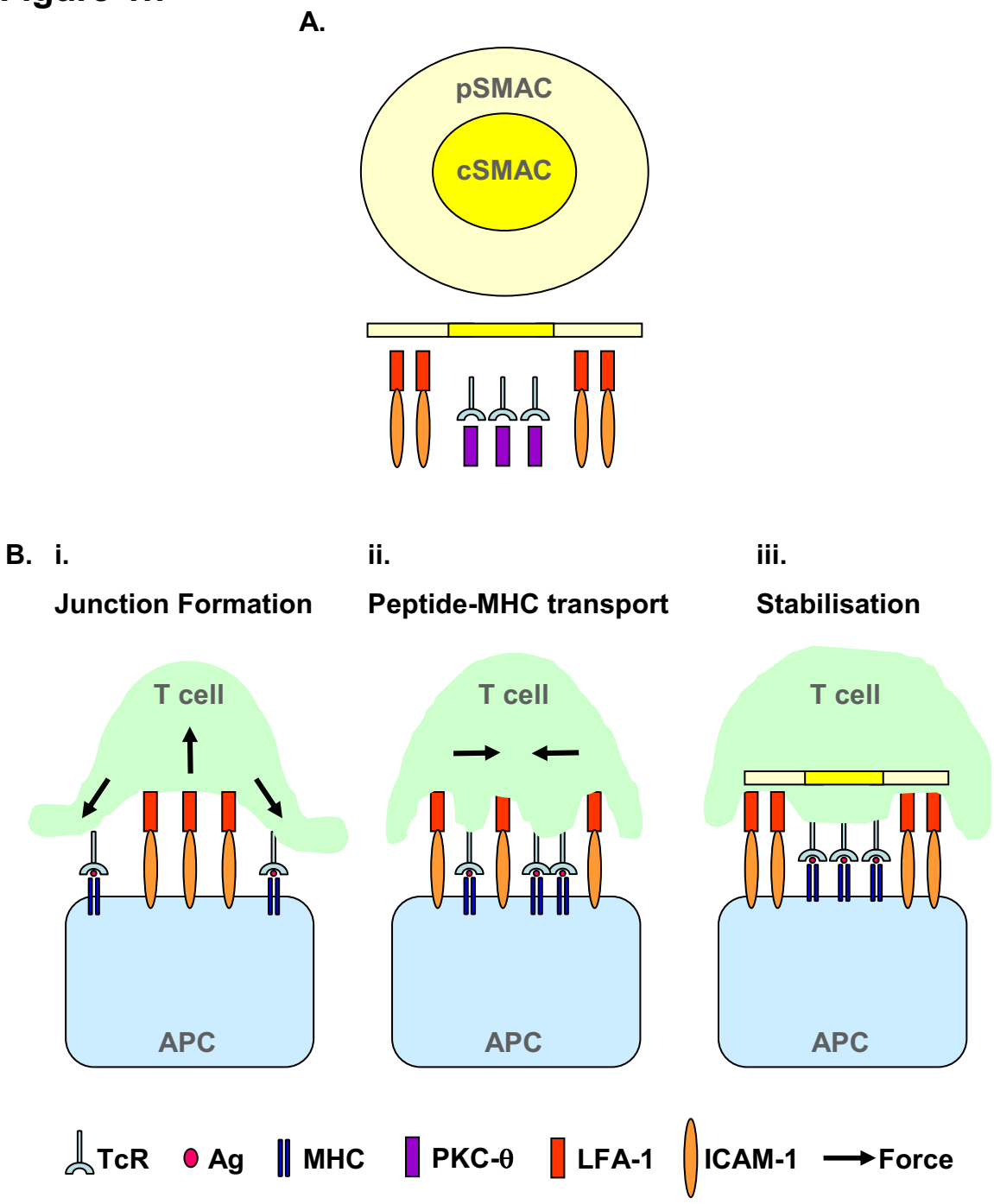
A.
pSMAC
cSMAC
B.
i.
Junction Formation
ii.
Peptide-MHC transport
iii.
Stabilisation
T cell
APC
T cell
APC
T cell
APC
TcR
Ag
MHC
PKC-θ
LFA-1
ICAM-1
Force

Figure 1.8

A.

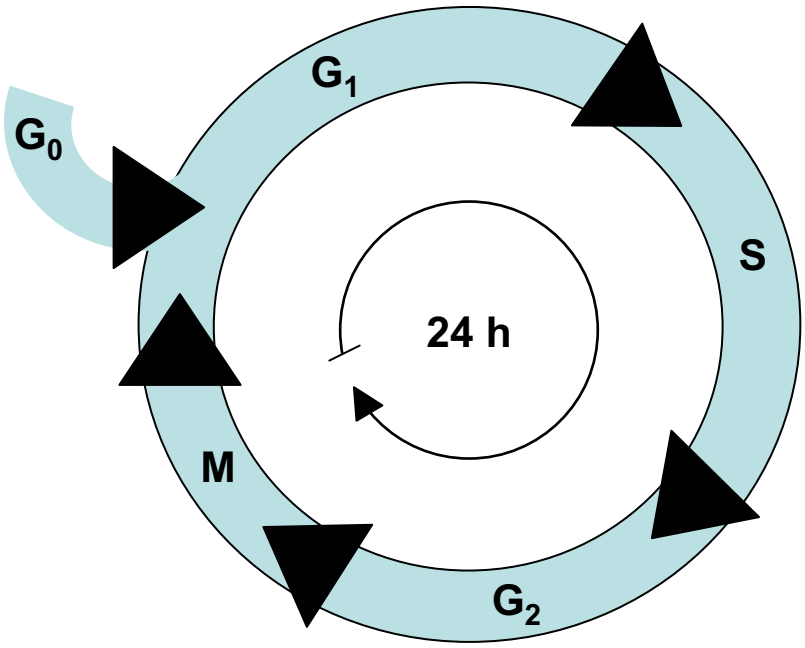
G1
G0
S
24 h
M
G2

B.

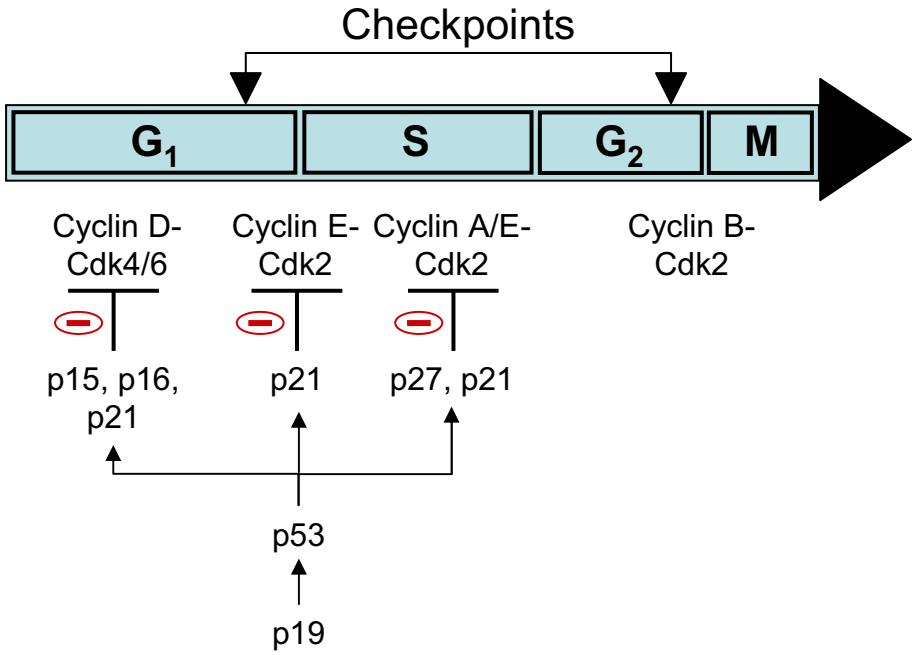
Checkpoints
G1
S
G2
M
Cyclin D-Cdk4/6
Cyclin E-Cdk2
Cyclin A/E-Cdk2
Cyclin B-Cdk2
p15, p16, p21
p21
p27, p21
p53
p19

Figure 1.9

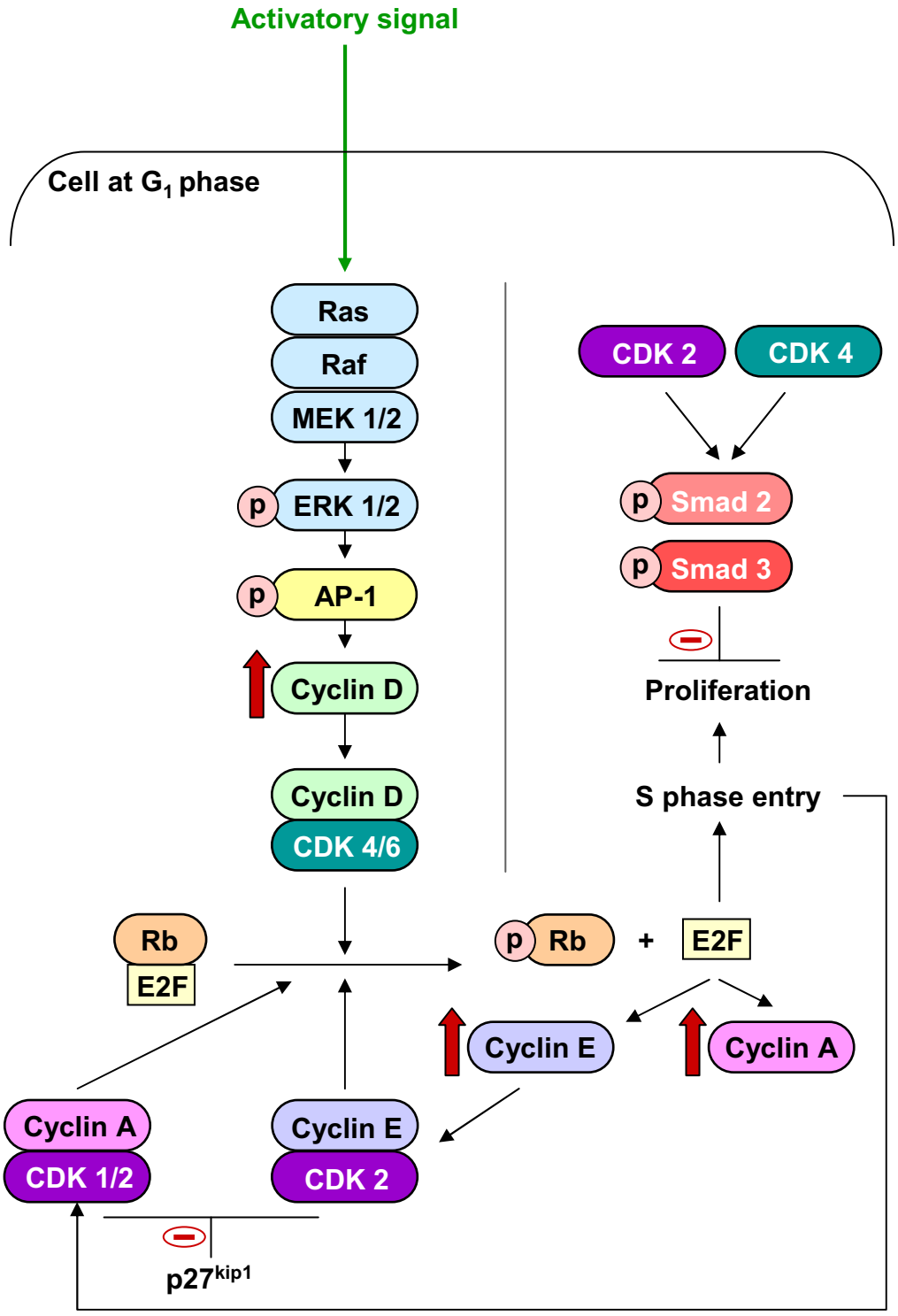
Activatory signal
Cell at G1 phase
Ras
Raf
MEK 1/2
p ERK 1/2
p AP-1
Cyclin D
Cyclin D
CDK 4/6
CDK 2
CDK 4
p Smad 2
p Smad 3
Proliferation
S phase entry
Rb
E2F
p Rb + E2F
Cyclin E
Cyclin A
Cyclin A
CDK 1/2
Cyclin E
CDK 2
p27kip1

Figure 1.10

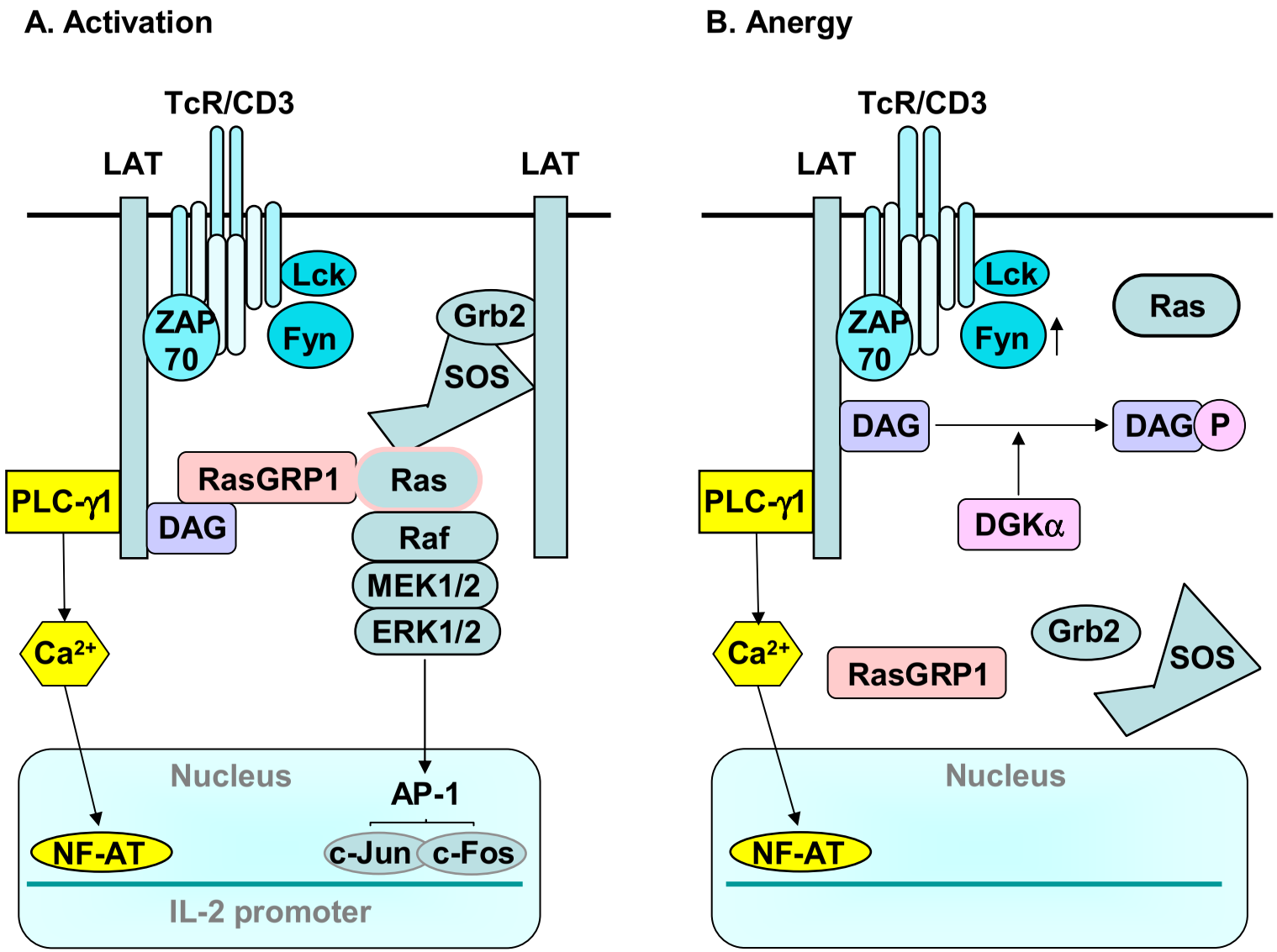
A. Activation
TcR/CD3
LAT
LAT
Lck
ZAP 70
Fyn
Grb2
SOS
RasGRP1
Ras
PLC-γ1
DAG
Raf
MEK1/2
ERK1/2
Ca2+
Nucleus
AP-1
NF-AT
c-Jun
c-Fos
IL-2 promoter
B. Anergy
TcR/CD3
LAT
Lck
ZAP 70
Fyn
Ras
DAG
DAG P
PLC-γ1
DGKα
Ca2+
RasGRP1
Grb2
SOS
Nucleus
NF-AT

Figure 1.11

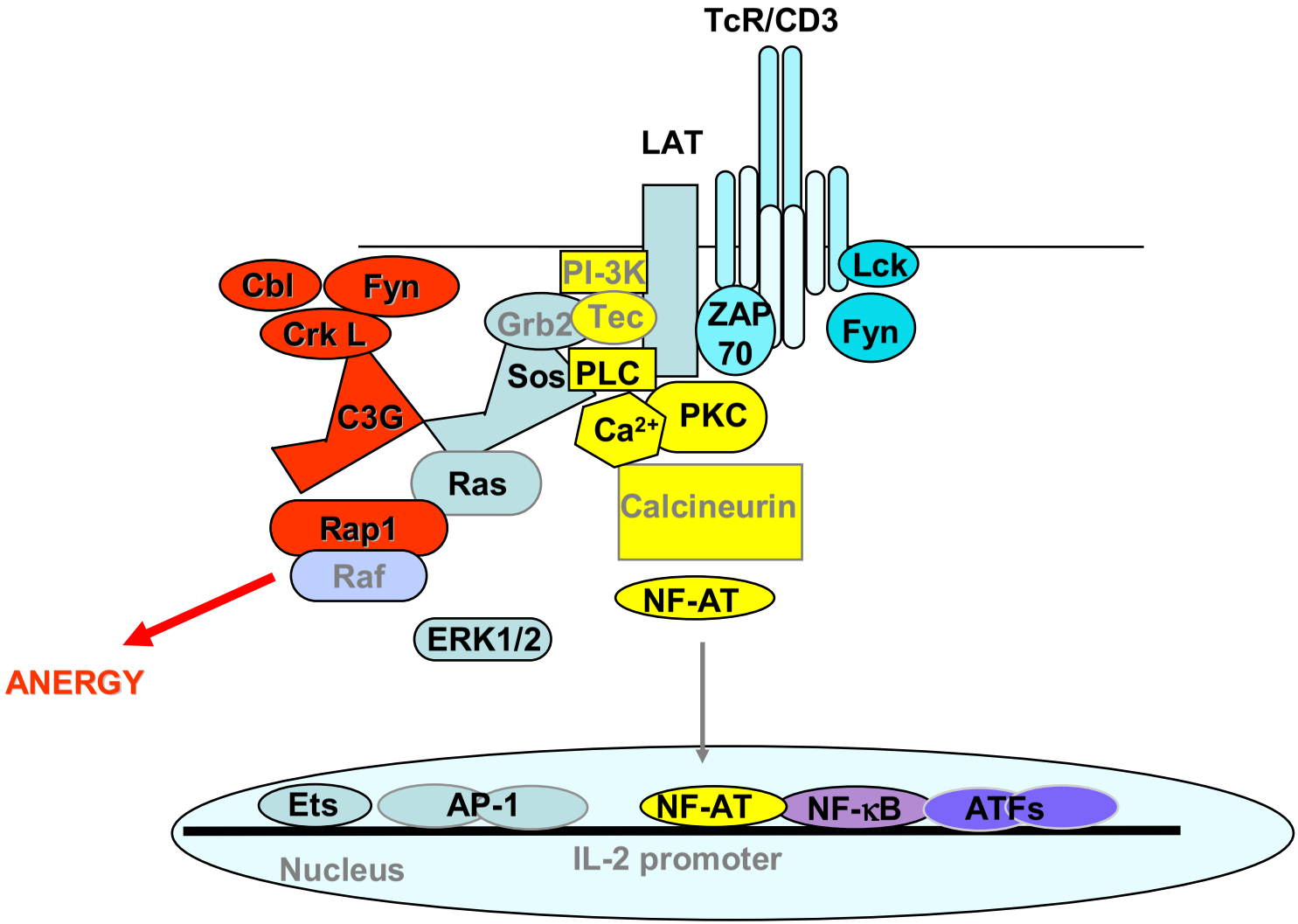
TcR/CD3
LAT
Lck
Fyn
ZAP 70
PI-3K
Tec
Grb2
Sos
PLC
Cbl
Fyn
Crk L
C3G
Ca2+
PKC
Ras
Calcineurin
Rap1
Raf
NF-AT
ERK1/2
ANERGY
Ets
AP-1
NF-AT
NF-κB
ATFs
Nucleus
IL-2 promoter

Figure 2.1

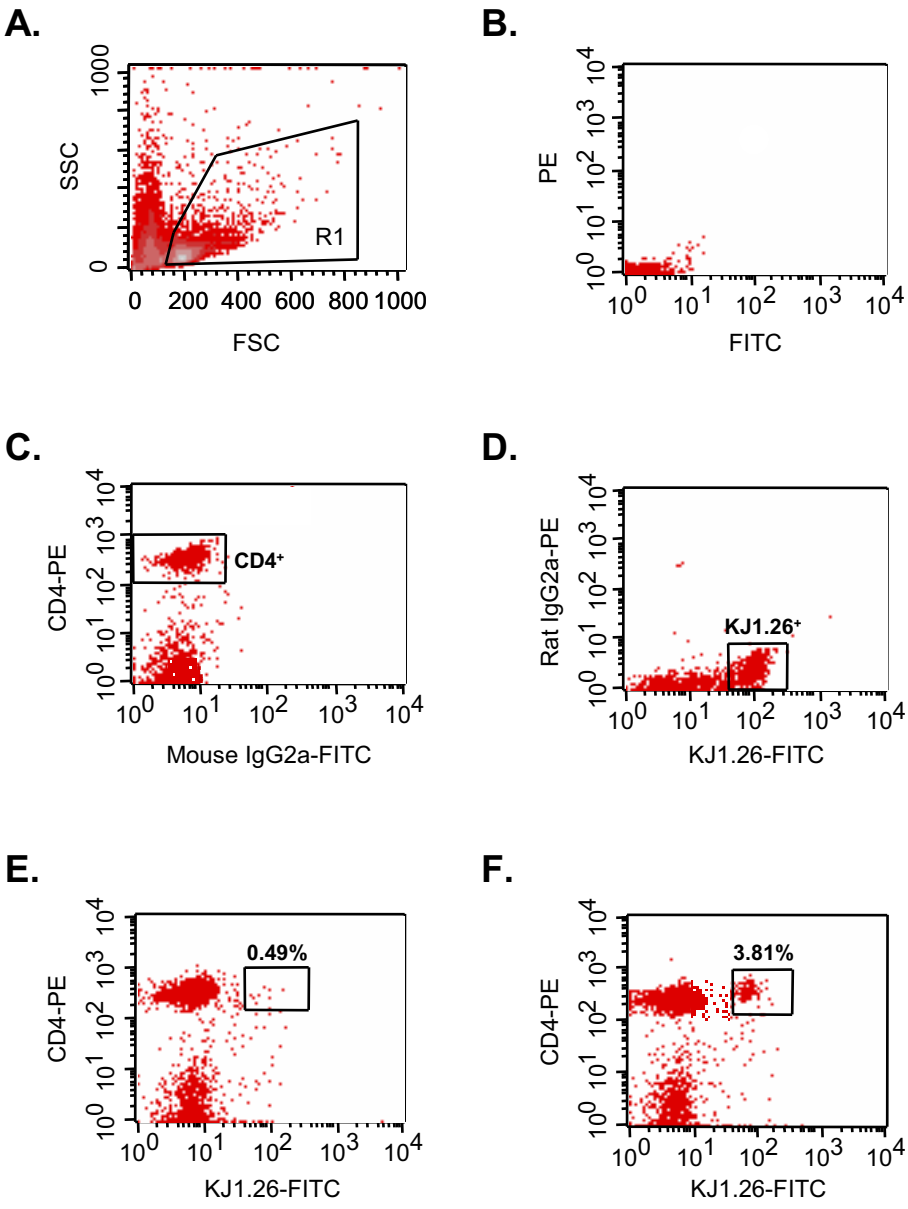
A.
SSC
1000
0
R1
0 200 400 600 800 1000
FSC
B.
PE
FITC
C.
CD4-PE
CD4+
Mouse IgG2a-FITC
D.
Rat IgG2a-PE
KJ1.26+
KJ1.26-FITC
E.
CD4-PE
0.49%
KJ1.26-FITC
F.
CD4-PE
3.81%
KJ1.26-FITC

Figure 2.2

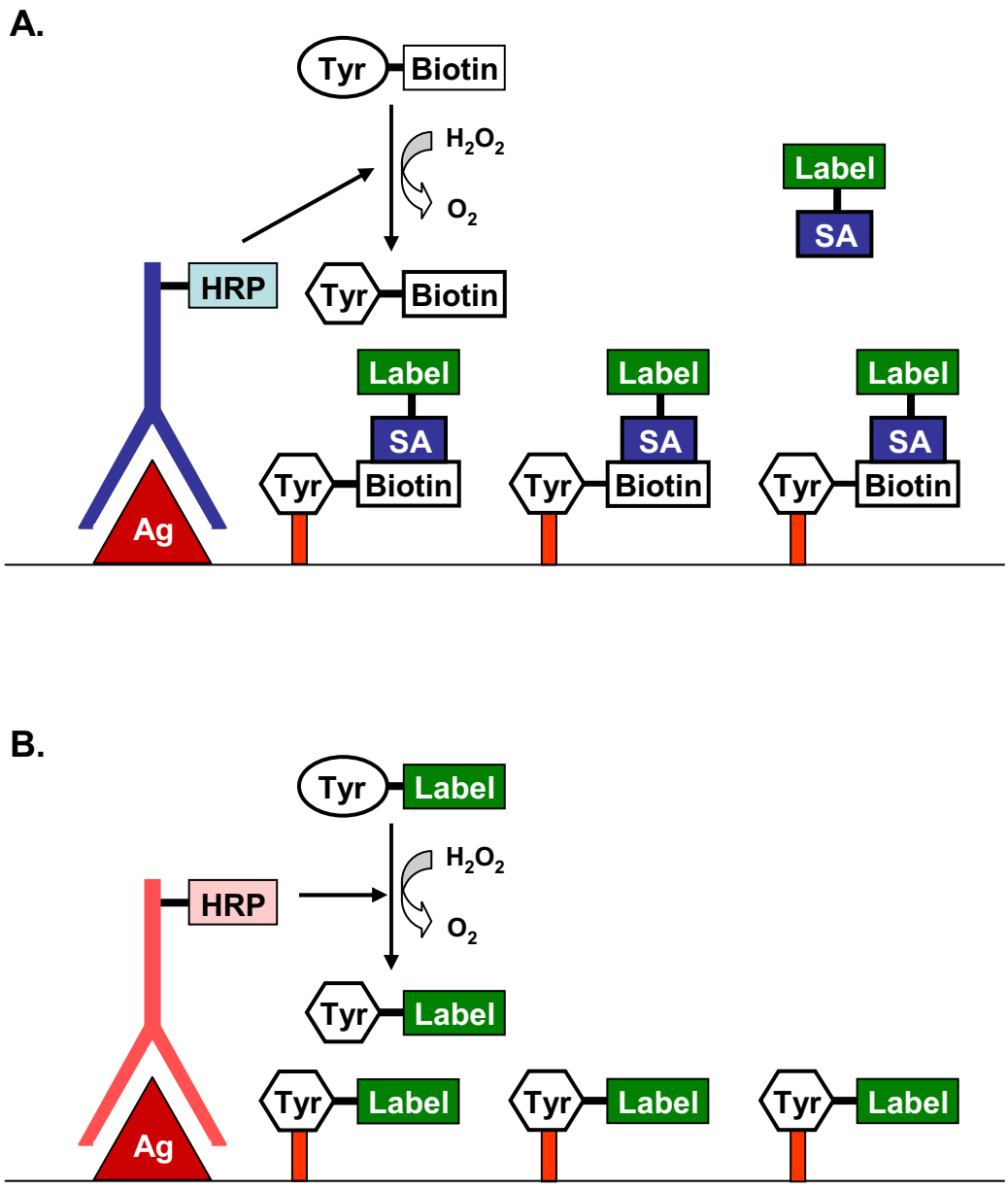
A.
Tyr
Biotin
H_2O_2
O_2
Label
SA
HRP
Tyr
Biotin
Label
SA
Tyr
Biotin
Label
SA
Tyr
Biotin
Label
SA
Tyr
Biotin
Ag
B.
Tyr
Label
H_2O_2
O_2
HRP
Tyr
Label
Tyr
Label
Tyr
Label
Tyr
Label
Ag

Figure 2.3

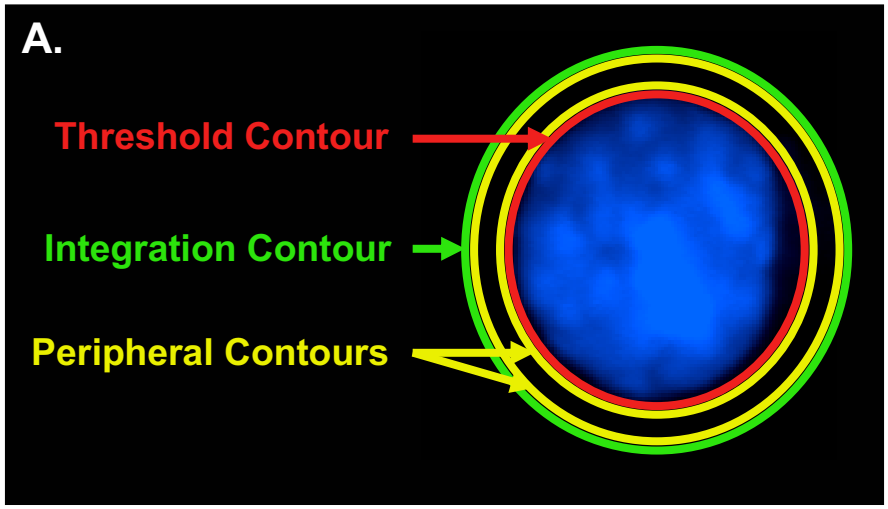
A.
Threshold Contour
Integration Contour
Peripheral Contours

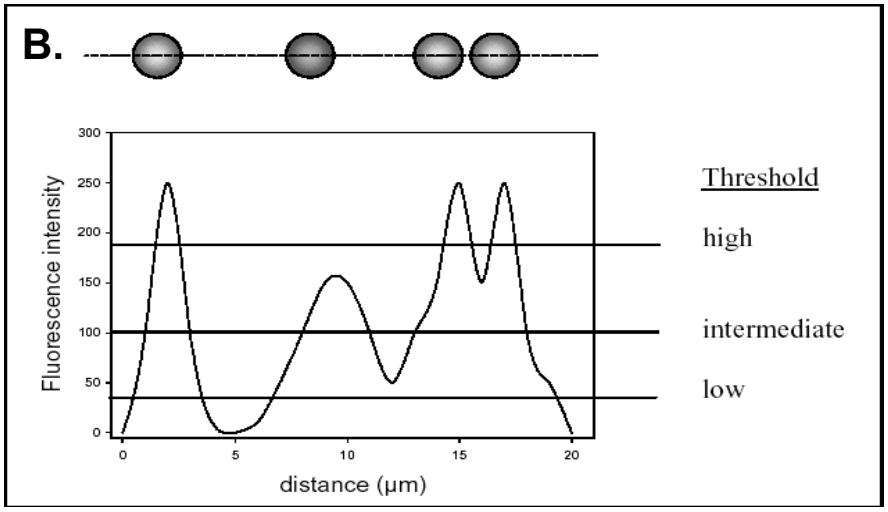
B.
Fluorescence intensity
300
250
200
150
100
50
0
0
5
10
15
20
distance (µm)
Threshold
high
intermediate
low

Figure 2.4

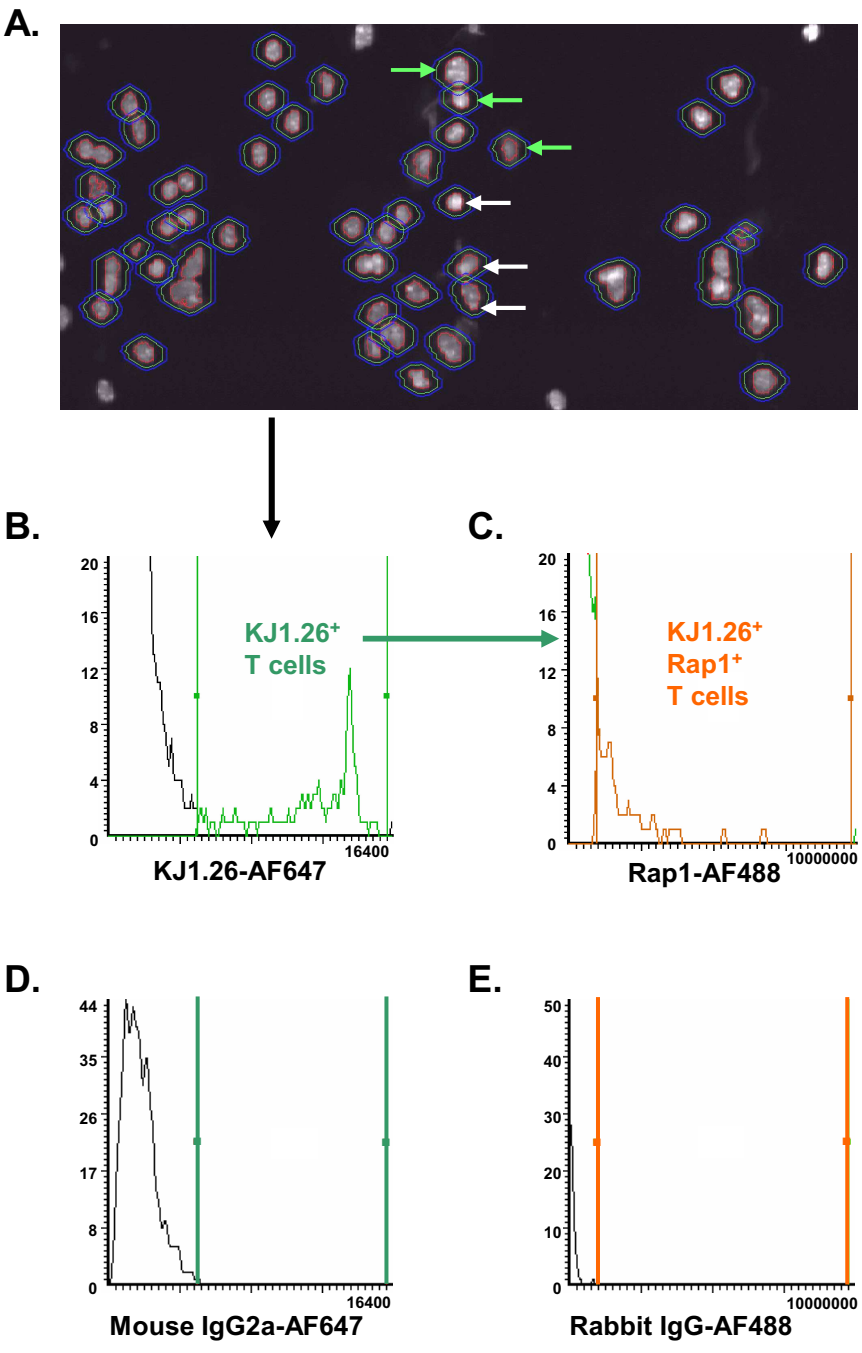
A.
B.
C.
KJ1.26+
T cells
KJ1.26+
Rap1+
T cells
20
16
12
8
4
0
16400
KJ1.26-AF647
10000000
Rap1-AF488
D.
E.
44
35
26
17
8
50
40
30
20
10
Mouse IgG2a-AF647
Rabbit IgG-AF488

Figure 2.5

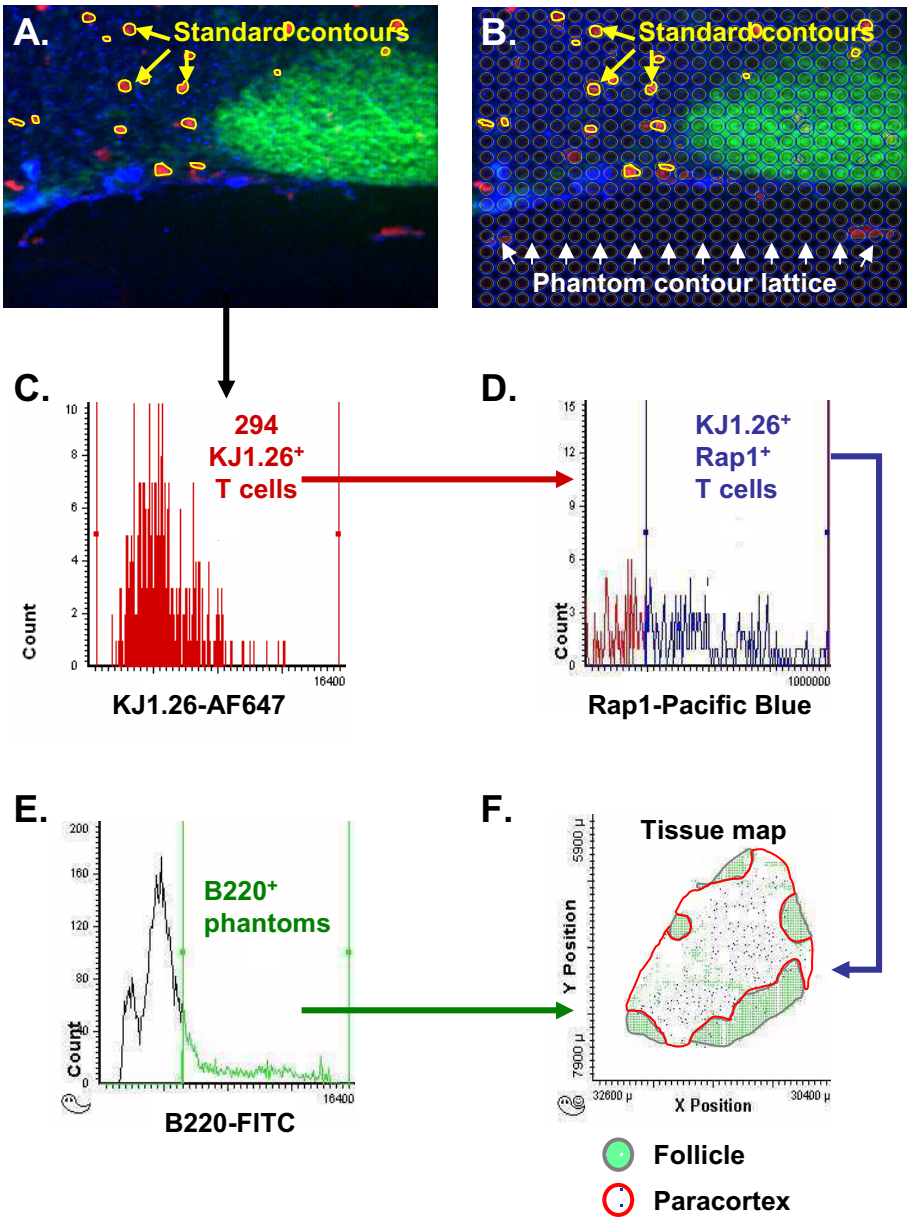
A.
Standard contours
B.
Standard contours
Phantom contour lattice
C.
294
KJ1.26+
T cells
Count
KJ1.26-AF647
D.
KJ1.26+
Rap1+
T cells
Count
Rap1-Pacific Blue
E.
B220+
phantoms
Count
B220-FITC
F.
Tissue map
Y Position
X Position
Follicle
Paracortex

Figure 2.6

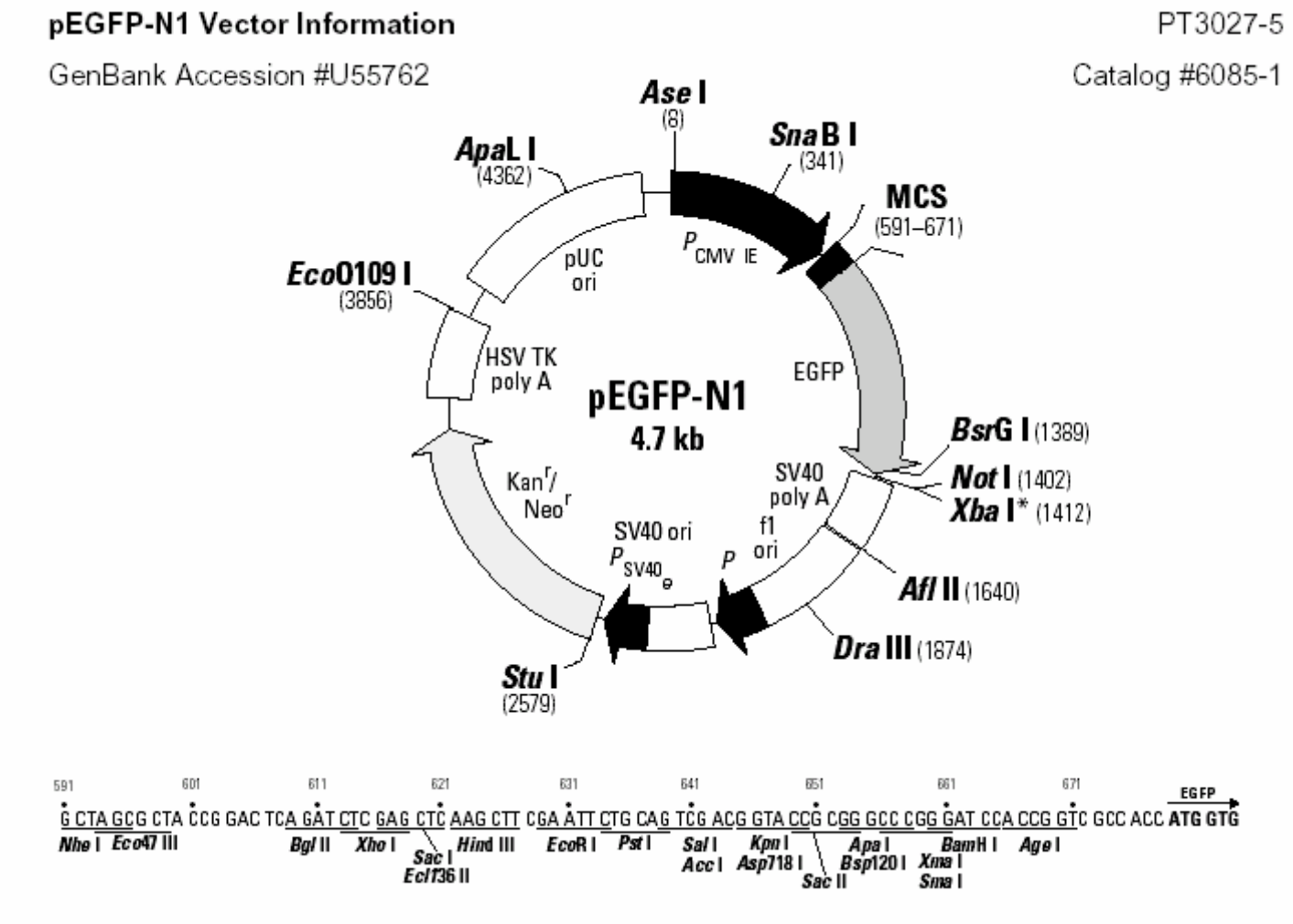
pEGFP-N1 Vector Information
PT3027-5
GenBank Accession #U55762
Catalog #6085-1
Ase I
(8)
Sna B I
(341)
ApaL I
(4362)
MCS
(591–671)
P CMV IE
pUC
ori
Eco0109 I
(3856)
HSV TK
poly A
EGFP
pEGFP-N1
4.7 kb
BsrG I (1389)
Not I (1402)
Xba I* (1412)
SV40
poly A
Kan r/
Neo r
f1
ori
SV40 ori
P SV40e
P
Afl II (1640)
Dra III (1874)
Stu I
(2579)
591
601
611
621
631
641
651
661
671
EGFP
G CTA GCG CTA CCG GAC TCA GAT CTC GAG CTC AAG CTT CGA ATT CTG CAG TCG ACG GTA CCG CGG GCC CGG GAT CCA CCG GTC GCC ACC ATG GTG
Nhe I Eco47 III
Bgl II
Xho I
Sac I
Ecl136 II
Hind III
EcoR I
Pst I
Sal I
Acc I
Kpn I
Asp718 I
Sac II
Apa I
Bsp120 I
BamH I
Xma I
Sma I
Age I

Figure 2.7

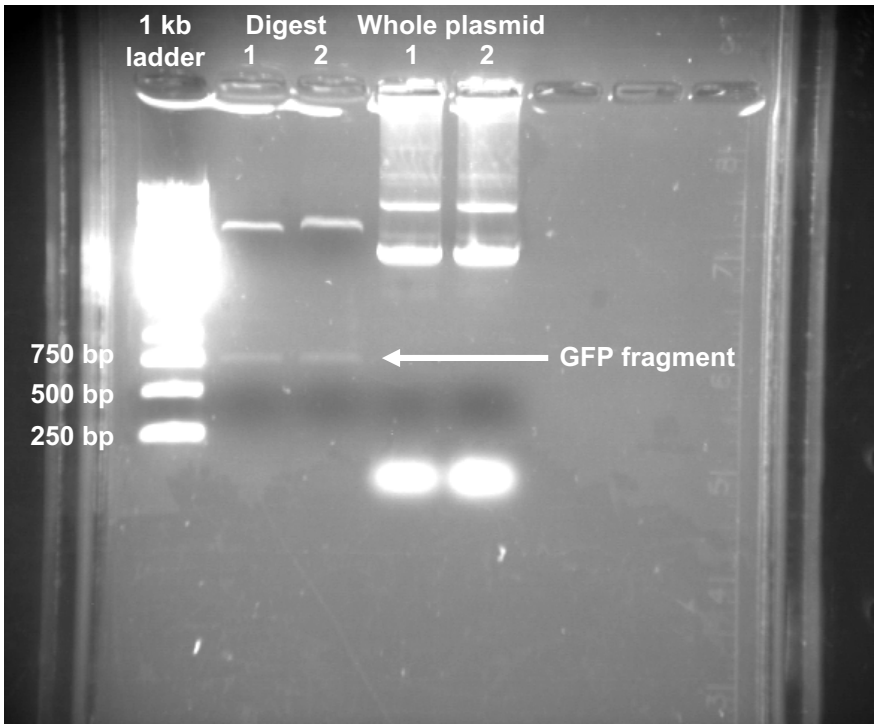
1 kb ladder
Digest 1
2
Whole plasmid 1
2
750 bp
500 bp
250 bp
GFP fragment

Figure 2.8

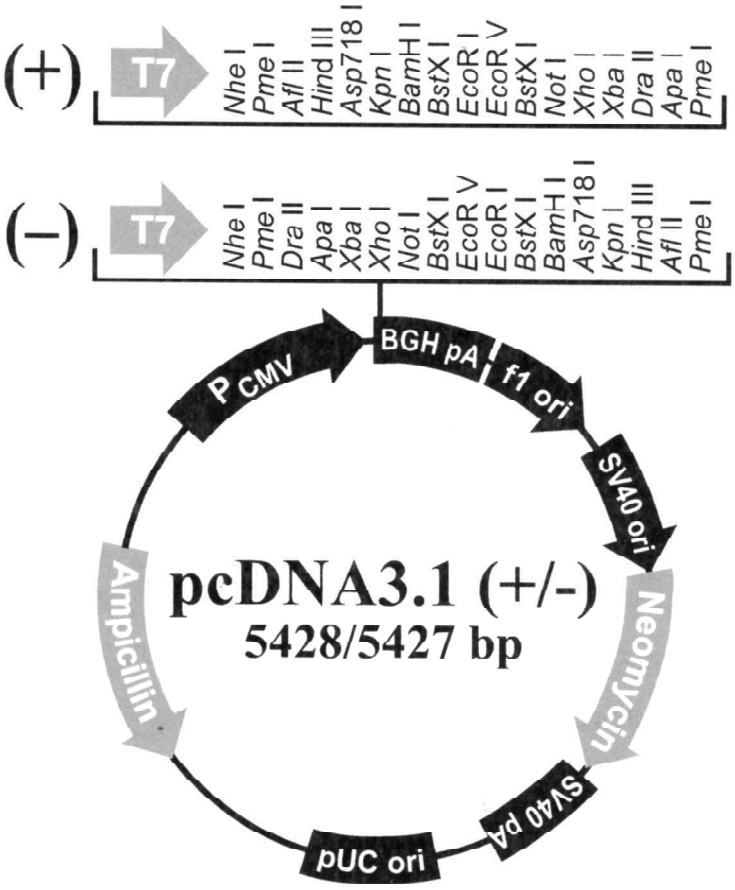
(+)
T7
Nhe I
Pme I
Afl II
Hind III
Asp718 I
Kpn I
BamH I
BstX I
EcoR I
EcoR V
BstX I
Not I
Xho I
Xba I
Dra II
Apa I
Pme I
(–)
T7
Nhe I
Pme I
Dra II
Apa I
Xba I
Xho I
Not I
BstX I
EcoR V
EcoR I
BstX I
BamH I
Asp718 I
Kpn I
Hind III
Afl II
Pme I
P CMV
BGH pA
f1 ori
SV40 ori
Neomycin
SV40 pA
pUC ori
Ampicillin
pcDNA3.1 (+/-)
5428/5427 bp

Figure 2.9

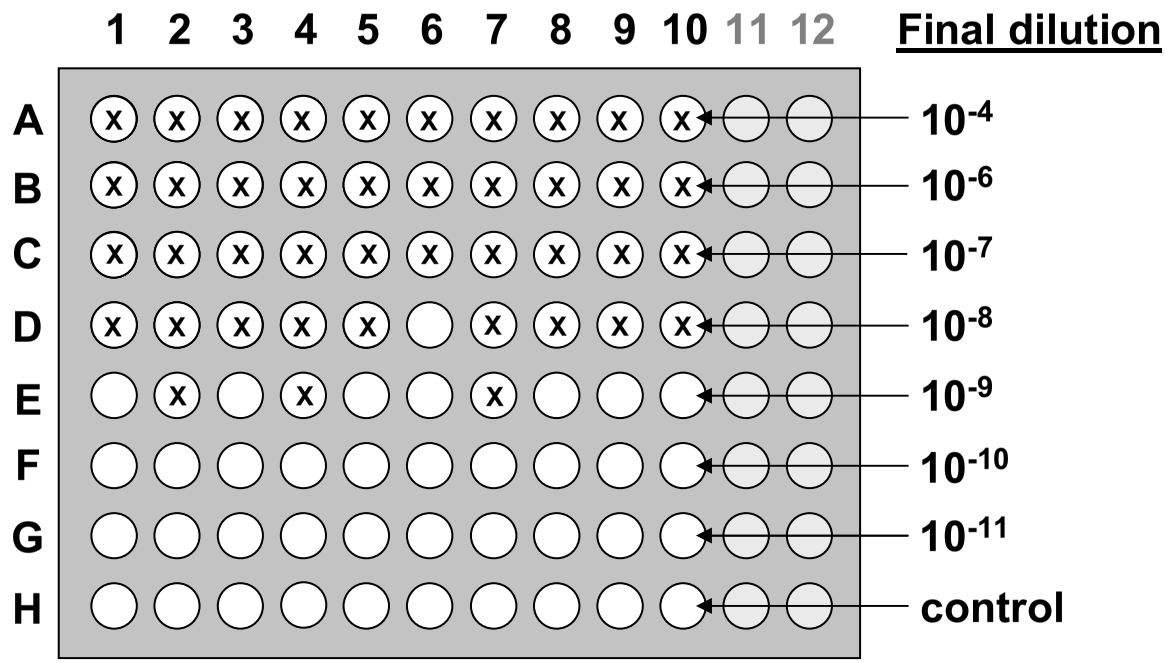
1 2 3 4 5 6 7 8 9 10 11 12
Final dilution
A
B
C
D
E
F
G
H
10-4
10-6
10-7
10-8
10-9
10-10
10-11
control

Specificity	Clone	Conjugate	Isotype
CD4	RM4-5	PE, APC, PerCP	Rat IgG2aκ
CD40	3/23	FITC	Rat IgG2aκ
CD45R/B220	RA3-6B2	FITC	Rat IgG2aκ
CD69	H1-2F3	FITC, PE	Hamster IgG1λ
CD80	16-10A1	FITC	Hamster IgG2κ
CD86	GL1	FITC	Rat IgG2aκ
I-Ad/MHC II	AMS-32.1	FITC	Mouse IgG2bκ
TcR KJ1-26*	DO11.10	Biotinylated	Mouse IgG2a
phospho-p44/42/pERK▲	N/A	Purified	Rabbit IgG
phospho-Kip1/p27^{kip1}▲	N/A	Purified	Rabbit IgG
Rap1 ▲▲	N/A	Purified	Rabbit IgG
phospho-Rb (Ser807/811) ▲	N/A	Purified	Rabbit IgG
phospho-cdc2 (Tyr15) ▲	N/A	Purified	Rabbit IgG
CAR**	RmcB	Purified	Mouse IgG1
IL-2	JES6-5H4	PE	Rat IgG2b
IFNγ	XMG1.2	PE	Rat IgG1

Table 2.1. Antibodies used for flow or laser scanning cytometry
All purchased from BD Pharmingen except: ▲Cell Signalling Technology, NEB; ▲▲ Santa Cruz Biotechnology, Santa Cruz, CA; *biotinylated in-house; **Upstate Biotechnology, Dundee, UK

Label	Excitation (nm)	Emission (nm)	Laser used to excite fluorochrome	Filter cube used to detect emission
Alexa Fluor® 350	346	442	UV	UV
DAPI	358	461	UV	UV
Cascade Blue™	400	425	UV	UV
Pacific Blue™	410	455	UV	UV
Fluorescein▲	494	518	Argon	D 530/30 nm
Alexa Fluor® 488	495	519	Argon	D 530/30 nm
Alexa Fluor® 647	650	668	Helium-Neon	H1 650/LP

Table 2.2. Fluorescence spectra and LSC laser/filter set-up information on labels used for laser scanning cytometry
All purchased from Invitrogen (Molecular Probes) except: ▲BD PharMingen.